European Spatial Data Research

July 2009

Digital Camera Calibration

by Michael Cramer

Official Publication Nº 55

Published by EuroSDR

Printed by Gopher, Amsterdam, The Netherlands

EUROPEAN SPATIAL DATA RESEARCH

PRESIDENT 2008 – 2010:
Antonio Arozarena, Spain

VICE-PRESIDENT 2009 – 2011:
Dieter Fritsch, Germany

SECRETARY-GENERAL:
Kevin Mooney, Ireland

DELEGATES BY MEMBER COUNTRY:

Austria: Michael Franzen
Belgium: Ingrid Vanden Berghe; Jean Theatre
Croatia: Željko Hećimović; Ivan Landek
Cyprus: Christos Zenonos; Michael Savvides
Denmark: Thorben Hansen; Lars Bodum
Finland: Risto Kuittinen; Juha Vilhomaa
France: Jean-Philippe Lagrange; Xavier Briottet
Germany: Dietmar Grünreich; Klement Aringer; Dieter Fritsch
Iceland: Magnús Guðmundsson; Eydís Líndal Finnbogadóttir
Ireland: Colin Bray, Ned Dwyer
Italy: Carlo Cannafoglia
Netherlands: Jantien Stoter; Aart-jan Klijnjan
Norway: Jon Arne Trollvik; Ivar Maalen-Johansen
Spain: Antonio Arozarena, Francisco Papí Montanel
Sweden: Anders Olsson; Anders Östman
Switzerland: Francois Golay; André Streilein-Hurni
United Kingdom: Malcolm Havercroft; Jeremy Morley

COMMISSION CHAIRPERSONS:

Sensors, Primary Data Acquisition and Georeferencing: Michael Cramer, Germany
Image Analysis and Information Extraction: Juha Hyyppä, Finland
Production Systems and Processes: André Streilein-Hurni, Switzerland
Data Specifications: Ulf Sandgren, Sweden
Network Services: Mike Jackson, United Kingdom

OFFICE OF PUBLICATIONS:

Bundesamt für Kartographie und Geodäsie (BKG)
Publications Officer: Andreas Busch
Richard-Strauss-Allee 11
60598 Frankfurt
Germany
Tel.: + 49 69 6333 312
Fax: + 49 69 6333 441

CONTACT DETAILS:

Web: www.eurosdr.net
President: president@eurosdr.net
Secretary-General: secretary@eurosdr.net
Secretariat: admin@eurosdr.net

EuroSDR Secretariat
Faculty of the Built Environment
Dublin Institute of Technology
Bolton Street
Dublin 1
Ireland

Tel.: +353 1 4023933

The official publications of EuroSDR are peer-reviewed.

EuroSDR Network

Digital Camera Calibration

Final Report

Report by Michael Cramer

Institut für Photogrammetrie (ifp), Universität Stuttgart, Germany

Abstract

This final report of the EuroSDR network on Digital Camera Calibration and Validation presents all results from empirical testing and summarizes the main findings. The project itself emphasizes the calibration and validation of digital airborne cameras, where mainly the geometric aspects were of concern. The project was officially finished in May 2007, after almost 3,5 years of project duration. Although the whole project was delayed for several reasons (originally a 2 year period was planned) it was finally a very successful one. This was mainly due to the input of numerous experts forming the EuroSDR Digital Camera Calibration network and their continuous support and active participation in empirical processing of test flight data. The description and analyses of the empirical second project phase is the main part of this report. Three empirical sensor test flights, namely from Leica Geosystems ADS40, Intergraph/ZI-Imaging DMC and Microsoft/Vexcel Imaging UCD were made available to interested network members. The active network members then used their own software and expertise to obtain the optimal results for geometric accuracy. Different software tools and mathematical models were involved during processing. Thus this test gives a broad overview on software, methodologies and expertise available for aerial triangulation of large-format digital airborne cameras. The empirical results clearly showed the importance of additional self-calibration during processing, which was necessary in all cases to obtain maximum geometric accuracy. Even though the results are based on material data already acquired in the years 2003/04 and some considerable improvements in software and hardware were made, the main results still seem to be relevant for the latest version sensor and data sets.

1 Introduction

With the advent of the first digital airborne photogrammetric imaging sensors in operational environments an immediate focus on the quality and performance of such cameras appeared. There definitely is a need for independent tests on sensor performance as well as investigations into the calibration of such digital mapping cameras. Calibration of mapping cameras is well established for the traditional analogue frame cameras but the process has to be modified when dealing with new digital sensors. Since the principal architecture of such digital systems is fairly heterogeneous (i.e. line scanning systems versus frame based solutions, multi-head large format systems versus single-head medium to small format systems, synchronous versus syntopic image data acquisition) individual procedures for system calibration are necessary. With an optional combination and in the case of line scanning systems mandatory tight integration of additional GPS/inertial components this situation becomes even more complex. Within this context a need for new and accepted calibration procedures as well as certification processes is evident. Such procedures will not only support digital camera system suppliers but are also of help for potential digital camera users. All this defined the background when EuroSDR decided to start an initiative on digital camera calibration and validation.

In October 2003 the EuroSDR project on Digital Camera Calibration and Validation was accepted and established officially. The goal was to derive the technical background for digital camera calibration and validation procedures based on scientific theory and empirical research. Research was based on a network of international experts in digital imaging that had to be established first (see Appendix A, page 45). At the time of project initiation legal and certification aspects were put to the background for the time being.

1.1 Objectives of the digital camera calibration project

The project on digital camera calibration and validation itself was divided into two project phases.

- Collection of publicly available material on digital airborne camera calibration to compile an extensive report describing the current practice and methods (phase 1).

- Empirical testing with the focus on the development of commonly accepted procedure(s) for airborne camera calibration and validation, based on the experiences and advice of individual experts (phase 2).

1.1.1 Theoretical phase 1

Phase 1 was finished by the first project year end of 2004. This first year was mainly dedicated to the start-up of the project including the acquisition of individual experts to form the network. Besides that a comprehensive report was compiled documenting the different approaches for sensor calibration in general and the calibration methods for digital cameras applied from system manufacturers so far (Cramer 2004). The report is mainly based on extracts from already published scientific papers amended with additional input from the system providers directly, like exemplarily provided calibration protocols for ADS40, DMC and UltracamD (UCD) systems. Additionally, the report is completed with an extensive bibliography on the topic of camera calibration including many of the fundamental publications. Many of these publications were also made available in digital PDF format. All this is publicly available. This phase 1 status report is also helpful for digital camera system users to gain experience in aspects of digital camera calibration.

The main conclusions from this theoretical phase 1 analysis are summarized as follows:

- A decreased use of standard collimator based laboratory calibration seems to be evident, whereas the importance of in-situ calibration is definitely increasing.

- Such in-situ calibrations, i.e. self-calibration determined from dedicated calibration flights, have to be undertaken by the users regularly, in order to validate and refine the manufacturer's system calibration parameters.

- Due to the fact that such self-calibrating techniques are not as common in traditional airborne photogrammetry, clear knowledge deficits, concerning the features and advantages of system calibration in flight, are present at this time on the users' side.

- It is interesting to note, that since compilation of the phase 1 report substantial changes in the design of the digital cameras and the manufacturer's calibration procedures have taken place. Leica Geosystems and Vexcel Imaging came up with their second generation sensor ADS40 2nd generation and UltracamX system. During the 21st ISPRS congress in Beijing (2008) the ADS80 and UltracamXp have been introduced. In addition new systems are continuously evolving, many of them using medium-format based multi-head sensors, like the Rolleimetric AIC multi-head series or AOS including oblique viewing capability, the IGI DigiCAM dual-head or quadro-head configurations, the Applanix DSS dualcam system, Intergraph/ZI-Imaging RMK D or the DiMAC three-head or oblique configurations. Each camera needs system specific calibration processes and independent validation.

With these many different systems and their various layouts it is not always easy to track the different ways of system calibration, as they are typically done by the manufacturers. Intergraph/ZI-Imaging has developed a calibration facility, where the geometric calibration of each individual DMC camera head is performed fully automatically (Hefele 2006). In addition a new concept for the in-flight calibration was presented (Dörstel 2007). For the UltracamX a (terrestrial) test site was installed for the calibration of individual camera heads (Gruber & Ladstädter 2008). Another interesting change in calibration concept was published by Tempelmann & Hinsken (2007). They introduced a modified parameter set for the geometric calibration of the ADS40 (2nd generation) camera. Now the exclusive calibration of ADS40 from calibration flights becomes feasible. No additional effort is spent in goniometer laboratory measurements any more. Such self-calibration is possible without any ground control, but a special calibration flight layout has to be followed (Tempelmann et al. 2003). A so-called burn-in flight, i.e. an individual system test and calibration using in-site calibration technologies, is now standard procedure for all of the three system providers mentioned above. These flights are typically done in manufacturer-owned test sites.

1.1.2 Empirical phase 2

The second phase focused on the empirical calibration and testing of a small number of data sets from different digital airborne cameras. Additional to the more theoretically oriented investigations of phase 1, in the second phase the individual network members themselves were now requested to investigate the performance of selected airborne cameras. Based on their individual software methodologies and expertise the participants tried to obtain the overall best geometric results using the most optimal system calibration for the individual flight campaign. In general, it was necessary to focus analysis on some of the technical aspects in a sequential order, starting with geometrical aspects and verification of accuracy potential. Analyses and discussions on radiometric and image quality aspects had been postponed to later follow up projects. The main aspect of empirical phase 2 was gathering of experience in individual system performance and finally recommendations of optimal procedures for the calibration and processing of digital image data. It clearly has to be pointed out that phase 2 did not concentrate on the direct comparison of geometric performance of different cameras, but on the definition and testing of sensor related self-calibration approaches for each camera type individually. The results from this second phase are discussed in more detail below.

It was expected that not all of the network members would actively participate in this second empirical phase. Nevertheless, 13 different institutions ultimately participated in this practical part and returned their processing results to the pilot centre (Table 1). The pilot centre provided test flight data obtained from the three large format digital airborne cameras commercially available at that time, namely the Leica Geosystems ADS40 (ADS, 1st generation, sensor head sh40) line scanning system and the Intergraph/ZI-Imaging DMC and Vexcel Imaging UCD frame based systems. As one can see from the table several participants processed more than one data set. The ADS data was analyzed by three participants only, whereas the UCD and DMC flights were processed seven and eight times, respectively. This distribution also was expected: Currently fewer photogrammetric institutions have the software and knowledge to correctly handle line images with their specific imaging geometry. Since DMC and UCD provide standard frame based images, the already implemented standard process chains used for analogue imagery can be used in principle. Nevertheless, even when using DMC and UCD frame imagery some modifications in processing might become necessary, which will be pointed out later.

In many cases the processing of data was done using different configurations or parameter sets during bundle adjustment. Thus, participants finally supported 157 different versions that have been evaluated by the pilot centre.

#	Institution	Code	Processed data set(s)
1	Institute Cartographic Catalunya, Barcelone, Spain	ICC	DMC
2	Lantmatäriet, Gävle, Sweden	LM	DMC
3	ITACyL, Valladolid, Spain	itacyl	UCD
4	Inpho, Stuttgart, Germany	inpho	DMC, UCD
5	CSIRO Information Sciences, Wembley, Australia	CSIRO	DMC, UCD
6	DLR, Berlin, Germany	DLR-B	ADS
7	University of Applied Science, Stuttgart, Germany	HfT	DMC
8	IPI, University of Hannover, Germany	IPI	DMC, UCD
9	ETH Zürich, Switzerland	ETH	ADS, DMC, UCD
10	University of Pavia, Italy	UoP	ADS
11	University of Nottingham, England	UoN	UCD
12	Intergraph/ZI-Imaging, Aalen, Germany	IngrZI	DMC
13	Vexcel, Graz, Austria	Vexcel	UCD

Table 1, Active participants in empirical phase 2

2 Empirical test flight data

The project activities in 2005 were mainly dedicated towards finding appropriate and publicly accessible empirical data sets for phase 2 analysis. Unfortunately there was no financial budget to perform test flights specially dedicated for this project. The original requirements on the test design were as follows: The sensors should have been flown in photogrammetric test ranges, providing a sufficient number of signalized ground control (GCP) and check points (ChP) – preferably all sensor data should have been acquired in the same test site. Additionally, the flight mission of each sensor should include two different flying heights. GPS/inertial data or at least GPS data should also have been available as

additional information for the sensor's exterior orientations. Although several European national mapping agencies as well as other companies kindly offered access to different test flight data, the finally chosen data sets could not fulfil all of the above requirements.

2.1 Photogrammetric test sites

In the end, two data sets acquired in the Norwegian Fredrikstad test site were exemplarily chosen for the DMC and UCD system. The DMC flight data were cordially provided by TerraTec (Norway); the UCD flights were made available through IFMS-Pasewalk (Germany). The Fredrikstad test site is one example of a specially designed photogrammetric test area with a sufficiently high number of signalized ground control points. The test site covers an area of 4.5 x 6 km² and consists of 51 well defined, permanently marked and regularly distributed control points. The accuracy of the GCPs in object space lies in the millimeter range. 20 of those points were made available and used as control points for the DMC and UCD processing. The remaining points were not distributed to the participants but used as independent check points for the absolute quality control performed. The site was already established in 1992 and is maintained by the Geomatics Section at the Norwegian University of Life Sciences. It is already well-known to the EuroSDR/OEEPE user community from former performance tests such as the OEEPE tests on GPS assisted aerial triangulation (Ackermann 1996) or integrated sensor orientation (Heipke et al. 2002).

The ADS40 data set was flown in the German test field Vaihingen/Enz. This field is maintained by the Institut für Photogrammetrie (ifp) at Universität Stuttgart and is also well known from former tests of digital airborne sensors or independent performance evaluations of integrated GPS/inertial systems (Cramer 2005). The site covers an area of 7.5 x 4.8 km², and more than 200 points are available as signalized and coordinated control and check points. Their distribution follows the ideal point distribution for fully signalized medium-scale (1:13000) wide angle analogue camera flights with 60% forward and side-lap conditions. All points are independently determined from static GPS surveys, with an estimated accuracy of 2cm for all three coordinate components. Again, only a sub-set of 12 control points was distributed for the ADS data processing; the remaining points served as independent check points for later absolute performance checks.

Both test sites provide a sufficient number of control and check points, all of them signalized, and therefore may serve as independent check points for geometric quality assurance. Since no radiometric or dedicated resolution targets were available for the time of flight only the geometric performance was investigated within phase 2.

At the time the selection empirical data sets for phase 2 had to be made, the three flights from the Fredrikstad (DMC and UCD) and Vaihingen/Enz (ADS) test sites were the only data made available to the pilot centre. Today, other data sets have appeared, in some cases even more appropriate for such investigations. Especially the test flight activities from the Finnish Geodetic Institute FGI within their Sjökulla test site have to be mentioned within this context (i.e. Honkavaara et al. 2006). None of those flights had been discovered within this EuroSDR test.

2.2 Image data acquisition

The basic characteristics of the three different sensor flights in the Fredrikstad and Vaihingen/Enz test sites are summarized in Table 2. All sensors were flown in two different flying heights resulting in different ground sampling distances (GSD) with individual block geometries. This can clearly be seen from the different overlap conditions.

The given ground sampling distance GSD is the theoretical value obtained from sensor pixel size and image scale. In the case of ADS40 this value is related to the non-staggered image data. The given number of images relates to the different image strips (pixel carpets) recorded by each of the ADS40 sensor lines. Each flight line consists of data from six simultaneously recording CCD lines, namely the pan-chromatic forward, nadir and backward looking A and B lines. Since the whole strip is acquired by all CCDs from three different viewing angles, ADS40 per se provides 100% overlap in flight direction. Unfortunately, additional GPS/inertial data were only available for the ADS40 flight. In the case of the DMC flight no additional GPS or GPS/inertial data was made available through the pilot centre. For the UCD project a GPS trajectory was processed and delivered but since the GPS test set-up was sub-optimal (long base line length >100km) the obtained positioning accuracy was limited and influenced by systematic offset and drift errors.

Flight	Altitude a. g. [m]	GSD [m]	# strips long/cross	% overlap long/cross	# Images	Additional data
ADS40 Vaihingen/Enz, June 26, 2004						
low	1500	0.18	4 / 2	100 / 44	36	GPS/INS
high	2500	0.26	3 / 3	100 / 70	36	GPS/INS
DMC Fredrikstad, October 10, 2003						
low	950	0.10	5	60 / 30	115	n.a.
high	1800	0.18	3	60 / 30	34	n.a.
UCD Fredrikstad, September 16, 2004						
low	1900	0.17	4 / 1	80 / 60	131	GPS
high	3800	0.34	2	80 / 60	28	GPS

Table 2, Flight parameters of phase 2 digital sensor flights

Figure 1 illustrates the block geometry for the block *DMC high* and *UCD low*, respectively. Although both flights were close to 2000m flying height above ground resulting in approximately 0.2m GSD each, they are of quite different layout. Due to the larger overlap between strips and one additional cross strip the UCD block is of considerably stronger geometric strength than the DMC block. This also positively influences the accuracy of the later object point determination and is one of the reasons why the different system accuracy from this test cannot be compared directly, although they were flown in the same test area.

It has to be mentioned that both frame based systems were flown relatively late in the year (September 16 and October 10 for UCD and DMC respectively) at 60deg northern latitude. This results in sun angles between 25-30deg maximum which are quite demanding environmental conditions. This was of negative influence on the radiometric image data quality. Therefore the data is not being used for the analysis of radiometric performance of digital airborne imaging. Furthermore some of the participants rightly complained about the limited visibility of signalized points within the DMC and UCD data, also due to the somewhat

limited radiometric image quality. This mainly affects the identification of image points and thus the performance of manual image coordinate measurements. In some cases of phase 2 evaluations not all check and control points had been measured. Therefore the pilot centre slightly modified phase 2 for DMC and UCD data. Within a second step image coordinates of all control and check points were carefully measured manually by the pilot centre itself and then provided to all participants together with the automatic tie point measurements. Now processing of participants could rely on the same set of pre-defined image coordinates. This second step of phase 2 was then denoted as phase 2b. For ADS40 no pre-defined image coordinates were provided (except for ETH evaluations of *ADS low* block). In that case all measurements were individually done by the participants by using the obtained ADS40 image strips.

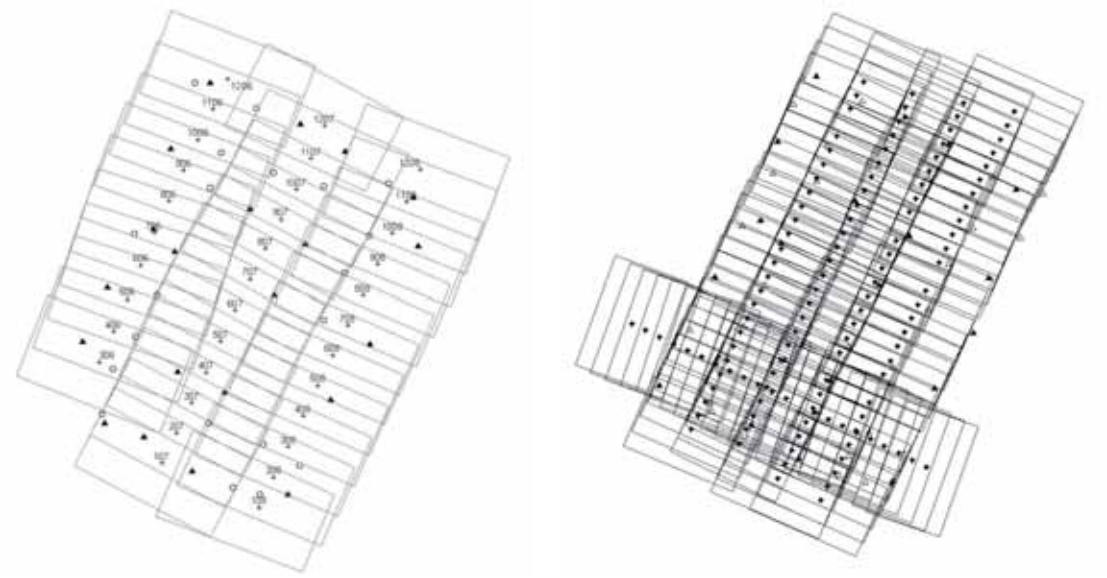

Figure 1, Block geometry of *DMC high* block (GSD 0.18m) (left) and *UCD low* block (GSD 0.17m) (right)

3 Test flight analyses

As already mentioned the main focus was on the estimation of the empirical geometric accuracy of the sensor systems and the influence of additional parameter sets during processing. Thus all participants did their own manual and automatic image coordinate measurements first. In case of phase 2b data the pre-measured image coordinates were used. Those measurements were then used as input for the succeeding aerial triangulation which finally leads to the adjusted coordinates of check points. These adjusted check point coordinates were then returned to the pilot centre together with a brief report from each participant mainly describing the concept and used additional parameters during their adjustment runs. Since the reference coordinates of check points were not provided to the participants in advance, they were used to obtain the absolute accuracy of the bundle adjustment. Unfortunately some of the reports provided by participants were only very rudimentary including

almost no or only brief descriptions on the performed investigations. After the absolute accuracy checks the pilot centre also prepared a report for each participant including the detailed results of the individual calculations. The main results from the other test participants dealing with the same data were also presented, but provided anonymously only. Besides, the results from the processing at the pilot centre were also part of this participant information. Thus, each participant was able to judge the quality of his evaluations compared to the results from the pilot centre and others. In some cases participants refined their processing and returned modified results afterwards.

All the following results are exclusively obtained from the three flight campaigns described in the previous section. Note that the flights were from 2003/04 and therefore might not fully reflect the current performance of today's digital sensor versions. Changes regarding hardware and sensor specific software processing might influence and improve today's sensor performance.

Table 3 shows the different software packages used for the image point measurement and the bundle adjustment, where image coordinate measurement was not necessary for the phase 2b data. As one can see almost all relevant software products used for measurements, point transfer and bundle adjustment were used during data processing. Besides, the additional parameter sets introduced for the different bundle adjustments are listed. In nearly all cases the participants tried different versions for their adjustments. Self-calibration was applied in general, but almost each participant also provided the solution without using additional parameters during AT. This was done mainly for comparison purposes. Besides standard additional parameter models, like orthogonal polynomials (Ebner or Grün model) or the physical relevant model provided by Brown, some evaluations were done with extended or modified additional parameter sets. These parameter sets were specially adapted to the camera specific sensor layout, i.e. the multi-head configurations of DMC and UCD cameras. Typically the two different flight heights were handled as two separate flights. A few participants used both flying heights for simultaneous adjustments. All sensor related results will be presented in more detail in the following sub-sections.

Process step	**Software**
Matching and point measurement (only for phase 2)	Manual, Match-AT, LPS, ISAT, GPro, PhotoMod, others
Bundle adjustment	Match-AT, ORIMA, InBlock, BLUH, Bingo, PhotoMod, ACX-Geotex, IS-PhotoT, others

Data set	**Additional parameter sets** (if applied)
DMC	Ebner, Grün, Polynom, BLUH Ebner/Grün per image quadrant, BLUH DMC specific
UCD	Ebner, Grün, BLUH Ebner/Grün per image patch, BLUH UCD specific
ADS40	Brown (with some extensions)

Table 3, Software packages and parameter sets in phase 2

3.1 ADS40 flight Vaihingen/Enz

3.1.1 Evaluations by the pilot centre

The ADS40 flight data were part of a joint project of the Institut für Photogrammetrie (ifp) and Leica Geosystems. The complete processing of the data was done by ifp, using the standard Leica process chain besides proprietary software products for bundle adjustment. More details on that test can be found in Cramer (2005). Again note, that GSD here relates to the non-staggered images, although the flight was done in so-called staggered mode. Nevertheless, images from A and B pan-chromatic CCD lines were always treated as separate images; no staggering was performed to combine A and B lines for each of the three viewing directions. Table 4 shows the geometric absolute accuracy (RMS) from investigations at the pilot centre obtained from 190 check point differences using standard GPro and ORIMA processing. 12 GCPs are introduced, exactly the same as also provided to the participants.

ADS flight	Self-calibration	RMS [m]		
		East	North	Vertical
low, GSD 0.18m	not applied	0.052	0.054	0.077
low, GSD 0.18m	applied	0.031	0.040	0.057
high, GSD 0.26m	not applied	0.066	0.060	0.100
high, GSD 0.26m	applied	0.064	0.059	0.087

Table 4, ADS40 results from pilot centre

Both flights were considered individually. Within the first version no additional self-calibration terms had been introduced in the bundle adjustment. In other words, the adjustment was done based on image point measurements from all image channels, and the 12 GCPs and GPS/inertial observations weighted with their accuracy estimated in Kalman filtering. Additional unknowns were introduced for the three boresight misalignment angles as well as for six GPS/inertial position and drift parameters, valid for the whole block only. Drift was almost not present. In the second run additional self-calibration was performed. The self-calibration model used by ORIMA can be related to the known Brown parameter model. Comparing the RMS values from both versions it is clearly obvious that in case of this ADS40 data sets additional self-calibration is only of minor influence on the resulting object point accuracy. The obtained refinement is very small for the *ADS high* flight, and of slightly larger influence for the *ADS low* block.

3.1.2 ADS results from participants

As already mentioned in Table 1 only DLR-B, UoP and ETH focused on the processing of ADS data. ETH only considered the 1500m block *ADS low*. The ETH analyses were restricted to the bundle adjustment only; image coordinates were provided by the pilot centre on request of ETH. The software used for point transfer and triangulation of three line sensor (TLS) imagery was developed at the ETH Zürich (Grün & Zhang 2003). The mathematical model and the methods of self-calibration are also published in Kocaman et al. (2006). **DLR-B** used an own processing chain to evaluate the ADS data. This software chain was originally developed for the orientation, DTM generation and orthophoto production of HRSC

data (Scholten et al. 2002). Some more detail can be seen from the statistics in B.1.3 and the report in C.2 provided by DLR-B. The results from UoP were achieved using standard Leica Geosystem processing software, i.e. GPro for tie point transfer and ORIMA for bundle adjustment. All participants investigated the two different flying heights as separate blocks. Rather than provide separate sets of estimated ChP coordinates DLR-B averaged the results from *ADS high* and *ADS low* to get the final coordinates of control points; thus their results are not included in Figure 2 and Figure 3 showing the exemplarily results (RMS accuracy) for the *ADS low* and *ADS high* block. The results from the self-calibration cases are given together with the non self-calibration variants. The obtained accuracy (RMS) for the DLR-B processing is about RMS_X=0.042m, RMS_Y=0.042m and RMS_Z=0.082m for the east, north and vertical coordinates respectively. No additional self-calibration was applied during processing; thus those results are consistent with the other results obtained without self-calibration. It is quite interesting to note that DLR-B also considered the subsequent process step, i.e. a height model and orthophotomosaic was processed from ADS data. This product generation is also part of their process chain and documented in the report in C.2 (page 86).

ETH did a very detailed analysis of data, but only focusing on the *ADS low* block. Their software supports different trajectory models to estimate the dynamics of sensor movements. The Lagrange interpolation model (LIM) and the direct georeferencing model (DGR) were used here. The LIM approach is similar to the orientation fix points in the ORIMA processing, whereas the DGR model relies more on the performance of a priori GPS/inertial trajectory information. Additionally, the number of self-calibration parameters varied. A full set of 18 additional parameters was introduced: namely 6 parameters describing the camera lens behaviour (1 focal length correction, 3 radial and 2 tangential distortions) amended by 4 additional parameters for each of the three scan-lines / viewing directions (2 principal point corrections, 1 scan line inclination, 1 affinity across flight direction). In some cases six of those parameters were eliminated. Note that all versions given here are based on the set of all 12 provided GCPs. ETH also does the similar processing based on a sub-set of four of those points. These variants are also included in their report. In general the DGR based versions obtained high quality and the more advanced LIM model does not improve the accuracy. This also indicates the high performance GPS/inertial trajectory computations. Using DGR with self-calibration obtains the best results. The RMS values are RMS_X=0.031m, RMS_Y=0.037m and RMS_Z=0.060m, which is fully consistent with the results from the pilot centre processing (see B.1.1 for statistical analyses and participant report in C.1 for more details). For the ETH versions use of additional parameters during adjustments mainly increases the geometric accuracy in the horizontal components.

In **UoP** processing two different GCP configurations were used. Besides the use of all 12 GCPs again a sub-set including only 6 GCPs was established. In the figures only the results from the 12 GCP case are displayed. Three different versions have been calculated for both GCP configurations: The first version *basic* does not use additional self-calibration parameters and also does not correct for IMU misalignment errors and GPS/inertial position drift and datum effects. Thus the second version *para* coincides with the non self-calibration case of the pilot centre evaluations. Here the additional parameters like IMU misalignment, datum transform and position drift are considered. Finally the version *self* also includes additional self-calibration. Comparing the results to the ETH results and the results from the pilot centre, the UoP results are slightly less accurate for the *ADS low* block. Especially in north component a systematic error seems to be present. The difference in north direction showed

a mean offset of about 5cm, which deteriorates the RMS value (see B.1.2 for details). The situation is different for the *ADS high* block. Here the UoP results in the horizontal components are better than the results obtained by PC, although both results are based on the same software. This somewhat reflects the situation in practice where smaller variations in final accuracy dependent on the users individual experience have to be expected.

In general the ADS results are of high accuracy. If one looks for the mean RMS value obtained from all self-calibration cases using the *ADS low* block, the horizontal accuracy is within 1/4 – 1/5 pix GSD, whereas the vertical accuracy is close to 1/3 pix GSD. Similar results are also obtained from the *ADS high* block. This is well within the accuracy expectations. Additional parameters during adjustment allow for the refinement of accuracy. But in general this accuracy increase is quite small and mainly visible in horizontal components.

The results from different participants are fairly consistent. Still it has to be kept in mind, that only 3 different institutions apart from the pilot centre itself were involved in the processing of the line scanner data set. Thus the statistical relevance is somewhat restricted.

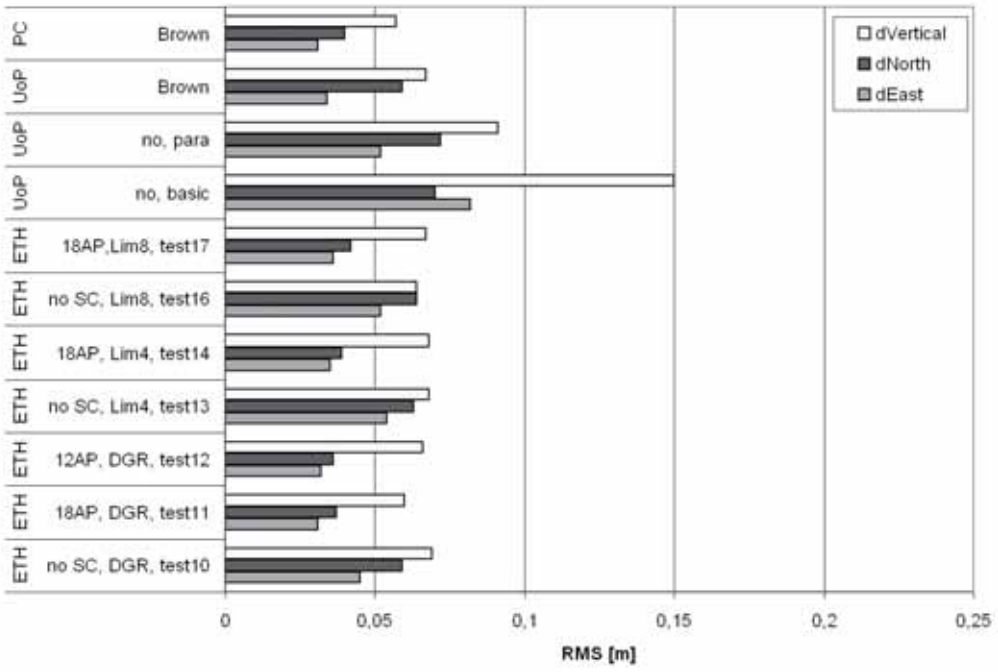

Figure 2, *ADS low* (phase 2) accuracy (RMS)

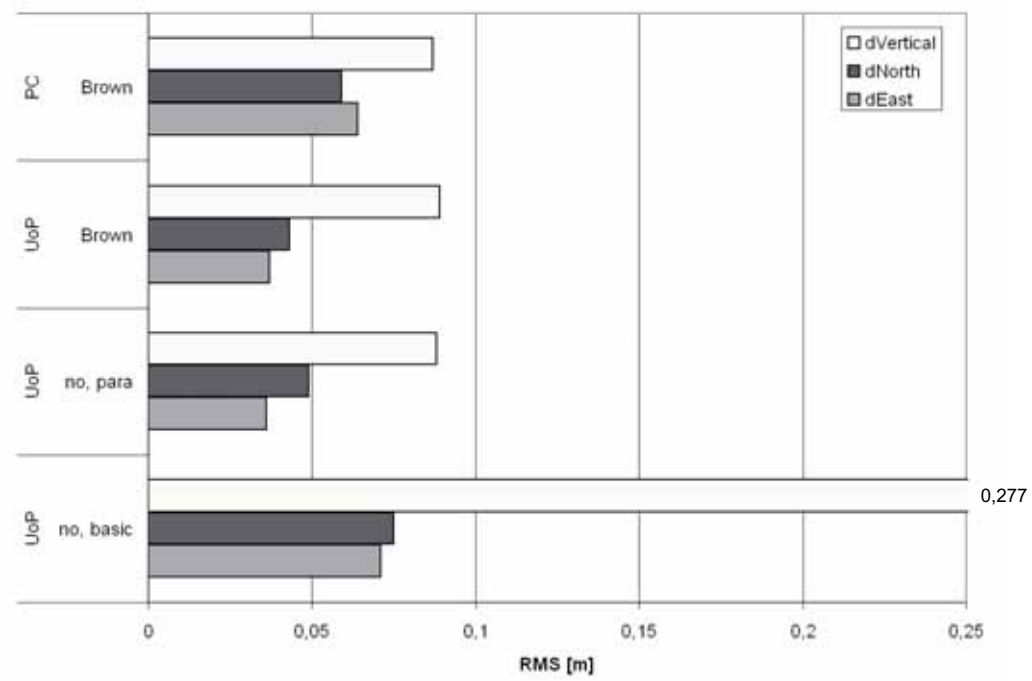

Figure 3, *ADS high* (phase 2) accuracy (RMS)

3.2 DMC and UCD flights Fredrikstad

3.2.1 Evaluations by the pilot centre

During processing of the Fredrikstad flights the pilot centre used different versions for each of the two flying heights of each camera. Within the first step conventional bundle adjustment without additional parameters was performed, based on 20 GCPs. The obtained RMS values from check point analysis for DMC data are as follows: RMS_X=0.097m, RMS_Y=0.054m and RMS_Z=0.14m. These numbers relate to the *DMC low* block (GSD 0.1m). Then the additional 44 parameters proposed by Grün were introduced. This mainly refines the accuracy in the east component. The accuracy obtained from *DMC low* is: RMS_X=0.056m, RMS_Y=0.054m and RMS_Z=0.124m. Again only 20 GCPs were used. Now the horizontal coordinates are of the same accuracy; the systematic error is compensated. The vertical accuracy is only marginally influenced. In the final step all available ground control (GCP and check points) were used to optimally determine the additional 44 parameters. Then the estimated parameters were fixed and a conventional AT was performed, again based on 20 GCPs only. The check point analysis results in RMS values of RMS_X=0.048m, RMS_Y=0.047m and RMS_Z=0.116m (*DMC low* block). This solution was used as "reference" solution. It has to be mentioned that, although all signalized object points had been used for control information this,is not necessarily the best solution. The self-calibration is based on a

standard (empirical) polynomial correction model only, which might be sub-optimal for the modelling of the 4 camera head geometry of the DMC and UCD.

Furthermore the choice of observation weights also influences the final solutions. All versions from the pilot centre were based on observation standard deviations of 3µm for image coordinates and 0.02m for horizontal and vertical control points. If for example the first, non self-calibration case is done with the following assumptions on standard deviations (image coordinates 1.2µm (automatic tie point transfer) and 3.6µm (manual measured image points); control points 0.01m for horizontal and vertical components) the obtained RMS values from check point analysis are significantly worse, mainly for the vertical component: RMS_X=0.118m, RMS_Y=0.051m and RMS_Z=0.247m. This clearly illustrates, that besides the choice of the mathematical model for self-calibration, the correct assumptions on a priori weights are also of major concern and in some cases might also have larger impact on the final accuracy than the applied parameter set for self-calibration.

Finally, for all UCD and DMC flights the processing was performed using the 44 parameters optimally estimated from all available control information on the ground and then used as fixed values – as described above. The standard deviations for observations were as follows: 3µm for image coordinates and 0.02m for all control point coordinates. This finally results in the absolute accuracy (RMS) given in Table 5. It is quite interesting to see that *DMC high* and *DMC low* show almost the same accuracy, although in general lower altitude flights should allow for better geometric accuracy. This might be due to the following reasons: First, the estimated sigma0, which is one factor within error propagation, is higher for the *DMC low* than for the *DMC high* flight. Second, the relative number of control points per image is higher for the *DMC high* block. Furthermore there are no control points within the side lap regions between two strips for the *DMC low* flight. This is especially of concern, since no GPS data was provided. And finally some errors in the control point object coordinates or some systematic errors in object space due to shadowing or meadows will influence the accuracy of signalized points. This also is of higher impact for lower altitude than higher altitude flights. Also remember the demanding radiometric quality of image data, which negatively affects the correct identification of points.

For the UCD flights similar performance is visible for the horizontal coordinates. Although the difference in flying height between the two UCD flights is about 2km, the horizontal accuracy is almost similar and comparable to the DMC accuracy. For the vertical component the UCD flights are of very high accuracy. This is mainly due to the very large overlaps resulting in much stronger block geometries than for the DMC blocks (consider the different flight designs described in Table 2).

Flight	Flying height, GSD	RMS [m]		
		East	North	Vertical
DMC low	950m, 0.10m	0.040	0.048	0.132
DMC high	1800m, 0.18m	0.048	0.047	0.116
UCD low	1900m, 0.17m	0.076	0.060	0.059
UCD high	3800m, 0.34m	0.048	0.068	0.103

Table 5, DMC and UCD results from pilot centre

3.2.2 DMC results from participants

Eight different institutions participated in the evaluation of the DMC flights. Three of them were active in both phase 2 and phase 2b, namely ICC, IPI and IngrZI. Inpho, HfT and LM only provided their results for phase 2, where ETH and CSIRO only participated in phase 2b. In all cases the image blocks were handled separately, except for IPI and CSIRO evaluations, where also a simultaneous block adjustment of both flying heights was done. Inpho only provided results from the combined adjustment of *DMC low* and *DMC high*. ICC, IPI and ETH used modified or specially designed self-calibration models to take care of the specific DMC sensor geometry. ICC introduces one set of Ebner correction polynomials for each of the four DMC image quadrants. IPI used the BLUH program offering different and flexible sets of additional parameters (Jacobsen 2007). The ETH software approach is similar to ICC, but the Grün parameters could also be introduced per image quadrant in addition to the Ebner model, as is done at ICC. The others worked with the already known correction models, like Ebner, Grün or Brown physical parameters.

DMC phase 2 results

As already mentioned the phase 2 results are based on the individual participants image coordinate measurements (manual and automatic), whereas for phase 2b all participating members have used the same set of pre-measured image coordinates. Since not all of the participants of phase 2 spent similar effort in the identification and measurement of control and especially check points (remember the sub-optimal image radiometry due to environmental conditions during flight) the available number of points for independent accuracy estimation is quite different. This also influences the later comparison of results.

The **ICC** results are based on automatic tie point measurements from MATCH-AT. The bundle adjustment was done with their own ACX-GeoTex software. As already mentioned, the Ebner 12 parameter model is introduced for each image quadrant separately. They still use the image point observations measured in the virtual image plane, but dependent on their location the individual observations contribute to the corresponding quadrant specific additional parameter set. The effect of such quadrant specific corrections is illustrated in Figure 4. As one can see the influence is in the range of about 1 pix which corresponds to 12µm in image plane. As one can see both blocks show a similar tendency but there are also differences, which might be due to the fact that the other effects are also compensated from the AP sets. The corresponding accuracy from check point analyses are given in B.2.1 (page 52). The ICC report is given in C.3 (page 103).

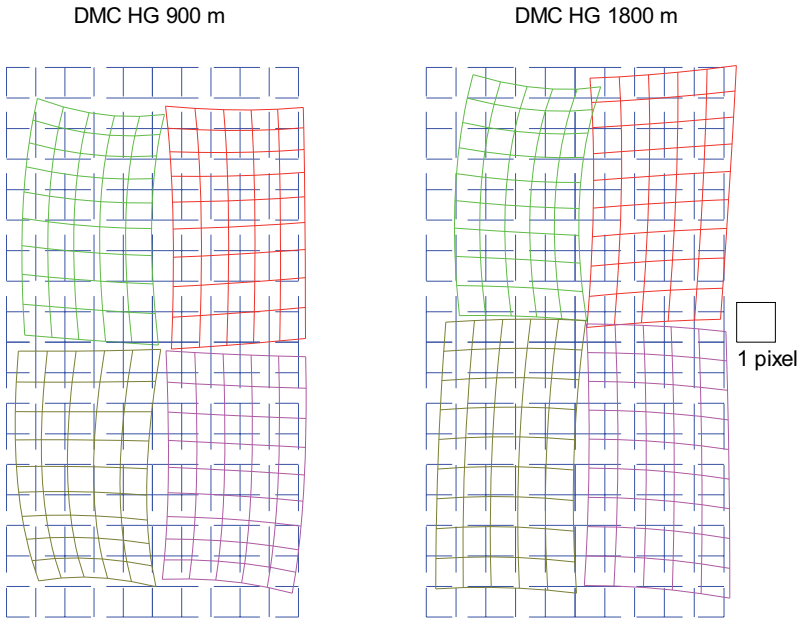

Figure 4, Distortions of additional parameters in the image space for blocks *DMC low* and *DMC high* (© ICC, 2006)

IPI was one of the most active members in the camera calibration network providing results from phase 2 and phase 2b processing for both DMC and UCD cameras. All processing results are based on the BLUH bundle adjustment software which offers sophisticated additional parameter sets that take care of the special geometry of the multi-head based large format airborne frame cameras, and others. The different additional parameter models are described in the IPI report (see C.4, page 113). The automatic tie points were measured using LPS. The adjustments were first done for the two flight heights separately. After that identical points from both flying heights were identified (by comparing the differences of adjusted object coordinates). Those additional 101 points were used to generate a stronger tie between the two blocks. This then allows for a common adjustment of both blocks. Several versions were calculated, i.e. without use of any self-calibration, with use of the BLUH standard 12 parameter set, which is different from the Ebner 12 additional parameters, and then also using additional DMC specific correction terms. The different variants are also explained in the IPI report (see C.4). From the DMC specific version only the one version using the BLUH parameters 1-12 (standard 12 parameters), 30-36 (DMC synchronization and perspective deformation) and 74-81 (DMC radial symmetric and focal length correction) is given. See B.2.2 for detailed results. Even though DMC specific additional parameters have been developed and implemented in BLUH their exclusive use is not sufficient to compensate for all the systematic effects. Therefore they have to be supplemented by the standard BLUH 12 parameter set.

The **inpho** company also participated in the empirical processing of the DMC phase 2 data. The processing was based on MATCH-AT used for automatic tie point transfer and adjustment. Additional adjustment runs were done by the InBlock software which offers more flexibility when using additional parameter models. Within InBlock the physical Brown

parameter model is also available. The automatic tie point transfer was done for both blocks separately first, but then all image coordinates were merged to perform a final adjustment with both flying heights in one data set. Thus, the tie between blocks is realized through the manual point measurements. The detailed results are given in B.2.3. Note also the short status report in C.5. Since inpho also processed the UCD data, the report relates to the findings from both data sets.

The DMC data was analyzed from **HfT** as part of a diploma thesis. Within their evaluations two programs, namely MATCH-AT and PhotoMod, were used. The first one uses automatic tie point generation. With PhotoMod all points were measured manually or semi-automatically since the automatic point transfer did not deliver reasonable results for this data set. This might also be partially due to the radiometry and the image content (water and forested areas), which was of larger influence for the automatic algorithms implemented in PhotoMod. In MATCH-AT runs the 44 parameter model by Grün is used for self-calibration. The PhotoMod adjustment used the independent model approach. Additional polynomial corrections were applied. The results are given in B.2.4 and the corresponding report can be found in C.6 (page 134). Although both software packages use different philosophies (automatic versus manual/semi-automatic, bundle versus independent model adjustment) the results obtained are quite similar.

The aerial triangulations performed at **LM** always rely on the assumption that GPS perspective centre coordinates are available, since all photo flights in Sweden are done with GPS support. From personal correspondence access to GPS data recorded during the DMC flights in Fredrikstad was possible for LM. These data obviously were not of standard quality and shift and drift corrections were introduced during processing. This data officially was not part of the evaluations and not available for the other test participants. Even the pilot centre also had no access to this GPS trajectory information. This has to be considered when comparing the LM evaluations to the results from other participants. During LM processing the 12 parameter Ebner model was used; all results were obtained from the MATCH-AT package. LM reported that high shift and drift corrections were estimated indicating that something is wrong in the GPS processing, preventing the use of position information as absolute values. The detailed results are given in B.2.5.

Finally the phase 2 results for DMC data from the manufacturer's evaluation (**IngrZI**) are given. Their self-calibration is based on the 12 Ebner parameters. The block adjustment was done in three steps: After free network adjustment to eliminate gross measurement errors, a sub-set of 7 control points was used for bundle adjustment to use the remaining GCP for check point analyses. The final adjustments were then based on all GCPs except two which again were used to have some independent quality control. The results from the different processing versions are given in B.2.6. A short report on their findings is included in C.7.

Figure 5 to Figure 7 summarize the above participant evaluations for the *DMC low* (GSD 0.1m), *DMC high* (GSD 0.18m) and *DMC both* data sets, respectively. The results from the pilot centre (PC) are also included. It is interesting to see that, for the *DMC low* case the horizontal accuracy (RMS) is typically in the range of 5cm or better corresponding to ½ pix GSD or better. For the vertical component the RMS is mostly in the range 1/2 to 1 pix GSD. Note that there are less accurate versions although self-calibration was applied. In horizontal components the accuracy seems to be more consistent. This again shows that the model used

for self-calibration is only one component in the whole process chain and its effect might be masked by other influences. For the *DMC high* data set the accuracy in absolute numbers is less compared to *DMC low*, which should have been expected. Nevertheless, if one looks at the horizontal accuracy, which is mostly about 6cm, this is only slightly worse compared to the *DMC low* block and corresponds to 1/3 pix GSD. The mean accuracy in height is about 1 pix and does not reach the 1/2 pix range. This is worse compared to the *DMC low* block. The results from combined adjustments are close to the DMC low results, even better for horizontal components. Obviously the stronger geometry of the combined block allows for the better estimation of additional parameters and the more accurate determination of object point coordinates.

Again, keep in mind that all these results are obtained from individually measured image observations (including the different choice of a priori weightings), slightly different check point configurations and of course from different software packages. Nevertheless, the variations in horizontal and vertical accuracy somewhat reflect the situation in practice. Even though all participants have used the same image and control point data set, the results obtained are different. This clearly reflects the impact of personal experience and software availability on the final result, which was pointed out before.

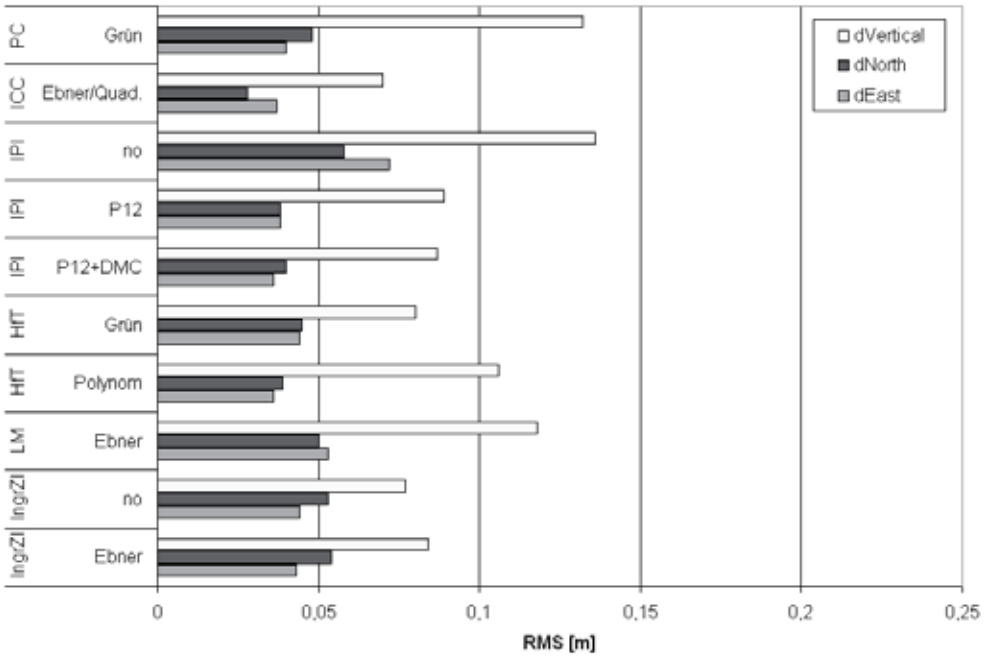

Figure 5, Accuracy (RMS) of participants results *DMC low* (phase 2)

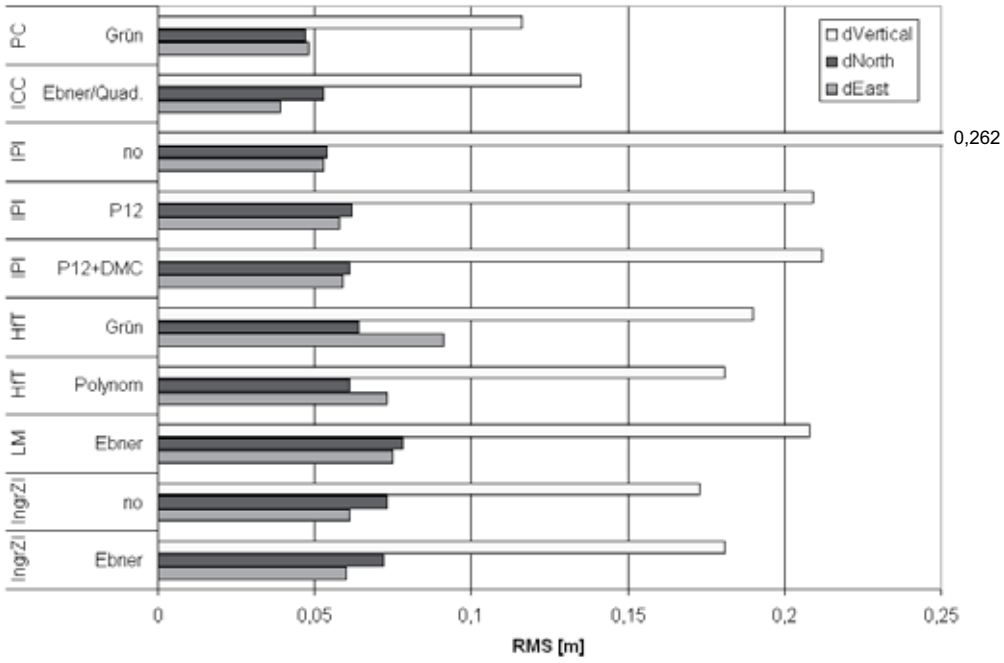

Figure 6, *DMC high* (phase 2) accuracy (RMS)

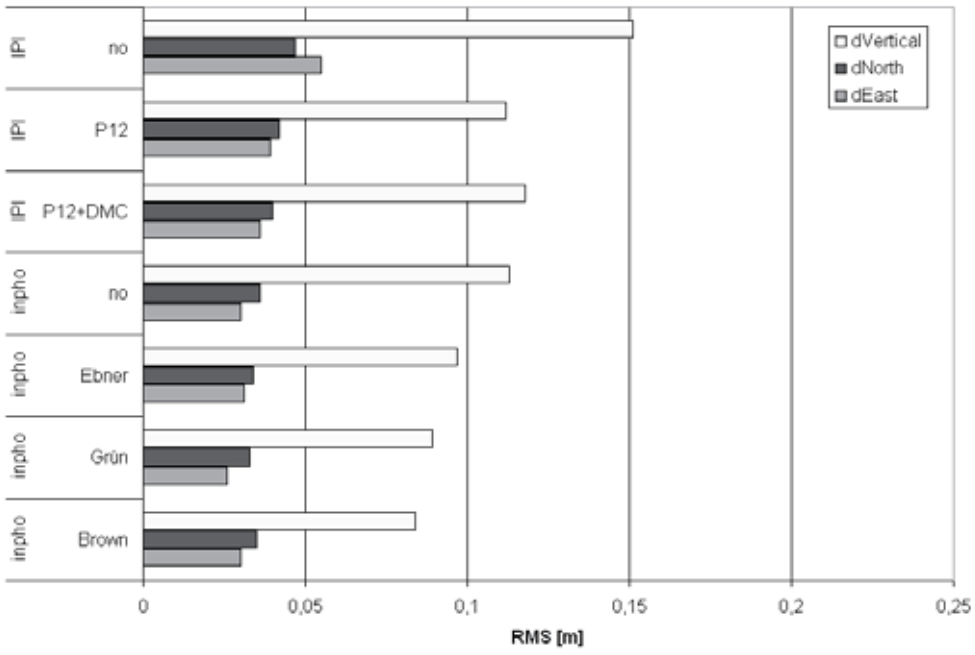

Figure 7, *DMC both* (phase 2) accuracy (RMS)

DMC phase 2b results

Different to the phase 2 results presented previously, the later extension to phase 2b relies on pre-measured sets of image coordinates, which were obtained at the pilot centre and delivered to all phase 2b participants afterwards. Thus the processing of each participant is based on the same set of image coordinate measurements, which allows for direct comparison of results. From that point of view this phase 2b may be more valuable since the influence of self-calibration and observation weightings is more clearly visible compared to the previous evaluations from phase 2.

Five different institutions dealt with the DMC phase 2b data, three of them already evaluated the phase 2 data sets, namely ICC, IPI and IngrZI. Two others (CSIRO and ETH) only delivered phase 2b results. In cases that participants were active in both parts of phase 2 they typically used the same configurations for block adjustments.

ICC, for example, again used the 12 Ebner parameter correction values introduced for each of the quadrants of the virtual image separately. In addition to the version provided for phase 2 two different settings of a priori weightings were introduced. The observation weights in detail can be seen from the table in B.2.7.

Figure 8 shows the influence on the final accuracy for the *DMC low* flight. The influence of a priori weightings is obvious especially for the accuracy in the vertical component. It is also interesting to compare the results from version 1 here with the ICC results already depicted in Figure 5. For both versions the a priori weightings and the self-calibration model are identical, the only difference are the image coordinates. As already described in phase 2 they were based on the participants' measurements; in phase 2b those observations were centrally supplied by the pilot centre. The difference in both ICC results is visible for *DMC low* and can only be explained by the assumption that the ICC image coordinate measurements used for phase 2 in this block have been of extraordinary performance. The differences are smaller if one compares the results from *DMC high* processing (Figure 6 and Figure 9). Nevertheless, this clearly illustrates the impact of high performance image observation measurements on the final result. Note that the ICC approach using the 12 Ebner parameters for each image quadrant in this case seems to be less effective than for the phase 2 data set. This can clearly be seen for the *DMC low* configuration.

As already mentioned **IPI** also repeated two processing versions, already used for the phase 2 data: The non self-calibration case and the case based on the BLUH specific 12 additional parameters. Those two variants can be directly compared to their corresponding results. Again compare the phase 2 results in Figure 5 and Figure 6 to the phase 2b results in Figure 8 and Figure 9. Both results are more consistent (compared to the previous findings from ICC) although smaller differences are also visible. Unfortunately the detailed a priori weight settings for the IPI phase 2 evaluations have not been reported. The two other IPI versions then take care of the DMC specific camera geometry. The additional parameter models obviously have been modified in BLUH since phase 2 evaluations. One version introduces additional parameters individually estimated for each virtual image quadrant (version P12-iDMC). Those parameters are different to the ones used in phase 2. The parameters (numbered 30-41, 74-77) are as follows: 4 additional parameters for DMC synchronization, 8 parameters for DMC perspective deformation of individual cameras and 4 parameters for

DMC radial symmetric distortion of original images, in addition to the standard 12 BLUH parameters. The new approach only uses two additional DMC parameters which are commonly estimated for all camera heads (image quadrants). They model the common viewing angle and the common effect of radial symmetric distortions for all four camera heads together (version P12-cDMC). For the *DMC low* configuration the use of DMC specific additional parameters is not of significant influence, which is different for the *DMC high* configuration where a certain although relatively small accuracy increase is visible when using the DMC specific correction terms.

A quite significant accuracy decrease in the east component for the *DMC high* data in phase 2b, which is visible for all cases that did not use any additional parameters, must to be mentioned. For the IPI processing even the use of the 12 BLUH parameters is not sufficient to fully compensate for this effect. With the additional individual DMC specific parameters the obtained east and north component accuracy is almost similar. If you compare the ICC evaluations, this effect is not visible at all, similar to the ETH results. More details on the IPI results and the report on phase 2b from participant are given in B.2.8 and C.9 (page 161).

CSIRO only uses the non self-calibration configuration and only participated in the phase 2b. They used an in-house bundle program for their processing, which so far has no additional self-calibration models implemented. CSIRO also provides a result based on the common adjustment of both flying heights. If one compares the results here to the non self-calibration cases from other participants, they are of the same accuracy. As already mentioned, the systematic effect in the x-coordinate of *DMC high* block configuration is clearly seen. Also see the detailed statistics (B.2.9) and participant report (C.10, page 172).

The **ETH** processing of phase 2b DMC data follows the ICC methodology. They also introduced existing mathematical self-calibration models estimated separately from observations from each individual image quadrant. The quadrants are defined in such a way that they have certain overlaps (buffers) of, in this case, 15 pix. Results when using 12 Ebner parameters or 44 Grün parameters per quadrant are compared to the non self-calibration case from ETH, or the corresponding results from ICC evaluations. Still, the different a priori weightings, as given in the detailed listing in B.2.10 have to be taken into account.

Finally the results from manufacturers processing are presented. **IngrZI** provided results from two different evaluations obtained by the Intergraph headquarters in Aalen and Huntsville, version v1 and v2 respectively. In principle both used the same software and methodology, i.e. the non self-calibrating case is compared to the case where the 12 Ebner parameters are introduced for the whole image only. Nevertheless, the assumptions on the a priori weightings are slightly different as one can see from section B.2.11. This of course is of influence on the results. Also note the submitted report which relates to the results from version v2 (C.11, page 174). Again it is interesting to compare phase 2b results to the previously discussed results from phase 2. Comparing the corresponding Figure 5 and Figure 8 for the results from *DMC low* and Figure 6 and Figure 9 for *DMC high* clear differences became obvious. For the evaluation of *DMC high* the accuracy of the east component in phase 2b is significantly worse (this general effect was mentioned before), although the accuracy in the vertical component seems to be slightly better. For *DMC low* the behaviour is the other way round. Here the vertical accuracy is significantly worse compared to the phase 2 processing. The horizontal accuracy is almost comparable.

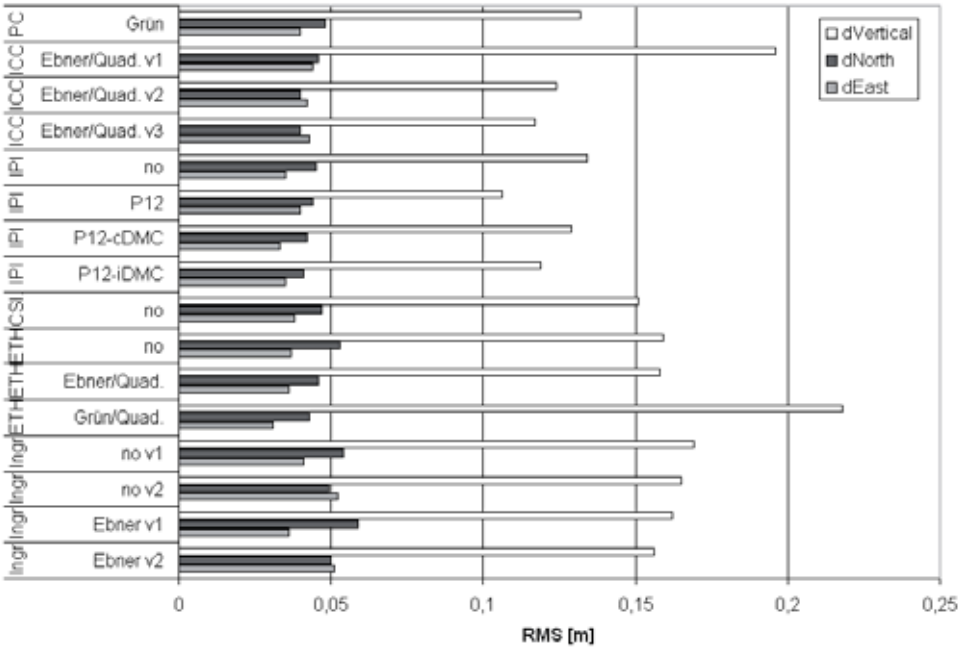

Figure 8, *DMC low* (phase 2b) accuracy (RMS)

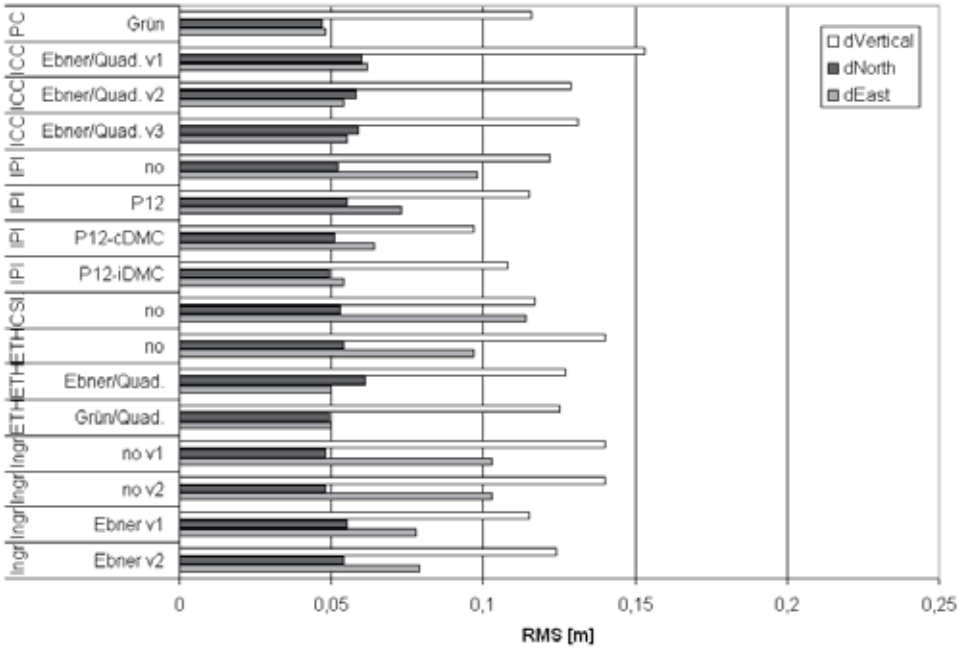

Figure 9, *DMC high* (phase 2b) accuracy (RMS)

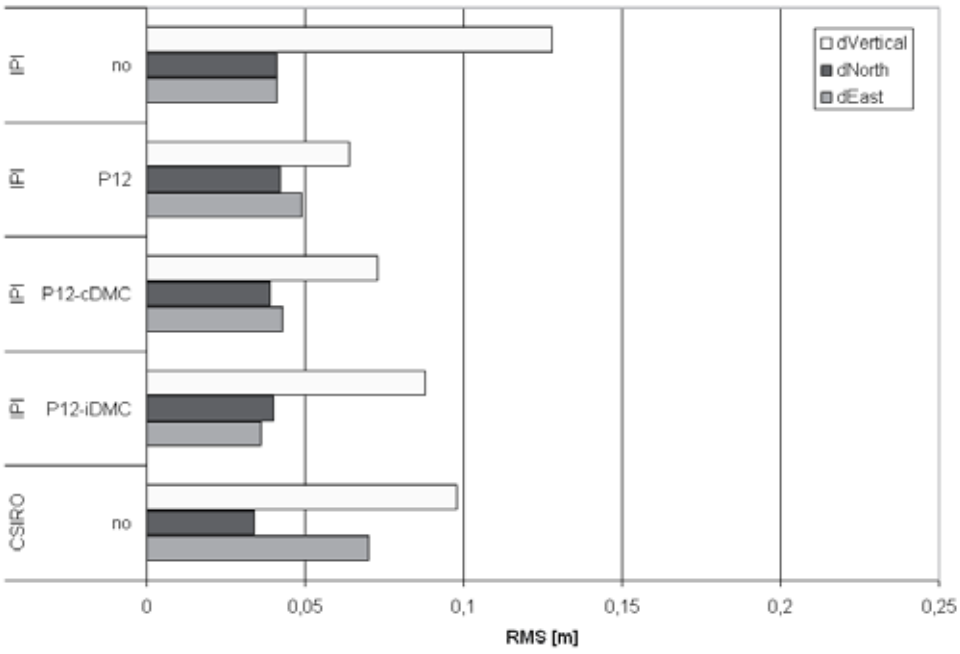

Figure 10, *DMC both* (phase 2b) accuracy (RMS)

For the DMC phase 2b data only IPI provided different results for the combined adjustment of *DMC low* and *DMC high* blocks. They are presented in Figure 10. The CSIRO results were only provided without self-calibration. Comparing the results of the combined adjustment to the separate handling of blocks the accuracy obtained is obviously higher, especially for the vertical coordinate component. A smaller improvement is also visible for the horizontal components, at least for the IPI results. Note that the systematic effect in the x-coordinate is still visible for the CSIRO case but not for the IPI versions, although this effect is present for IPI *DMC high* as well. In general the results from the combined adjustments lead to the conclusion that the overall block geometry is more stable and consistent if both blocks are adjusted in parallel. This obviously is enforced by the lack of GPS perspective centre observations.

To finally put together the findings from phase 2b DMC data processing: The results from this processing, where all participants used the same set of image coordinates clearly showed the role of different parameter sets for self-calibration overlaid by the effects from individual weighting of observations. Obviously the influence of observation weighting in some cases even exceeds the influence of different self-calibration models. Nevertheless, it is hard to recommend an optimal method of DMC data processing. This especially becomes obvious, when the results from the phase 2 and phase 2b are compared to each other. This is especially visible from the different ICC evaluations. This proves that the quality and also distribution of image point observations is of influence on the final accuracy. In general one has the feeling the phase 2b data set *DMC low* is of less accuracy than the phase 2 evaluation of most of the participants. This might only be due to the different image observations. This situation is slightly different for the *DMC high* block. Here one has the impression that

results from phase 2b are of better accuracy. This at least is the case for the vertical component; the east coordinate on the other hand is worse, since influenced by the previously mentioned systematic effect. When finally comparing the absolute accuracy from check point analysis to the nominal GSD for the two different blocks (*DMC low*: 0.1m, *DMC high*: 0.18m) the performance is fairly well within the 1/2 pix range for the horizontal for both phases (although slightly worse for the east component in phase 2b *DMC high*). With the height component the sub-pixel accuracy could only be achieved in *DMC high* (phase 2b) and most of the phase 2 evaluations (*DMC low* and *DMC high*). With the image observations from phase 2b *DMC low* the vertical accuracy is above one pixel in all cases. This proves that the final accuracy cannot only be attributed to the camera alone, the observations themselves also play a major role!

3.2.3 UCD results from participants

Within this section the results from UCD evaluations are presented. As mentioned before, seven different institutions participated in the processing of UCD data. CSIRO and IPI participated in both phase 2 and phase 2b. These two were also the only ones, who both looked at the flights combined and separately. Inpho provided results from common adjustment of both UCD flying heights only. UoN, itacyl and inpho participated in phase 2, ETH and Vexcel provided results for phase 2b only. Itacyl only focused on the processing of *UCD low* flight.

The phase 2 processing – similar to the DMC data evaluations – are based on the individual image coordinate measurements from each participant, whereas the phase 2b results presented below all use the pre-defined image coordinates measured and distributed through the pilot centre. As for all the other test data most participants provided results from different versions to be evaluated at the pilot centre. UoN used the standard Brown parameters and a proprietary (IESSG) approach for self-calibration, but also provided a non self-calibration version. Itacyl only provided a non self-calibration case, but with the use of GPS offset and drift parameters. They "prefer to avoid using autocorrelation parameters, because the ones included in Match-AT are specific for film cameras". Nevertheless, as results from other evaluations showed, self-calibration is certainly of positive influence on the object point accuracy, even when the parameter sets originally designed for film-based single optic systems are used. The inpho results were based on Grün and Brown parameter models, but estimated from simultaneous adjustment of both flights. IPI has considered the block in both ways: separate and combined. Some more details are described below.

UCD phase 2 results

itacyl only provided results from the *UCD low* block. They themselves declare their results as preliminary only. The processing was based on the automatic tie point transfer and AT from using the Match-AT software package. GPS perspective centre coordinates were introduced with additional offset and drift parameters to correct for expected systematic errors due to baseline length. No self-calibration parameters were applied. Obviously automatic tie point transfer between images from both flying heights was also successfully done, but such results have not been reported to the pilot centre. The accuracy from check

point analyses is given in B.3.1 (page 69), and the itacyl report can be found in C.12 (page 190).

Both flying heights were considered within one AT in the **inpho** processing. The AT results were done using two different bundle adjustment packages Match-AT and InBlock. In both AT packages the Match-AT tie points have been used. Additionally the GPS drift corrections are applied. InBlock was used for the estimation of Brown additional parameters; Match-AT only allows for the polynomial correction models (here the Grün model was introduced). For comparison one version without the use of self-calibration parameters was also processed. The following Figure 11 illustrates the remaining residuals in image space for the non self-calibration case compared to the use of the Grün correction model. The decrease in residuals is obvious. Some more details from inpho related to their own processing can be found in the short report which was already cited in the context of DMC evaluations (C.5, page 132). The statistics of check point differences are given in B.3.2 (page 69). Inpho also mentioned that the influence of additional self-calibration is more significant for UCD compared to their results from the DMC data set. It should also be mentioned that the influence of self-calibration models is converted to a correction grid, which then can be used for all later production steps.

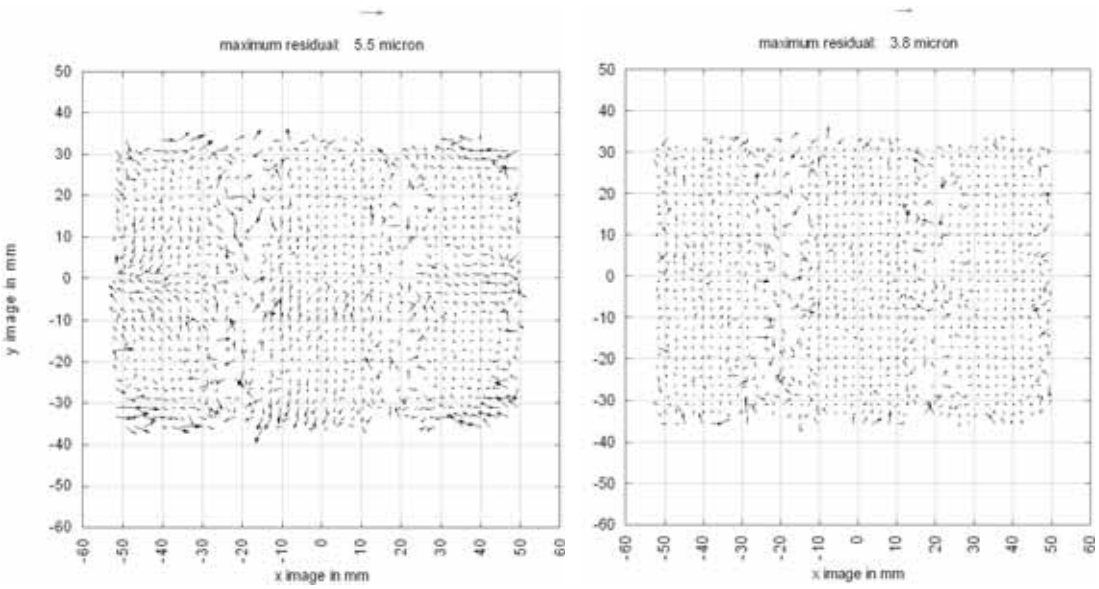

Figure 11, Remaining image residuals in *UCD both* block: no self-calibration (left), using additional Grün parameters (right) (© inpho, 2006)

The UCD results from **CSIRO** are again based on their own software developments. All points were measured manually; tie points were only introduced in case an insufficient number of control and check points was available per model. No additional self-calibration parameters were estimated but, as already done during the DMC processing the image blocks were triangulated as single blocks as well as in a combined way. Different block configurations were tested, i.e. with or without use of the cross-strip from *UCD low*. Some more

details on the block configurations can be seen from the CSIRO report in C.13 (page 194). The full statistics of check point analyses are given in B.3.3 (page 70).

Extensive evaluations were also done by **IPI**. Based on the BLUH bundle adjustment program special sets of additional parameters designed for the UCD imaging geometry were introduced. These additional parameters (numbered 42 - 73 in BLUH) take care of the scale, shift in x/y and rotation of each of the 9 individual CCD arrays used in the four different focal planes. These UCD specific parameters were combined with the 12 standard BLUH parameters. The following Figure 12 shows the effect of using the 12 standard BLUH parameters and then additionally adding the UCD specific parameters compared to the non self-calibrating case. The example is taken from the processing where both blocks *UCD low* and *UCD high* were used in a combined adjustment. As one can clearly see there is a decrease in image residuals visible. The RMS values change from 1µm (no self-calibration), 0.8µm (using standard 12 BLUH parameters only) to finally 0.6µm (all parameters used for self-calibration).

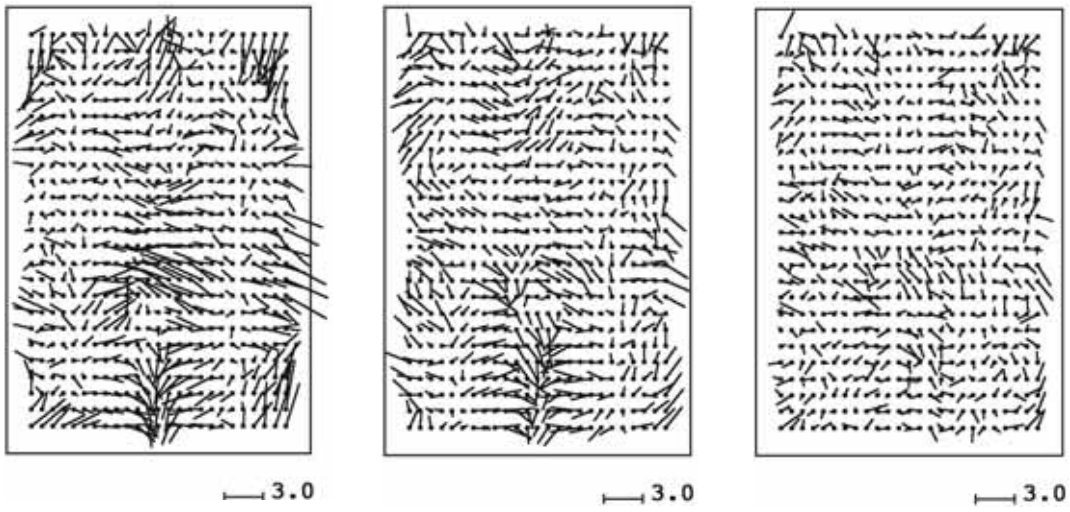

Figure 12, Influence of additional parameters in image space for *UCD both* block: no self-calibration case (left), using 12 BLUH standard parameters (middle), using all parameters including UCD specific terms (right) (© IPI, 2006)

The statistics from check point analyses are given in B.3.4 (page 71). It has to be mentioned that in this case the accuracy numbers have not been calculated by the pilot centre but by IPI itself. Since IPI was already involved in one of the former EuroSDR/OEEPE test, where the Frederikstad test site was used, accuracy was obtained from the check point coordinates already available from the former tests. This is mentioned in the extensive reports from IPI (see C.14, page 199). Additionally note that the accuracy given by IPI is the standard deviation (std.dev.), whereas in all other cases the RMS and mean values have been delivered through the pilot centre evaluation. Thus no direct comparison to the results from other participants are possible, at least they have to be done carefully, since RMS and std.dev. values are different especially when differences from check point analyses show constant offsets.

UoN also focused on the processing of the UCD data sets. Both flying heights were treated as separate blocks. The results are all based on LPS for tie point matching and ORIMA for bundle adjustment. The non calibration case is compared to the self-calibration adjustment using the Brown parameter model. As a third version an own approach is presented (called IESSG approach), where systematic residuals are identified and quantified after bundle adjustment and then directly corrected to image coordinates. After that the bundle adjustment is repeated using these corrected image coordinates but now no additional self-calibration parameters are used. From UoN's point of view this approach is advantageous because

- it can be applied to any multi-lens camera system with little or no change to the method;
- it only requires some post processing software to analyse the residuals not a change to existing aerial triangulation software;
- it can consider systematic effects on image coordinates from any sources and not just those dependent on modelling optical geometry.

More details on this IESSG method and the processing itself are given in the UoN report (see C.15, page 231). The statistics from check point analyses are listed in B.3.5 (page 73).

The above participant results are all summarized in Figure 13 (*UCD low* block, GSD 17cm), Figure 14 (*UCD high* block, GSD 34cm) and Figure 15 (*UCD both*, both blocks considered in one adjustment). The results from the pilot centre (PC) are also included, although those results are always based on the use of all available control points for an optimal determination of the introduced Grün parameters. Thus comparison with the others is not directly possible. The results from the PC somewhat reflect the maximum accuracy potential assuming that the applied set of self-calibration parameters is also the optimal one. Whether this is the case for the Grün parameters used in the PC evaluations cannot be answered. Additionally keep in mind that for IPI evaluations the standard deviations already determined from IPI itself are plotted. In all other cases the error bars reflect the RMS values.

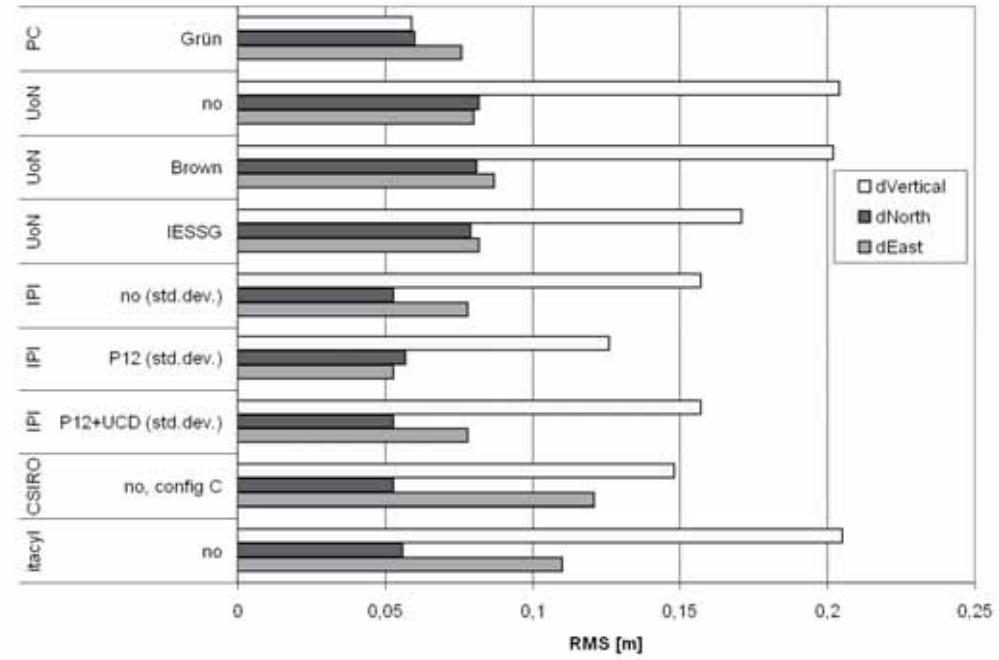

Figure 13, Accuracy (RMS) of participants results *UCD low* (phase 2)

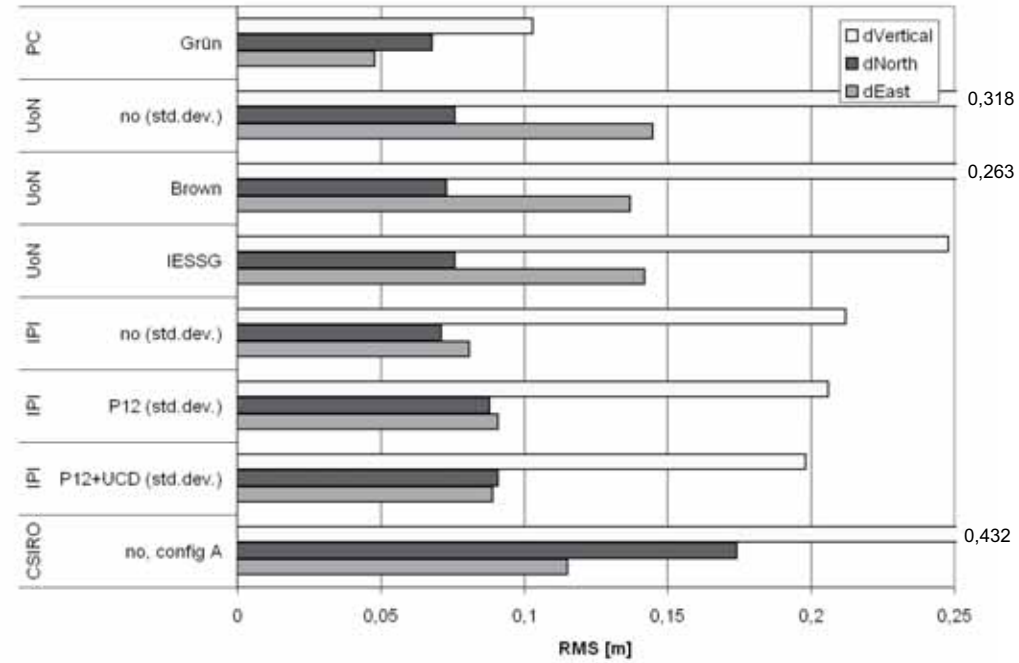

Figure 14, *UCD high* (phase 2) accuracy (RMS)

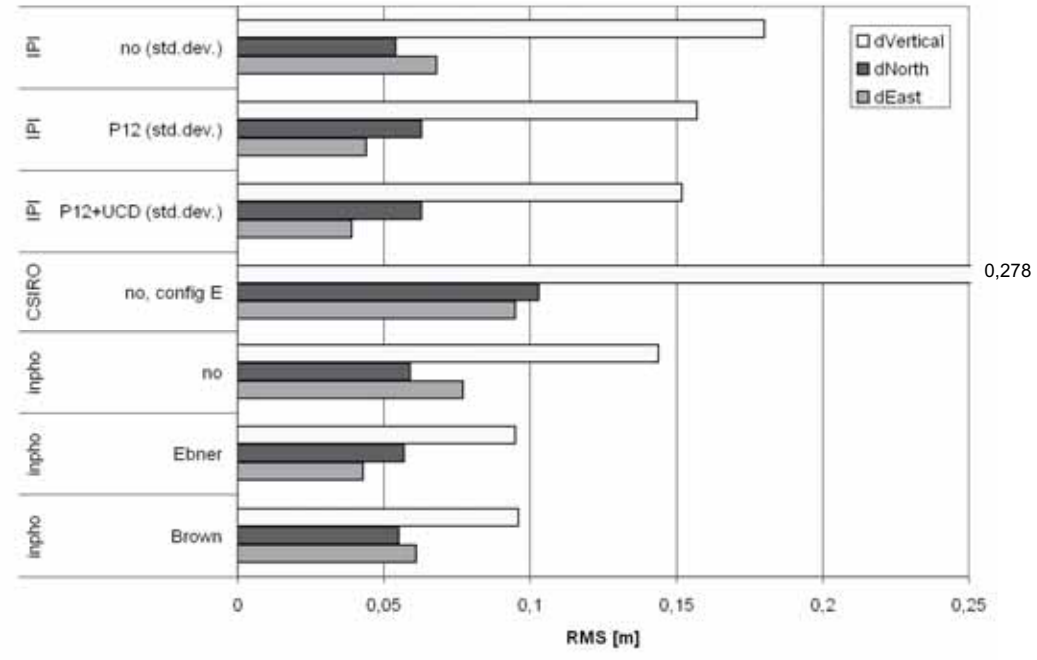

Figure 15, *UCD both* (phase 2) accuracy (RMS)

Comparing the different results some larger variations are obvious although principally all participants evaluated the same two UCD image blocks and had access to the same set of control points. This should be expected due to different image point observables and different software and adjustment models used. Additionally the different weightings and the handling of the GPS observations are of influence. One also can see the influence of self-calibration, which typically refines the accuracy in the vertical component. The influence of self-calibration in horizontal accuracy is not so obvious. Still it seems to be difficult to compare between the self-calibrating cases from different participants. The accuracy achieved is still quite different in some cases. If one calculates a mean accuracy from all self-calibration evaluations (assuming that the IPI standard deviations are similar to the expected RMS values) the following values are obtained for the *UCD low* block: 7.5cm (RMS_X), 6.6cm (RMS_Y) and 14.3cm (RMS_Z). This accuracy corresponds to better than 1/2 pix GSD in horizontal and better than 1 pix (0.8 GSD) in vertical axes. For the *UCD high* block the mean accuracy from self-calibrating cases is as follows: 10.1cm (RMS_X), 7.9cm (RMS_Y) and 20.4cm (RMS_Z). Again the corresponding GSD related values are about 1/4 – 1/3 pix in horizontal and 2/3 pix in vertical. It is interesting to see, that the object accuracy related to GSD is higher for the *UCD high* block, although this block only consists of two parallel flight lines without additional cross strips. Potential errors in the precise definition of signalized object points in imagery, caused by the non optimal image radiometry for UCD flights, might be one factor for the relatively higher accuracy from *UCD high* compared to *UCD low*. If the two blocks are considered in the same adjustment the accuracy is better than the accuracy values from the individual block analyses. The mean accuracy from the self-calibration cases for *UCD both* is about 4.5cm (RMS_X), 5.0cm (RMS_Y) and 11.3cm (RMS_Z). Thus common observations from *UCD high* and *UCD low* are of positive influence on the

overall block stability and performance. This combined adjustment of both blocks finally reaches the highest accuracy, which again shows the positive influence of multiple overlapping images. Similar effects already have been shown for the DMC evaluations.

UCD phase 2b results

Similar to the processing of DMC data, a second phase 2b was additionally introduced for the UCD processing, where pre-defined sets of image coordinates delivered by the pilot centre were distributed to participants. Thus all evaluations were based on the same set of image observations. CSIRO and IPI contributed to both phases, where ETH and Vexcel only provided results for the phase 2b data sets.

The **CSIRO** processing was based on the same configurations already used for the phase 2 evaluations, i.e. different configurations with/without use of the cross strip and separate or combined adjustment of both blocks. Unfortunately CSIRO did not explicitly mention the weights used for their observations in AT. Only non self-calibration cases have been done. The statistics from check point analyses are given in B.3.6 (page 74) and the corresponding report can be seen in C.16 (page 247).

The **IPI** configurations applied for phase 2b are also similar to the phase 2 processing. The following three cases are used for each block separately and then for the common adjustment of both blocks: (1) no self-calibration, (2) self-calibration using the standard BLUH 12 parameter and (3) self-calibration based on standard 12 BLUH parameters in addition to the Ultracam specific parameters 42-73. The a priori weightings for the observations for the IPI evaluations were 2µm for image coordinates and 2cm for object coordinates for all cases, except for the vertical component in the combined adjustment of both blocks. Here the accuracy of object point height was assumed to be 4cm. The statistics of check point differences are presented in B.3.7 (page 76) and the corresponding IPI report can be found in C.17 (page 251). From IPIs findings the use of UCD specific parameters is necessary if one looks at the influence on image coordinate residuals, although their effect is not clearly seen in the results from check point differences.

During the evaluation from **ETH** different options for the weighting of observations and also different methods for the self-calibration were tried. Finally nine different versions for each of the UCD low and UCD high block were tested during the processing phase. Not all variants were successful. Finally the analyses were focused on the non self-calibration case, the standard self-calibration case based on 44 Grün parameters used for the whole image and then two different methods trying to model the UCD specific sensor geometry. Here the 12 Ebner or 44 Grün parameters are introduced separately for each of the nine image patches forming the virtual large format UCD image. A small 15 pixel buffer between the neighbouring image patches is present. The a priori weights are 3µm for image observations and 2cm of object coordinates in all cases. No common adjustment of both blocks was done by ETH. The statistics of check point differences are presented in B.3.8 (page 78). Unfortunately no ETH report explaining some more details of their UCD evaluations was made available.

Finally the UCD system provider **Vexcel** also provided results for the phase 2b analyses. The statistics are displayed in B.3.9 (page 80). Unfortunately, the individual observation weights and applied self-calibration terms used have not been documented. There is no report

available. But it was confirmed that self-calibration was applied for processing. The two blocks were adjusted separately.

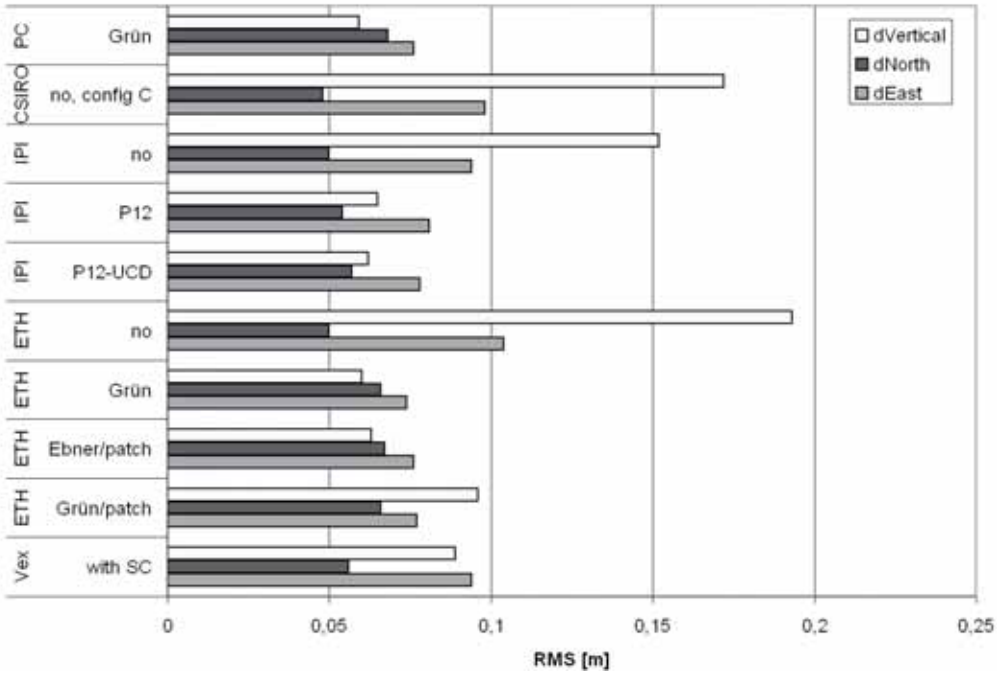

Figure 16, *UCD low* (phase 2b) accuracy (RMS)

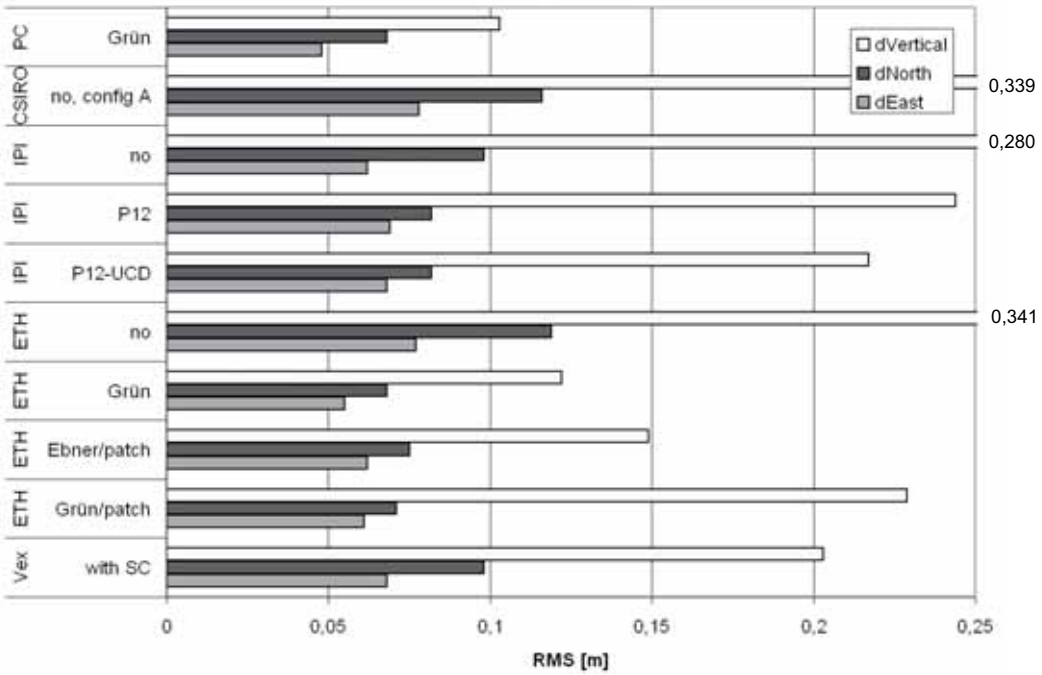

Figure 17, *UCD high* (phase 2b) accuracy (RMS)

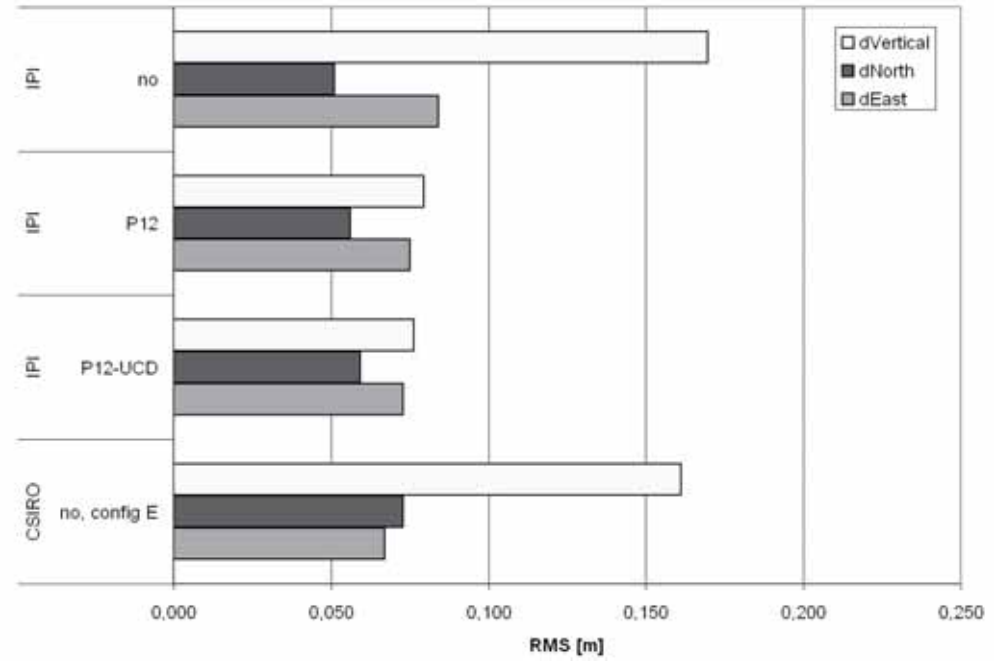

Figure 18, *UCD both* (phase 2b) accuracy (RMS)

Figure 16, Figure 17 and Figure 18 now compare the previously described results from different approaches for UCD phase 2b data processing. Since in phase 2b all evaluations were based on the same set of image coordinates, variations in RMS values are only due to the different adjustment models and observations weights. As one can see for all configurations the use of additional parameters increases the accuracy. This is especially obvious for the height component. If one focuses on the IPI evaluations the use of the 12 standard BLUH parameters (P12) is almost sufficient for the *UCD low* and *UCD both* configurations but performs worse in case of the *UCD high* block. The addition of UCD specific parameters does not significantly increase the performance, except for the *UCD high* block. Similar trends can be seen from the ETH evaluations. Here also additional parameter sets were introduced for each of the nine UCD image patches separately, but here, different to the IPI processing, the "standard" Grün and Ebner parameters were used. From ETH results this approach does not really improve the overall accuracy. For the *UCD high* block the accuracy even decreases. In addition to the UCD specific corrections terms, in this case the use of 44 Grün parameters seem to perform reasonably. This model was also used by the pilot centre (PC). Especially for the *UCD high* block this approach obtains best results, still keeping in mind that the accuracy numbers are always influenced by the slightly different observations weights as chosen by individual participants. If one computes the mean RMS values from all the versions using self-calibration the accuracy numbers obtained are as follows: For the *UCD low* block mean RMS values are RMS_X=7.9cm, RMS_Y=6.2cm and RMS_Z=7.1cm which corresponds to better than 1/2 pix in x- and y-component. The vertical components relate to the same accuracy range. For the *UCD high* block the numbers are as follows: RMS_X=6.2cm, RMS_Y=7.8cm and RMS_Z=18.1cm. In this case the GSD related values are about 1/5 pix in horizontal and about 1/2 pix in vertical axis. Here especially the accuracy obtained in the horizontal component is quite high. It is also interesting to see that the results from the *UCD both* combined block configuration are almost similar to the *UCD low* block.

4 Summary and conclusion

The previous section 3 tried to illustrate the detailed results from individual evaluations obtained by test participants. Even though the descriptions and analyses are amended by the detailed statistics in Appendix B and the participants reports in Appendix C (if available), only an overview on the comprehensive findings of this project was possible, due to the complexity of data material and software used. Nevertheless, the most important facts obtained are summarized below.

Self-calibration is obviously necessary to improve the quality of object point determination for all three tested camera systems ADS, DMC and UCD. With self-calibrating aerial triangulation for the ADS flight the horizontal accuracy is in the range of 1/5 pix and the vertical accuracy in the range of 1/3 pix. For DMC the accuracy is about 1/4 – 1/2 pix and 1/2 – 1 pix for horizontal and vertical components respectively. And finally in the case of UCD the resulting accuracy is about 1/4 – 1/3 pix horizontal and 1/3 – 1 pix for vertical component. Again note, these values are obtained from these three empirical test data sets only and are always dependent on the applied mathematical model. Each block has its own geometry. Furthermore the version of processing software also including the sensor providers' software used for image pre-processing (like image stitching for UCD and DMC frame

based sensors) is of concern. Since the time of data acquisition and preparation there has been some considerable refinement in those sensor related software packages. Additionally, in the case of UCD and DMC the radiometric quality might also be of influence on the obtained accuracy. Thus these numbers cannot be transferred to other current projects in general but have to be verified from additional investigations.

The accuracy increase obtained in object point determination using self-calibration is higher for DMC and UCD compared to ADS. Additionally, the systematic corrections for UCD are more significant compared to DMC.

In some cases specially designed self-calibration parameter sets adapted to sensor geometry are necessary. For ADS the standard model based on Brown parameters is sufficient. For the frame based systems DMC and UCD extended or modified self-calibration models had been used. Alternatively high order correction polynomials like the 44 parameter Grün model in some cases also led to the most accurate results. The use of only 12 additional parameters like Ebner or the BLUH standard parameters seems not to be sufficient to compensate for the systematic errors in the hereby analysed data sets.

Besides the self-calibration model the a priori weighting of observations is of larger influence. In some case the choice of weighting factors even exceeds the influence of the self-calibration model applied.

It is quite interesting to see that all three system manufacturers that participated in this project looked into more detail in their software processing again to overcome or minimize the need for self-calibration methods. Their refinements are already published (see above). These system refinements were surely pushed by investigations such as this EuroSDR project.

5 Outlook

When this EuroSDR Camera Calibration and Validation network was initiated originally radiometric aspects and other sensor formats like medium-format based systems should also have been covered, but only the geometry has been treated here. Thus EuroSDR designed two follow-up projects that now cover those aspects that have not been treated in the Digital Camera Calibration and Validation initiative and additionally adds a further initiative now focusing on the legal aspects of system calibration and certification.

5.1 Medium format digital cameras

The first more technology oriented project was launched in autumn 2007 and deals with the *geometric and radiometric performance of digital medium format cameras*. Currently considerable developments in medium format cameras are obvious (several systems providing up to 39Mpix resolution like IGI dIGIcam, Rollei AIC, DiMAC, Applanix DSS and others). Such cameras will play a growing future role in the photogrammetric market and also might become of interest for the national mapping agencies. Formerly used as single

head sensor only, quite often parallel to airborne lidar systems, later developments are based on multi-head (dual-head or quaddro-head design) configurations, which at least in case of image size and ground coverage may fully compete with the "traditional" large format systems, covered in this study. A first project report reflecting this current situation and first remarks on their accuracy potential is already available (Grenzdörffer 2008).

5.2 Radiometric performance of digital cameras

In addition, a second EuroSDR project focusing on the *radiometric performance of large format digital cameras* was started in spring 2008. This activity should also investigate the influence of pan-sharpening, which is often used in processing of large format sensor image data. The first phase of the project is a theoretical evaluation of the radiometric aspects of geomatic (spaceborne, airborne, photogrammetric large-format, medium-format, hyperspectral, etc.) imaging. The task will be accomplished through a literature research and a query for various interest groups dealing with image radiometry (sensor manufacturers, image producers and image users). In the second more practically oriented phase the individual radiometric sensor performance will be evaluated from true flight data.

5.3 European digital airborne camera certification (EuroDAC²)

The most important EuroSDR decision was to officially instigate a project to take forward the issue of *European Digital Airborne Camera Certification – EuroDAC²* by EuroSDR. The coordination is between the European National Mapping and Cadastre Agencies (NMCAs) while cooperating closely with all relevant digital airborne mapping camera suppliers and other experts. The initiative will lead to a European wide accepted certification procedure substituting the traditional analogue mapping camera certification. Based on the experience and network discussions from the former and still ongoing more technically oriented EuroSDR projects this EuroDAC² initiative is the somewhat logical continuation.

The certification of new digital camera systems is a hot issue worldwide today. Many of those activities are driven by existing and ongoing projects like the quality assurance plan developed by the US Geological Survey USGS. Close co-operation has already been established between EuroSDR and USGS to align both concepts as much as possible. The latest details on these initiatives are published in Cramer (2008) and Stensaas & Lee (2008).

6 Acknowledgments

The author would like to acknowledge all members of the EuroSDR Digital Camera Network for their continuous support and fruitful discussions. Special thanks has to be expressed to all people and institutions actively involved in the empirical phase 2 evaluations. Without their contributions the results of this project would not have been possible. The author would also like to thank the system suppliers Leica Geosystems, Intergraph/ZI-Imaging and Microsoft/Vexcel for supporting this project and the companies TerraTec (Norway) and IFMS-Pasewalk (Germany) for data provision. Special thanks finally has to be expressed to Werner

Schneider who did most of the data handling and preparation and was also responsible for all the tedious and time consuming image measurements and final accuracy checks!

7 References

Ackermann, F. (1996): Experimental Tests on Fast Ambiguity Solutions For Airborne Kinematic GPS Positioning, in: 'International Archives of Photogrammetry and Remote Sensing', Vol. 31/6, ISPRS Congress Vienna, pp. 1-6.

Cramer, M. (2004): The EuroSDR network on digital camera calibration, Report Phase 1 (Status, Oct. 16, 2004), digitally available at http://www.ifp.uni-stuttgart.de/eurosdr/EuroSDR-Phase1-report.pdf, 53 pages.

Cramer, M. (2005): 10 Years ifp test site Vaihingen/Enz – an independent performance study, in Fritsch (ed.): Photogrammetric Week 05, pp. 79-92, Wichmann Verlag, Karlsruhe, also digitally available at http://www.ifp.uni-stuttgart.de/publications/phowo05/120cramer.pdf

Cramer, M. (2008): The EuroSDR Approach on Digital Airborne Camera Calibration and Certification, International Archives of Photogrammetry and Remote Sensing IAPRS 27(B4), pp. 1753-1758, Proceedings 21. ISPRS Congress, Beijing 2008, digitally published on CD, 6 pages.

Dörstel, C. (2007): DMC- (R)evolution on geometric accuracy, in Fritsch (ed.): Photogrammetric Week 07, pp. 81-88, Wichmann Verlag, Karlsruhe, also digitally available at http://www.ifp.uni-stuttgart.de/publications/phowo07/110Doerstel.pdf.

Grenzdörffer, G. (2008): Medium format digital cameras - a EuroSDR project, International Archives of Photogrammetry and Remote Sensing IAPRS 27(B1), pp. 1043-1050, Proceedings 21. ISPRS Congress, Beijing 2008, digitally published on CD, 8 pages.

Gruber, M. & Ladstädter, R. (2008): Calibrating the digital large format aerial camera UltraCamX, Proc. International Calibration and Orientation Workshop (EuroCOW) 2008, Castelldefels, Spain, digitally available on CD-ROM, 8 pages.

Grün, A. & Zhang, L. (2003): Sensor Modeling for Aerial Triangulation with Three-Line-Scanner (TLS) Imagery. Journal of Photogrammetrie, Fernerkundung, Geoinformation, 2/2003, pp. 85-98.

Hefele, J. (2006): Calibration experience with the DMC, International Calibration and Orientation Workshop EuroCOW 2006, 25 - 27 January 2006, Castelldefels, Spain, Digitally published on CD, 6 pages.

Heipke, C., Jacobsen, K. & Wegmann, H. (2002): Integrated sensor orientation: Test report and workshop proceedings, OEEPE Official publication No. 43 (accessible from www.eurosdr.net), 302 pages.

Honkavaara, E., Jaakkola, J., Markelin, L., Nurminen, K. & Ahokas, E. (2006): Theoretical and empirical evaluation of geometric performance of multi-head large format photogrammetric sensors, International Archives of Photogrammetry and Remote Sensing IAPRS, 36(A1), ISPRS Commission I Symposium, Paris 2006, digitally published on CD, 6 pages.

Jacobsen, K. (2007): Geometry of digital frame cameras, ASPRS 2007 annual conference, Tampa, Florida, US, May 7-11, 2007, digitally published on CD, 12 pages.

Kocaman, S., Zhang, L. & Grün, A. (2006): Self-calibrating triangulation of airborne linear CCD cameras. International Calibration and Orientation Workshop EuroCOW 2006, 25 - 27 January 2006, Castelldefels, Spain, Digitally published on CD, 6 pages.

Scholten, F., Gwinner, G. & Wewel, F. (2002): Angewandte Digitale Photogrammetrie mit der HRSC, Photogrammetrie-Fernerkundung-Geoinformation, 5, Schweizenbarth'sche Verlagsbuchhandlung, Stuttgart, pp. 317-332.

Stensaas, G. & Lee, G. (2008), Driving toward a worldwide acceptance procedure for digital airborne sensors, International Archives of Photogrammetry and Remote Sensing IAPRS 27(B1), pp. 561-566, Proceedings 21. ISPRS Congress, Beijing 2008, digitally published on CD, 6 pages.

Tempelmann, U., Hinsken, L. & Recke, U. (2003): ADS40 calibration and verification process, in Grün/Kahmen (eds.): Proceedings on Optical 3-D Measurement Techniques VI, Zürich, Switzerland, pp. 48-54.

Tempelmann, U. & Hinsken, L. (2007): Hardware improvements of the ADS40 sensor heads SH51/52 and how they allow a better camera model for self calibration, in Grün/Kahmen (eds.): Proceedings on Optical 3-D Measurement Techniques VIII, Zürich, Switzerland, pp. 187-193.

A Members of the EuroSDR Digital Camera Calibration network

Status: July 2007

#	Organization	Network member(s)
System providers		
I.1	ADS 40, Leica Geosystems	U. Tempelmann, P. Fricker, Dr. U. Beisl, Dr. G. Ferrano
I.2	DMC, Intergraph/ZI-Imaging	C. Dörstel, Dr. M. Madani
I.3	Ultracam, Microsoft/Vexcel	Dr. M. Gruber
I.4	DIMAC, Dimac Systems	P. Louis, J. Losseau
I.5	DSS, Applanix Corp.	Dr. M. Mostafa
I.6	Starimager, Starlabo Corp.	Dr. K. Tsuno
I.7	3-DAS-1, Wherli & Ass. Inc.	Dr. H. Wherli
I.8	DigiCAM, IGI mbh	Dr. J. Kremer, M. Müller
Industry & other software developers		
II.1	ISTAR	Dr. P. Nonin
II.2	GEOSYS Technology Solutions	Dr. B. Ameri
II.3	Vito	Mr. J. Everaerts
II.4	Optical Metrology Centre	Dr. T. Clarke
II.5	ORIMA	Dr. L. Hinsken
II.6	inpho	T. Heuchel
II.7	DLR Oberpfaffenhofen	Prof. M. Schroeder, Dr. P. Reinartz, Dr. R. Müller, Dr. M. Lehner
II.8	DLR Berlin	F. Scholten, K. Gwinner
II.9	dgap	D. Stallmann
II.10	CSIRO	X. Wu
II.11	stereocarto	T. F. de Sevilla Riaza
II.12	Geosense Ltd.	A. Clarence
University		
III.1	Ohio State University	Prof. T. Schenk, Prof. D. Merchant
III.2	ETH Zürich	Prof. A. Grün, Dr. M. Baltsavias, S. Kocaman, H. Eisenbeiss, J. A. Parian
III.3	University of Glasgow	Prof. G. Petrie
III.4	University of Rostock	Dr. G. Grenzdörffer
III.5	University of Stuttgart	Dr. N. Haala, Dr. M. Cramer
III.6	University of Hannover	Prof. C. Heipke, Dr. K. Jacobsen
III.7	Humboldt University Berlin	Prof. R. Reulke
III.8	University of Applied Sciences Stuttgart	Prof. E. Gülch
III.9	University of Applied Sciences Anhalt	Prof. H. Ziemann
III.10	Institute de Geomatica Castelldefels	Dr. I. Colomina
III.11	Norwegian University of Life Sciences	Dr. I. Maalen-Johansen
III.12	University of Nottingham	Dr. M. Smith
III.13	University of Pavia	Prof. V. Casella, Dr. M. Franzini
III.14	University of Leon	B. A. Pérez
III.15	University of Hamburg	Prof. H. Spitzer

#	Organization	Network member(s)
National mapping agencies & other authorities		
IV.1	Swedish Land Survey	Dr. D. Klang, D. Akerman
IV.2	Finnish Geodetic Institute	Prof. R. Kuittinen, Prof. J. Hyyppä
IV.3	British Ordnance Survey	P. Marshall
IV.4	Swisstopo – Landestopographie, Suisse	Dr. A. Streilein, Dr. S. Bovet
IV.5	US Geological Survey	G. Stensaas, Dr. G. Y. G. Lee, J. Christopherson
IV.6	ICC Barcelona	Dr. J. Talaya, R. Alamus
IV.7	IGN France	Dr. M. Deseilligny
IV.8	Bundesamt für Eich- und Vermessungswesen, Austria	M. Franzen
IV.9	Instituto Cartográfico Valenciano	R. Fernández
IV.10	ITACyL - Junta de Castila y León	D. A. Nafría
IV.11	Bayrisches Landesamt für Vermessung	W. Stößel
IV.12	Institut Géographique National, Belgium	J. Théatre, S. Roovers

B Detailed statistics for participants results

Reference coordinate of check point	$\underline{x}_i^{GPS}$
Adjusted coordinate of check point	$\underline{x}_i^{pho}$
Number of used check points	n
Mean [m]	$\overline{m} = \frac{1}{n} \cdot \sum_{i=1}^{n} \left(\underline{x}_i^{GPS} - \underline{x}_i^{pho} \right)$
RMS [m]	$RMS = \sqrt{\frac{1}{n} \cdot \sum_{i=1}^{n} \left(\underline{x}_i^{GPS} - \underline{x}_i^{pho} \right)^2}$

B.1 ADS detailed results

B.1.1 ETH-ADS

The ETH processing is based on a powerful bundle program developed at ETH Zürich. The program allows for the introduction of different trajectory models and different parameter sets for self-calibration. In this case the direct georeferencing model (DGR) is compared against the lagrange interpolation trajectory model (LIM). The available parameter set for camera calibration uses 18 parameters (maximum). The camera lens parameters (changes in focal length (1 parameter), radial symmetric distortion (3 parameters) and decentring distortion (2 parameters)) are extended by an additional 4 parameters which are introduced for each sensor CCD line separately. They estimate the distance of the individual CCD line centre from the principal point of the lens (2 parameters), the scan line inclination angle and the affinity across flight direction (2 parameters). Since only the data of the 3 panchromatic lines were used, this altogether results in the 18 parameter set-up. ETH also tries two different control point distributions: 12 GCP versus 4 GCP. Only the 12 GCP results are given in detail here (versions test10 – test18). The remaining versions (test1 – test9) use the same parameters but were based on 4 GCP only, where test1 case corresponds to the test10 version, test2 to test11 and so forth. Note, that only the processing of ADS low block was done by ETH and the image coordinate measurements were delivered from the pilot centre.

Configuration

Flying height	low
Software used in matching	manual point measurements provided by pilot centre
SW used for bundle	ETH, 12 GCP

Check point analysis (version Test10, DGR, no SC)

	ΔEast [m]	ΔNorth [m]	ΔVertical [m]
Mean	-0.008	-0.021	0.007
RMS	**0.045**	**0.059**	**0.069**

Accuracy obtained from 190 check point differences

Check point analysis (version Test11, DGR, 18 add. params for SC)

	ΔEast [m]	ΔNorth [m]	ΔVertical [m]
Mean	-0.008	-0.010	-0.005
RMS	**0.031**	**0.037**	**0.060**

Accuracy obtained from 190 check point differences

Check point analysis (version Test12, DGR, only 12 add. params for SC)

	ΔEast [m]	ΔNorth [m]	ΔVertical [m]
Mean	-0.002	-0.008	-0.002
RMS	**0.032**	**0.036**	**0.066**

Accuracy obtained from 190 check point differences

Check point analysis (version Test13, LIM-4, no SC)

	ΔEast [m]	ΔNorth [m]	ΔVertical [m]
Mean	-0.019	-0.023	0.003
RMS	**0.054**	**0.063**	**0.068**

Accuracy obtained from 190 check point differences

Check point analysis (version Test14, LIM-4, 18 add. params for SC)

	ΔEast [m]	ΔNorth [m]	ΔVertical [m]
Mean	-0.010	-0.012	-0.013
RMS	**0.035**	**0.039**	**0.068**

Accuracy obtained from 190 check point differences

Check point analysis (version Test15, LIM-4, only 16 add. params for SC)

	ΔEast [m]	ΔNorth [m]	ΔVertical [m]
Mean	-0.015	-0.013	-0.013
RMS	**0.037**	**0.041**	**0.070**

Accuracy obtained from 190 check point differences

Check point analysis (version Test16, LIM-8, no SC)

	ΔEast [m]	ΔNorth [m]	ΔVertical [m]
Mean	-0.014	-0.027	0.006
RMS	**0.052**	**0.064**	**0.064**

Accuracy obtained from 190 check point differences

Check point analysis (version Test17, LIM-8, 18 add. params for SC)

	ΔEast [m]	ΔNorth [m]	ΔVertical [m]
Mean	-0.009	-0.016	-0.009
RMS	**0.036**	**0.042**	**0.067**

Accuracy obtained from 190 check point differences

Check point analysis (version Test18, LIM-8, only 16 add. params for SC)

	ΔEast [m]	ΔNorth [m]	ΔVertical [m]
Mean	-0.013	-0.018	-0.009
RMS	**0.037**	**0.045**	**0.068**

Accuracy obtained from 190 check point differences

B.1.2 UoP-ADS

UoP uses the standard Leica Geosystems process line for the data processing. In general three different versions were processed: The basic case uses no camera calibration parameters and does not implement any correction of boresight alignment at all, i.e. uses the GPS/inertial exterior orientations as delivered. The para case then still uses no camera parameter refinement but implements additional parameters, such as the datum transform, the IMU misalignment and the drifts. The final self-calibration case then performs self-calibration besides the additional parameters from the para case. Only results from the cases based on 12 control points are given here. UoP also does processing with 6 GCPs only.

Configuration

Flying height	low
Software used in matching	GPro
SW used for bundle	ORIMA, 12 GCP

Check point analysis (case basic, no SC, no boresight alignment)

	ΔEast [m]	ΔNorth [m]	ΔVertical [m]
Mean	0.064	-0.059	0.133
RMS	**0.082**	**0.070**	**0.150**

Accuracy obtained from 190 check point differences

Check point analysis (case para, no SC, but boresight and datum parameters)

	ΔEast [m]	ΔNorth [m]	ΔVertical [m]
Mean	-0.016	-0.055	0.051
RMS	**0.052**	**0.072**	**0.091**

Accuracy obtained from 190 check point differences

Check point analysis (case self, including camera SC and boresight and datum parameters)

	ΔEast [m]	ΔNorth [m]	ΔVertical [m]
Mean	-0.018	-0.048	0.006
RMS	**0.034**	**0.059**	**0.067**

Accuracy obtained from 190 check point differences

Configuration

Flying height	high
Software used in matching	GPro
SW used for bundle	ORIMA, 12 GCP

Check point analysis (case basic, no SC, no boresight alignment)

	ΔEast [m]	ΔNorth [m]	ΔVertical [m]
Mean	0.057	-0.050	0.263
RMS	**0.071**	**0.075**	**0.277**

Accuracy obtained from 132 check point differences

Check point analysis (case para, no SC, but boresight and datum parameters)

	ΔEast [m]	ΔNorth [m]	ΔVertical [m]
Mean	0.002	-0.014	0.018
RMS	**0.036**	**0.049**	**0.088**

Accuracy obtained from 132 check point differences

Check point analysis

	ΔEast [m]	ΔNorth [m]	ΔVertical [m]
Mean	0.007	-0.013	-0.005
RMS	**0.037**	**0.043**	**0.089**

Accuracy obtained from 132 check point differences

B.1.3 DLR-B-ADS

DLR-B carried out the processing for each of the two flying heights separately, but they only delivered the check point coordinates obtained from later averaging of both results. Thus no flying height specific results could be given, although during the triangulation process the blocks were treated independently. Interesting to note, that besides the IMU misalignment angles additional time offsets for camera positions and attitudes from GPS/inertial were estimated. No additional self-calibration was applied during processing. All analyses were done with the 12 control point configuration. The DLR-B results are based on their own evaluation and processing system for multi-line pushbroom scanners. They also used this software chain to automatically generate a height model and orthophotomosaic.

Configuration

Flying height	Blocks treated separately, but ChP coordinates obtained from later averaging, no separate adjusted ChP coordinates delivered to pilot centre
Software used in matching	DLR
SW used for bundle	DLR, 12 GCP

Check point analysis (no camera SC)

	ΔEast [m]	ΔNorth [m]	ΔVertical [m]
Mean	0.007	-0.002	-0.034
RMS	**0.042**	**0.042**	**0.082**

Accuracy obtained from 185 check point differences

B.2 DMC detailed results

B.2.1 ICC-DMC

The ICC processing is by automatic tie point measurements by MATCH-AT and additional manual measurement of control and check points. To refine the block tie, additional tie points were measured manually. Only the self-calibration case was performed, where the set of additional 12 Ebner parameters was estimated for each image quadrant. The a priori standard deviations were set to 2µm for the automatically derived image points and 6µm for the manual measurements. The accuracy of GCP was set to 3cm in planimetry and 5cm in height component.

Configuration

Flying height	low
Software used in matching	MATCH-AT
SW used for bundle	ACX-GeoTex, 23 GCP

Check point analysis (12 additional parameters per quadrant camera SC)

	ΔEast [m]	ΔNorth [m]	ΔVertical [m]
Mean	0.001	0.007	0.008
RMS	**0.037**	**0.028**	**0.070**

Accuracy obtained from 21 check point differences

Configuration

Flying height	high
Software used in matching	MATCH-AT
SW used for bundle	ACX-GeoTex, 21 GCP

Check point analysis (12 additional parameters per quadrant camera SC)

	ΔEast [m]	ΔNorth [m]	ΔVertical [m]
Mean	0.006	0.031	0.002
RMS	**0.039**	**0.053**	**0.135**

Accuracy obtained from 19 check point differences

B.2.2 IPI-DMC

The IPI processing was based on the automatic tie point transfer using the LPS software The later bundle adjustments were all done with the BLUH program package. The blocks were processed separately first. Afterwards identical points were identified by comparing the obtained object point coordinates. Since they were generated from automatic tie point transfer they obtained different point numbers for each of the two blocks and therefore were treated as separate points. After renumbering those points were used to enforce the connection between the two blocks and then the common adjustment of the two flying heights was done.

Configuration

Flying height	low
Software used in matching	LPS
SW used for bundle	BLUH

Check point analysis (no self-calibration)

	ΔEast [m]	ΔNorth [m]	ΔVertical [m]
Mean	0.006	0.010	0.044
RMS	**0.072**	**0.058**	**0.136**

Accuracy obtained from 20 check point differences

Check point analysis (standard 12 BLUH parameters)

	ΔEast [m]	ΔNorth [m]	ΔVertical [m]
Mean	0.009	0.007	0.024
RMS	**0.038**	**0.038**	**0.089**

Accuracy obtained from 20 check point differences

Check point analysis (standard 12 BLUH parameters plus additional individual DMC specific parameters 30-36 and 74-81)

	ΔEast [m]	ΔNorth [m]	ΔVertical [m]
Mean	0.009	0.012	0.029
RMS	**0.036**	**0.040**	**0.087**

Accuracy obtained from 20 check point differences

Configuration

Flying height	high
Software used in matching	LPS
SW used for bundle	BLUH

Check point analysis (no self-calibration)

	ΔEast [m]	ΔNorth [m]	ΔVertical [m]
Mean	-0.023	0.013	0.098
RMS	**0.053**	**0.054**	**0.262**

Accuracy obtained from 18 check point differences

Check point analysis (standard 12 BLUH parameters)

	ΔEast [m]	ΔNorth [m]	ΔVertical [m]
Mean	-0.014	0.020	0.010
RMS	**0.058**	**0.062**	**0.209**

Accuracy obtained from 18 check point differences

Check point analysis (standard 12 BLUH parameters plus additional individual DMC specific parameters 30-36 and 74-81)

	ΔEast [m]	ΔNorth [m]	ΔVertical [m]
Mean	-0.005	0.022	0.003
RMS	**0.059**	**0.061**	**0.212**

Accuracy obtained from 18 check point differences

Configuration

Flying height	both
Software used in matching	LPS
SW used for bundle	BLUH

Check point analysis (no self-calibration)

	ΔEast [m]	ΔNorth [m]	ΔVertical [m]
Mean	-0.012	0.009	0.056
RMS	**0.055**	**0.047**	**0.151**

Accuracy obtained from 20 check point differences

Check point analysis (standard 12 BLUH parameters)

	ΔEast [m]	ΔNorth [m]	ΔVertical [m]
Mean	-0.007	0.011	0.042
RMS	**0.039**	**0.042**	**0.112**

Accuracy obtained from 20 check point differences

Check point analysis (standard 12 BLUH parameters plus additional individual DMC specific parameters 30-36 and 74-81)

	ΔEast [m]	ΔNorth [m]	ΔVertical [m]
Mean	-0.007	0.013	0.042
RMS	**0.036**	**0.040**	**0.118**

Accuracy obtained from 20 check point differences

B.2.3 inpho-DMC

The inpho results are based on MATCH-AT tie point transfer and subsequent adjustments in MATCH-AT and InBlock. Only the results from the common adjustments of blocks have been submitted. The tie between blocks is realized through the manually measured points.

Configuration

Flying height	both
Software used in matching	MATCH-AT
SW used for bundle	MATCH-AT and InBlock

Check point analysis (MATCH-AT, no self-calibration)

	ΔEast [m]	ΔNorth [m]	ΔVertical [m]
Mean	0.010	-0.001	-0.039
RMS	**0.030**	**0.036**	**0.113**

Accuracy obtained from 18 check point differences

Check point analysis (MATCH-AT, additional Ebner parameters)

	ΔEast [m]	ΔNorth [m]	ΔVertical [m]
Mean	0.008	0.001	-0.034
RMS	**0.031**	**0.034**	**0.097**

Accuracy obtained from 18 check point differences

Check point analysis (MATCH-AT, additional Grün parameters)

	ΔEast [m]	ΔNorth [m]	ΔVertical [m]
Mean	0.007	0.001	-0.032
RMS	**0.026**	**0.033**	**0.089**

Accuracy obtained from 18 check point differences

Check point analysis (InBlock, additional Brown parameters)

	ΔEast [m]	ΔNorth [m]	ΔVertical [m]
Mean	0.004	0.000	-0.031
RMS	**0.030**	**0.035**	**0.084**

Accuracy obtained from 18 check point differences

B.2.4 HfT-DMC

HfT used two different software packages for the analysis of data. The MATCH-AT and the Russian PhotoMod product. In PhotoMod most of the points were measured manually since the automatic tie point transfer did not deliver reasonable results in this case. Also note that PhotoMod uses the method of independent stereo pairs for block adjustment. Additional polynomial correction is also performed. Both evaluations were done independently, i.e. no image observations were transferred between the different software packages.

Configuration

Flying height	low
Software used in matching	MATCH-AT (automatic tie point transfer) PhotoMod (manual or semi-automatic point measurements)
SW used for bundle	MATCH-AT (bundle adjustment) and PhotoMod (independent model adjustment)

Check point analysis (MATCH-AT, additional Grün parameters)

	ΔEast [m]	ΔNorth [m]	ΔVertical [m]
Mean	0.028	-0.016	0.020
RMS	**0.044**	**0.045**	**0.080**

Accuracy obtained from 19 check point differences

Check point analysis (PhotoMod, additional polynomial correction)

	ΔEast [m]	ΔNorth [m]	ΔVertical [m]
Mean	0.003	0.011	-0.024
RMS	**0.036**	**0.039**	**0.106**

Accuracy obtained from 21 check point differences

Configuration

Flying height	high
Software used in matching	MATCH-AT (automatic tie point transfer) PhotoMod (manual or semi-automatic point measurements)
SW used for bundle	MATCH-AT (bundle adjustment) and PhotoMod (independent model adjustment)

Check point analysis (MATCH-AT, additional Grün parameters)

	ΔEast [m]	ΔNorth [m]	ΔVertical [m]
Mean	0.018	-0.017	-0.016
RMS	**0.091**	**0.064**	**0.190**

Accuracy obtained from 19 check point differences

Check point analysis (PhotoMod, additional polynomial correction)

	ΔEast [m]	ΔNorth [m]	ΔVertical [m]
Mean	0.043	-0.020	-0.059
RMS	**0.073**	**0.061**	**0.181**

Accuracy obtained from 19 check point differences

B.2.5 LM-DMC

The LM processing also used GPS trajectory information that was made available to LM through personal correspondence. This data was neither available for the remaining participants nor the pilot centre. The GPS coordinate observations showed significant offset and drift effects and thus they only were used as relative observations. The results are obtained from the MATCH-AT software.

Configuration

Flying height	low
Software used in matching	MATCH-AT
SW used for bundle	MATCH-AT

Check point analysis (MATCH-AT, 12 Ebner parameters and GPS (corrected by additional GPS shift and drift parameters))

	ΔEast [m]	ΔNorth [m]	ΔVertical [m]
Mean	-0.011	-0.012	0.028
RMS	**0.053**	**0.050**	**0.118**

Accuracy obtained from 21 check point differences

Configuration

Flying height	high
Software used in matching	MATCH-AT
SW used for bundle	MATCH-AT

Check point analysis (MATCH-AT, 12 Ebner parameters and GPS (corrected by additional GPS shift and drift parameters))

	ΔEast [m]	ΔNorth [m]	ΔVertical [m]
Mean	0.015	-0.014	0.030
RMS	**0.075**	**0.078**	**0.208**

Accuracy obtained from 20 check point differences

B.2.6 IngrZI-DMC

The processing at IngrZI used the ISAT for automatic tie point matching and IS Photo-T for later bundle adjustment. The flying heights were treated separately. Again the results for the non self-calibration case are compared to the results when using the 12 Ebner parameters during adjustment.

Configuration

Flying height	low
Software used in matching	ISAT
SW used for bundle	IS Photo-T, 21 GCP

Check point analysis (no self-calibration)

	ΔEast [m]	ΔNorth [m]	ΔVertical [m]
Mean	0.002	0.024	0.028
RMS	**0.044**	**0.053**	**0.077**

Accuracy obtained from 19 check point differences

Check point analysis (using 12 Ebner parameters for self-calibration)

	ΔEast [m]	ΔNorth [m]	ΔVertical [m]
Mean	0.000	0.024	0.041
RMS	**0.043**	**0.054**	**0.084**

Accuracy obtained from 19 check point differences

Configuration

Flying height	high
Software used in matching	ISAT
SW used for bundle	IS Photo-T, 18 GCP

Check point analysis (no self-calibration)

	ΔEast [m]	ΔNorth [m]	ΔVertical [m]
Mean	0.005	0.029	0.071
RMS	**0.061**	**0.073**	**0.173**

Accuracy obtained from 19 check point differences

Check point analysis (using 12 Ebner parameters for self-calibration)

	ΔEast [m]	ΔNorth [m]	ΔVertical [m]
Mean	0.004	0.029	0.078
RMS	**0.060**	**0.072**	**0.181**

Accuracy obtained from 19 check point differences

B.2.7 ICC-P2B-DMC

The ICC used the same processing approach as for phase 2 data. Three different versions for a priori weightings of observations were considered during processing. The values chosen for a priori std.dev. of observations are listed in the following table. The same settings were used for the low and high blocks. Note that the version 1 observations settings correspond to the values also used previously for phase 2 processing.

Version	Std.Dev. [µm] Automatic tie points observation	Std.Dev. [µm] manual point measurements	Std.Dev. [m] Horizontal control points	Std.Dev. [m] Vertical control points
Vers. 1	2	6	0.03	0.05
Vers. 2	2	2.5	0.02	0.025
Vers. 3	4	5	0.02	0.025

Configuration

Flying height	low
SW used for bundle	ACX-GeoTex

Check point analysis (12 additional parameters per quadrant, vers. 1 observation weights)

	ΔEast [m]	ΔNorth [m]	ΔVertical [m]
Mean	0.007	0.005	0.085
RMS	**0.044**	**0.046**	**0.196**

Accuracy obtained from 21 check point differences

Check point analysis (12 additional parameters per quadrant, vers. 2 observation weights)

	ΔEast [m]	ΔNorth [m]	ΔVertical [m]
Mean	0.002	0.004	0.036
RMS	**0.042**	**0.040**	**0.124**

Accuracy obtained from 21 check point differences

Check point analysis (12 additional parameters per quadrant, vers. 3 observation weights)

	ΔEast [m]	ΔNorth [m]	ΔVertical [m]
Mean	-0.002	0.007	0.032
RMS	**0.043**	**0.040**	**0.117**

Accuracy obtained from 21 check point differences

Configuration

Flying height	high
SW used for bundle	ACX-GeoTex

Check point analysis (12 additional parameters per quadrant, vers. 1 observation weights)

	ΔEast [m]	ΔNorth [m]	ΔVertical [m]
Mean	0.017	-0.015	-0.030
RMS	**0.062**	**0.060**	**0.153**

Accuracy obtained from 20 check point differences

Check point analysis (12 additional parameters per quadrant, vers. 2 observation weights)

	ΔEast [m]	ΔNorth [m]	ΔVertical [m]
Mean	0.005	-0.011	-0.006
RMS	**0.054**	**0.058**	**0.129**

Accuracy obtained from 20 check point differences

Check point analysis (12 additional parameters per quadrant, vers. 3 observation weights)

	ΔEast [m]	ΔNorth [m]	ΔVertical [m]
Mean	0.005	-0.012	-0.009
RMS	**0.055**	**0.059**	**0.131**

Accuracy obtained from 20 check point differences

B.2.8 IPI-P2B-DMC

IPI was the only phase 2b participant who also used both data sets in a combined adjustment and tested several configurations. All processing runs were done with the same set of observation weightings as given below. Additionally to the two versions without any self-calibration and with use of the standard BLUH 12 parameter set, a version considering additional parameters for each individual DMC camera head (better quarters of virtual image) and one version based only on 2 special additional parameters common for all DMC heads were tested. Thus, in total, results from four versions were provided for evaluation. Note that the DMC specific additional parameter sets obviously weremodified in BLUH between the phase 2 and phase 2b processing.

Version	Std.Dev. [µm] Automatic tie points observation	Std.Dev. [µm] manual point measurements	Std.Dev. [m] Horizontal control points	Std.Dev. [m] Vertical control points
Vers. 3	3	3	0.02	0.04

Configuration

Flying height	low
SW used for bundle	BLUH

Check point analysis (no self-calibration)

	ΔEast [m]	ΔNorth [m]	ΔVertical [m]
Mean	0.002	0.011	0.038
RMS	**0.035**	**0.045**	**0.134**

Accuracy obtained from 21 check point differences

Check point analysis (BLUH 12 parameter set for self-calibration)

	ΔEast [m]	ΔNorth [m]	ΔVertical [m]
Mean	0.002	0.010	0.026
RMS	**0.040**	**0.044**	**0.106**

Accuracy obtained from 21 check point differences

Check point analysis (BLUH 12 parameter set plus 2 additional DMC specific parameters 79+80)

	ΔEast [m]	ΔNorth [m]	ΔVertical [m]
Mean	-0.001	0.008	0.046
RMS	**0.033**	**0.042**	**0.129**

Accuracy obtained from 21 check point differences

Check point analysis (BLUH 12 parameter set plus additional DMC camera head specific parameters 30-41 and 74-77)

	ΔEast [m]	ΔNorth [m]	ΔVertical [m]
Mean	-0.003	0.006	0.042
RMS	**0.035**	**0.041**	**0.119**

Accuracy obtained from 21 check point differences

Configuration

Flying height	high
SW used for bundle	BLUH

Check point analysis (no self-calibration)

	ΔEast [m]	ΔNorth [m]	ΔVertical [m]
Mean	0.053	-0.002	-0.043
RMS	**0.098**	**0.052**	**0.122**

Accuracy obtained from 20 check point differences

Check point analysis (BLUH 12 parameter set for self-calibration)

	ΔEast [m]	ΔNorth [m]	ΔVertical [m]
Mean	0.028	-0.012	-0.042
RMS	**0.073**	**0.055**	**0.115**

Accuracy obtained from 20 check point differences

Check point analysis (BLUH 12 parameter set plus 2 additional DMC specific parameters 79+80)

	ΔEast [m]	ΔNorth [m]	ΔVertical [m]
Mean	0.028	-0.015	-0.029
RMS	**0.064**	**0.051**	**0.097**

Accuracy obtained from 20 check point differences

Check point analysis (BLUH 12 parameter set plus additional DMC camera head specific parameters 30-41 and 74-77)

	ΔEast [m]	ΔNorth [m]	ΔVertical [m]
Mean	-0.002	-0.016	-0.022
RMS	**0.054**	**0.049**	**0.108**

Accuracy obtained from 20 check point differences

Configuration

Flying height	both
SW used for bundle	BLUH

Check point analysis (no self-calibration)

	ΔEast [m]	ΔNorth [m]	ΔVertical [m]
Mean	0.014	0.003	-0.053
RMS	**0.041**	**0.041**	**0.128**

Accuracy obtained from 21 check point differences

Check point analysis (BLUH 12 parameter set for self-calibration)

	ΔEast [m]	ΔNorth [m]	ΔVertical [m]
Mean	0.016	0.004	-0.006
RMS	**0.049**	**0.042**	**0.064**

Accuracy obtained from 21 check point differences

Check point analysis (BLUH 12 parameter set plus 2 additional DMC specific parameters 79+80)

	ΔEast [m]	ΔNorth [m]	ΔVertical [m]
Mean	0.015	0.002	-0.015
RMS	**0.043**	**0.039**	**0.073**

Accuracy obtained from 21 check point differences

Check point analysis (BLUH 12 parameter set plus additional DMC camera head specific parameters 30-41 and 74-77)

	ΔEast [m]	ΔNorth [m]	ΔVertical [m]
Mean	-0.001	0.004	-0.004
RMS	**0.036**	**0.040**	**0.088**

Accuracy obtained from 21 check point differences

B.2.9 CSIRO-P2B-DMC

CSIRO used an own aerial triangulation software for the processing of phase 2b. Since the software obviously has no additional self-calibration models implemented (at the time of data processing) only the non self-calibration case was considered. The data from the two flying heights were also processed in one common adjustment besides the results from separate processing. The a priori weightings used have not been reported.

Configuration

Flying height	low
SW used for bundle	In house (proprietary) software

Check point analysis (no self-calibration)

	ΔEast [m]	ΔNorth [m]	ΔVertical [m]
Mean	0.013	0.005	0.018
RMS	**0.038**	**0.047**	**0.151**

Accuracy obtained from 21 check point differences

Configuration

Flying height	high
SW used for bundle	In house (proprietary) software

Check point analysis (no self-calibration)

	ΔEast [m]	ΔNorth [m]	ΔVertical [m]
Mean	0.059	0.002	-0.010
RMS	**0.114**	**0.053**	**0.117**

Accuracy obtained from 20 check point differences

Configuration

Flying height	both
SW used for bundle	In house (proprietary) software

Check point analysis (no self-calibration)

	ΔEast [m]	ΔNorth [m]	ΔVertical [m]
Mean	0.042	0.009	-0.057
RMS	**0.070**	**0.034**	**0.098**

Accuracy obtained from 21 check point differences

B.2.10 ETH-P2B-DMC

The results from ETH are based on an in house software package. For self-calibration the standard available parameter sets defined by Ebner or Grün are introduced for each image quadrant. The quadrants can be defined in such a way, that they have certain overlaps with each other. The results presented here have used overlaps of 15pix. For a priori weighting the same parameters as the pilot centre were introduced. During data processing other weights and weighting options were tried but their results are not given here.

Version	Std.Dev. [µm] Automatic tie points observation	Std.Dev. [µm] manual point measurements	Std.Dev. [m] Horizontal control points	Std.Dev. [m] Vertical control points
all	3	3	0.02	0.02

Configuration

Flying height	low
SW used for bundle	In house (proprietary) software

Check point analysis (no self-calibration)

	ΔEast [m]	ΔNorth [m]	ΔVertical [m]
Mean	0.009	0.011	0.064
RMS	**0.037**	**0.053**	**0.159**

Accuracy obtained from 20 check point differences

Check point analysis (12 Ebner parameters per quadrant)

	ΔEast [m]	ΔNorth [m]	ΔVertical [m]
Mean	0.009	0.008	0.036
RMS	**0.036**	**0.046**	**0.158**

Accuracy obtained from 20 check point differences

Check point analysis (44 Grün parameters per quadrant)

	ΔEast [m]	ΔNorth [m]	ΔVertical [m]
Mean	0.008	0.003	0.006
RMS	**0.031**	**0.043**	**0.218**

Accuracy obtained from 20 check point differences

Configuration

Flying height	high
SW used for bundle	In house (proprietary) software

Check point analysis (no self-calibration)

	ΔEast [m]	ΔNorth [m]	ΔVertical [m]
Mean	0.049	-0.002	-0.037
RMS	**0.097**	**0.054**	**0.140**

Accuracy obtained from 20 check point differences

Check point analysis (12 Ebner parameters per quadrant)

	ΔEast [m]	ΔNorth [m]	ΔVertical [m]
Mean	0.007	-0.011	0.002
RMS	**0.050**	**0.061**	**0.127**

Accuracy obtained from 20 check point differences

Check point analysis (44 Grün parameters per quadrant)

	ΔEast [m]	ΔNorth [m]	ΔVertical [m]
Mean	-0.014	-0.005	-0.040
RMS	**0.050**	**0.049**	**0.125**

Accuracy obtained from 20 check point differences

B.2.11 IngrZI-P2B-DMC

IngrZI delivered two independent results form the processing done in their two branches in Aalen (version v1) and Huntsville (version v2). Both used the same software for bundle adjustment (ISAT) and the 12 Ebner parameters for self-calibration. Both versions used different a priori weightings which, most likely, are the reasons for the later (small) differences in results. For version v1 different weights were used for the low and high flight respectively. In version v2 the same weights were introduced for both blocks.

Version	Std.Dev. [µm] Automatic tie points observation	Std.Dev. [µm] manual point measurements	Std.Dev. [m] Horizontal control points	Std.Dev. [m] Vertical control points
v1 low	5	5	0.06	0.08
v1 high	5	5	0.10	0.10
v2	3	3	0.06	0.08

Configuration

Flying height	low
SW used for bundle	ISAT

Check point analysis (version v1 low, no self-calibration)

	ΔEast [m]	ΔNorth [m]	ΔVertical [m]
Mean	0.016	0.012	0.072
RMS	**0.041**	**0.054**	**0.169**

Accuracy obtained from 21 check point differences

Check point analysis (version v2, no self-calibration)

	ΔEast [m]	ΔNorth [m]	ΔVertical [m]
Mean	0.026	0.014	0.068
RMS	**0.052**	**0.049**	**0.165**

Accuracy obtained from 21 check point differences

Check point analysis (version v1 low, 12 Ebner parameters for self-calibration)

	ΔEast [m]	ΔNorth [m]	ΔVertical [m]
Mean	0.018	0.014	0.076
RMS	**0.036**	**0.059**	**0.162**

Accuracy obtained from 21 check point differences

Check point analysis (version v2, 12 Ebner parameters for self-calibration)

	ΔEast [m]	ΔNorth [m]	ΔVertical [m]
Mean	0.027	0.010	0.083
RMS	**0.051**	**0.050**	**0.156**

Accuracy obtained from 21 check point differences

Configuration

Flying height	high
SW used for bundle	ISAT

Check point analysis (version v1 high, no self-calibration)

	ΔEast [m]	ΔNorth [m]	ΔVertical [m]
Mean	0.041	-0.001	-0.033
RMS	**0.103**	**0.048**	**0.140**

Accuracy obtained from 20 check point differences

Check point analysis (version v2, no self-calibration)

	ΔEast [m]	ΔNorth [m]	ΔVertical [m]
Mean	0.042	-0.002	-0.030
RMS	**0.103**	**0.048**	**0.140**

Accuracy obtained from 20 check point differences

Check point analysis (version v1 high, 12 Ebner parameters for self-calibration)

	ΔEast [m]	ΔNorth [m]	ΔVertical [m]
Mean	0.004	0.014	-0.029
RMS	**0.078**	**0.055**	**0.115**

Accuracy obtained from 20 check point differences

Check point analysis (version v2, 12 Ebner parameters for self-calibration)

	ΔEast [m]	ΔNorth [m]	ΔVertical [m]
Mean	0.001	0.014	-0.028
RMS	**0.079**	**0.054**	**0.124**

Accuracy obtained from 20 check point differences

B.3 UCD detailed results

B.3.1 itacyl-UCD

Only results from the *UCD low* block are provided. Note that itacyl itself declared the results as preliminary only to document their ongoing data evaluation process. But no additional or final results were provided later.

Configuration

Flying height	low
Software used in matching	MATCH-AT
SW used for bundle	MATCH-AT

Check point analysis (no self-calibration but GPS-offset and drift params)

	ΔEast [m]	ΔNorth [m]	ΔVertical [m]
Mean	-0.012	-0.002	0.146
RMS	**0.110**	**0.056**	**0.205**

Accuracy obtained from 13 check point differences

B.3.2 inpho-UCD

The inpho results are based on MATCH-AT tie point transfer and subsequent adjustments in MATCH-AT and InBlock. Both blocks are considered in one bundle adjustment. The tie between blocks is realized through the manually measured points.

Configuration

Flying height	both
Software used in matching	MATCH-AT
SW used for bundle	MATCH-AT and InBlock

Check point analysis (MATCH-AT, no self-calibration, GPS-offset and drift)

	ΔEast [m]	ΔNorth [m]	ΔVertical [m]
Mean	-0.029	0.006	0.072
RMS	**0.077**	**0.059**	**0.144**

Accuracy obtained from 12 check point differences

Check point analysis (MATCH-AT, additional Ebner parameters, GPS-offset and drift)

	ΔEast [m]	ΔNorth [m]	ΔVertical [m]
Mean	0.000	0.013	0.029
RMS	**0.043**	**0.057**	**0.095**

Accuracy obtained from 12 check point differences

Check point analysis (InBlock, additional Brown parameters, GPS-offset and drift)

	ΔEast [m]	ΔNorth [m]	ΔVertical [m]
Mean	-0.007	0.020	0.030
RMS	**0.061**	**0.055**	**0.096**

Accuracy obtained from 12 check point differences

B.3.3 CSIRO-UCD

Different to other evaluation the CSIRO results are exclusively based on manually measured image points. Own software is used for the AT and no additional self-calibration was done. All results are obtained without the use of GPS observed perspective centre coordinates.

Configuration

Flying height	low
Software used in matching	Only manual measurements
SW used for bundle	Own software development

Check point analysis (no SC, no GPS data used, configuration B (no cross strip used in AT))

	ΔEast [m]	ΔNorth [m]	ΔVertical [m]
Mean	0.025	-0.001	0.107
RMS	**0.118**	**0.048**	**0.151**

Accuracy obtained from 15 check point differences

Check point analysis (no SC, no GPS data used, configuration C (all strips used in AT))

	ΔEast [m]	ΔNorth [m]	ΔVertical [m]
Mean	0.019	0.010	0.093
RMS	**0.121**	**0.053**	**0.148**

Accuracy obtained from 14 check point differences

Configuration

Flying height	high
Software used in matching	Only manual measurements
SW used for bundle	Own software development

Check point analysis (no SC, no GPS data used, configuration A (using all high flight lines))

	ΔEast [m]	ΔNorth [m]	ΔVertical [m]
Mean	0.011	0.012	-0.033
RMS	**0.115**	**0.174**	**0.432**

Accuracy obtained from 17 check point differences

Configuration

Flying height	both
Software used in matching	Only manual measurements
SW used for bundle	Own software development

Check point analysis (no SC, no GPS data used, configuration D (using no cross strip in AT))

	ΔEast [m]	ΔNorth [m]	ΔVertical [m]
Mean	0.031	0.019	0.010
RMS	**0.091**	**0.100**	**0.266**

Accuracy obtained from 17 check point differences

Check point analysis (no SC, no GPS data used, configuration E (using all strips in AT))

	ΔEast [m]	ΔNorth [m]	ΔVertical [m]
Mean	0.028	0.024	0.002
RMS	**0.095**	**0.103**	**0.278**

Accuracy obtained from 17 check point differences

B.3.4 IPI-UCD

The IPI results are all obtained from BLUH adjustments, where the automatic tie point transfer was done with the Leica LPS software. Different to other evaluations, here the statistics from check point analyses were done by IPI itself, and are already reported in the corresponding IPI reports. Note that IPI has only computed the standard deviations (std.dev.); no RMS and mean values are reported. Thus, only the std.dev. is given in the following tables. Within the IPI reports the use of GPS observations is not explicitly mentioned.

Configuration

Flying height	low
Software used in matching	LPS
SW used for bundle	BLUH

Accuracy (**Std.Dev**) from check point analysis (as *delivered by IPI*)

Case	ΔEast [m]	ΔNorth [m]	ΔVertical [m]
No self-calibration	0.078	0.053	0.157
SC, BLUH params 1-12	0.053	0.057	0.126
SC, BLUH params 1-12 and UCD params 42-65	0.048	0.057	0.124

Accuracy obtained from 8 check point differences, located in centre of the block

Configuration

Flying height	high
Software used in matching	LPS
SW used for bundle	BLUH

Accuracy (**Std.Dev**) from check point analysis (as *delivered by IPI*)

Case	ΔEast [m]	ΔNorth [m]	ΔVertical [m]
No self-calibration	0.081	0.071	0.212
SC, BLUH params 1-12	0.091	0.088	0.206
SC, BLUH params 1-12 and UCD params 42-73	0.089	0.091	0.198

Accuracy obtained from 8 check point differences, located in centre of the block

Configuration

Flying height	both
Software used in matching	LPS
SW used for bundle	BLUH

Accuracy (**Std.Dev**) from check point analysis (as *delivered by IPI*)

Case	ΔEast [m]	ΔNorth [m]	ΔVertical [m]
No self-calibration	0.068	0.054	0.180
SC, BLUH params 1-12	0.044	0.063	0.157
SC, BLUH params 1-12 and UCD params 42-65	0.039	0.063	0.152

Accuracy obtained from 8 check point differences, located in centre of the block

B.3.5 UoN-UCD

In UoN analyses both blocks are evaluated separately. Two different self-calibration cases are considered. The standard Brown parameter approach is compared to an alternative calibration model proposed by UoN, here mentioned IESSG approach. The non self-calibration also was computed to serve as a reference. GPS observations obviously were not introduced during adjustments.

Configuration

Flying height	low
Software used in matching	LPS
SW used for bundle	ORIMA

Check point analysis (no SC)

	ΔEast [m]	ΔNorth [m]	ΔVertical [m]
Mean	-0.020	0.043	0.008
RMS	**0.080**	**0.082**	**0.204**

Accuracy obtained from 13 check point differences

Check point analysis (SC using Brown parameters (int. orientation and radial distortion only)

	ΔEast [m]	ΔNorth [m]	ΔVertical [m]
Mean	-0.016	0.046	-0.019
RMS	**0.087**	**0.081**	**0.202**

Accuracy obtained from 13 check point differences

Check point analysis (IESSG method (refined image coordinates used in AT (no add. SC))

	ΔEast [m]	ΔNorth [m]	ΔVertical [m]
Mean	0.000	0.045	-0.045
RMS	**0.082**	**0.079**	**0.171**

Accuracy obtained from 12 check point differences

Configuration

Flying height	high
Software used in matching	LPS
SW used for bundle	ORIMA

Check point analysis (no SC)

	ΔEast [m]	ΔNorth [m]	ΔVertical [m]
Mean	-0.038	0.009	-0.082
RMS	**0.145**	**0.076**	**0.318**

Accuracy obtained from 12 check point differences

Check point analysis (SC using Brown parameters (int. orientation and radial distortion only)

	ΔEast [m]	ΔNorth [m]	ΔVertical [m]
Mean	-0.034	0.006	-0.060
RMS	**0.137**	**0.073**	**0.263**

Accuracy obtained from 12 check point differences

Check point analysis (IESSG method (refined image coordinates used in AT (no add. SC))

	ΔEast [m]	ΔNorth [m]	ΔVertical [m]
Mean	-0.032	0.005	-0.060
RMS	**0.142**	**0.076**	**0.248**

Accuracy obtained from 12 check point differences

B.3.6 CSIRO-P2B-UCD

CSIRO used an own aerial triangulation software for the processing of phase 2b. No additional self-calibration models were used. The two flying heights were also processed in one common adjustment besides the separate processing. The a priori weightings used have not been reported.

Configuration

Flying height	low
SW used for bundle	In house (proprietary) software

Check point analysis (no self-calibration, configuration B (only long strips from low block, without cross strip))

	ΔEast [m]	ΔNorth [m]	ΔVertical [m]
Mean	-0.009	-0.011	0.043
RMS	**0.103**	**0.047**	**0.213**

Accuracy obtained from 15 check point differences

Check point analysis (no self-calibration, configuration C (all strips from low block))

	ΔEast [m]	ΔNorth [m]	ΔVertical [m]
Mean	-0.010	-0.007	0.039
RMS	**0.098**	**0.048**	**0.172**

Accuracy obtained from 15 check point differences

Configuration

Flying height	high
SW used for bundle	In house (proprietary) software

Check point analysis (no self-calibration, configuration A (all strips used))

	ΔEast [m]	ΔNorth [m]	ΔVertical [m]
Mean	-0.010	0.016	-0.042
RMS	**0.078**	**0.116**	**0.339**

Accuracy obtained from 15 check point differences

Configuration

Flying height	both
SW used for bundle	In house (proprietary) software

Check point analysis (no self-calibration, configuration D (only long strips used))

	ΔEast [m]	ΔNorth [m]	ΔVertical [m]
Mean	-0.014	-0.010	0.011
RMS	**0.067**	**0.075**	**0.181**

Accuracy obtained from 13 check point differences

Check point analysis (no self-calibration, configuration E (all available strips used))

	ΔEast [m]	ΔNorth [m]	ΔVertical [m]
Mean	-0.023	-0.005	0.014
RMS	**0.067**	**0.073**	**0.161**

Accuracy obtained from 13 check point differences

B.3.7 IPI-P2B-UCD

All IPI processing runs were done with the same set of observation weightings as given below. For each block (first separate then in combined adjustment) the non self-calibration case is compared to the results from self-calibration using the standard 12 BLUH parameters only and then the version where the 12 BLUH parameters are added with Ultracam specific correction terms 42-73.

Version	Std.Dev. [μm] Automatic tie points observation	Std.Dev. [μm] manual point measurements	Std.Dev. [m] Horizontal control points	Std.Dev. [m] Vertical control points
Low	2	2	0.02	0.02
High	2	2	0.02	0.02
Both	2	2	0.02	0.04

Configuration

Flying height	low
SW used for bundle	BLUH

Check point analysis (no self-calibration)

	ΔEast [m]	ΔNorth [m]	ΔVertical [m]
Mean	-0.003	-0.002	0.025
RMS	**0.094**	**0.050**	**0.152**

Accuracy obtained from 15 check point differences

Check point analysis (12 BLUH parameters for self-calibration)

	ΔEast [m]	ΔNorth [m]	ΔVertical [m]
Mean	0.008	0.006	0.015
RMS	**0.081**	**0.054**	**0.065**

Accuracy obtained from 15 check point differences

Check point analysis (12 BLUH parameters and UCD specific terms 42-73 for SC)

	ΔEast [m]	ΔNorth [m]	ΔVertical [m]
Mean	0.010	0.008	0.016
RMS	**0.078**	**0.057**	**0.062**

Accuracy obtained from 15 check point differences

Configuration

Flying height	high
SW used for bundle	BLUH

Check point analysis (no self-calibration)

	ΔEast [m]	ΔNorth [m]	ΔVertical [m]
Mean	-0.012	0.019	-0.050
RMS	**0.062**	**0.098**	**0.280**

Accuracy obtained from 15 check point differences

Check point analysis (12 BLUH parameters for self-calibration)

	ΔEast [m]	ΔNorth [m]	ΔVertical [m]
Mean	-0.028	0.025	0.014
RMS	**0.069**	**0.082**	**0.244**

Accuracy obtained from 15 check point differences

Check point analysis (12 BLUH parameters and UCD specific terms 42-73 for SC)

	ΔEast [m]	ΔNorth [m]	ΔVertical [m]
Mean	-0.003	0.017	0.039
RMS	**0.068**	**0.082**	**0.217**

Accuracy obtained from 15 check point differences

Configuration

Flying height	both
SW used for bundle	BLUH

Check point analysis (no self-calibration)

	ΔEast [m]	ΔNorth [m]	ΔVertical [m]
Mean	-0.009	0.006	0.057
RMS	**0.084**	**0.051**	**0.170**

Accuracy obtained from 15 check point differences

Check point analysis (12 BLUH parameters for self-calibration)

	ΔEast [m]	ΔNorth [m]	ΔVertical [m]
Mean	0.000	0.008	0.024
RMS	**0.075**	**0.056**	**0.079**

Accuracy obtained from 15 check point differences

Check point analysis (12 BLUH parameters and UCD specific terms 42-73 for SC)

	ΔEast [m]	ΔNorth [m]	ΔVertical [m]
Mean	-0.001	0.009	0.021
RMS	**0.073**	**0.059**	**0.076**

Accuracy obtained from 15 check point differences

B.3.8 ETH-P2B-UCD

The ETH results were based on their proprietary software which allows for the modelling of the UCD sensor geometry. This is performed by introducing the standard Grün or Ebner parameters for each of the 9 image patches, i.e. corresponding patches in the virtual large format UCD image. In all cases for both blocks the same observations weights were used.

Version	Std.Dev. [µm] Automatic tie points observation	Std.Dev. [µm] manual point measurements	Std.Dev. [m] Horizontal control points	Std.Dev. [m] Vertical control points
Low	3	3	0.02	0.02
High	3	3		

Configuration

Flying height	low
SW used for bundle	ETH proprietary software

Check point analysis (no self-calibration)

	ΔEast [m]	ΔNorth [m]	ΔVertical [m]
Mean	-0.009	0.000	0.046
RMS	**0.104**	**0.050**	**0.193**

Accuracy obtained from 15 check point differences

Check point analysis (SC, one set of Grün parameters for whole image)

	ΔEast [m]	ΔNorth [m]	ΔVertical [m]
Mean	0.005	0.014	0.012
RMS	**0.074**	**0.066**	**0.060**

Accuracy obtained from 15 check point differences

Check point analysis (SC, 9 Ebner sets, one for each of the 9 image patches/regions)

	ΔEast [m]	ΔNorth [m]	ΔVertical [m]
Mean	0.006	0.015	0.022
RMS	**0.076**	**0.067**	**0.063**

Accuracy obtained from 15 check point differences

Check point analysis (SC, 9 Grün sets, one for each of the 9 image patches/regions)

	ΔEast [m]	ΔNorth [m]	ΔVertical [m]
Mean	0.006	0.012	0.019
RMS	**0.077**	**0.066**	**0.096**

Accuracy obtained from 15 check point differences

Configuration

Flying height	High
SW used for bundle	ETH proprietary software

Check point analysis (no self-calibration)

	ΔEast [m]	ΔNorth [m]	ΔVertical [m]
Mean	-0.014	0.017	-0.027
RMS	**0.077**	**0.119**	**0.341**

Accuracy obtained from 15 check point differences

Check point analysis (SC, one set of Grün parameters for whole image)

	ΔEast [m]	ΔNorth [m]	ΔVertical [m]
Mean	-0.001	0.016	-0.026
RMS	**0.055**	**0.068**	**0.122**

Accuracy obtained from 15 check point differences

Check point analysis (SC, 9 Ebner sets, one for each of the 9 image patches/regions)

	ΔEast [m]	ΔNorth [m]	ΔVertical [m]
Mean	-0.015	0.017	-0.051
RMS	**0.062**	**0.075**	**0.149**

Accuracy obtained from 15 check point differences

Check point analysis (SC, 9 Grün sets, one for each of the 9 image patches/regions)

	ΔEast [m]	ΔNorth [m]	ΔVertical [m]
Mean	-0.006	0.010	-0.075
RMS	**0.061**	**0.071**	**0.229**

Accuracy obtained from 15 check point differences

B.3.9 Vexcel-P2B-UCD

The Vexcel results were based on the Bingo bundle adjustment program. Obviously self-calibration was applied but unfortunately no details were given on the models used. The a priori weightings used have also not been reported.

Configuration

Flying height	Low
SW used for bundle	Bingo

Check point analysis (with SC))

	ΔEast [m]	ΔNorth [m]	ΔVertical [m]
Mean	0.017	-0.001	0.024
RMS	**0.094**	**0.056**	**0.089**

Accuracy obtained from 15 check point differences

Configuration

Flying height	High
SW used for bundle	Bingo

Check point analysis (with SC))

	ΔEast [m]	ΔNorth [m]	ΔVertical [m]
Mean	0.003	-0.002	0.006
RMS	**0.068**	**0.098**	**0.203**

Accuracy obtained from 15 check point differences

C Reports from participants

Triangulation of Vaihingen ADS40 Low-Altitude Flight Dataset
Test Results and Evaluation

Sultan Kocaman, Armin Gruen
ETH Zurich, Institute of Geodesy and Photogrammetry, 8092, Zurich
<skocaman> <agruen> @geod.baug.ethz.ch
http://www.photogrammetry.ethz.ch

1 Summary

Algorithms and software for a complete photogrammetric processing chain for TLS imagery have been developed at our Institute, ETH Zurich, since the year 2000. For the triangulation of TLS imagery, a modified bundle adjustment algorithm with the possibility of use of three different trajectory models was developed (Gruen and Zhang, 2003) and in the meantime tested with data of several sensors, including a variety of satellite imagery. In the latter phase of sensor modeling, the potential systematic error sources of the airborne linear array sensor imagery are examined and the self-calibration capabilities of the TLS sensors are investigated by introducing (at first instance) 16 additional parameters (AP) to the TLS sensor model. The mathematical model and parameter determinability testing methods of the self-calibration has been published by Kocaman et al. (2006); and the first test results from the ADS40 dataset acquired over Vaihingen Testfield and from the SI-100 sensor acquired over Yoriichio Testfield are provided in the same work.

In this study, the initial AP set is extended to 18 parameters. The first 6 parameters belong to the camera lens, that are changes in focal length (Δc), 3 radial symmetric lens distortion parameters (k_1, k_2, k_3), and 2 decentering distortion parameters (p_1, p_2). The distortion model of Brown (1971) is used for this purpose. 4 additional parameters per CCD line are defined to model the respective systematic errors: the distance of the CCD line center from the principal point of the lens (x_0 ,y_0), the scan line inclination angle (θ), and the affinity parameter in across flight direction (s_y). The definition of the parameters allows to extend the self-calibration model for multiple lenses and n-number CCD line sensors. Data from three panchromatic lines of ADS40 are used for the triangulation tests given in the following section.

2 Results & Evaluation

Two of the developed trajectory models, the Lagrange Interpolation Model (LIM) and the Direct Georeferencing (DGR) Model, are used for testing. 18 different tests are performed using two different ground control point (gcp) sets (4 and 12 gcps). The test results from both gcp configurations are provided in Table 1 and Table 2. In both tables, results of the DGR model, and LIM with 4 and with 8 orientation fixes are presented. The self-calibration method is applied with a full-set and a reduced-set of additional parameters and compared with the results obtained without self-calibration. The parameter elimination algorithm as proposed by Gruen (1985) is used. The numbers of the APs in the final sets are different in each test and the removed parameters are given in Table 3. All APs are initially introduced as free (unconstrained) observations.

The results can briefly be assessed as following:

- The DGR is a more stable model than the LIM, in particular when a small number of GCPs is employed. Using a higher number of GCPs is of importance when LIM is used. Other conditions to use the LIM safely, such as the network configuration, stochastical model, pre-processing of the trajectory, etc., should be investigated more in-depth. In general the performance of the LIM (and PPM) models under diverse network conditions is not well understood yet.

- Basically 4 control points are enough to model the trajectory when the DGR model is used. A higher number of control points provides a slight improvement in the accuracy values of the DGR model. The improvement can be observed both in the RMSE values, which are computed using check points coordinates, and also in the network geometry, which can be analyzed from the standard deviations (sigma values) of points' ground coordinates computed using the covariance matrix elements.
- Use of self-calibration improves the overall accuracy in all tests.
- The best RMSE values are obtained using the DGR model with self-calibration. Considering the ground sample distance (GSD) = 15.6 cm, the RMSE values correspond to 0.22 pixel in planimetry and 0.38 pixel in height.
- It is noted that the more advanced LIM model does not improve the results (RMSE) compared to DGR. This is an indication that the measured GPS/INS values are of exceptional accuracy in the Vaihingen test, a fact which has not been observed by us in other projects. Here with DGR and self-calibration one comes close to the theoretically expected values (compare RMSEs with STDs). In case of LIM there is still a substantial gap between RMSEs and STDs, which cannot be explained at this point yet and which leaves room for improvement.

Table 1: Vaihingen Testfield ADS40 low-altitude flight dataset, triangulation results using 4 ground control points. The best value(s) in each row is coloured.

Test id	*Test 1*	*Test 2*	*Test 3*	*Test 4*	*Test 5*	*Test 6*	*Test 7*	*Test 8*	*Test 9*
Trajectory Model	*DGR*	*DGR*	*DGR*	*LIM-4*	*LIM-4*	*LIM-4*	*LIM-8*	*LIM-8*	*LIM-8*
Self-calibration model	*N.A.**	*18 AP*	*12 AP*	*N.A.**	*18 AP*	*14 AP*	*N.A.**	*18 AP*	*14 AP*
RMSE planimetry (cm)	5.6	3.5	3.4	6.2	3.9	4.2	6.1	4.1	4.4
RMSE Z (cm)	7.5	6.4	6.8	7.3	6.7	9.0	7.0	6.6	8.3
Sigma planimetry (cm)	3.6	2.5	3.5	2.5	2.4	2.4	2.4	2.2	2.2
Sigma Z (cm)	6.3	5.4	5.9	5.1	5.9	4.9	5.0	5.6	4.7
Sigma naught (μ)	1.78	1.61	1.62	1.72	1.59	1.60	1.61	1.49	1.50

** N.A.: Not applicable (self calibration has not been applied).*

Table 2: Vaihingen Testfield ADS40 low-altitude flight dataset, triangulation results using 12 ground control points. The best value(s) in each row is coloured.

Test id	*Test 10*	*Test 11*	*Test 12*	*Test 13*	*Test 14*	*Test 15*	*Test 16*	*Test 17*	*Test 18*
Trajectory Model	*DGR*	*DGR*	*DGR*	*LIM-4*	*LIM-4*	*LIM-4*	*LIM-8*	*LIM-8*	*LIM-8*
Self-calibration model	*N.A.**	*18 AP*	*12 AP*	*N.A.**	*18 AP*	*16 AP*	*N.A.**	*18 AP*	*16 AP*
RMSE planimetry (cm)	5.2	3.4	3.4	5.9	3.7	3.9	5.8	3.9	4.1
RMSE Z (cm)	6.9	6.0	6.6	6.8	6.8	7.0	6.4	6.7	6.8
Sigma planimetry (cm)	2.9	2.3	2.7	2.5	2.3	2.3	2.3	2.2	2.2
Sigma Z (cm)	5.6	4.9	5.1	5.1	5.0	5.1	5.0	4.8	4.9
Sigma naught (μ)	1.78	1.61	1.61	1.72	1.58	1.59	1.61	1.48	1.49

** N.A.: Not applicable (self calibration has not been applied).*

Table 3: Deleted additional parameters in related tests.

	DGR	LIM-4	LIM-8
4 gcp	Test-3: Δc, $x_{0\_forward}$, x_{0_nadir}, y_{0_nadir}, s_{y_nadir}, θ_{nadir}	Test-6: Δc, k_1, y_{0_nadir}, s_{y_nadir}	Test-9: Δc, k_1, y_{0_nadir}, s_{y_nadir}
12 gcp	Test-12: Δc, $x_{0\_forward}$, $y_{0\_backward}$, x_{0_nadir}, s_{y_nadir}, θ_{nadir}	Test-15: y_{0_nadir}, s_{y_nadir}	Test-18: y_{0_nadir}, s_{y_nadir}

REFERENCES

Brown, D.C., 1971. Close-Range Camera Calibration. Photogrammetric Engineering, 37 (8), pp. 855-866.

Gruen, A., 1985. Data Processing Methods for Amateur Photographs. Photogrammetric Record, 11 (65), pp. 567-579.

Gruen, A., Zhang, L., 2003. Sensor modeling for aerial triangulation with Three-Line-Scanner (TLS) imagery. Photogrammetrie, Fernerkundung, Geoinformation 2003, No.2, pp. 85-98

Kocaman S., Zhang, L., Gruen, A., 2006. Self-calibrating Triangulation of Airborne Linear Array CCD Cameras, EuroCOW 2006 International Calibration and Orientation Workshop, Castelldefels, Spain, 25-27 Jan. (proceedings on CD-ROM).

EuroSDR network “Digital Camera Calibration”

Sensor: ADS40

Report of German Aerospace Center (DLR), Berlin-Adlershof

FRANK SCHOLTEN, KLAUS GWINNER, THOMAS ROATSCH

Frank.Scholten@dlr.de
Klaus.Gwinner@dlr.de
Thomas.Roatsch@dlr.de

This report documents the evaluation, performed at DLR, Berlin-Adlershof, of geometrical aspects of ADS40 data provided within the EuroSDR network “Digital Camera Calibration”. The evaluation was conducted by use of DLR’s photogrammetric processing system for multi-line pushbroom scanners, originally developed for orientation, DTM generation, ortho-rectification, and mosaicking of HRSC data.

1 Test Data

(provided by ifp Stuttgart / LEICA GEOSYSTEMS)

Image Data
- ADS40 data, flight June 26, 2004
- test site Vaihingen/Enz, approx. 35 km^2
  (extension approx. 7 km East-West x 5 km North-South)
- Flight 1 (approx. 2,500 m above ground)
  3 long strips (East-West)
  3 cross strips (North-South)
- Flight 2 (approx. 1,500 m above ground)
  4 long strips (East-West)
  2 cross strips (North-South)

Orientation Data
- camera calibration data (LEICA *.cam files)
- original DGPS/INS data (APPLANIX POS/AV SBET file)
- LEICA orientation data files (LEICA *.odf files)

Point information
- 12 ground control points
- 202 check points

2 Data preparation

DLR’s experience on multi-line pushbroom scanners is based on its own evaluation and processing system (WEWEL et al., 2000; SCHOLTEN et al., 2002; SCHOLTEN & GWINNER, 2004). In order to prepare the ADS40 data set for the integration into this software system and to enable a standardised and automated evaluation, the provided data had to be converted in terms of data formats, file nomenclature, labelling etc.

After this conversion the data of this specific ADS40 camera define a simulated HRSC-AX camera. The steps applied to each data file are the following:

- **Conversion of 16bit-TIFF files to DLR's internal 8bit format**

  For further processing the 16bit image data are converted from TIFF to DLR's internal format and then (focussing on geometrical aspects) to 8bit files by adequate histogram stretching.

- **Conversion of LEICA'S camera calibration files to DLR specifications**

  Metric x/y focal plane coordinates of all CCD-elements of all CCD-lines are stored together with the nominal focal length (62.7 mm).

- **Integration of APPLANIX SBET file as orientation data set**

  The distinct description of all necessary definitions of angular rotations is a central and often crucial point within investigations of orientation data (fundamental rotations, rotation directions, coordinate system rotations vs. rotation matrices for vector transformation, integration of IMU-misalignment, etc.), in particular if such data are exchanged between different systems.

  In order to avoid possible misinterpretations or erroneous conclusions only the original orientation of the ADS test flight, as described in the post-processed APPLANIX SBET file, has been used within this investigation, rather than the more or less poorly documented orientation data files (**.odf*).

- **Transformation of files from Leica nomenclature to HRSC nomenclature**

  The 6 provided ADS sensors, 2 staggered forward sensors (F28A/B), 2 staggered backward sensors (B14A/B), and 2 staggered nadir sensors (N00A/B), have been converted to the nominal HRSC-AX sensors as follows:

  ADS F28A -> HRSC-AX S2
  ADS F28B -> HRSC-AX P2
  ADS N00A -> HRSC-AX ND
  ADS N00B -> HRSC-AX IR
  ADS B14B -> HRSC-AX P1
  ADS B14A -> HRSC-AX S1

  The HRSC-AX owns 5 panchromatic channels s1,s2,p1,p2, and nd. Therefore the 6th ADS N00B sensor was re-named to one of HRSC's 4 color channels, in this case the near-infrared channel ir.

- **Adding data prefixes (containing time information) to each image line**

  In order to connect the image data lines to the correct orientation data, DLR's image format requires a line prefix in front of each image lines which contains the image line acquisition time. It is derived from the start time of each image strips and the integration time of the data take, i.e. 1.5 ms for the 1,500 m flight resp. 2.5 ms for the 2,500 m flight.

- **Adding image/calibration labels describing sensor-specific information**

  Information about the sensor which is related to the data file is documented within DLR's image label entries. Label entries also document other properties, such as geo-location for map-referenced data and the processing history.

3 Block Orientation

The photogrammetric orientation procedures and the associated analyses have been done for both, the 1,500 m flight as well as for the 2,500 m flight. Both blocks, each formed by 6 image strips, have been analyzed independently, in order to detect variations in time of the investigated alignment values and/or time offsets, caused e.g. by variable flight conditions and/or manoeuvres.

The arrangement of flight strips in both flights differ slightly (see Figure 1). Within the 2,500 m flight neighbouring strips have been flown sequentially, at least the cross strips (N->S, S->N, N->S), while the along strips have a side-overlap of approx. 75 % and thus provide 2 pairs of strips with alternating heading.

Within the 1,500 m flight the 2 cross strips have both been flown from S->N and the 4 neighbouring along strips have not been flown sequentially, so they are arranged E->W, E->W, W->E, W->E. and provide only one pair of strips with alternating heading.

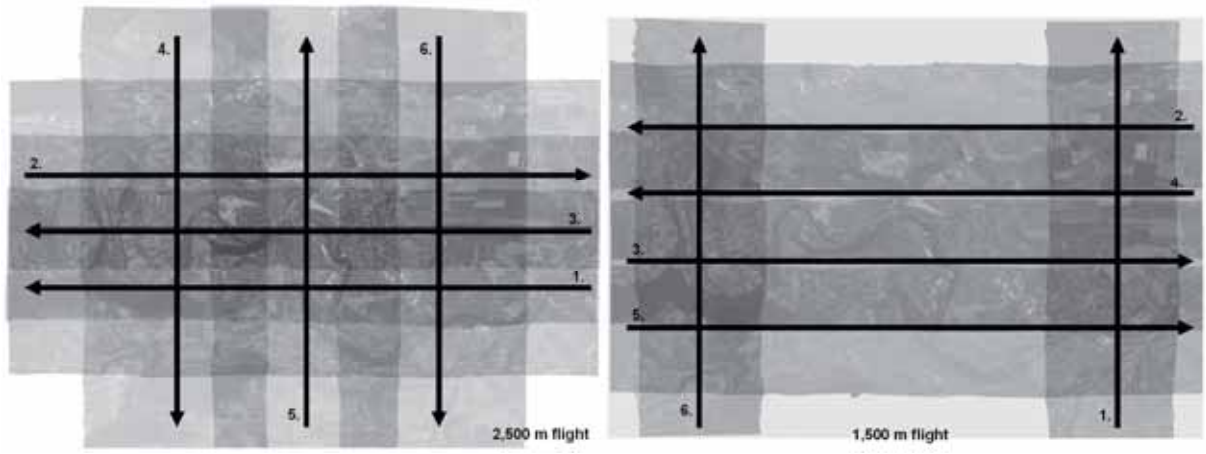

Figure 1: Strip arrangement

Previous investigations on multi-line scanner block geometry (SCHOLTEN et al., 2001; SUJEW et al., 2002), in particular for HRSC-AX applications, have shown that a strip constellation of sequentially flown strips with alternating heading, which nearly was used for the 2,500 m flight provides the best geometry for the subsequent photogrammetric analysis, in particular for the analysis and control of time offsets.

Therefore, the 2,500 m flight has been chosen for a more detailed investigation. In addition, the 1,500 m flight was used to check for its block stability under reduced conditions (sub-optimal strip constellation and, thus, reduced point measurement density).

The analysis of image orientation is based on the following initial data:

- camera calibration for each sensor as described within the files **.cam*
- calibrated IMU-alignment as provided in file *misalignment.dat*
- orientation as described in the APPLANIX SBET file *sbet_ln200.out*

The photogrammetric investigation of image orientation contains the following steps:

- Derivation of nominal orientation data for each strip, sensor, image line
- Measurement of block-internal tie-points, ground control points, and check points

- Photogrammetric analysis of block stability
- Determination of absolute block orientation
- Derivation of object point coordinates for given check points

Remark: The working reference frame for this photogrammetric investigation is the body-centered WGS84 system, since this is the standard reference frame for DLR's processing system. Results of the investigations (point coordinates, accuracies, etc.) have additionally been transformed to the given local system in a final step in order to follow the guidelines of this EuroSDR network.

3.1 Derivation of nominal orientation data for each strip, sensor, image line

The pre-requisite for the following photogrammetric investigations is the availability of orientation data. The binary SBET file contains these values for the entire flight (position is given in WGS84, pointing is given for the IMU measurement axes with respect to a topocentric frame defined at the actual position by x to the local North, z to the nadir, and y completing a right-handed system).

First, the initial position and attitude values for each image line of each sensor file of each image strip is derived by liner interpolation within the 200 Hz SBET data at the time-tags of each images line (preserving the original angular definitions of rotations (ω,ϕ,κ) from the IMU-axes to the actual topocentric frame).

In a second step the initial values for the IMU-misalignment are taken into account and the rotation angles ω, ϕ, κ , defined w.r.t. the local topocentric frames, are converted to a rotation defined by a ϕ, ω, κ sequence to the body-fixed Earth-centered WGS84 reference frame. Values for the actual IMU/camera-alignment, resp. the deviation from the nominal alignment, will be determined within the subsequent photogrammetric adjustment.

3.2 Measurement of block-internal tie-points, ground control points, and check points

3 different types of points have been measured and used within this investigation. For each point image coordinates have been measured manually in all 6 stereo channels (backward, forward, nadir) in both staggered files (A, B), except the 6th ADS-sensor N00B which was ignored within this investigation.

The applied point measurement tool allows a measurement accuracy of about 0.2 pxl (i.e. 1.3 micron).

- block-internal tie-points (TPs)

  TPs are defined as image points, which are visible in each of the used 5 stereo data sets of an image strip. The measured TPs are independent from other points (ground control and check points). Clearly defined natural or man-made features (road markings, manhole covers, etc.) haven been selected. In order to tie the entire block TPs are defined within the overlap between adjacent strips.

Figure 2 gives an overview of the TP distribution within the 2,500 m flight. It shows 38 TPs (yellow dots), 5 of these TPs are not visible in all stereo channels of adjacent strips and have therefore not been used as real tie points but only for strip-internal stability.

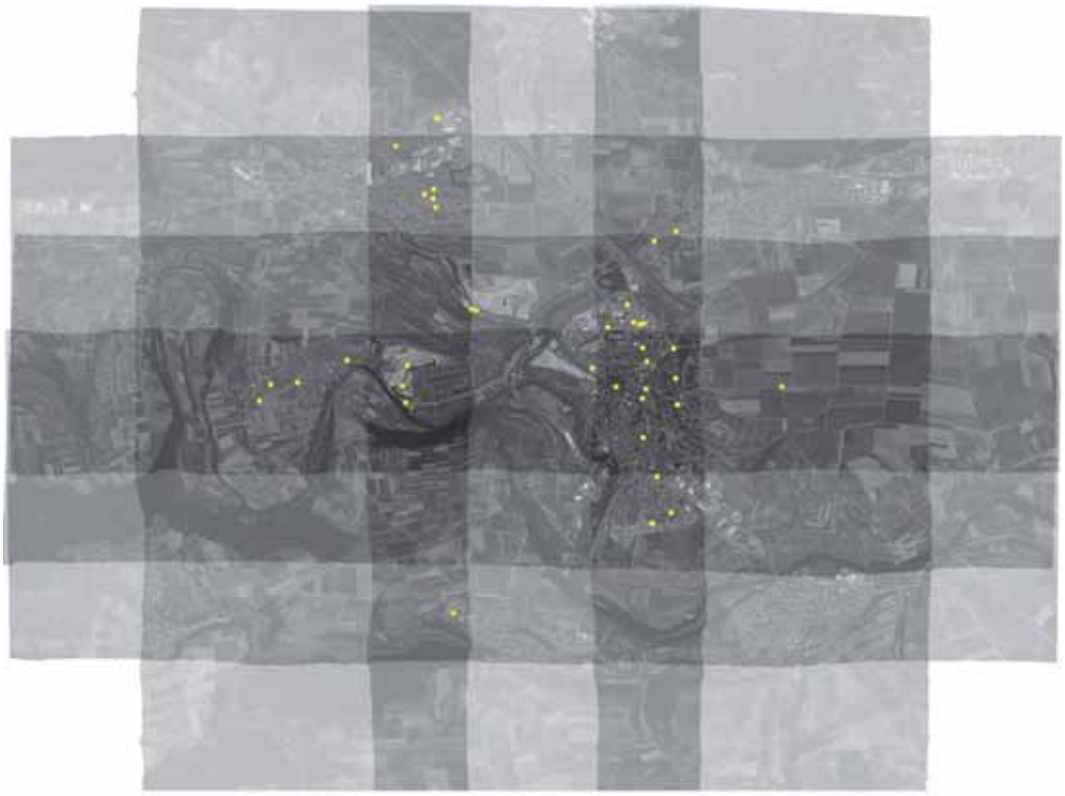

Figure 2: Tie point distribution (2,500 m flight)

Figure 3 gives an overview of the TP distribution (yellow dots) within the 1,500 m flight. It shows 10 TPs, 1 of these used for strip-internal stability only.

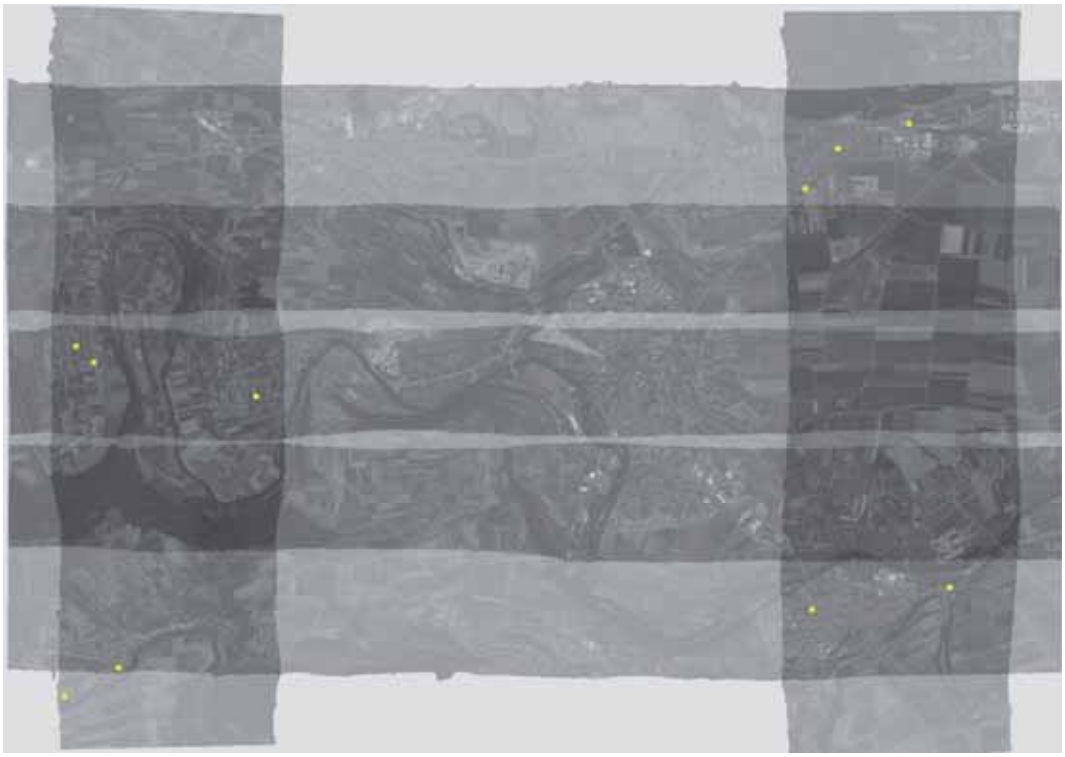

Figure 3: Tie point distribution (1,500 m flight)

- ground control points (GCPs)

  The 12 given GCPs have also been measured in all strips / all stereo channels as far as visible within the data.

  Figure 4 shows the GCP distribution (red dots) within the 2,500 m flight.

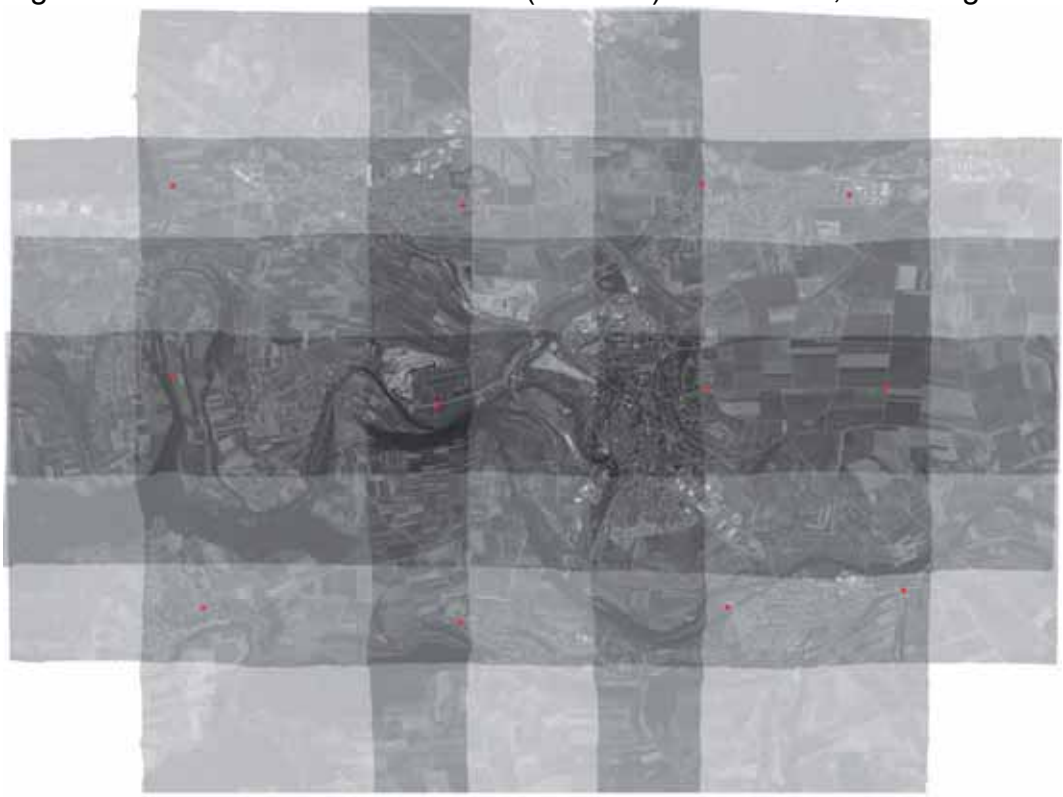

Figure 4: GCP distribution (2,500 m flight)

Figure 5 shows the GCP distribution (red dots) within the 1,500 m flight.

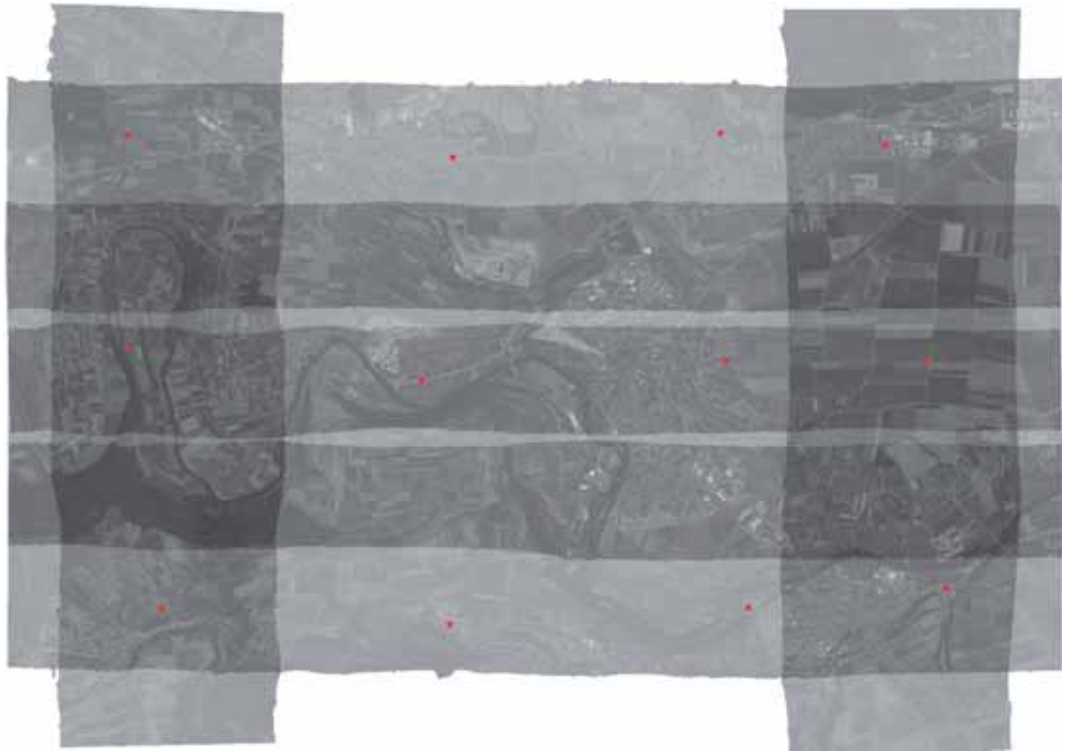

Figure 5: GCP distribution (1,500 m flight)

- check points (CPs)

  The 192 given CPs have also been measured in all strips / all stereo channels as far as visible within the data.

  Figure 6 shows the CP distribution (green dots) within the 2,500 m flight.

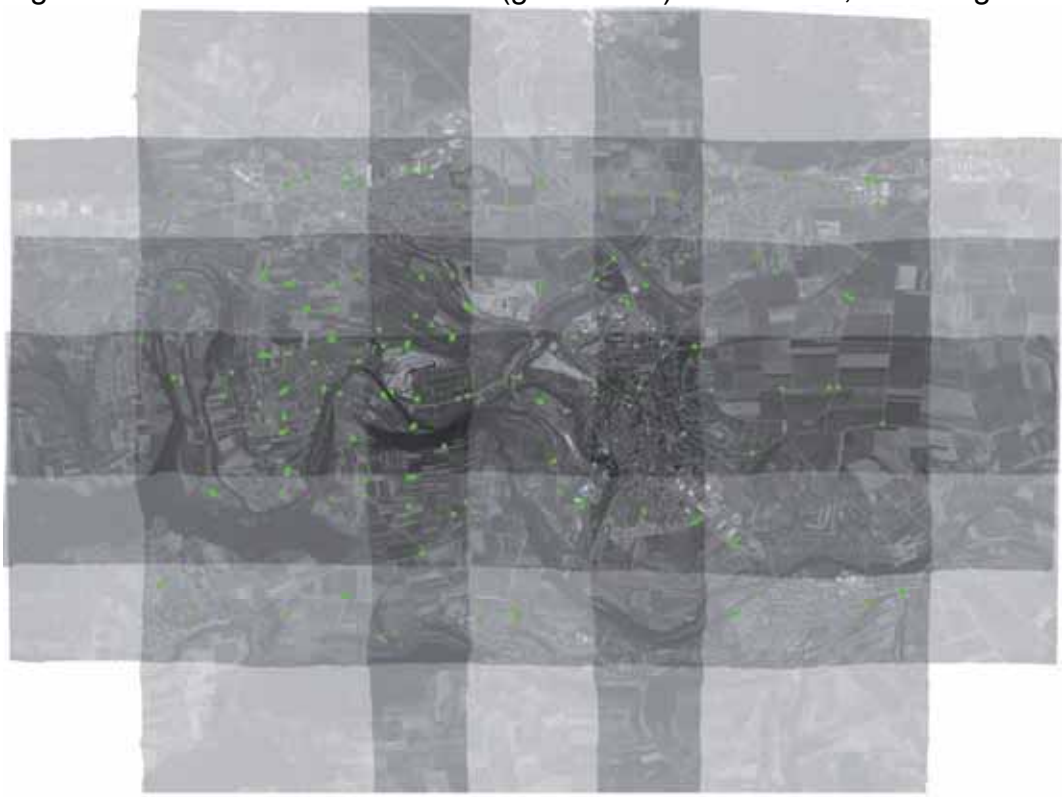

Figure 6: Check point distribution (2,500 m flight)

Figure 7 shows the CP distribution (green dots) within the 1,500 m flight.

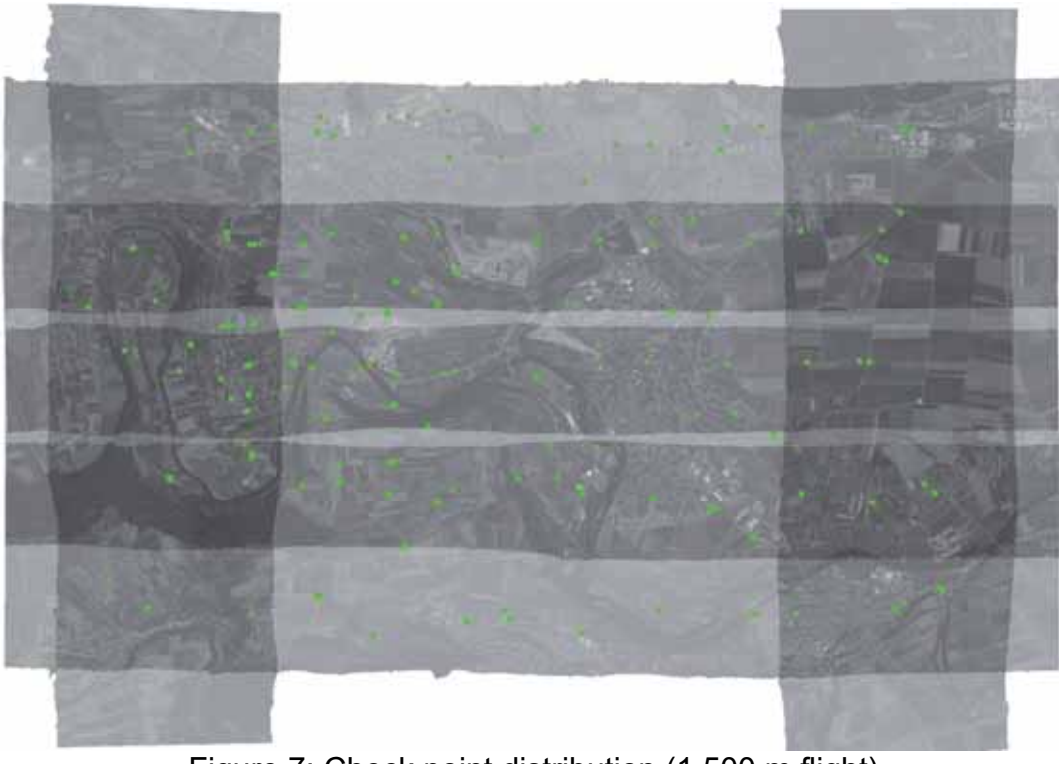

Figure 7: Check point distribution (1,500 m flight)

3.3 Photogrammetric analysis of block stability

The stability and accuracy of a block of multi-stereo line scanner data and its orientation information can be determined by the analysis of two aspects:

- the strip-internal stability: how precise do multi-stereo observations of a specific tie point form a 3D object point ?
- the block (strip-to-strip) accuracy: how precise do identical points (tie points), determined independently within overlapping strips, form a common object point ?

An optimization process, in which the strip-internal error and the strip-to-strip error have been minimized, was used to determine the following parameters, for both flights separately:

- IMU alignment ($\Delta\omega$, $\Delta\phi$, $\Delta\kappa$)
- time offsets for GPS position (Δt_pos) and for angular data (Δt_ang)

The results of this optimization are shown in Table 1:

Complete blocks of 6 strips	**Altitude 1,500 m** IFOV 0.006 deg GSD 15.6 cm scan rate 1.5 ms Ground speed 56 m/s	**Altitude 2,500 m** IFOV 0.006 deg GSD 25,9 cm scan rate 2.5 ms Ground speed 56 m/s
IMU alignment $\Delta\omega$ $\Delta\phi$ $\Delta\kappa$	0.033 deg -0.923 deg -0.262 deg	0.031 deg -0.925 deg -0.266 deg
Time offsets Δt_pos Δt_ang	 4.5 ms -2.0 ms	 7.8 ms 0.0 ms
Mean TP strip-internal accuracy 3D forward intersection acc., 1σ rms	7.1 cm	6.9 cm
Mean TP strip-to-strip accuracy 3D stand. deviation of $\lvert TP_{str}-TP_{mean}\rvert$, 1$\sigma$ rms)	15.4 cm	17.8 cm

The results can be described as follows:

- The mean accuracy achieved for flight 2,500 m shows values well below the original pixel resolution.
- The differences for the determined alignment angles is also well below the IFOV of the ADS40 camera.
- Although based only on reduced tie points information and although not having flown in an ideal strip arrangement, the orientation of the 1,500 m flight also yields sub-pixel accuracy.
- No significant time offsets for angular orientation values could be detected.
- Time offsets for position differ to the extent of one pixel.
- No evidence for systematic calibration errors has been detected by the analysis of the strip-internal accuracy (strip-internal forward ray intersection error less than half the original pixel resolution).
- Photogrammetric adjustment without using staggered stereo channels showed no degradation of the achieved accuracy.

Because of the flight strip arrangement and its higher point density, the 2,500 m flight has been used for further analysis of the characteristics of the parameters. Pairs and

sub-blocks of strips with alternating heading were formed to study the determined alignment angles and time offsets (see Table 2)

Altitude 2,500 m							
Sub-blocks	**along 1 / 2**	**along 2 / 3**	**along 1 / 2 / 3**	**cross 4 / 5**	**cross 5 / 6**	**cross 4 / 5 / 6**	**all 6 strips**
IMU-alignment							
$\Delta\omega$ [deg]	0.031	0.031	0.031	0.034	0.030	0.032	0.031
$\Delta\phi$ [deg]	-0.921	-0.920	-0.922	-0.929	-0.925	-0.927	-0.925
$\Delta\kappa$ [deg]	-0.264	-0.266	-0.265	-0.269	-0.266	-0.267	-0.266
Δt_pos [ms]	12.9	14.1	12.1	2.8	5.8	4.2	7.8
Δt_ang [ms]	0.0	1.0	1.0	1.0	0.0	0.0	0.0
strip-int. accuracy [cm]	7.0	5.5	6.5	4.8	5.9	6.1	6.9
block accuracy [cm]	17.8	10.0	15.2	14.7	9.7	15.6	17.8

Although providing an overall sub-pixel accuracy within the 2,500 m flight, a clear variation of the IMU ϕ (phi) alignment and a slightly variable κ (kappa) alignment can be seen for the 2 sub-blocks of along and cross strips. The reason for this is most probably not a physical change of the alignment but a varying quality of the horizontal levelling and the orientation to the North, which was derived by the IMU measurements and the subsequent DGPS/INS post-processing. These components are not modelled, so that their influence is integrated into the alignment model. Experience in other flight campaigns show that during the flight it is essentially important to stick to all restrictions concerning flight manoeuvres (adequate in-flight alignment, maximum roll angle during turns, etc). As a follow-up effect of the variations which correspond to a forward/backward displacement) the time offset for position (Δt_pos) was internally determined with different values, thus (at least partly) compensating these displacements. Since the reason of the effect and the time of its appearance can not clearly be detected and reconstructed outside the DGPS/INS post-processing and because of its sub-pixel extent, the alignment and time offsets used in the following investigations are those determined for all 6 strips together.

3.4 Determination of absolute block orientation

The determination of IMU alignment and time offsets as well as the optimization of the internal block stability had been done based on image data alone (without any ground reference). The absolute orientation of the derived blocks was then determined using the provided GCPs. Results are shown in Table 3a:

Absolute orientation at 12 GCP	**Altitude 1,500 m**	**Altitude 2,500 m**
Mean systematic offset:		
Δx / Δy / Δz (WGS84)	-6.3 / -1.7 / -9.4 cm	8.9 / -2.5 / 4.2 cm
ΔE / ΔN / ΔH (Local system)	-0.7 / -1.3 / -11.3 cm	-3.9 / -3.6 / 8.7 cm
Residuals after correction of systematic offsets:		
Mean |Δx| / |Δy| / |Δz| (WGS84)	5.7 / 3.0 / 6.2 cm	7.9 / 2.7 / 7.2 cm
Mean |ΔE| / |ΔN| / |ΔH| (Local system)	3.1 / 3.6 / 8.1 cm	3.6 / 3.0 / 10.5 cm
Mean 3D residual	10.0 cm	12.3 cm
(Min 3D - Max 3D)	1.5 - 21.6 cm	3.3 - 22.6 cm

From Table 3a it can be seen that:

- Based on the previously determined values, derived for IMU alignment and time offsets without any ground control, only small systematic offsets (absolute orientation) have been detected for both flights:

    - 1,500 m: 1 - 2 cm horizontal, 11 -12 cm vertical
    - 2,500 m: 4 - 5 cm horizontal, 8 - 9 cm vertical

- After the removal of these systematic offsets, the mean 3D residuals, detected at the given GCPs, are smaller than the original pixel resolution.

Residuals at each GCP and for both flights are given in Tables 3b and 3c:

GCP residuals [cm] after removal of syst. offsets: Altitude 1,500 m

	WGS84			Local			3D
GCP #	Δx	Δy	Δz	ΔE	ΔN	ΔH	
10101	-14.1	-6.5	-15.0	-4.2	1.4	-21.1	21.6
10601	-0.9	-1.9	-11.3	-1.7	-6.5	-9.3	11.5
11002	0.1	-1.0	1.1	-1.0	0.8	0.8	1.5
11301	7.9	-5.8	4.9	-7.0	-2.0	8.2	11.0
30102	9.7	4.0	2.9	2.4	-5.8	8.9	10.9
30501	5.9	-2.8	12.0	-3.7	3.8	12.6	13.7
31001	4.4	0.1	13.0	-0.6	5.3	12.7	13.7
31301	6.3	0.2	2.2	-0.8	-3.3	5.8	6.7
50101	-4.0	3.7	1.2	4.3	3.3	-1.3	5.6
50601	-10.4	3.5	-3.4	5.1	5.1	-9.0	11.5
51001	-3.3	2.3	-0.4	2.8	1.9	-2.2	4.0
51201	-1.2	4.0	-7.0	4.1	-4.2	-5.6	8.2
Mean residual |Δ|	5.7	3.0	6.2	3.1	3.6	8.1	10.0

GCP residuals [cm] after removal of syst. offsets: Altitude 2,500 m

	WGS84			Local			3D
GCP #	Δx	Δy	Δz	ΔE	ΔN	ΔH	
10101	1.8	10.7	2.4	10.3	-1.7	3.3	10.9
10601	6.0	-1.9	9.5	-2.8	2.0	10.9	9.7
11002	-15.7	-0.7	-16.3	1.8	1.1	-22.5	22.6
11301	7.5	-1.1	14.9	-2.3	4.3	16.0	16.7
30102	-11.3	2.5	-5.3	4.2	4.6	-11.1	12.7
30501	-5.9	2.5	0.2	3.4	4.2	-3.4	6.4
31001	-5.4	-1.7	-10.5	-0.8	-2.7	-11.6	14.2
31301	-8.8	-0.2	-7.9	1.2	1.4	-11.7	11.8
50101	-0.7	0.6	-3.2	0.7	-1.7	-2.8	3.3
50601	6.2	-1.8	7.2	-2.7	0.3	9.3	9.7
51001	13.7	-8.9	6.6	-10.9	-4.8	13.0	17.6
51201	12.1	0.2	2.8	-1.7	-7.2	10.0	12.4
Mean residual |Δ|	7.9	2.7	7.2	3.6	3.0	10.5	12.3

3.5 Derivation of object point coordinates for given check points

10102	-3365.770	-2000.253	368.413
10301	-2464.630	-2059.843	355.822
10401	-1906.375	-1883.144	357.333
10402	-1877.611	-1904.374	356.348
10501	-1412.973	-2245.802	312.025
10701	-276.321	-2026.255	327.714
10702	-223.025	-2094.983	323.321
10801	386.427	-2209.564	320.968
10901	1055.699	-2018.936	247.449
11001	2115.581	-1802.472	245.829
11101	2246.471	-2051.687	278.126
11201	3099.727	-2003.696	246.818
11302	3519.259	-1850.454	257.386
20201	-3174.388	-893.647	260.593
20202	-3170.686	-874.073	257.929
20301	-2517.863	-913.752	254.739
203101	-2523.757	-569.454	253.932
203102	-2530.864	-570.160	254.026
203103	-2471.186	-700.358	254.251
203104	-2460.547	-689.686	254.393
203105	-2464.250	-658.596	254.030
203106	-2524.506	-915.643	254.871
203107	-2500.154	-289.389	269.101
203108	-2518.704	-303.601	269.873
20401	-2031.011	-946.253	287.061
204101	-1827.661	-360.502	294.401
204102	-1817.611	-357.734	294.639
204103	-1711.010	-758.819	307.393
204104	-1699.322	-758.760	308.288
204105	-1711.371	-918.301	304.343
204106	-1706.247	-912.966	304.619
20501	-1283.287	-736.834	325.539
205101	-938.389	-429.227	323.405
205102	-1234.345	-734.061	326.571
205103	-1242.164	-736.053	326.480
205104	-850.508	-1090.982	351.033
205105	-842.212	-1089.100	351.170
205106	-1280.253	-1022.850	329.295
205107	-1280.843	-1007.815	328.962
20601	-733.665	-974.955	346.322
20701	184.939	-871.202	260.741
20702	-152.718	-881.590	276.510
20801	398.652	-966.620	253.653
20901	1003.679	-1061.996	271.093
21001	1552.436	-1128.329	263.496
21101	2298.860	-1011.947	291.157
21201	2911.263	-1085.112	313.477
21301	3361.469	-924.503	301.081
21302	3451.343	-1003.723	282.856
30101	-3569.028	232.712	289.012
30201	-3087.963	55.120	260.999
30301	-2735.238	-13.114	288.357
303101	-2704.128	445.036	348.821
303102	-2646.360	446.702	350.282
303103	-2514.304	96.486	285.501
303104	-2484.462	112.510	284.152
303105	-2101.675	137.857	253.439
303106	-2104.300	117.634	253.122
303107	-2494.492	-143.399	269.689
303108	-2490.545	-157.823	269.728
30401	-1947.031	83.772	255.821
304101	-1772.677	394.070	255.440
304102	-1762.084	392.251	255.441
304104	-1523.993	56.257	252.545
304105	-1530.185	72.600	252.549
305101	-1206.481	29.178	275.413
305102	-1195.338	29.771	275.661
305103	-1226.910	-226.996	252.604
305104	-1247.343	-246.453	252.670
30601	-704.565	58.524	252.608
30602	-802.034	31.329	254.196
30701	-0.032	-0.041	251.094
30702	-18.746	6.526	251.082
30801	521.261	159.494	288.930
30901	958.367	137.067	292.971
31101	2340.888	133.889	362.547
31201	2885.046	143.559	357.291
31302	3322.078	-205.779	332.502
40101	-3492.700	1118.923	257.076
40102	-3504.620	1113.087	257.124
40201	-3298.860	668.402	256.405
40301	-2452.974	1147.772	333.559
403101	-2673.393	1193.392	329.440
403102	-2685.545	1250.756	325.571
403103	-2480.467	1145.639	333.906
403104	-2432.944	1149.456	333.450
403105	-2456.815	467.796	353.070
403106	-2444.391	471.462	353.299
403107	-2294.745	904.845	365.283
403108	-2261.003	902.048	365.341
40401	-2017.181	1152.715	329.896
404101	-1784.090	1240.293	315.015
404102	-1775.108	1234.962	315.029
404103	-1996.765	898.695	359.598
404104	-1991.117	898.291	359.183
404105	-2047.656	601.233	354.765
404106	-2017.227	605.640	355.612
404107	-1569.328	703.330	357.024
404108	-1526.346	543.595	351.729
40501	-1154.608	1207.860	299.132
405101	-855.565	1235.317	271.860
405102	-857.284	1227.443	271.611
405103	-1157.121	1211.043	298.955
405104	-1152.248	1206.440	299.247
405105	-1219.405	834.005	332.980
405106	-1062.246	749.106	329.494
405107	-1287.325	579.410	343.524
405108	-1296.354	550.855	344.224
405109	-854.334	636.622	318.847
405110	-860.580	616.812	320.829
40601	-708.096	918.126	268.316
40701	-0.049	1124.360	292.201
40702	-1.324	1182.215	296.037
40801	541.146	1185.912	273.494
40901	1024.590	1135.668	293.560
41001	1836.703	1161.283	304.925
41101	2279.453	1267.872	303.296
41102	2343.441	1655.175	311.254
41201	2990.496	1274.423	318.097
41301	2968.139	1042.986	318.693
41302	3020.667	1014.666	320.369
50102	-3592.544	2009.923	304.407
50201	-3052.262	2142.600	295.083
50202	-2999.181	1958.943	292.481
50301	-2466.342	2121.990	285.862
50401	-1874.093	2260.159	274.955
50402	-1898.829	2128.815	275.650
50501	-1274.880	2255.188	277.896
50701	6.702	2148.551	302.759
50702	-1.787	2156.498	302.767
50801	685.912	2019.340	293.455
50901	982.737	2016.937	288.439
51002	1641.659	2164.849	279.815
51101	2362.077	2178.233	288.242
51301	3174.599	2159.048	293.189
51302	3255.982	2142.264	292.956
910101	-3701.565	-1782.236	384.920
910501	-1148.676	-1470.764	364.448
910502	-1143.837	-1462.950	364.269
910601	-604.279	-2120.457	321.549
910602	-602.795	-2118.338	321.527
911001	1902.541	-2048.492	263.089
911002	1890.349	-2052.019	263.000
911202	3178.401	-1949.007	246.113
911301	3502.753	-1832.636	254.438
920701	128.803	-577.247	266.647
920801	396.210	-1015.155	252.896
920802	678.165	-1145.506	275.849
920803	518.697	-607.887	251.833
921001	1505.983	-1162.266	263.159
921003	1885.143	-1398.143	250.344
921004	1892.270	-1386.026	250.343
921005	1388.838	-310.293	289.302
921101	1725.865	-315.864	324.398
921102	2052.585	-499.734	305.505
930103	-3881.884	610.208	257.610
930201	-2996.048	283.238	289.362
930301	-2643.631	-187.214	273.519
930302	-2171.835	-84.761	254.990
930304	-2715.837	445.997	348.278
930305	-2690.842	446.650	349.222
930306	-2652.546	447.905	350.149
930401	-2202.828	380.908	276.553
930403	-1445.910	97.582	254.656
930602	-212.857	242.057	253.132
930801	330.043	636.540	303.495
930901	1180.703	582.216	311.600
930902	1494.044	542.394	322.200
931001	1652.759	114.331	354.625
931101	2799.793	144.945	358.604
940601	-690.050	909.180	267.609
940802	707.097	1393.913	289.795
940803	840.997	965.136	290.738
940804	1002.334	1337.803	299.340
940901	1363.017	1364.426	309.193
941301	3149.757	1434.062	313.829
950302	-2470.450	2117.892	285.689
950401	-1759.823	2091.802	276.371
950501	-1105.270	2258.520	278.293
950601	-756.639	1903.726	289.150
950602	-759.692	2307.708	282.895
950603	-306.947	1914.969	296.284
950801	417.175	1690.112	299.830
950901	1299.498	2021.382	283.546
951001	1595.571	1970.744	280.188
951002	1943.521	2175.154	285.887
951101	2369.410	2191.427	288.740
951201	2977.444	1993.533	301.035
951302	3270.619	1923.869	300.880

Table 4: Check point coordinates (E, N, H) in the local coordinate system

Using the previously determined IMU-alignment and time offsets for both flights the final 3D object point coordinates of the check points (CPs) have been calculated, as far as the points were visible and as precise they could be identified within the image data. Table 4 gives the coordinates of all check points in the local coordinate system (Appendix A contains both coordinates in the local and in the WGS84 system).

4 DEM and Orthoimage generation

The final exterior orientation, derived by the photogrammetric block adjustment, has been used for a final automated derivation of geocoded 3D data of the visible surface and, subsequently, orthorectified image data. This has been done for both flights, but the 1,500 flight with less sidelap of the strips and thus containing more occlusions offered no improvement compared to the 2,500 m flight. Therefore, for these investigations only the 2,500 m flight was used for the generation of a DEM.

4.1 Generation of Digital Elevation Models

Based on the 3 sensors of ADS40, a DEM of the visible surface has been derived by multi-stereo area-based matching and multiple forward ray intersection. Only one sensor for each view (forward, backward, nadir) has been used. Additional staggered data for stereo/nadir showed no visible effect within 3D modelling. For the 2,500 m flight almost 1.5 Billion object points have been derived. The mean 3D forward ray intersection error of these mass points is about 8 cm. An example for the distribution and a histogram of the intersection accuracy within an image strip is shown in Figure 8 for the first strip of the 2,500 m flight (intersection better than the ground pixel resolution in green/yellow, worse intersections in yellow/red). No trend can be seen for the accuracy distribution from the center of the strip to its border, which proves that at least the κ (kappa) component of the alignment estimation is generally well determined. Only the North-East part shows a local degradation which might be caused by temporary vibrations which have not been measured by the IMU (e.g. because of its high frequency). Again, as within the photogrammetric adjustment, these mass points show no evidence of any systematic calibration errors.

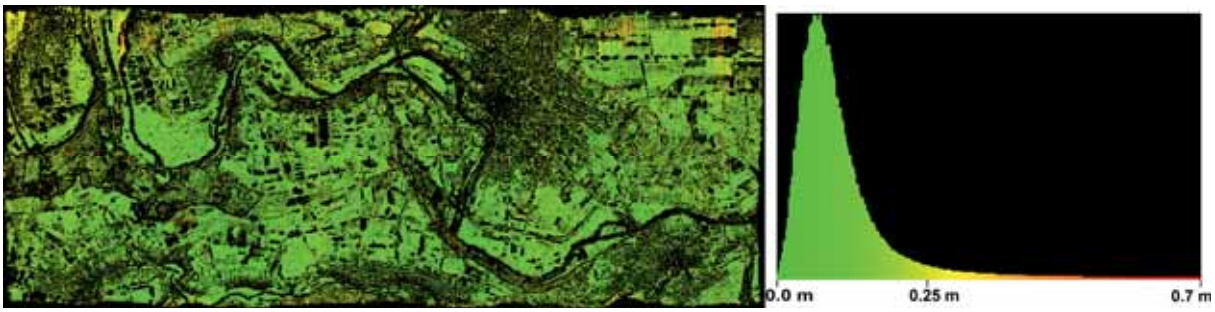

Figure 8: Forward ray intersection accuracy (first strip of 2,500 m flight)

It has to be taken into account that the imaging geometry of the ADS is not optimized w.r.t. 3D modelling of urban areas. Compared to data from sensors that provide 2 different forward and backward channels and/or a narrow-angle optics, it has to be noted that surface modelling based on image matching is more affected by occlusions. Thus, the accuracy of 3D surface point generation is partly degraded e.g. in urban areas, at forest borders or steep terrain slopes (which also reduces the local quality of ortho-rectification in such areas). Nevertheless, multiple image acquisition of the test area by along and cross strips as well as the high geometric accuracy in the range of 1 - 2 decimeters yields a coverage of approx. 73 % (see Figure 9).

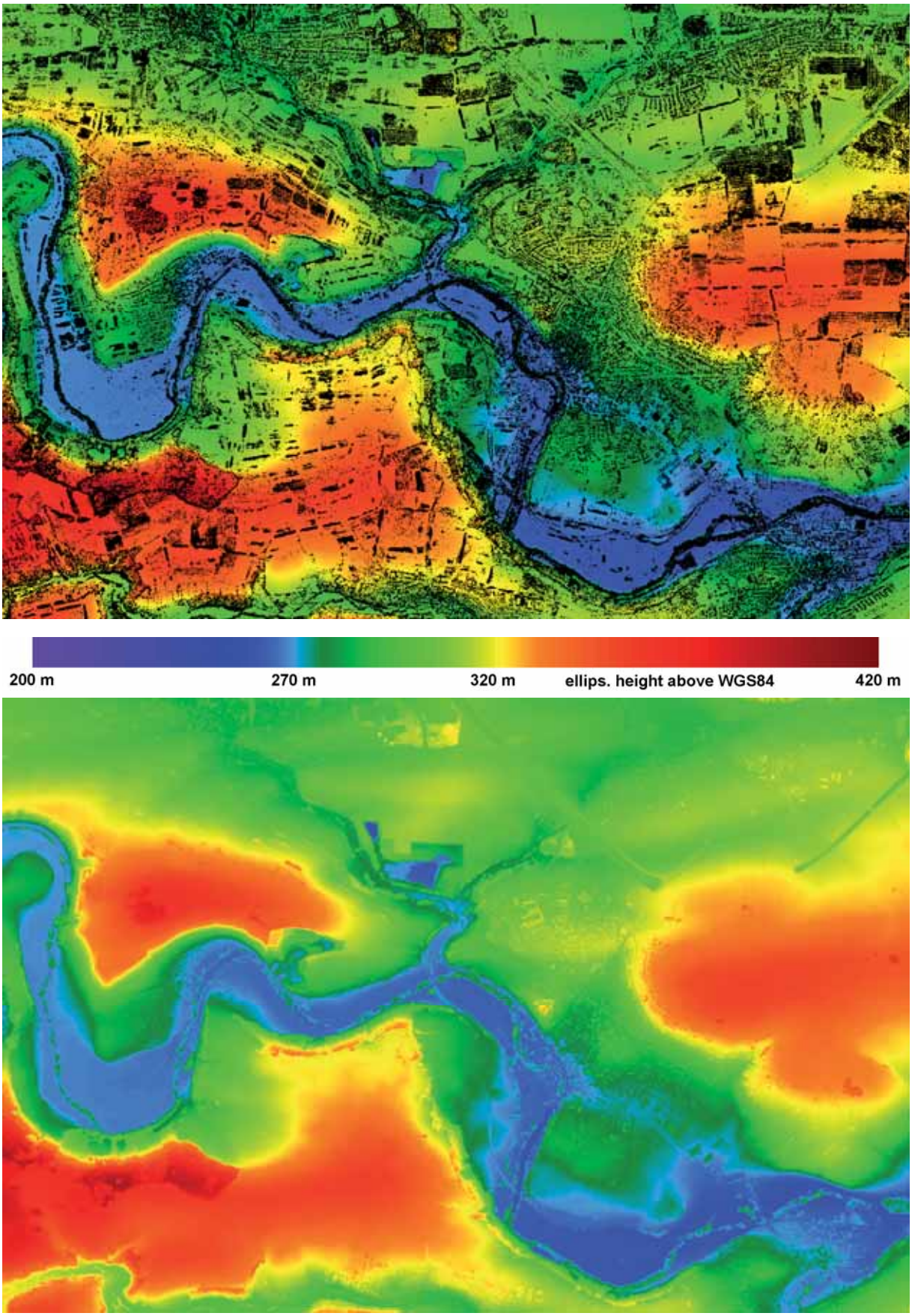

Figure 9: 50 cm raster DEM (top: coverage, gaps in black, bottom: interpolated DEM)

The 3D point distribution allowed for the automated interpolation of a final 50 cm raster DEM of the test area without any manual interaction/editing (Figure 9, Appendix B contains the full resolution DEM data).

Figure 10 shows the DEM and a subset in a shaded relief representation.

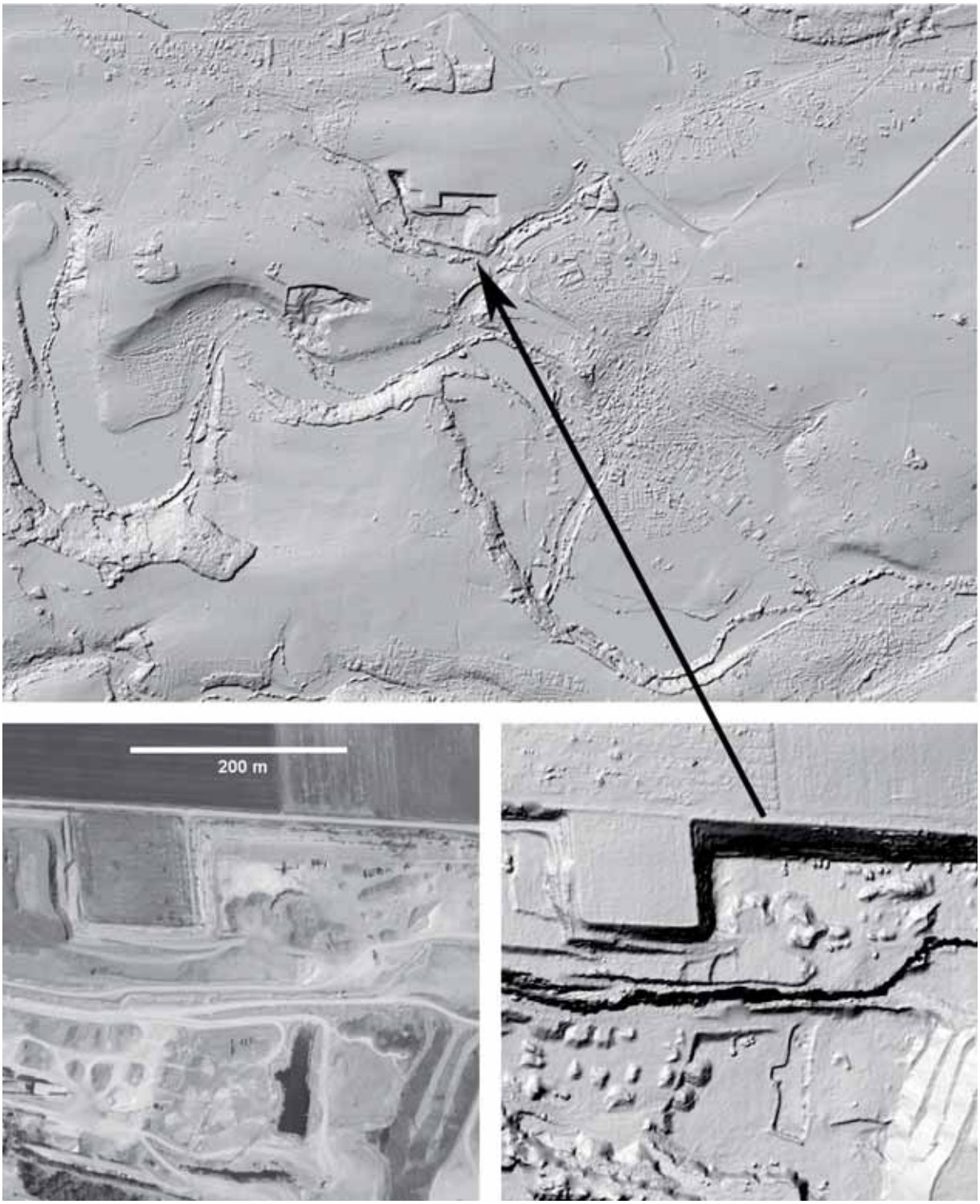

Figure 10: Shaded relief of 50 cm raster DEM (overview and subset), lower left: subset of 25 cm/pxl orthoimage mosaic

4.1 Orthoimage generation and mosaicking

Based on the DEM, orthoimages of each image strip and an orthoimage mosaic has been derived with 25 cm/pxl for the 2,500 m flight (see Figure 11, Appendix C contains the full resolution orthoimage mosaic). The original ADS40 data, provided in 16 bit data format, have been converted to 8 bit data for this representation.

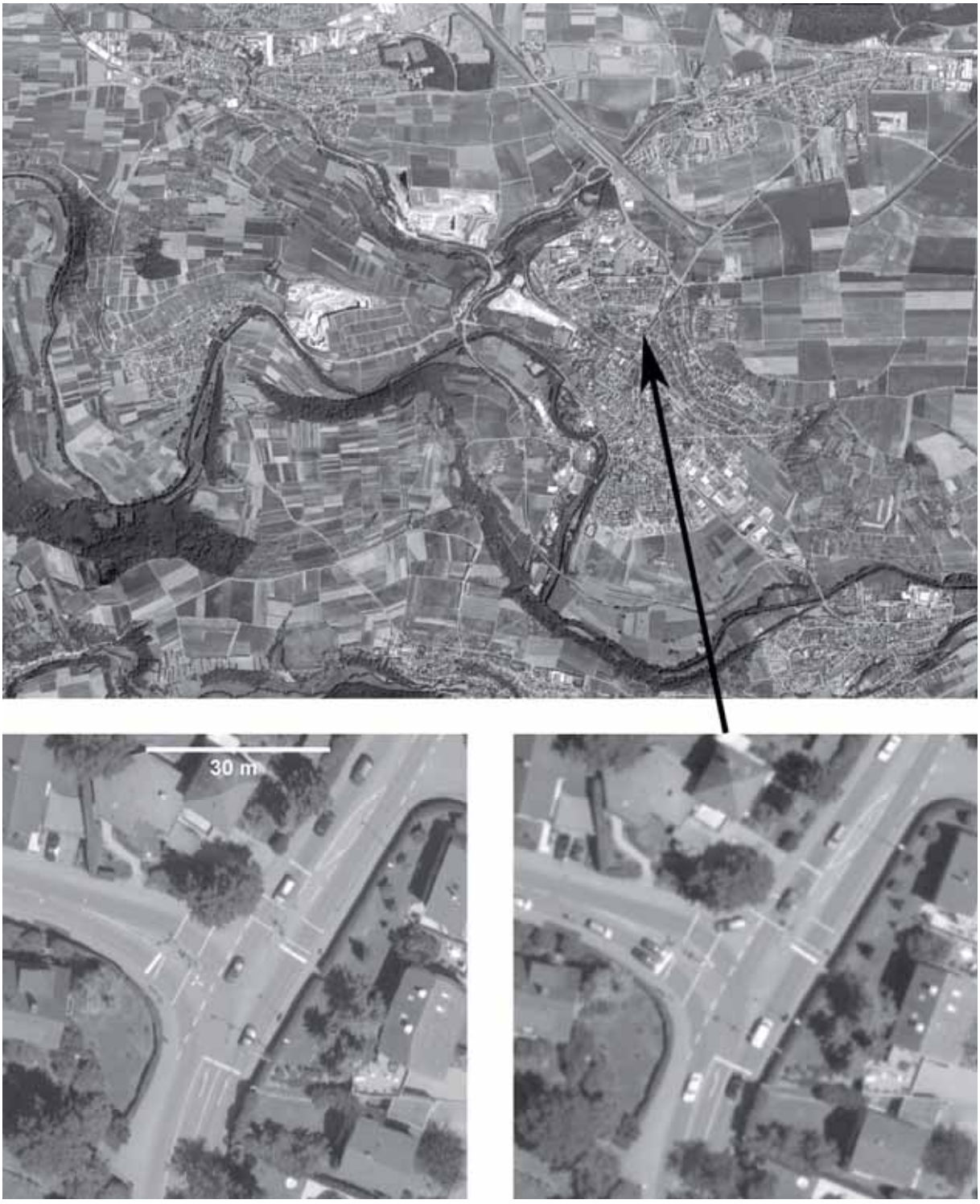

Figure 10: Orthoimage mosaic: top: 25 cm/pxl ,
lower subsets: right: 25 cm/pxl from 2,500 m flight
for comparison: left: 15 cm/pxl from 1,500 m flight

Ortho-rectification has been performed only for one of the two staggered nadir files. The combined used of staggered data sets within the ortho-rectification process might improve the nominal/theoretical image resolution, but this requires a special resampling technique in which final orthoimage grayvalues are derived simultaneously from both input data sets. Since such a resampling algorithm is not yet implemented in our processing system, this theoretical improvement could not be proven.

5 Summary of the ADS40 test flight analysis

- The entire photogrammetric analysis was based on the provided original interior orientation (camera calibration) and the original exterior orientation (APPLANIX POS/AV SBET file).
- No evidence for camera calibration errors has been found.
- Actual IMU alignment (including/modelling possible orientation errors of the SBET solution) and time offsets for position and attitude values in the SBET file have been determined for both flights.
- Within the 2,500 m flight a significant change of the ϕ (phi) and slight change of the κ (kappa) component of the IMU alignment was found between the along and cross strip blocks (indicating changes of accuracy of estimation of orientation during DGPS/INS post-processing, most probably caused by inadequate flight constellation).
- After photogrammetric adjustment a strip-internal accuracy of well below the original pixel size could be derived. The relative strip-to-strip accuracy within the blocks corresponds at least to the size of the original pixels.
- Staggered stereo data have been used within the photogrammetric adjustment, but neglecting them yielded no degradation of the achieved accuracy.
- The systematic offsets of the absolute positioning of the blocks w.r.t. the reference frames could be detected at GCPs. These offsets are only few centimeters laterally and approx. 10 cm vertically. After correction of this systematic component the mean residuals at the GCPs are 1 - 4 cm laterally and 8 - 12 cm vertically.
- Adjusted coordinates of the given check points have been derived and provided (although some points offered only poor signalization/visibility).
- The test data could be processed to a 50 cm DEM and 25 cm/pxl orthoimage mosaic in automated processes (without manual interaction/editing).

Although the investigations during this test define the first comprehensive application of DLR's software system to ADS40 data, the photogrammetric analyses yielded promising results. DEM and orthoimage mosaics have been derived in automated process and define products of high quality, at least for open areas. Specific adjustments of the processing parameters, which were selected in this study as for the HRSC-AX case, are likely to allow for some further improvements, particularly w.r.t. the DEM quality. 3D modelling and orthoimage generation using ADS40 data, in particular of urban areas, can benefit from these first experiences and from upcoming investigations. But, manual interaction/editing of the DEM at occlusions may still be necessary if LEICA's ADS40 data are to be used for the generation of 3D city models.

6 References

F. SCHOLTEN, F. WEWEL, S. SUJEW, High Resolution Stereo Camera – Airborne (HRSC-A): 4 Years of Experience in Direct Sensor Orientation of a Multi-Line Pushbroom Scanner. In: International Society for Photogrammetry and Remote Sensing, Proceedings of Joint Workshop "Sensors and Mapping from Space 2001", Veröffentlichungen des Instituts für Photogrammetrie und Geoinformation, Universität Hannover, (2001).

F. SCHOLTEN, G. GWINNER, F. WEWEL, Angewandte Digitale Photogrammetrie mit der HRSC. Photogrammetrie-Fernerkundung-Geoinformation, 5, E. Schweizerbart´sche Verlagsbuchhandlung, Stuttgart, Germany, pp. 317-332, (2002).

F. SCHOLTEN & K. GWINNER, Operational Parallel Processing in Digital Photogrammetry - Strategy and Results using Different Multi-Line Cameras. International Archives of Photogrammetry and Remote Sensing, Vol. XXXV, Part B, pp. 408-413, Istanbul, Turkey, (2004).

S. SUJEW, F. SCHOLTEN, F. WEWEL, R. PISCHEL, GPS/INS-Systeme im Einsatz mit der HRSC - Vergleich der Systeme Applanix POS/AV-510 und IGI AEROcontrol-IId. Photogrammetrie-Fernerkundung-Geoinformation, 5, E. Schweizerbart´sche Verlagsbuchhandlung, Stuttgart, Germany, pp. 333-340, (2002).

F. WEWEL, F. SCHOLTEN, K. GWINNER, High Resolution Stereo Camera (HRSC) – Multispectral 3D-Data Acquisition and Photogrammetric Data Processing. Canadian Journal of Remote Sensing, Vol. 26, No. 5, pp. 466-474, Ottawa, Canada, (2000).

Berlin-Adlershof, June 2006

Appendices:

Appendix A: DLR-Scholten_checkpoints.lis
Appendix B: DLR-Scholten_dem.raw
Appendix C: DLR-Scholten_orthomos.tif.bz2
Appendix D: DLR-Scholten_dem-orthomos.readme

INSTITUT CARTOGRÀFIC DE CATALUNYA

REPORT

EuroSDR "Digital Camera Calibration".
Data set: DMC data on Fredrikstad test site

R.Alamús, W. Kornus, J.Talaya
Institut Cartogràfic de Catalunya
Parc de Montjuïc 08038 Barcelona SPAIN
ralamus@icc.es, wkornus@icc.es, talaya@icc.es

INTRODUCTION

GOAL

Description of analysis carried out at the ICC with the EuroSDR data. Method and models used are described.

REFERENCE DOCUMENTS

Reference	DOCUMENT	DATE
D_1	EuroSDR-Phase2-Schedule.pdf	Stuttgart, February 17, 2006
D_2	EuroSDR-Phase2-Data.pdf	Stuttgart, February 20, 2006
D_3	EuroSDR-Members-Feb202006.pdf	Stuttgart, February 20, 2006
D_4	README-DMC-DataDisc.pdf	Stuttgart, March 24, 2006

GENERAL OVERVIEW

In this section a general overview description of the data set and process is done.

DATA SET

Data set evaluated is “DMC data, test site Fredrikstad” described in documents D_2 and, in a closer detail, D_4.

Due to the fact that all 12-bit images were saturated and unusable for aerotriangulation work, the whole process has been carried out using 8-bits images.

WORKFLOW

Ground control points (GCP) are manually and stereoscopically measured in an INTERGRAPH (INGR) digital stereo station.

In a second step, photogrammetric observations of tie points are automatically derived by Inpho’s Match-AT software using the manually measured GCP. Automatically generated tie points are visually checked focusing in strip and photo connections. In weak photo (and/or strip) connection areas, manual insertion is carried out by means of manual edition (manual tie point measurement).

Bundle block adjustment is carried out with the in-house ACX-GeoTex software (Match-AT is exclusively used for the automatic production of photogrammetric observations).

Due to the absence of GPS data and to unknowing the coordinate reference system for the control points coordinates, the bundle block adjustment is performed in Cartesian coordinates. 4 sets of additional parameters have been included in the adjustment: a set of 12 self-calibration parameters per image quarter.

DATA SET ANALYSIS

Data sets have been processed independently.

DMC HG 900m

In this block 16 511 photogrammetric observations of 5 036 tie points (which were automatically derived by Match-AT software), 23 GCP, 21 check points and 55 manual tie points were entered into the bundle adjustment. GCP and check points were stereoscopically measured. The 55 manual tie points were manual and monoscopically measured in the areas where automatically derived tie points showed weak photo and strip connection.

In the bundle block adjustment there is estimated an additional set of 12 self-calibration parameters for each image quadrant.

The *a priori* standard deviations were set to 2 μm for the automatically derived tie points and 6 μm for the manual photogrammetric observations. Accuracy for GCP was set to 3 cm in planimetry and 5 cm in height.

DMC HG 1800m

In this block 6 388 photogrammetric observations of 1 998 tie points (which were automatically derived by Match-AT software), 21 GCP, 20 check points and 30 manual tie points were entered into the bundle adjustment. GCP and check points were stereoscopically measured. The 30 manual tie points were manual and monoscopically measured in the areas where automatically derived tie points showed weak photo and strip connection.

In the bundle block adjustment there is estimated an additional set of 12 self-calibration parameters for each image quadrant.

The *a priori* standard deviations were set to 2 μm for the automatically derived tie points and 6 μm for the manual photogrammetric observations. Accuracy for GCP was set to 3 cm in planimetry and 5 cm in height.

ON THE USE OF ADDITIONAL PARAMETERS

According to ICC experiences (see Alamús et al. 2005, and Alamús 2006) the aero-triangulation of DMC images requires highly accurate control (GPS and ground points) in order to overcome systematic errors in height when appropriate self-calibration parameters cannot be estimated. Since the current data sets do not include any GPS observations it is necessary to estimate an appropriate set of self-calibration parameters in the adjustment.

In Figure 1 the effect of the estimated additional parameters for the 2 blocks DMC HG 900m and DMC HG 1800m is graphically represented. Although the two blocks show similar tendencies there are also presenting some differences in the parameters, this could be due to the fact that the self calibration parameters are also modeling weak block configuration.

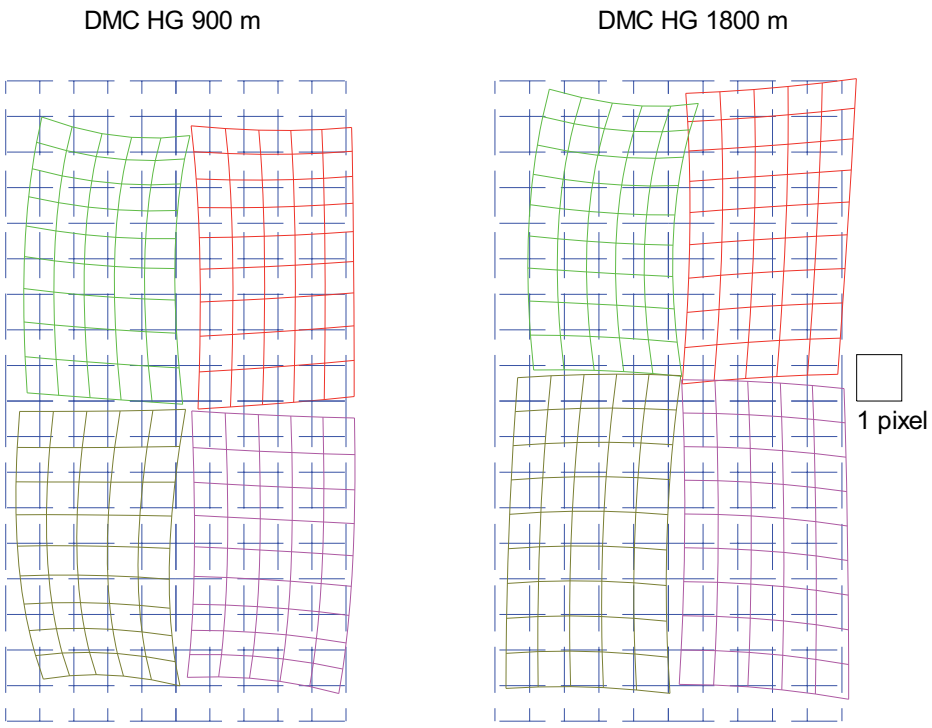

Figure 1: Distortions of additional parameters in the image space for blocks DMC HG 900 m and DMC HG 1800 m.

RESULTS

In this section, results are discussed and check point coordinates are provided.

DMC HG 900m

The check points have been split into 2 groups: A first group of 4 points, which only have been measured in 2 images and a second group of 17 check points, which have been measured at least in 3 images.

Check points adjusted coordinates are in ANNEX 1: DMCHG 900 m.

DMC HG 1800m

13 of the 20 check points are only 2-ray points. Only 7 points (35%) could be identified and measured in more than 2 images, which in this case means 3 images. Obviously, the analysis on the full set of check points including the 13 2-ray check points will be highly affected by the operator pointing accuracy and, thus, shows up the performance of the camera only to a limited extent.

Check points adjusted coordinates are in ANNEX 2: DMCHG 1800 m.

Table 1 shows the adjusted check points of the high altitude block in comparison to the corresponding adjusted coordinates of the low altitude block.

	No.	X [m]			Y [m]			H [m]		
	points	mean	σ	rms	mean	σ	Rms	mean	σ	rms
2-ray	13	0.00	0.04	0.04	0.02	0.05	0.05	-0.04	0.21	0.20
3-ray	7	0.00	0.05	0.05	0.02	0.04	0.04	-0.02	0.13	0.12
all	20	0.00	0.05	0.04	0.02	0.04	0.05	-0.03	0.18	0.18

Table 1: Statistical results comparing adjusted coordinated for check points of the DMC HG 1800m block against the DMC HG 900m block. Units are in meters.

The two check points no. 1 and no.18 are estimated with very high residuals in height of -48 cm and -39 cm, respectively. Both are 2-ray points and situated in areas in the northern corner of the block, where the automatic tie point generation has produced unsatisfactory results, mainly due to unfavourable image illumination conditions. If the points 1 and 18 are excluded from the analysis, an rms height differences of 0.12 m is obtained for all points, which is the same value as for the 6 3-ray-points.

COMMENTS

Despite most of the following comments have been already discussed in sections above, in this section results are commented, focusing specially on the use of additional parameters. Furthermore, the questions of document D_1 are explicitly answered.

"What processing software was used for data evaluation (i.e. point transfer, bundle adjustment)?"

As explained in section above (see subsection workflow):

- GCP have been measured stereoscopically using INGR digital stereo workstations,
- manual tie points have been measured monoscopically using INGR digital stereo workstations,
- automatic tie points have been derived by Match-AT, weak connection areas have been edited adding manual tie points,
- Bundle block adjustment has been performed using ACX-GeoTex.

"What kind of parameter set was used for AT? Is the use of additional parameters necessary? Which model was applied?"

As explained in the section above (see subsection data set analysis), a set of 12 self-calibration parameters per quadrant has been used. In more detail: photogrammetric observations have been split in four groups per image (based on the image coordinates). Each group corresponds to a quadrant (i.e. to a high resolution head image). A single set of 12 self-calibration parameters (as described by Ebner 1975) per quadrant is used.

With this approach, the 4-head convergent geometry of the DMC is considered and, somehow, modeled.

As commented in the sub-sections "on the use of additional parameters", additional parameters are necessary, at least for the current block configuration lacking GPS observations.

"In case you have introduced additional parameter sets within processing, how will this additional parameters be used within further processing chain like DTM generation?"

Optimal use of such parameters should come by implementing the rigorous model applied in AT in the software package used for DTM generation or stereocompilation. As most of commercial software has implemented a more general model, which is different to the one used in AT, an absolute orientation per image of the model has to be performed using adjusted object and image coordinates of tie points in the model.

"Were the two flying heights used separately or in combined approach?"

They were used separately. This way it is possible to evaluate the camera performance at different heights.

As can be seen in figure 1, additional parameters are significantly different at different flying heights. Moreover, only GCP and check points are common in both blocks. These two facts do not support the convenience of processing both flights together.

"What are the general findings obtained from this specific data set? What is your personal feeling on the data quality and performance of this specific data set?"

Geometric data quality and performance is consistent with our personal experience with DMC data. Image quality is not discussed because ICC focused on geometric aspects and 12-bit images could not be analyzed.

"What are your personal experiences with other digital sensor flights of the same type of sensor (in case such experience is available)? Does this result match the experiences from former flights?"

The results are consistent with the ICC experience with the first digital camera of the ICC.

"What is your personal recommendation on optimal processing flow for this specific type of digital sensor data? How will you handle such kind of data in future?"
We can not fully answer this question because to our opinion the optimal processing flow should include GPS observations, which are not available in that case.

ANNEX 1: DMCHG 900 m

In this section it is included the file with the adjusted check points coordinates. Notice that points have been separated in 2 parts: the first one is the relation of 4 check points with only 2 photogrammetric observations; the second part is the relation of 17 points with more than 3 photogrammetric observations.

The following list has the check point adjusted coordinates, its theoretical standard deviations and correlations. Units are in meters.

… deleted by M. Cramer …

ANNEX 2: DMCHG 1800 m

In this section it is included the file with the adjusted check points coordinates. Notice that points have been separated in 2 parts: the first one is the relation of 13 check points with only 2 photogrammetric observations; the second part is the relation of 7 points with 3 photogrammetric observations.

The following list has the check point adjusted coordinates, its theoretical standard deviations and correlations. Units are in meters.

… deleted by M. Cramer …

REFERENCES

Alamús R., Kornus W., Palà V., Pérez F., Arbiol R., Bonet R., Costa J., Hernández J., Marimon J., Ortiz M.A., Palma E., Pla M., Racero S., Talaya J., 2005. Validation process of the ICC digital Camera. In: ISPRS Hannover workshop 2005 "High-Resolution Earth Imaging for Geospatial Information", 17-20th May 2005, Hannover (Germany) – on CD-ROM.

Alamús R., Kornus W., Talaya J., 2006. Studies in DMC Geometry. In: ISPRS Journal of Photogrammetry and Remote Sensing Theme issue "Digital aerial cameras", to be published.

Ebner, H., 1975. Automatische Kompensation Systematischer Fehler bei der Blockausgleichung mit Unabhängigen Modellen. In: Vorträge des Lehrgangs Numerische Photogrammetrie (III). Esslingen 1975. Institut für Photogrammetrie, Universität Stuttgart Schriftenreihe, Heft 1, 1976.

Institut für Photogrammetrie und GeoInformation
Universität Hannover

Nienburger Str. 1
D-30167 Hannover

Tel.: ++49-511/762-2485
Fax: ++49-511/762-2483
e-mail: jacobsen@ipi.uni-hannover.de
http://www.ipi.uni-hannover.de

Dr.-Ing. Karsten Jacobsen

Hannover, May, 25th ,2006

EuroSDR digital camera test

Investigation of DMC block Fredrikstad, Norway

1. STATISTICS

block configuration:

113 images flying height: 988m, mean ground height 67m image scale 1 : 7 667
34 images flying height: 1866m, mean ground height 65m image scale 1 : 15 003

An automatic aero triangulation has been made with LPS, the block adjustment and analysis has been made with the Hannover program system BLUH.

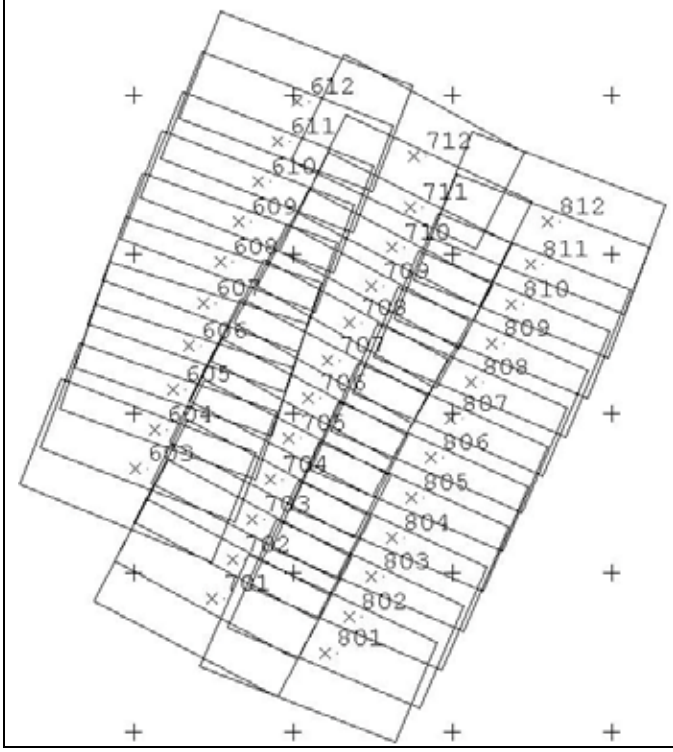

Fig. 1: configuration of upper flight level

the image numbers have been changed like shown to ascending numbers in the flight lines

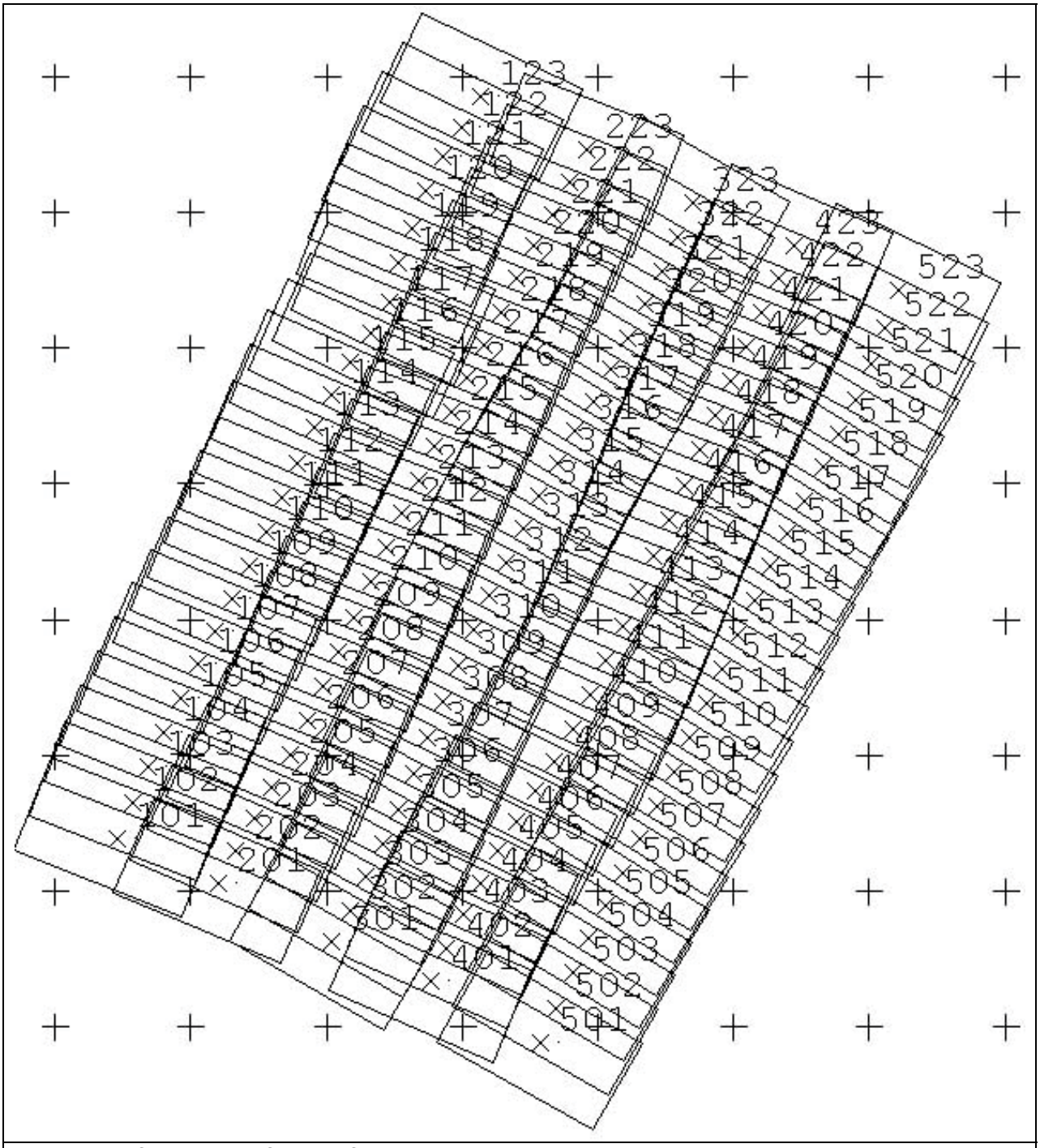

Fig. 2: configuration of lower flight level

the image numbers have been changed like shown to ascending numbers in the flight lines

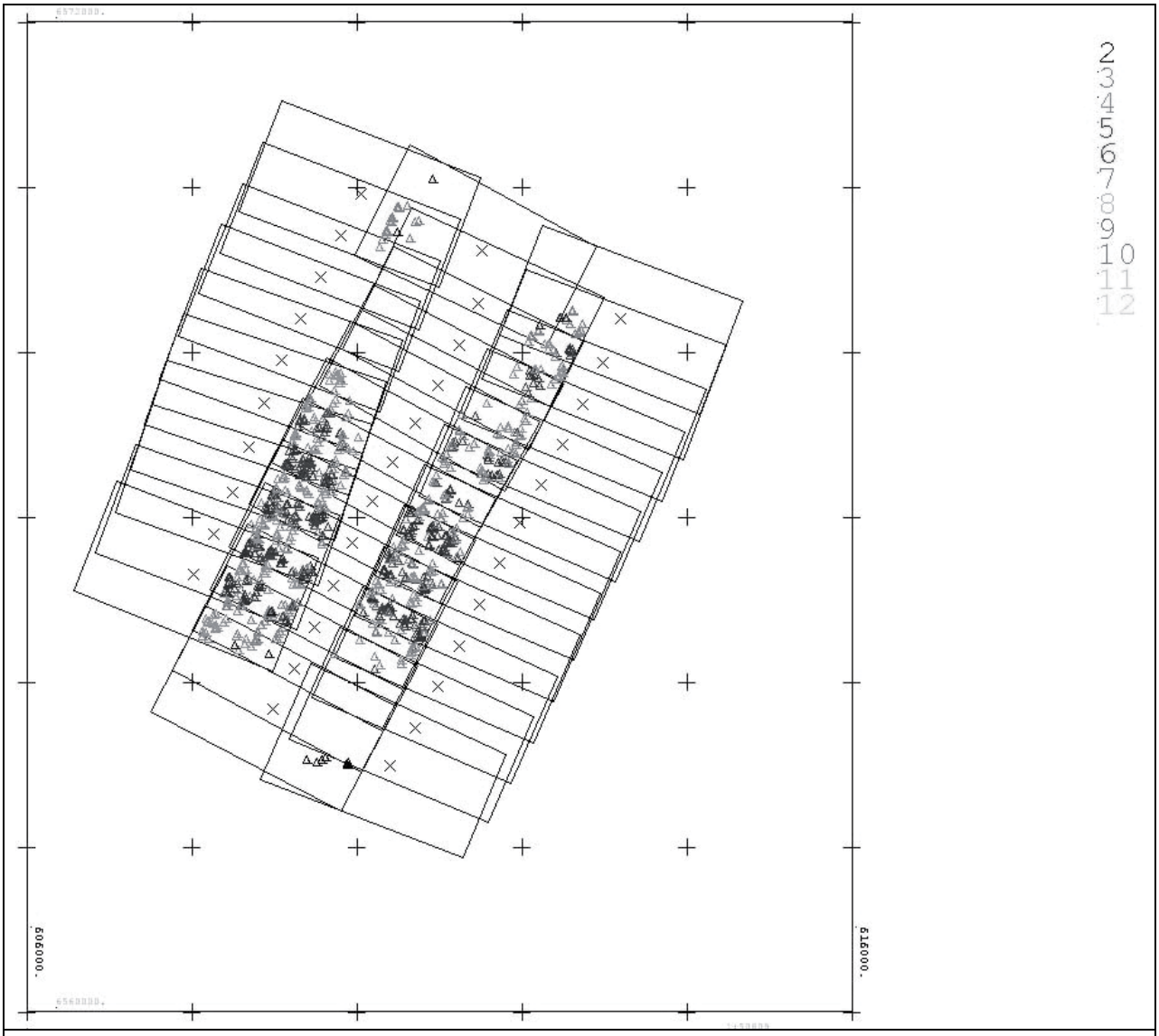

Fig. 3: tie points of flight lines upper flight level
the colour corresponds to the number of images / point (see upper right)

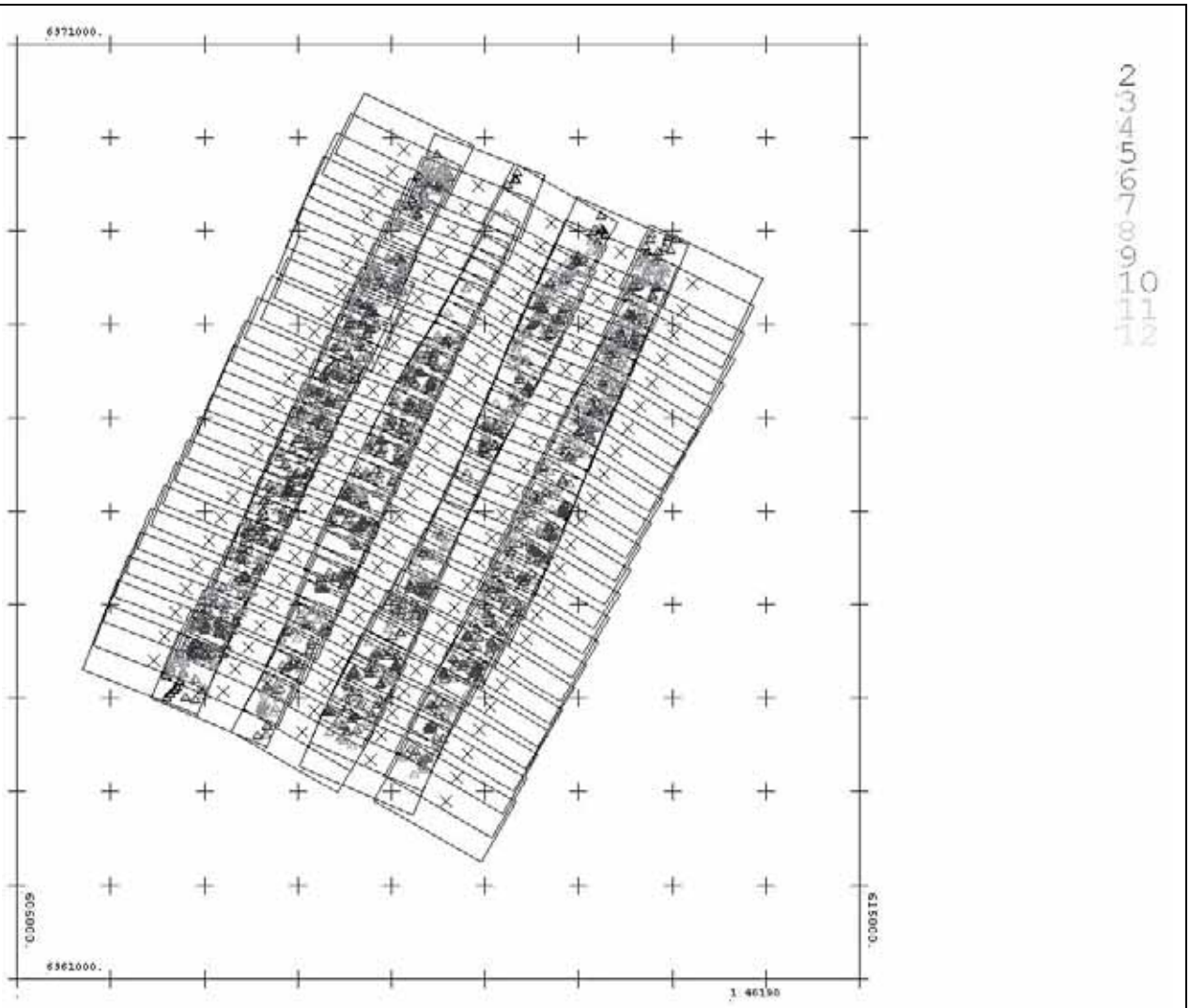

Fig. 4: tie points of flight lines lower flight level
the colour corresponds to the number of images / point (see upper right)

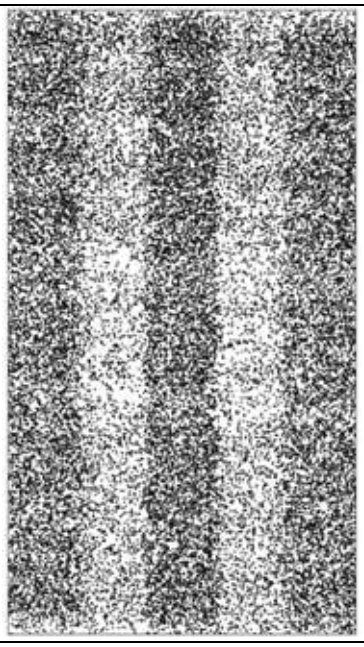

Fig. 5: distribution of points in the images – overlay of all images

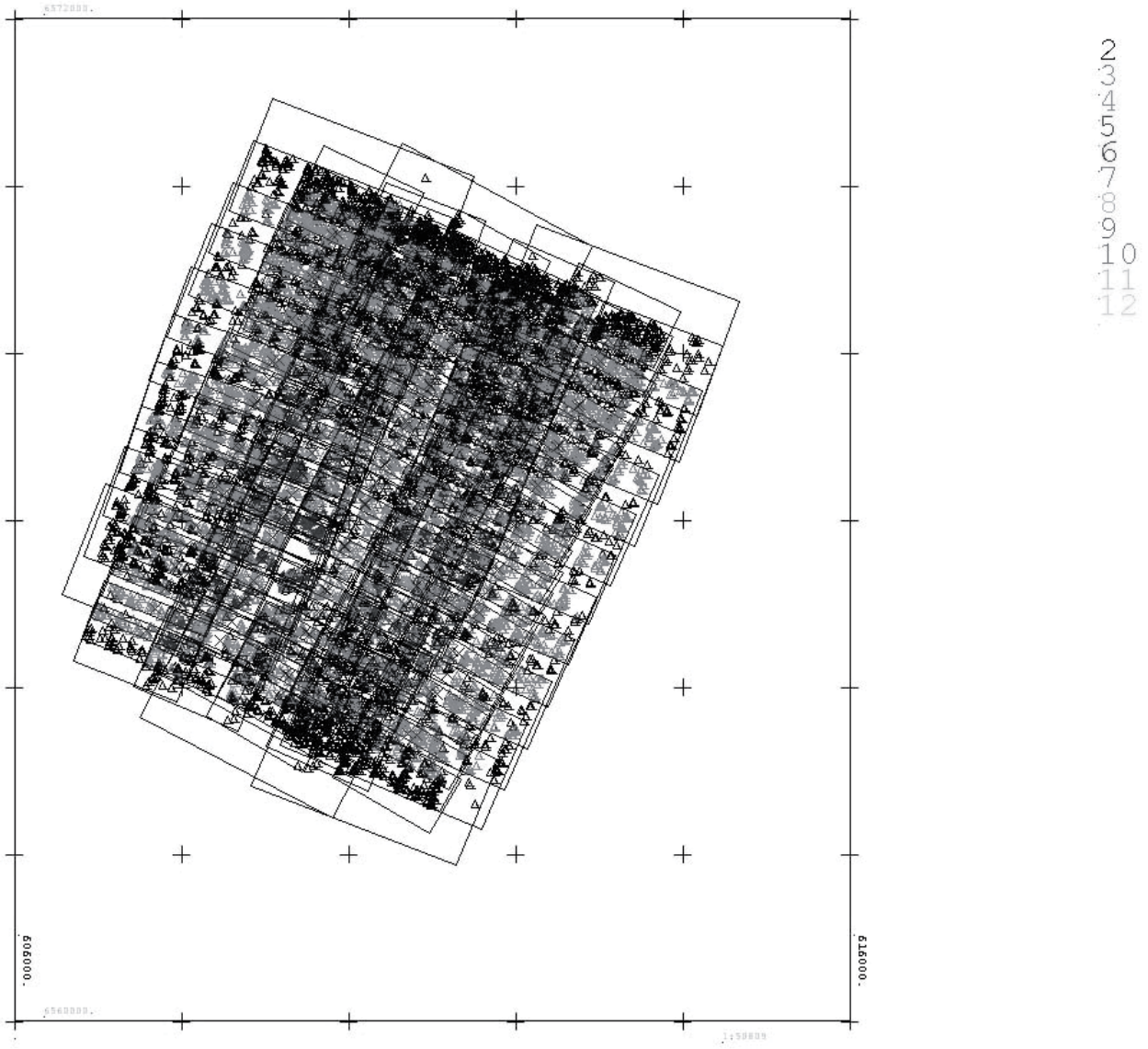

Fig. 6: all points of the full block
colour coded corresponding to the number of images / points (see upper right)

```
NUMBER OF PHOTOS/OBJECT POINT
 PHOTOS/POINT     2     3     4     5     6     7     8     9    10
 POINTS:       4610  5778   853   945   551    11     6     3     3

 MAX PHOTOS/POINT           :     12
 OBJECT POINTS              :  12761
 PHOTOS                     :    149
 PHOTO POINTS               :  38191

 MINIMUM AND MAXIMUM OF PHOTO COORDINATES
  X MINIMUM =  -45.873  X MAXIMUM =   45.887
  Y MINIMUM =  -82.730  Y MAXIMUM =   82.737
```

NUMBER OF POINTS PER PHOTO
==========

101	141	102	202	103	202	104	180	105	171
106	174	107	178	108	174	109	152	110	170
111	176	112	181	113	182	114	176	115	185
116	221	117	256	118	247	119	248	120	239
121	284	122	295	123	205	201	122	202	188
203	194	204	156	205	155	206	158	207	164
208	160	209	155	210	177	211	196	212	189
213	194	214	186	215	207	216	238	217	263
218	274	219	261	220	222	221	336	222	463
223	328	301	94	302	137	303	163	304	161
305	155	306	151	307	138	308	158	309	167
310	167	311	165	312	144	313	146	314	169
315	193	316	217	317	224	318	202	319	214
320	216	321	273	322	315	323	231	401	101
402	156	403	156	404	158	405	149	406	166
407	164	408	167	409	160	410	168	411	166
412	174	413	160	414	166	415	187	416	223
417	231	418	237	419	244	420	256	421	239
422	233	423	175	501	103	502	153	503	146
504	133	505	140	506	138	507	138	508	134
509	137	510	143	511	149	512	158	513	144
514	145	515	168	516	200	517	205	518	213
519	235	520	245	521	243	522	251	523	175
603	459	604	665	605	645	606	633	607	605
608	525	609	496	610	501	611	501	612	330
701	331	702	513	703	538	704	542	705	546
706	554	707	494	708	442	709	393	710	406
711	409	712	240	801	295	802	490	803	471
804	500	805	528	806	497	807	516	808	468
809	424	810	476	811	496	812	305		

General information about data acquisition and block characteristics

Figures 3 and 4 indicate problems of the flight lines tie. This is caused by forest in these areas. It was not possible to get reliable tie points between the flight lines in the area around images 610 / 710 in the upper flight level and 220 / 320 as well as 311 / 411. We tried to add manual measured points but this also failed.

Not all control and check points are reliable; they could not be measured in all theoretic possible images because of the forest. In addition the point identification was very difficult. By this reason the block is not optimal for test of the best data handling, but nevertheless an analysis of the image geometry for systematic image errors is possible. Because of the just parallel flight lines the systematic image errors cannot be separated totally from the influence of the control points – for such an analysis crossing flight lines should be used.

The points are distributed well in the images (figure 5), so systematic image errors can be analysed well.

2. ADDITIONAL PARAMETERS

The detailed analysis has been made with program system BLUH. BLUH includes general additional parameters and a set of parameters especially fitted to the geometry of the DMC as well as the UltraCam. The self calibration with additional parameters is able to determine geometric discrepancies between the mathematical model of perspective images and the real image geometry – this difference is called “systematic image errors” even if it is an error of the mathematic model.

The additional parameters may be correlated. High correlations may cause geometric problems in block areas not well supported by control points. By this reason in program BLUH the additional parameters are checked for correlation, total correlation and by Student-test. Too high correlated parameters and parameters with too small Student – test values are removed automatic from the adjustment.

Additional parameters in BLUH

```
1 = ANGULAR AFFINITY
2 = AFFINITY
3 - 6 = GENERAL DEFORMATION
7 - 8 = TANGENTIAL DISTORTION
9 = RADIAL SYMMETRIC R*R*R  10 - 11 RADIAL SYMMETRIC HIGHER DEGREE
12 = GENERAL DISTORTION

13 = FOCAL LENGTH  14, 15 = PRINCIPAL POINT
   FOR COMBINED ADJUSTMENT WITH GPS 13 - 15 REQUIRED FOR GPS-SHIFT
16 - 18 POSSIBLE GPS-DRIFT   19-20 GPS-DATUM  21= T*T
22 - 26 FOR PANORAMIC CAMERA
27 - 28 RADIAL SYMMETRIC FOR FISHEYE
29      DMC EXCENTRICITY   30 - 33 DMC SYNCHRONIZATION
34 - 41 DMC PERSPECTIVE DEFORMATION OF SINGLE CAMERAS
42 - 49 ULTRACAM SCALE  50 - 65 ULTRACAM SHIFT  66 - 73 ULTRACAM ROTATION
74 - 77 DMC RADIAL SYMMETRIC ORIGINAL IMAGES  78 - 81 DMC FOCAL LENGTH
ORIGINAL IMAGES
```

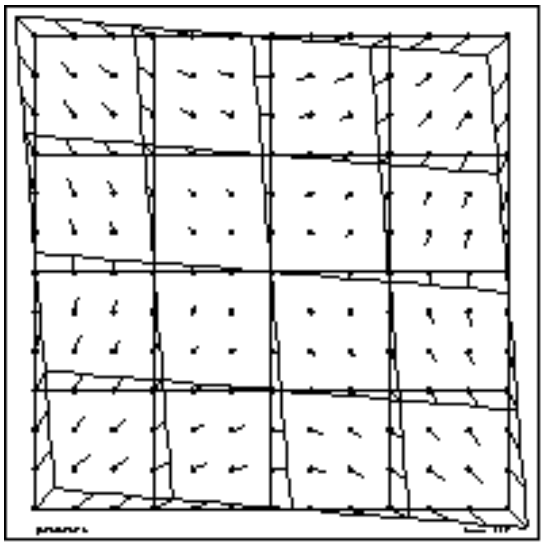

parameter 1

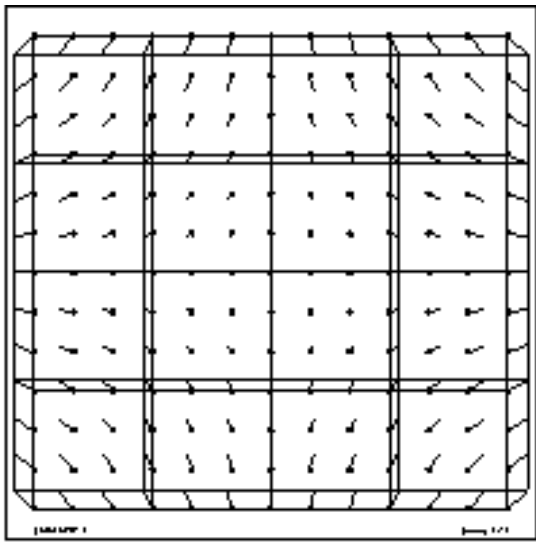

parameter 2

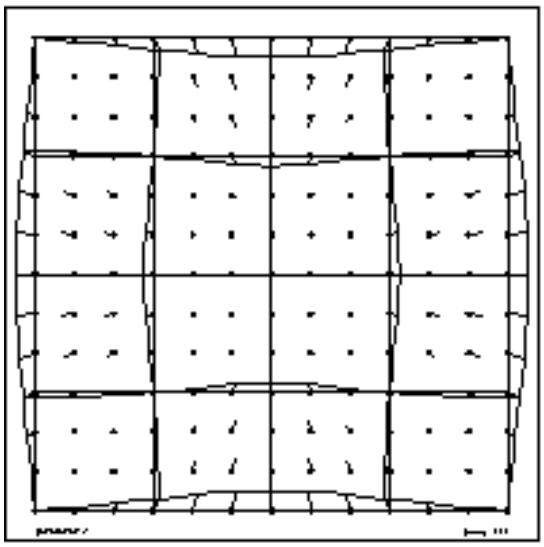

parameter 3 ↑

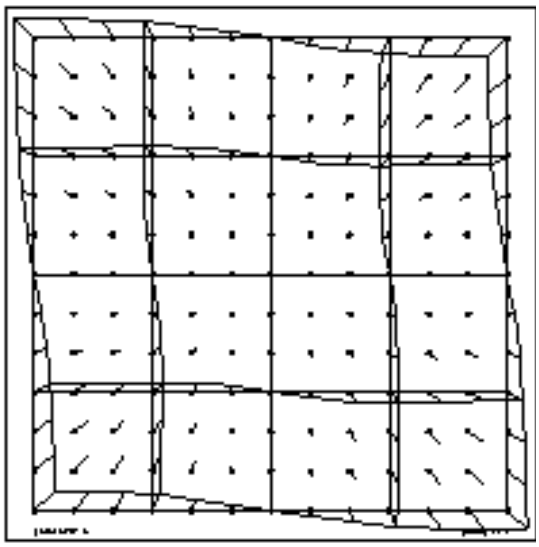

parameter 4 ↑

parameter 5 ↓

parameter 6 ↓

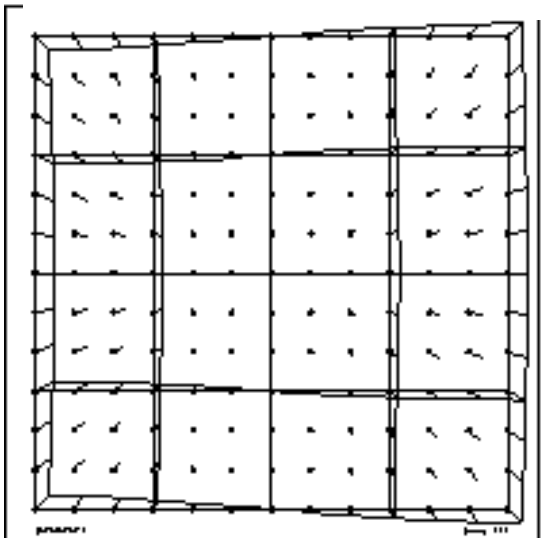

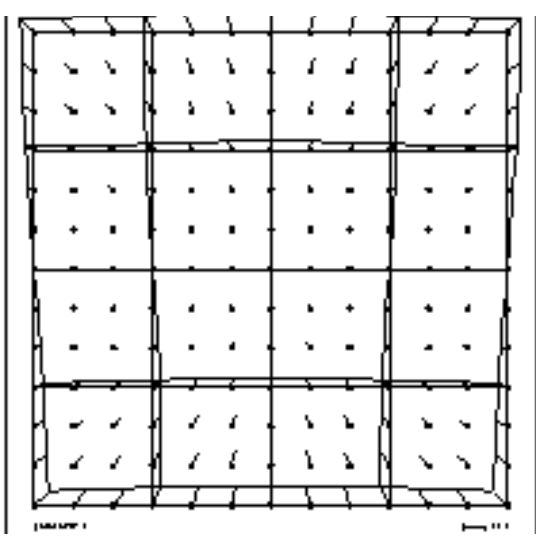

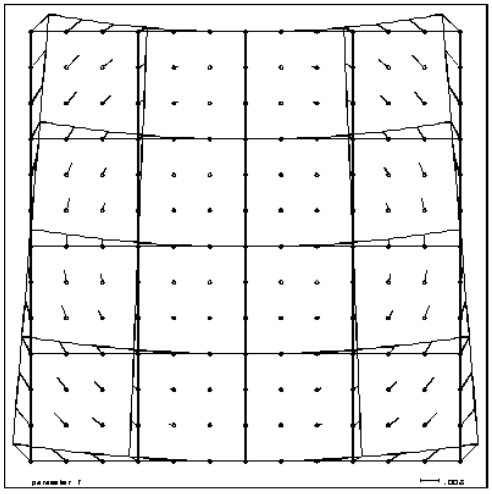

parameter 7

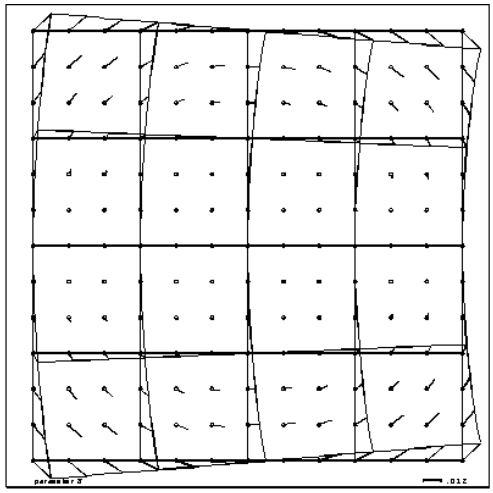

parameter 8

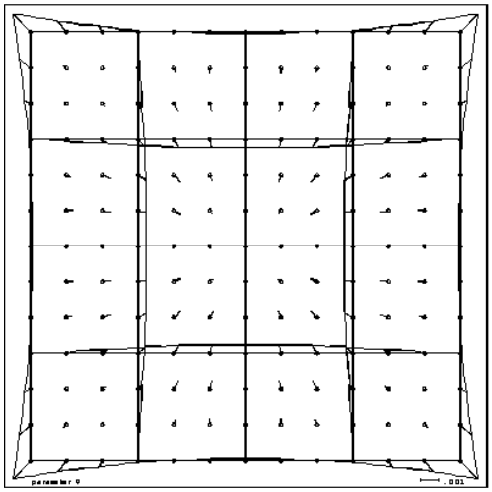

parameter 9 ↑

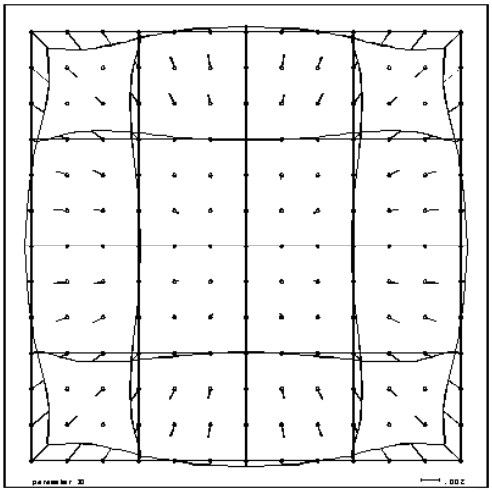

parameter 10 ↑

parameter 11 ↓

parameter 12 ↓

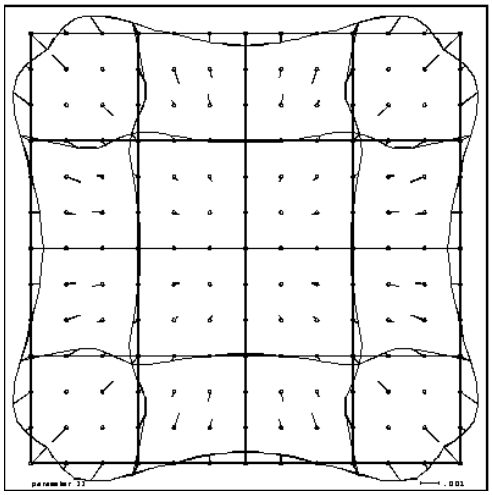

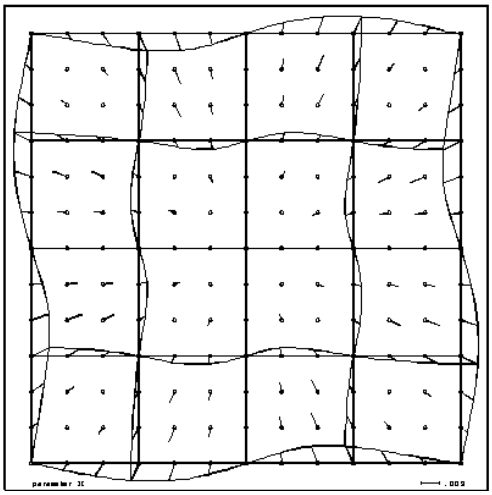

Special additional parameters for DMC in program system BLUH:

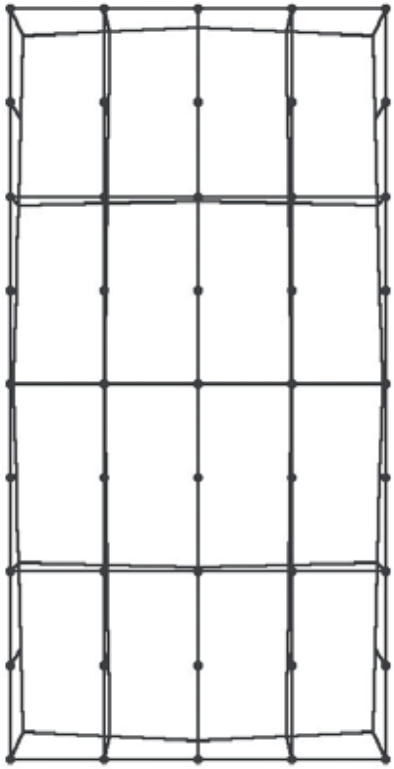

29: Influence of offset of the 4 panchromatic cameras:

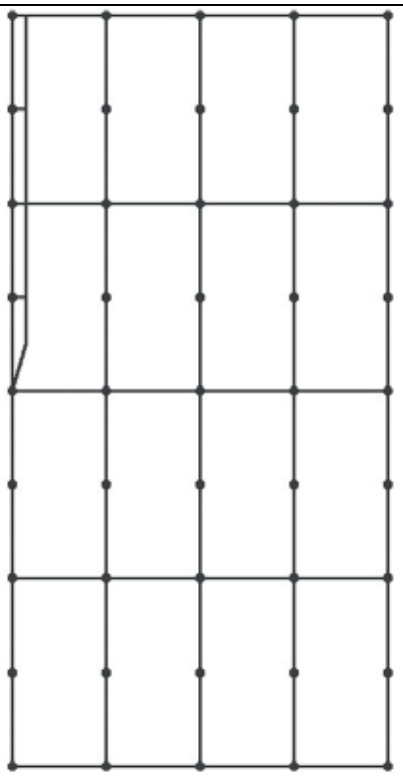

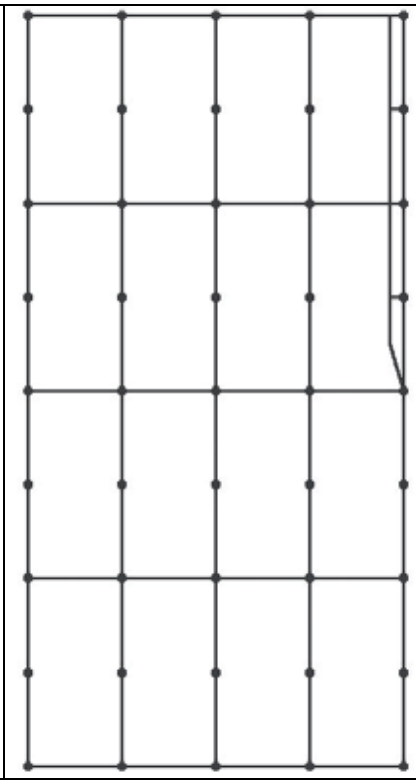

parameter

32 33

for synchronization error of individual cameras

$x' = x + P32 * (x^2 - 32x)$

32	33
31	30

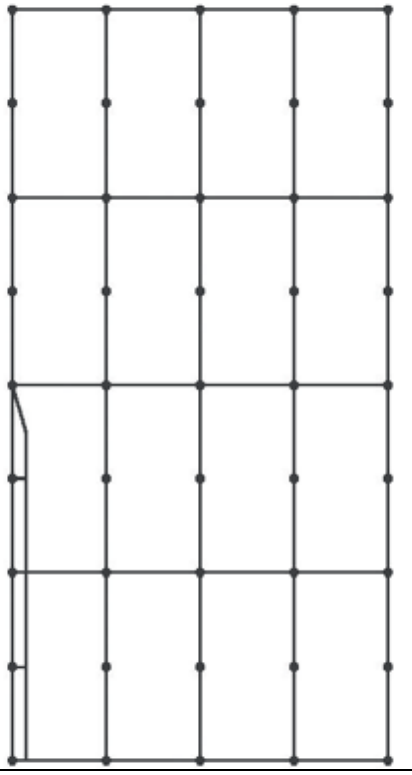

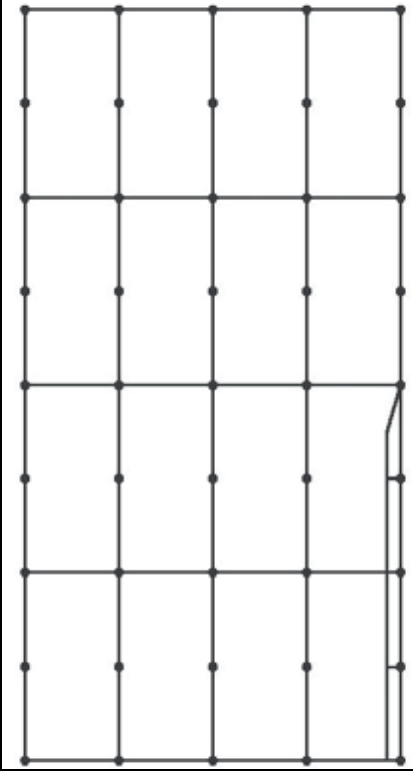

parameter

31 30

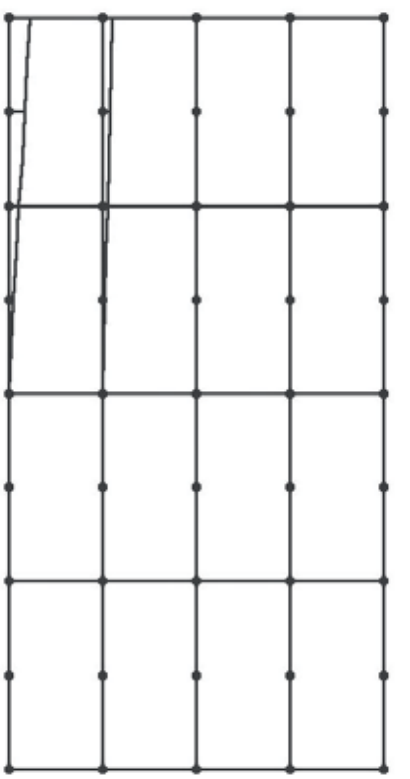

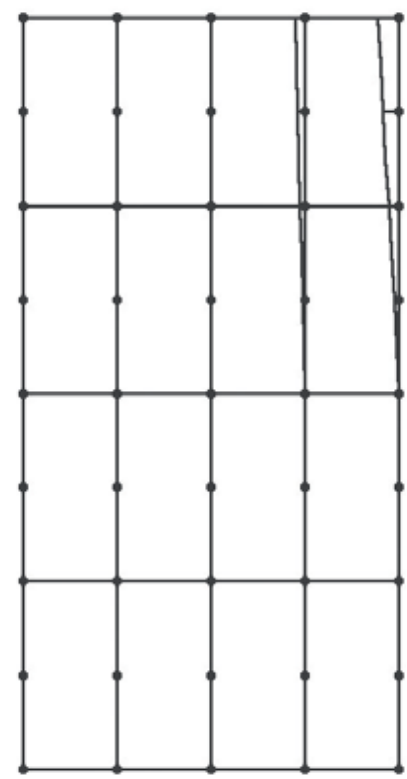

parameter 36 37

x-part of orientation error of individual camera

x’=x+P36*x*y

36	37
35	34

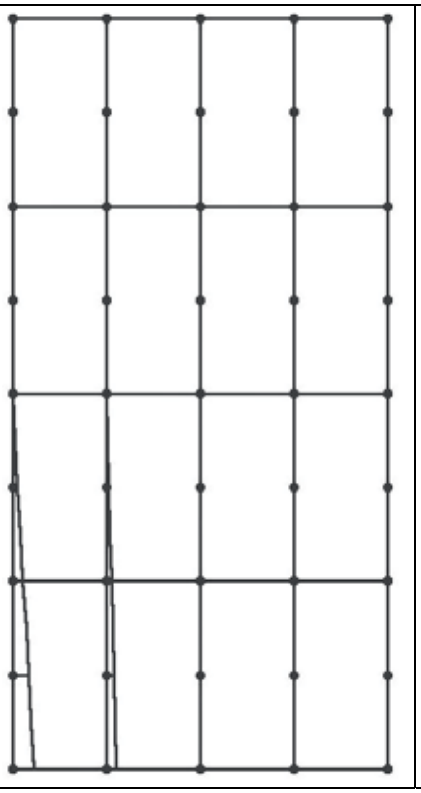

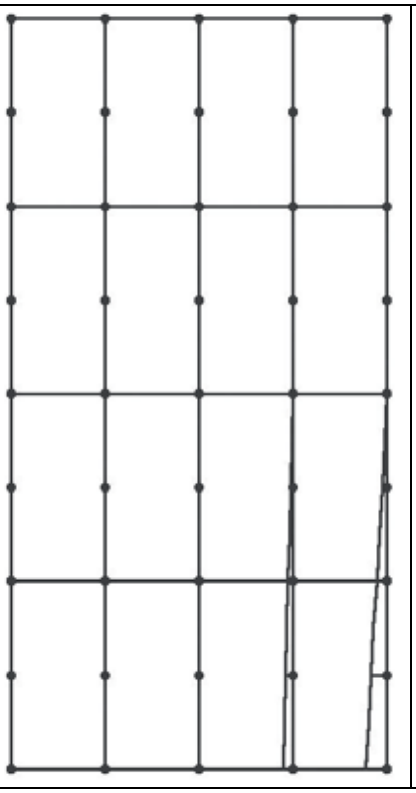

parameter 35 34

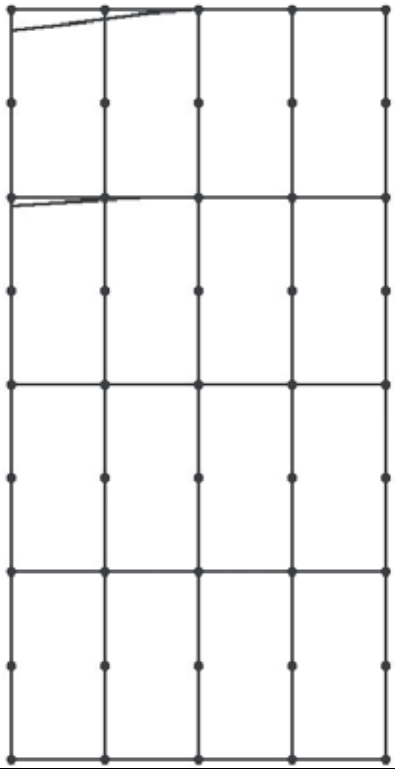

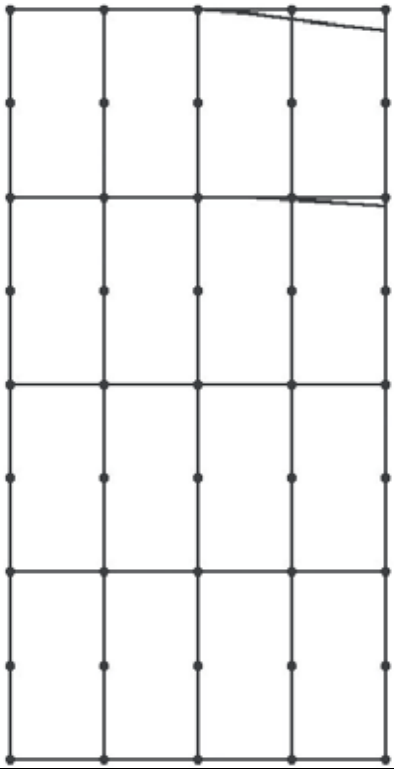

parameter 40 41

y-part of orientation error of individual camera

y'=y+P40*x*y

40	41
39	38

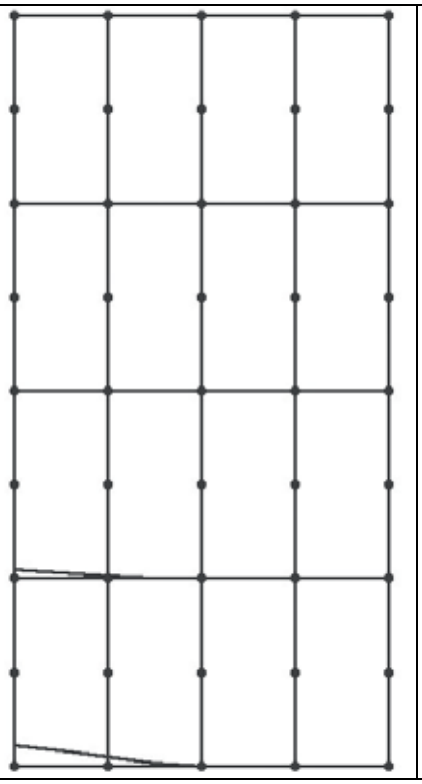

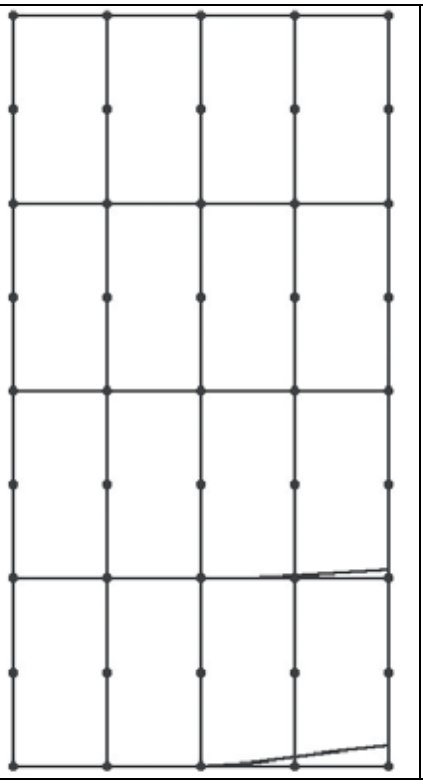

parameter 39 38

parameters 74 – 77: radial symmetric parameters for original DMC panchromatic cameras

The additional parameters 74 – 77 can determine radial-symmetric effects of the original panchromatic DMC cameras. These cameras are rotated against the artificial image plane in the x-direction approximately +/-10.1° and in the y-direction approximately +/-17.9°. The original sub-images do have 4096 x 7168 pixels with a pixel size of 12µm. In the original sub-images following formulas are used:

$x' = x + (r^2 - 1849) * x*r \qquad y' = y + (r^2 - 1849)*y*r$

This relation exists for all the 4 cameras separately and the geometric effect is projected to the artificial image plane.

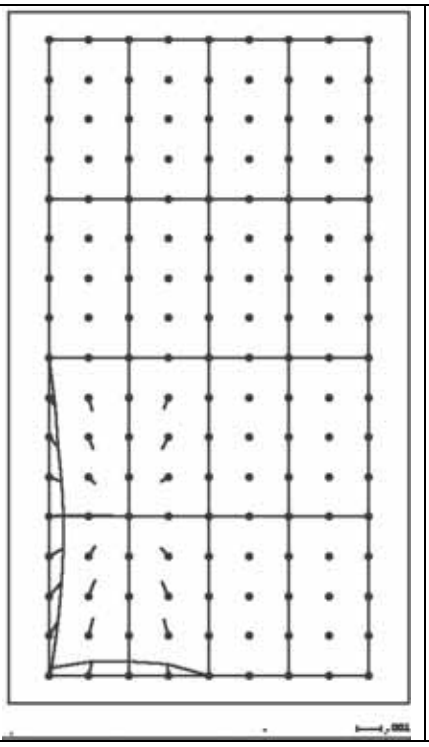

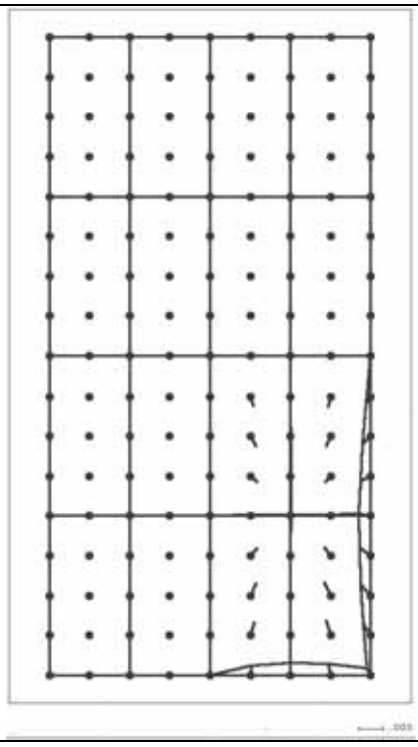

parameter 75 (left)
74 (right)

75 74

for $r^3 - c*r$ in original sub-images projected to reference plane

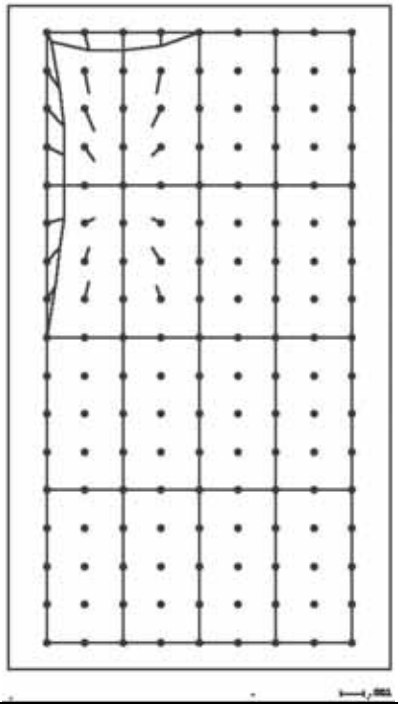

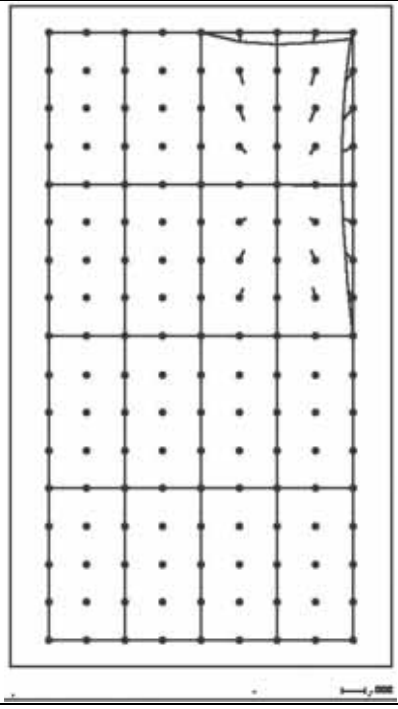

parameter 76 (left)
77 (right)

76 77

for r^3 -c*r in original sub-images projected to reference plane

parameters 78 – 81: remaining influence of focal length of original DMC panchromatic cameras

Difference in the image scale is respected by fitting the 4 panchromatic sub-images of the DMC together. A remaining influence may be still available. The linear component of differences in the focal length may be still present. This second order effect can be fitted with the additional parameters 78 – 81.

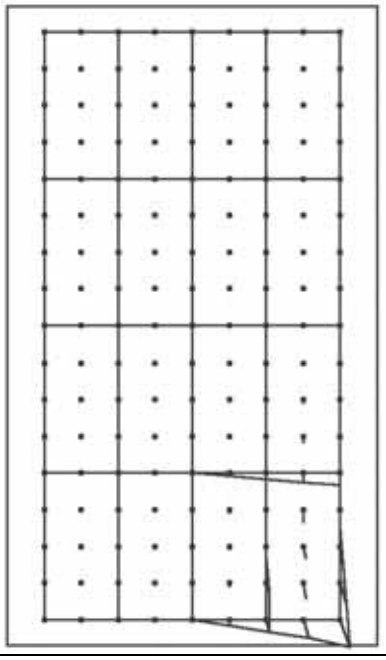

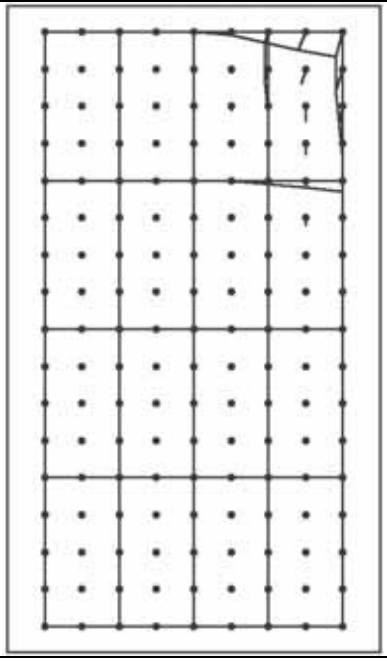

parameter 78 (left)
81 (right)

80 81
79 78
arrangement of additional parameters

79 and 80 do have a corresponding effect

3. ANALYSIS OF BLOCK FREDERICKSTAD

Only control points have been available, an analysis with check points was not possible.

	add. parameters	used	sigma0	RMSX	RMSY	RMSZ
1	without		3.94	5.9	3.0	14.9
2	1 - 12	2,3,5,7-10,12	3.89	5.4	2.4	5.8
3	**1-12 A**	**1H,2-5H+L,7-10H+L,12H+L**	**3.88**	**5.1**	**2.7**	**4.9**
4	29-41,74-81	30-36,38,74-81	3.87	7.4	3.6	13.8
5	30-36,74-81 A	25 parameters	3.86	7.5	3.9	12.6
6	1-12,30-36,74-81	22 parameters	3.83	5.0	2.3	6.3
7	**1-12,30-36,74-81 A**	**40 parameters**	**3.81**	**4.6**	**2.5**	**6.0**

Table 1: comparison of different block adjustments
add. parameters = initiated additional parameters A = separate for upper and lower flying height
used = finally used parameters H=upper L=lower flying height

The numbers in the first column are corresponding to the results e.g. adjusted ground coordinates of adjustment without additional parameters in daxyz.1

Program BLUH shows the discrepancies at the control point based on the adjusted orientation and a common intersection – this is a realistic estimation of the problems at the control points not splitting of the error component of the image coordinates. Most programs are showing only an unrealistic small part of the discrepancies which can be manipulated very easy to any result. By this reason a comparison of the results cannot be based on the root mean square discrepancies at the control points, only a comparison with independent check points is possible. But in this case the manual identification of the check points was very difficult leading mainly to a comparison of random pointing accuracy of the check points.

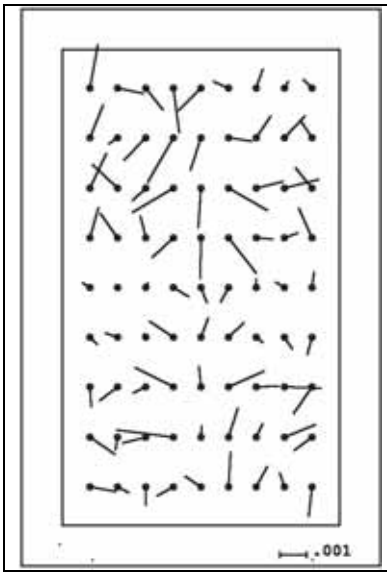

Fig. 7: averaged image coordinate residuals of block adjustment without additional parameters

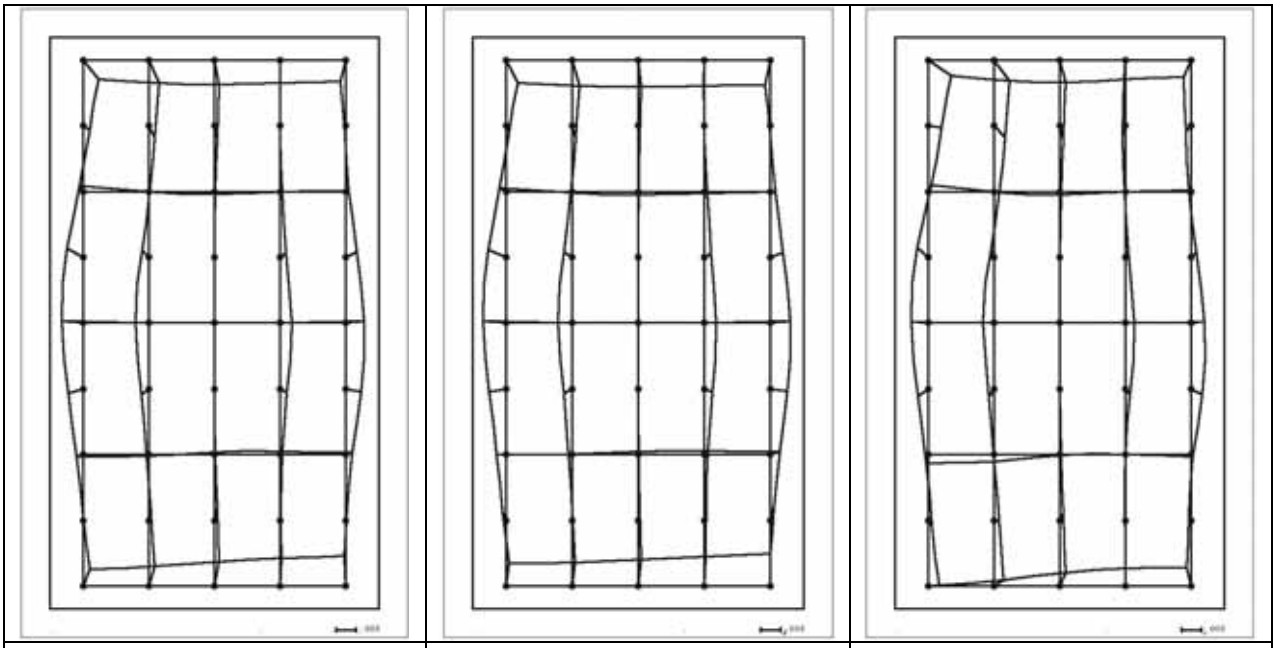

case 2	case 3 lower images	case 3 upper images

Fig. 8: systematic image errors

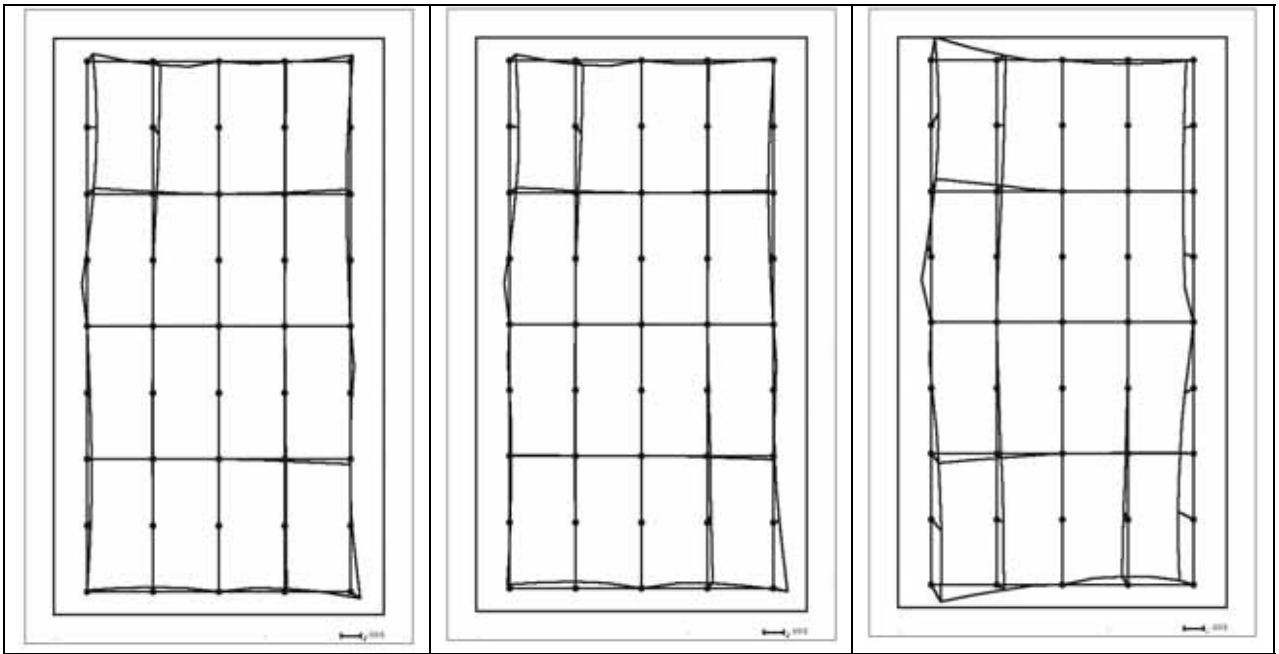

case 4	case 5 lower images	case 5 upper images

Fig. 9: systematic image errors

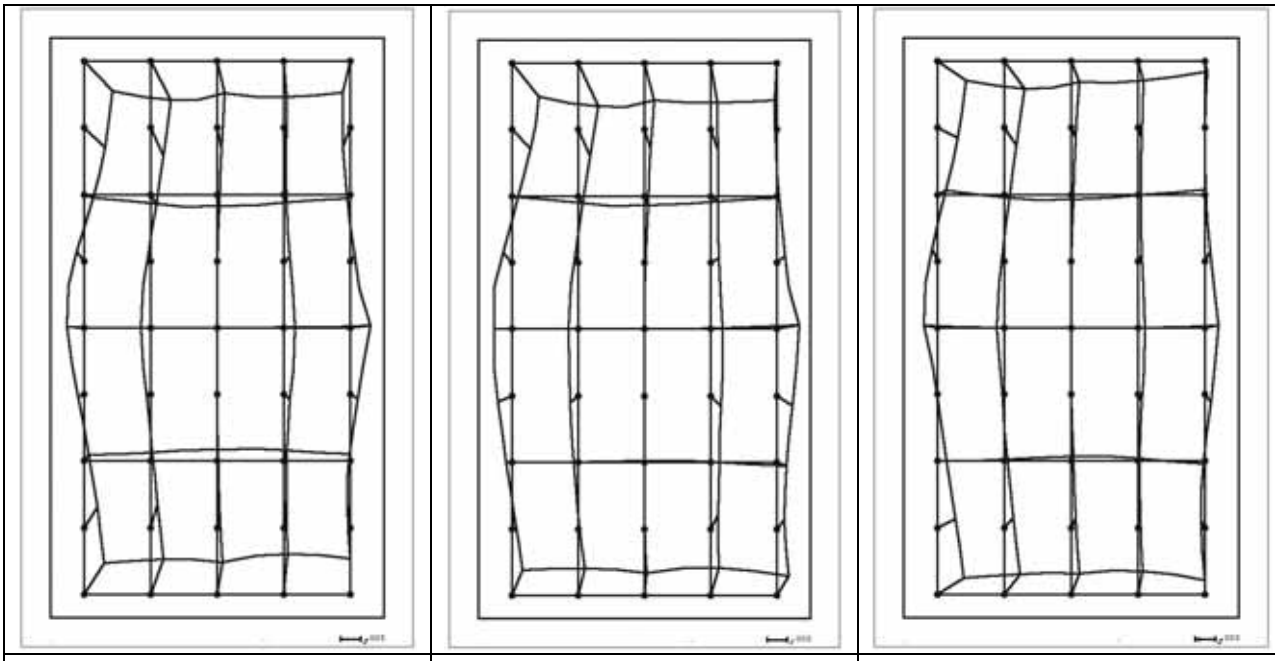

case 6	case 7 lower images	case7 upper images

Fig. 10: systematic image errors

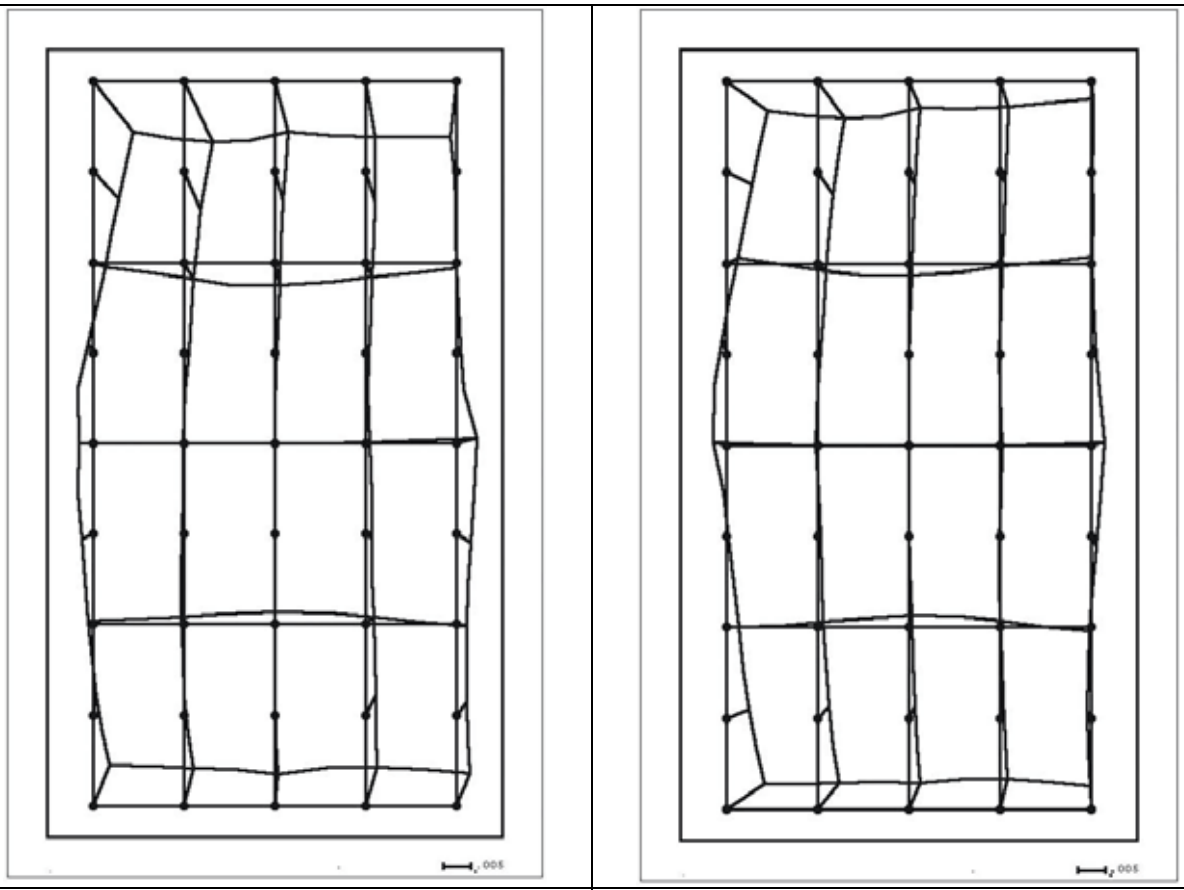

case 7 lower images without radial symmetric component	case7 upper images without radial symmetric component

Fig. 11: systematic image errors without radial symmetric component

There is no doubt an adjustment with self-calibration by additional parameters is required.

The dominating part of the systematic image errors can be fitted with the standard additional parameters (1-12) of program BLUH. The special additional DMC parameters do have only a limited influence and over all they are not really improving the adjustment. Like in the case of the block adjustment of the DMC block Rubi from ICC Barcelona the block adjustment can be handled without loss of accuracy by the general additional parameters. This was also the case for an analysis of UltraCam data over Istanbul.

The special DMC parameters are not able to fit the systematic effects, in addition the general parameters have to be used.

Institut für Photogrammetrie und GeoInformation
Universität Hannover

Nienburger Str. 1
D-30167 Hannover

Tel.: ++49-511/762-2485
Fax: ++49-511/762-2483
e-mail: jacobsen@ipi.uni-hannover.de
http://www.ipi.uni-hannover.de

Dr.-Ing. Karsten Jacobsen

Hannover, 26.6.2006

EuroSDR DMC camera test Frederikstad

Separate computation for lower and upper flying height

lower flying height: root mean square differences [cm]

	add par	control points			sigma0	check points		
1	without	7.7	4.2	13.3	4.23	6.8	6.0	13.8
2	1 -12	4.2	2.3	5.2	4.19	3.6	3.9	9.2
6	1-12,30-36,74-81	4.0	2.5	5.6	4.13	3.4	4.0	8.8

upper flying height: root mean square differences [cm]

	add par	control points			sigma0	check points		
1	without	7.1	4.7	27.2	3.41	7.2	5.4	26.9
2	1 -12	5.1	3.6	12.0	3.34	6.8	6.1	16.2
6	1-12,30-36,74-81	4.6	3.5	12.3	3.31	7.6	6.0	16.6

What processing software has been used for data evaluation?

MATCH-AT for point measurement/extraction/transfer and adjustment. InBlock for ppa and fc determination.

What kind of parameter set was used for AT? Is the use of additional parameter necessary? Which model was applied?

DMC data set : different models used (12 Ebner, 44 Grün and Brown) but no significant need for additional parameters could be detected for this data set.

UltraCam: different models used (12 Ebner, 44 Grün and Brown) systematic corrections are more significant compared to DMC for this data set. (compare attached file with image residual plots)

In case you have introduced additional parameters set within processing, how will this additional parameters be used within further processing chain like DTM generation?

Corrections from additional parameters are stored as a calibration grid and will be used in all additional production steps.

Were the two flying heights used separately or in a combined approach?

Two flying height were processed separately for point extraction, merged and final adjustment with MATCH-AT has been done with both flying height in one data set.

What are the general findings obtained from this specific data set ? What is your personal feeling on the data quality and performance of the this specific data set?

It was quite difficult to identify control/check points. Without the given orientation, this step would have been quite sensitive to identification errors.

INPHO GmbH
Smaragdweg 1
70174 Stuttgart - Germany

Tel.: +49 711 2288 10
Fax: +49 711 2288 111

E-mail: tobias@inpho.de
Web: www.inpho.de

What are your personal experiences with other digital sensor flights of the same type of sensor? Does this result match the experiences from former flights?

Yes, for both camera types there have been blocks processed where systematic errors could be seen in image residuals after block adjustment. But quite often these errors become only visible in blocks with greater extensions (some hundreds images).

What is your personal recommendation on optimal processing flow for this specific type of digital sensor data? How will you handle such kind of data in future?

We expect in future “more stable” calibrated cameras from the manufacture side. I hope that they will better understand the geometrical behaviour of the cameras due to their practical experiences. Large format cameras need to be as stable so that on the fly calibration are not needed for standard applications. On sight calibration can be expensive due to additional overhead. Having 2 different flying heights is no standard application case in aerial projects and it is questionable if customers would pay for this additional calibration procedure. INPHO's software has possibilities to check for remaining systematic image deformations and a possibility to create “new calibrated” cameras by adding a correction grid which is used during further processing. This is important for QA/QC procedures. We think that with this concept we can handle the current available digital frame cameras and the related issues. But the goal for all photogrammetric multihead large format cameras should be the ability to create ideal virtual images which are geometrically and radiometrically corrected to an expected quality level during the after flight postprocessing.

INPHO GmbH
Smaragdweg 1
70174 Stuttgart - Germany

Tel.: +49 711 2288 10
Fax: +49 711 2288 111

E-mail: tobias@inpho.de
Web: www.inpho.de

EuroSDR Test Phase 2 – Digital Camera Calibration – DMC data sets

Report

HFT-Stuttgart Results

July 2006

Natalia Zheltukhina, Moscow State University of Geodesy and Cartography

(as part of a Diploma Thesis at Stuttgart University of Applied Sciences)

glazastick@yandex.ru

and

Prof. Dr.-Ing. Eberhard Gülch, Stuttgart University of Applied Sciences

eberhard.guelch@hft-stuttgart.de

Abstract

In this research were used two digital aerial triangulation programs: MATCH-AT 4.0.6 and PhotoMod 4.0.398. Both were applied to the EuroSDR Camera calibration data sets DMC-low and DMC-high. As a result the adjusted coordinates of unknown check points and this report are delivered. Both aerial blocks have been triangulated independently from each other. This work is part of the Diploma Thesis of Mrs. Natalia Zheltukhina during her stay at Stuttgart University of Applied Sciences.

Data sets and preparations

Two blocks of the EuroSDR DMC data set were used. They were two blocks of panchromatic aerial images, made from different heights with the Z/I Imaging DMC camera.

Test size extension - 5×6,5 km; main flight direction from northwest to southwest. Uncompressed images 16bit/pix were wrongly defined (they were overexposed and most part of information were lost due to a bug in the Intergraph conversion software used by the EuroSDR pilot center). This bug was reported and as a consequence the raw format images were used. Raw format images are in tiled tiff format, jpeg compressed, 12bit/pix. They could be directly used in MATCH-AT, for working with these images in PhotoMod they were converted to 8 bit/pix. Coordinates of ground control points (GCP) are known with several mm accuracy. Also results from a priory PatB bundle adjustment, to be used, as approximate exterior orientation, and sketches of GCP and of check points were available. As well their coordinates of check points were given with 1m accuracy to lighten the process of finding them in the images. Still some of the points were rather difficult to identify and to measure.

The first block - project DMC_low: flying height 950 m, scale ≈ 1:7900, 5 long strips (115 images), no cross lines, approximate 60% forward lap and 30% side lap, 23 ground control points and 21 check points (cf. also Figure 1). The pixel size is 12 µm.

Expected accuracy for this block:

$$dz \approx 0{,}01\% \times H_f = 0.095m$$

$$dx = dz \approx 5\mu m \times scalefactor = 0.039m$$

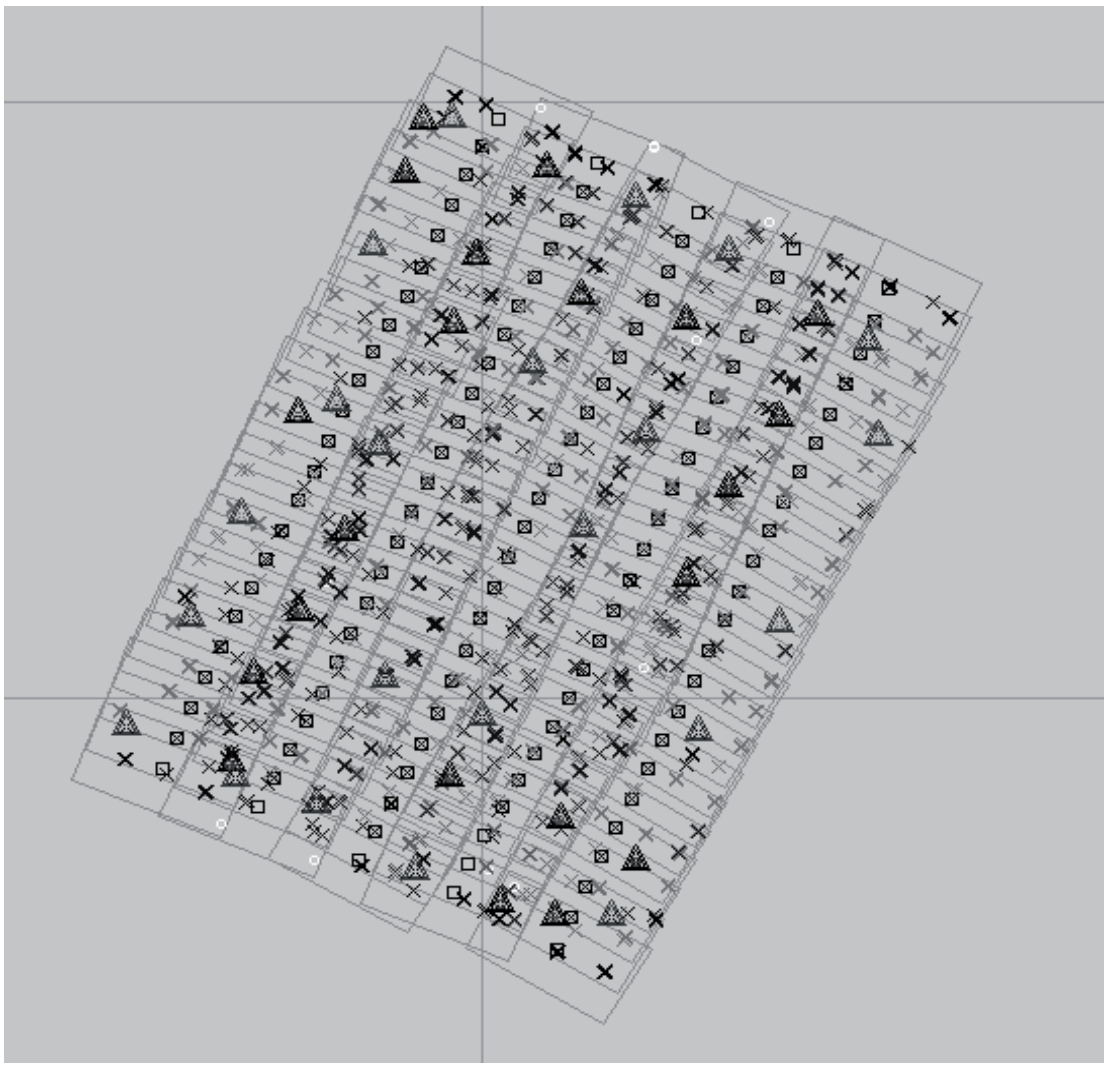

Figure 1: Schema of DMC_low block

The second block – project DMC_high: flying height 1800 m, 3 long strips (34 images), scale ≈ 1:15000, no cross lines, approximate 60% forward lap and 30% side lap, 21 ground control points and 20 check points (cf. also Figure 2). The pixel size is 12 µm.

Expected accuracy for this block:

$$dz \approx 0{,}01\% \times H_f = 0.18m$$

$$dx = dz \approx 5\mu m \times scalefactor = 0.075m$$

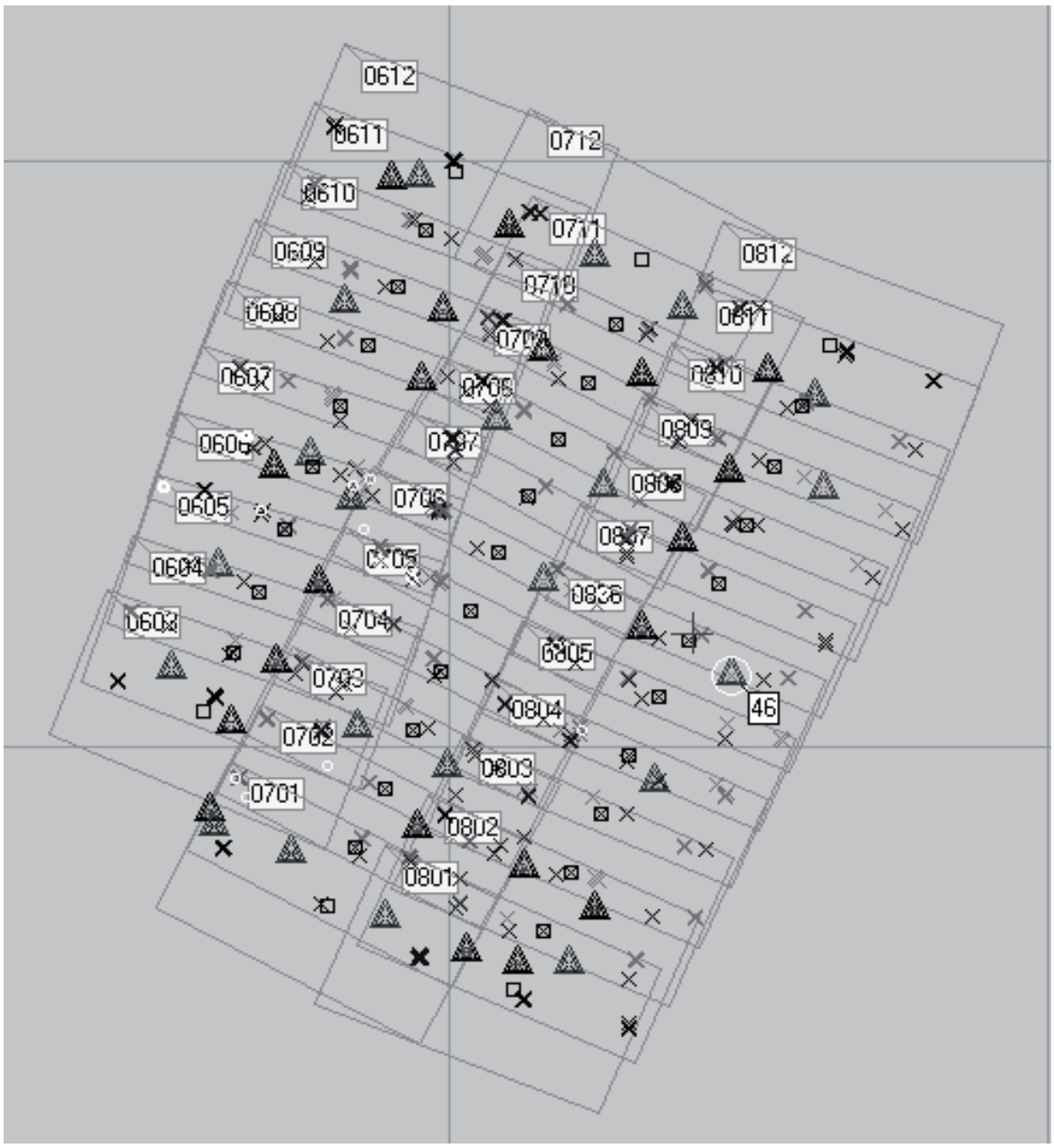

Figure 2: Schema of DMC-low block.

Description of experiments and results

The following chapters describe the experiments and the results. Details are provided in Appendix A and B for the MATCH-AT runs (.prj and .cnt files) as well as settings for PhotoMod in Appendix C.

Both projects DMC-low and DMC-high were performed independently, i.e. there was no combination of both blocks in the aerial triangulation process.

Photo measurements

In MATCH-AT the photo measurements were made in two steps:

1. Manual measurements of ground control and check points
2. Automatic search for tie points (default parameters were used: 6 levels of pyramid (5-0), standard quantity of points, default strategy of matching and so on).

In DMC_high several tie points had to be added manually on the edges of block (about 15 points).

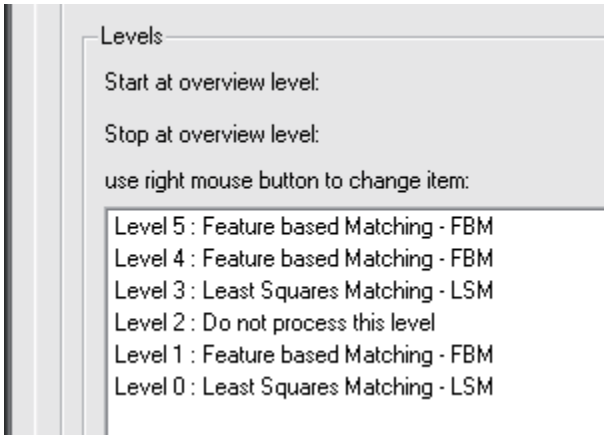

Figure 3: Automatic tie-point matching strategies in MATCH-AT.

In PhotoMod all measurements were made manually (semi-automatically), because the automatic triangulation did not give satisfying results (the reason of it is big areas, covered with trees and water, where algorithm used in PhotoMod seems not to work properly).

Adjustment parameters used

In MATCH-AT the bundle adjustment with self calibration (44 parameters) was used, The adjustment was performed without using information about GPS.

In PhotoMod the method of independent stereopairs was used. The weights of ground control points is set to 3 and polynomial correction was used.

Adjusted coordinates of check points

In the following four tables are given the final results for both DMC projects with MATCH-AT and with PhotoMod.

Table 1: MATCH-AT DMC-low. Adjusted coordinates of check points.

Check point ID	E [m]	N [m]	Height [m]
1	609521.8423	6569846.011	95.06879
12	608182.7357	6565194.791	77.14222
13	608558.523	6565721.151	66.79465
14	608907.3331	6566394.13	71.01039
144	611215.0314	6563612.36	39.30096
16	609769.4353	6568129.769	82.82711
17	609945.1213	6568708.744	65.80551
18	610506.7339	6569436.943	82.65287
20	610782.7116	6568376.124	92.02361
28	609743.0921	6564317.456	77.38011
33	611606.3075	6568156.213	110.9799
35	612655.5919	6568198.274	69.86521
36	612347.0657	6567348.344	69.69456
37	611943.3124	6566758.34	91.3071
38	611604.215	6565996.303	103.56343
40	610623.7368	6563966.181	73.61725
42	610567.9088	6563150.286	75.46724
51	610137.3319	6563264.169	78.33877
52	608004.5566	6564458.777	39.67508
7	608533.4741	6567383.55	71.20296
3	609388.4028	6569394.507	80.63173

Table 2: PhotoMod - DMC-low. Adjusted coordinates of check points.

Check point ID	E [m]	N [m]	Height [m]
1	609521.753	6569846.131	95.073
12	608182.800	6565194.719	7.330
13	608558.575	6565721.120	66.767
14	608907.293	6566394.060	70.881
144	611215.097	6563612.380	39.228
16	609945.169	6568708.672	65.972
18	610507.340	6569437.243	81.985
20	610782.743	6568376.058	92.052
28	609743.101	6564317.434	7.595
3	609388.449	6569394.490	80.774
33	611606.292	6568156.166	111.100
35	612655.603	6568198.169	70.085
36	612347.104	6567348.335	69.807
37	611943.345	6566758.347	91.349
38	611604.241	6565996.322	103.586
40	610623.808	6563966.171	73.604
42	610567.906	6563150.252	75.285
51	610137.291	6563264.153	78.107
52	608004.610	6564458.754	39.805
7	608533.402	6567383.512	71.191

Table 3: MATCH-AT DMC-high. Adjusted coordinates of check points.

Check point ID	E [m]	N [m]	Height [m]
1	609521.8049	6569846.168	95.23441
12	608182.6698	6565194.848	76.97084
13	608558.5222	6565721.174	66.81415
14	608907.1885	6566394.117	71.00017
144	611215.0195	6563612.38	39.2975
16	609769.4279	6568129.791	82.93196
17	609945.0821	6568708.77	66.25492
18	610507.308	6569437.231	82.33292
20	610782.75	6568376.036	92.10865
28	609743.0025	6564317.453	77.69812
33	611606.2276	6568156.149	110.89748
35	612655.6713	6568198.239	69.90317
36	612347.1132	6567348.267	69.63997
37	611943.4474	6566758.29	91.10936
38	611604.2429	6565996.314	103.4009
40	610623.7589	6563966.259	73.35695
42	610567.9876	6563150.39	75.49241
51	610137.5219	6563264.133	78.3539
52	608004.2902	6564458.947	39.18372
7	608533.4105	6567383.492	70.92768

Table 4: PhotoMod - DMC-high. Adjusted coordinates of check points.

Check point ID	E [m]	N [m]	Height [m]
1	609521.711	6569846.160	95.283
12	608182.714	6565194.823	77.232
13	608558.500	565721.070	66.921
14	608907.257	6566394.086	70.975
144	611215.148	6563612.471	39.401
16	609769.455	6568129.820	82.960
17	609945.109	6568708.760	66.089
18	610507.289	6569437.054	82.296
20	610782.713	6568376.068	91.973
28	609743.084	6564317.476	77.592
33	611606.278	6568156.207	110.875
35	612655.642	6568198.295	69.305
36	612347.095	6567348.310	69.547
37	611943.389	6566758.348	91.188
38	611604.253	6565996.419	103.802
40	610623.736	6563966.203	73.755
42	610567.877	6563150.357	75.253
51	610137.305	6563264.129	78.267
52	608004.369	6564458.847	39.732
7	608533.330	6567383.467	71.192

Some comments:

Points 17 and 18 are very difficult to identify, i.e. also very difficult to measure.
Point 35 gives problems in PhotoMod DMC-high project. We have not yet found the reason for it.
Point 52 gives problems in MATCH-AT DMC-high project. We have not yet found the reason for it.

Sigma naught

The following Sigma naught values have been reached with MATCH-AT:

MATCH-AT - DMC_low: σ_0 = 1.5 µm (Point 18 was eliminated by the program)

MATCH-AT - DMC_high σ_0 = 2.1 µm

This means in both cases better than or equal 1/6 of the pixel size.

Quality at ground control points

In the following tables (Table 5 and Table 6) are given the residuals at ground control points for both DMC projects with MATCH-AT and with PhotoMod each.

Table 5: Residuals on ground control points for both AT results in project DMC_low

MATCH-AT - DMC_low			PhotoMod - DMC_low		
RMS (m)			RMS (m)		
dX	dY	dZ	dX	dY	dZ
0.017	0.015	0.005	0.007	0.008	0.008

Table 6: Residuals on ground control points for both AT results in project DMC_high.

MATCH-AT - DMC_high			PhotoMod - DMC_high		
RMS (m)			RMS (m)		
dX	dY	dZ	dX	dY	dZ
0.003	0.003	0.002	0.030	0.022	0.086

Quality at ground control points (as provided by first feedback of pilot center)

The above adjusted coordinates had been submitted to the EuroSDR test pilot center and as a first result we received summarized RMS values at the to us unknown check points by the pilot center.

In the following four tables are given the RMS values at check points for both DMC projects with MATCH-AT and with PhotoMod. The pilot center has also individually excluded the check points that we had marked as difficult to measure. By this exclusion of recognized bad points, the results are significantly improved further.

Table 7: Residuals on check points (result provided by the pilot center on our provided results) for MATCH-AT results in project DMC_low.

MATCH-AT			DMC_low	
RMS (m)			Number of	
dx	dy	dz	points	
0.104	0.072	0.225	20	
0.091	0.064	0.190	19	without point 52
0.090	0.057	0.180	18	without points 17, 52

Table 8: Residuals on check points (result provided by the pilot center on our provided results) for PhotoMod results in project DMC_low.

PhotoMod			DMC_low	
RMS (m)			Number of	
dx	dy	dz	points	
0.072	0.060	0.231	20	
0.073	0.061	0.181	19	without point 35

Table 9: Residuals on check points (result provided by the pilot center on our provided results) for MATCH-AT results in project DMC_high.

Match-AT			DMC_high	
RMS (m)			number of	
dx	dy	dz	points	
0.153	0.069	0.162	21	
0.053	0.520	0.085	20	without point 18
0.044	0.045	0.080	19	without points 1, 18

Table 10: Residuals on check points (result provided by the pilot center on our provided results) for PhotoMod results in project DMC_high.

PhotoMod	Dmc_high		
RMS (m)			number of
dx	dy	dz	points
0.036	0.039	0.106	21

Some conclusions

It is clear from the results presented above that in these two digital aerial triangulation programs it is possible to reach the same accuracy. However in Photomod it took much more time, due to much lower degree of automation

At present time automatic triangulation in MATCH-AT works better and faster than in PhotoMod. The reason are certainly the differences in the used algorithms. The most time-consuming process in the PhotoMod program is the creation of the block layout, especially, with using feature based matching. Feature based matching is also used in Match-AT but it is not used on the level 0 of pyramid there. Another reason is the process of rejection points in PhotoMod, when rejection is done by vertical parallax. Sometimes there are situations when because of one bad point a lot of good ones are skipped and finally there are not enough points left.

However, PhotoMod has some other advantages, like a very user-friendly interface for any kind of manual measurements and the opportunity to measure points in stereo. There is such an opportunity in MATCH-AT but it is more difficult to do it there, at least without training.

Considering aerial triangulation itself, and not taking into account the possibilities of automatic search and matching of tie points, it is in both projects possible to reach in PhotoMod the same accuracy of measurements as in MATCH-AT.

Appendix A – MATCH-AT .prj and .cnt files for project DMC-low

```
$PROJECT 1.5
  $PROJECT_NAME : def_project
  $USER_ID : def_user
  $STARTING_DATE : Sun Jul 02 17:00:10 2006
  $LAST_CHANGE : Mon Jul 10 09:09:52 2006
  $IMAGE_TYPE : Aerial
  $STD_DEV_OBJECT_POINTS : 0.020000
  $STD_DEV_OBJECT_Z_POINTS : 0.020000
  $STD_DEV_IMAGE_POINTS : 0.002400
  $STD_DEV_IMAGE_GC_POINTS : 0.004000
  $SDS_OBJ_GROUP_XY :  -1.000000 -1.000000 -1.000000 -1.000000
  $SDS_OBJ_GROUP_Z :  -1.000000 -1.000000 -1.000000 -1.000000
  $IMPORTED_DATA : autoprj
  $REFRACT_CORR_DEFAULT : On
  $CURV_CORR_DEFAULT : On
  $DISTORT_CORR_DEFAULT : On
  $LINEAR_UNITS_OF_OBJECT : m
  $LINEAR_UNITS_OF_IMAGE : mm
  $ANGULAR_UNITS : deg
  $WARNING_LEVEL : 0
  $REPORT_LOGFILE : .\1_low.log
$END
$AAT
  $AAT_DIR : .\
  $AAT_CNT : .\1_low.cnt
  $TPG_FILE : This_file_entry_is_no_longer_supported_in_vesion_3.5_and_higher
  $GPS_FILE : This_file_entry_is_no_longer_supported_in_vesion_3.5_and_higher
  $INS_FILE : This_file_entry_is_no_longer_supported_in_vesion_3.5_and_higher
  $GPS_MODE : Off
  $DRIFT_PAR : Off
  $GPS_EXC : 0.000000 0.000000 0.000000
  $GPS_STD : 0.100000 0.100000 0.100000
  $INS_MODE : Off
  $INS_DRIFT : Off
  $BORE_SIGHT_ALIGNEMENT : Off
  $INS_STD : 0.010000 0.010000 0.010000
  $END_LAP : 65.000000
  $SIDE_LAP : 25.000000
  $STRIPS :
    1     -154.02   0.00   0.00       610118.23      6569860.59 { 0123 0122 0121
          0120 0119 0118 0117 0116 0115 0114 0113 0112 0111 0110
          0109 0108 0107 0106 0105 0104 0103 0102 0101 }
    2      26.42   0.00   0.00       608220.89      6564082.75 { 0201 0202 0203
          0204 0205 0206 0207 0208 0209 0210 0211 0212 0213 0214
          0215 0216 0217 0218 0219 0220 0221 0222 0223 }
    3     -153.75   0.00   0.00       611699.98      6569080.32 { 0323 0322 0321
          0320 0319 0318 0317 0316 0315 0314 0313 0312 0311 0310
          0309 0308 0307 0306 0305 0304 0303 0302 0301 }
    4      26.46   0.00   0.00       609762.46      6563364.17 { 0401 0402 0403
```

```
        0404 0405 0406 0407 0408 0409 0410 0411 0412 0413 0414
        0415 0416 0417 0418 0419 0420 0421 0422 0423 }
    5    -154.66   0.00   0.00       613210.88      6568434.57 { 0523 0522 0521
        0520 0519 0518 0517 0516 0515 0514 0513 0512 0511 0510
        0509 0508 0507 0506 0505 0504 0503 0502 0501 }
  $END_STRIPS
  $GRUBER :
    0     33.00  63.00  11.00
    1     33.00   0.00  11.00
    2     33.00 -63.00  11.00
    3      0.00 -63.00  11.00
    4    -33.00 -63.00  11.00
    5    -33.00   0.00  11.00
    6    -33.00  63.00  11.00
    7      0.00  63.00  11.00
    8      0.00   0.00  11.00
  $END_GRUBER
$END



#
# Control parameter for matching strategy
#
$OVW_TO_START     5
$OVW_TO_STOP     0
$OVWS_TO_JUMP     1
$OVW_TO_ADD_TIES_SINGLE     4
$OVW_INIT_TO_START     6
$OVW_INIT_TO_STOP     5
$REFINE_WITH_LSM     ON
$MAX_IMAGES     3000
$MAX_NEW_TIES_MULT     1
$MAX_NEW_TIES_SINGLE     2
$NUM_TIE_THRES     2
$PTS_PER_TPC     3
$MAX_PTS_PER_IMAGE     100
$STRATEGY     FROM_TPG
$TPC_STRATEGY     MAKE_OK
$INIT_DEM
$USE_DEM     OFF
$REFINE_DEM     OFF
$PROJECT_FILE     .\1_low.prj
$USE_MAN_AS_TPC     ON
$MATCHINGSEQUENCE      FBM FBM LSM SKIP FBM LSM
$FACTORFIRSTLEVEL     1.000000
$CREATENUMERICIDS     ON
$TRACKPOINTSFROMLEVEL     ON
#
```

```
# Control parameter for block adjustment
#
$SELFCALIBRATION     ON
$SELFCALPARAMETER     44
$NO_ELIM_MAN_POINTS     OFF
#
# Control parameter for feature-based matching techniques
#
$MATCH_WINDOW_SIZE     100
$WINDOW_SIZE     5
$NON_MAX_WINDOW     5
$QMIN     0.500000
$WMIN     0.100000
$FILTER_TYPE     BOX
$CORRELATION_COEFFICIENT     0.920000
$WINDOW_RHO     5
$PARALLAX_BOUND     30
$REDUCTION     OFF
$REDUCT_FACTOR     0.005000
$EPILINE     OFF
$EPI_DIST     0.500000
$INTEREST_VALUE     OFF
$MAX_INT_RATIO     100.000000
$RESAMPLING_TYPE     BILIN
$SUBPIXEL     OFF
$NOSIGN     ON
$THIN_OUT     OFF
#
# Control parameter for least squares matching techniques
#
$LSM_WIN_SIZE     21
$MARGIN     6
$MAX_ITERATIONS     20
$LSM_RHO     0.930000
```

Appendix B – MATCH-AT .prj and .cnt files for project DMC-high

```
$PROJECT 1.5
  $PROJECT_NAME : def_project
  $USER_ID : def_user
  $STARTING_DATE : Sun Jul 09 15:00:35 2006
  $LAST_CHANGE : Mon Jul 24 10:04:55 2006
  $IMAGE_TYPE : Aerial
  $STD_DEV_OBJECT_POINTS : 0.010000
  $STD_DEV_OBJECT_Z_POINTS : 0.020000
  $STD_DEV_IMAGE_POINTS : 0.002400
  $STD_DEV_IMAGE_GC_POINTS : 0.004000
  $SDS_OBJ_GROUP_XY :  -1.000000 -1.000000 -1.000000 -1.000000
  $SDS_OBJ_GROUP_Z :  -1.000000 -1.000000 -1.000000 -1.000000
  $IMPORTED_DATA : autoprj
  $REFRACT_CORR_DEFAULT : On
  $CURV_CORR_DEFAULT : On
  $DISTORT_CORR_DEFAULT : On
  $LINEAR_UNITS_OF_OBJECT : m
  $LINEAR_UNITS_OF_IMAGE : mm
  $ANGULAR_UNITS : deg
  $WARNING_LEVEL : 0
  $REPORT_LOGFILE : .\ph_m.log
$END
$AAT
  $AAT_DIR : .\
  $AAT_CNT : .\1_high.cnt
  $TPG_FILE : This_file_entry_is_no_longer_supported_in_vesion_3.5_and_higher
  $GPS_FILE : This_file_entry_is_no_longer_supported_in_vesion_3.5_and_higher
  $INS_FILE : This_file_entry_is_no_longer_supported_in_vesion_3.5_and_higher
  $GPS_MODE : Off
  $DRIFT_PAR : Off
  $GPS_EXC : 0.000000 0.000000 0.000000
  $GPS_STD : 0.100000 0.100000 0.100000
  $INS_MODE : Off
  $INS_DRIFT : Off
  $BORE_SIGHT_ALIGNEMENT : Off
  $INS_STD : 0.010000 0.010000 0.010000
  $END_LAP : 65.000000
  $SIDE_LAP : 25.000000
  $STRIPS :
    6      24.43   0.00   0.00       607958.81      6565312.63 { 0603 0604 0605
         0606 0607 0608 0609 0610 0611 0612 }
    7     -154.36   0.00   0.00       611613.22      6569150.58 { 0712 0711 0710
         0709 0708 0707 0706 0705 0704 0703 0702 0701 }
    8      25.52   0.00   0.00       610546.70      6562939.28 { 0801 0802 0803
         0804 0805 0806 0807 0808 0809 0810 0811 0812 }
  $END_STRIPS
  $GRUBER :
    1     80.00  85.00  20.00
```

```
   2     80.00   0.00  20.00
   3     80.00 -85.00  20.00
   4      0.00 -85.00  20.00
   5    -80.00 -85.00  20.00
   6    -80.00   0.00  20.00
   7    -80.00  85.00  20.00
   8      0.00  85.00  20.00
   9      0.00   0.00  20.00
 $END_GRUBER


#
# Control parameter for matching strategy
#
$OVW_TO_START     5
$OVW_TO_STOP     0
$OVWS_TO_JUMP     1
$OVW_TO_ADD_TIES_SINGLE     4
$OVW_INIT_TO_START     6
$OVW_INIT_TO_STOP     5
$REFINE_WITH_LSM     ON
$MAX_IMAGES     3000
$MAX_NEW_TIES_MULT     1
$MAX_NEW_TIES_SINGLE     2
$NUM_TIE_THRES     2
$PTS_PER_TPC     3
$MAX_PTS_PER_IMAGE     100
$STRATEGY     FROM_TPG
$TPC_STRATEGY     MAKE_OK
$INIT_DEM
$USE_DEM     OFF
$REFINE_DEM     OFF
$PROJECT_FILE     .\1_high.prj
$USE_MAN_AS_TPC     ON
$MATCHINGSEQUENCE      FBM FBM LSM SKIP FBM LSM
$FACTORFIRSTLEVEL     1.000000
$CREATENUMERICIDS     ON
$TRACKPOINTSFROMLEVEL     ON
#
# Control parameter for block adjustment
#
$SELFCALIBRATION     ON
$SELFCALPARAMETER     44
$NO_ELIM_MAN_POINTS     OFF
#
```

```
# Control parameter for feature-based matching techniques
#
$MATCH_WINDOW_SIZE     100
$WINDOW_SIZE     5
$NON_MAX_WINDOW     5
$QMIN     0.500000
$WMIN     0.100000
$FILTER_TYPE     BOX
$CORRELATION_COEFFICIENT     0.920000
$WINDOW_RHO     5
$PARALLAX_BOUND     30
$REDUCTION     OFF
$REDUCT_FACTOR     0.005000
$EPILINE     OFF
$EPI_DIST     0.500000
$INTEREST_VALUE     OFF
$MAX_INT_RATIO     100.000000
$RESAMPLING_TYPE     BILIN
$SUBPIXEL     OFF
$NOSIGN     ON
$THIN_OUT     OFF
#
# Control parameter for least squares matching techniques
#
$LSM_WIN_SIZE     21
$MARGIN     6
$MAX_ITERATIONS     20
$LSM_RHO     0.930000
```

Appendix C – Parameters used in PhotoMod for both DMC projects

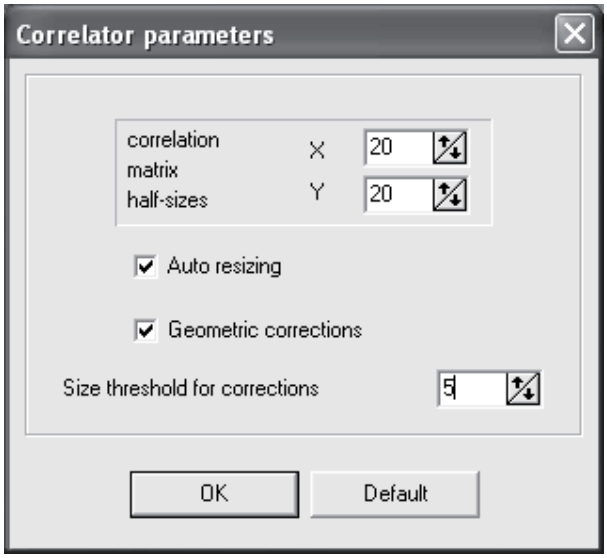

Figure 4: Properties of correlator, used for semi-automatical measurements in both DMC projects.

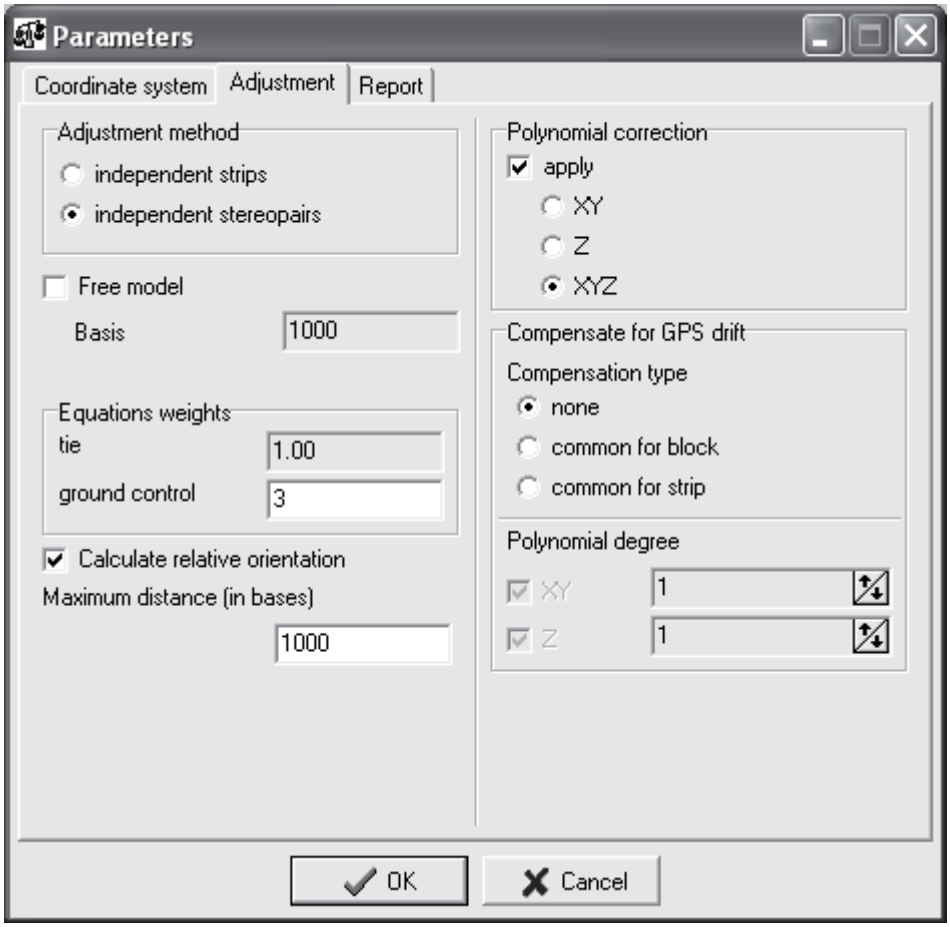

Figure 5: Parameters of adjustment in PhotoMod for both DMC projects.

Christoph Dörstel
Hardware Development Centre
Manager Software Development
Intergraph (Deutschland) GmbH
Phone: +49 (0)7361 8895 80
Fax: +49 (0)7361 8895 29
E-mail: christoph.doerstel@intergraph.com www.intergraph.com

Results of EuroSDR Block
Data processed by Intergraph

Data Sets:
Following data were provided by EuroSDR and used for our tests.

	High altitude	Low altitude	Comment
Name	Fredrikstad_High	Fredrikstad_Low	
Camera	DMC	DMC	
Hg [m]	1800	990	
Scale	1:16000	1:8000	
# images	34	115	
# Control Points	20	23	
# Check Points	22	23	Accuracy within 1 m, noise added

Processing:
This chapter presents a brief overview about the procedure we applied for processing the blocks. The processing steps introduced in sequential order.

- Tie point measurements by use of ISAT (Version 5.0)
- Free block adjustment to eliminate erroneous measurements and additional measurement of tie points in weak areas
- First Block Adjustment using 7 control points in the “von Gruber areas” of the block plus one control point in the centre. Double check delivered control points and block stability. No elimination of control points for further processing. When using self calibration all self calibration parameters were activated (12 parameters). Adjustments done in two modes:
  - Without self calibration
  - With self calibration
- Second Block Adjustment with all given control points and using 2 of them as check points. These results present the final block results.
- Final computation includes delivered check points. Precise coordinates for these points are computed.

Measurements:
Measurements of the check and control points were performed in mono comparator mode. Just in case the control points showed large z-residuals the height measurement was performed as stereo measurement. In general the given control points could be well identified and measured, except some laying in the shadow (eg. 26, 47, 50) or placed on a slope (48). The same can be said about given check points: some were hooded e.g. by trees (42) or in the shadow (eg. 7, 17, 51). Measurement accuracy in those points may lack a little. Target quality was good in the low altitude project and a bit poor in the high altitude project because of unchanged target size.

Noticeable problems:
For the block adjustment no DGPS and IMU measurements were available, but the number of control points was sufficient. A better stabilization of the high altitude block could have been achieved by additional control points in the overlapping area of the strips or one cross strip.

Results:
Best accuracies were achieved when applying self calibration. Without self calibration parameters the residuals in the control as well as in the check points were unacceptable. A correction for atmospheric conditions such as refraction is needed.

The final residuals in the check points were taken from the second block adjustment. In that case just real control points (without noise) were used. The final computation shows of course higher RMS residuals in the check points due the noise computed into these points. The maximum residuals in the check points were discovered in different points. In the below table for the low altitude flight the maximum residual of 3,4 cm in X was measured in check point 6, where the maximum residuals of -4,1 cm and -12,5 cm in Y and Z were measured in check point 31 (see comment).

	High altitude	**Low altitude**	**Comment**
Name	Fredrikstad_High	Fredrikstad_Low	
Sigma [µm]	2,3	3,1	
RMS control X/Y/Z [cm]	4,1 / 2,7 / 2,5	3,1 / 3,8 / 3,7	High - 18 points Low – 21 points
Max ground residuals X/Y/Z [cm]	9,1 / 5,0 / 4,6	6,3 / 6,4 / 8,6	
CP Used as check points	6 + 31	15 + 31	
RMC check X/Y/Z [cm]	7,5 / 2,5 / 7,9	2,4 / 2,9 / 9,7	High – 2 points Low – 2 points
Max residuals in check points X/Y/Z [cm]	10,1 / -3,5 /-10,6	3,4 / -4,1 / -12,5	In check point High – 6 / 31 / 31 Low – 15 / 31 / 31

Conclusions:
In general the reached accuracies are within the expected range. There is a surprising accuracy difference in the X and Y coordinates, which we were not able to explain. This was not further investigated, but could be related to the flight direction and the FMC compensation? Interestingly this is more obvious in the high altitude block than in the low altitude block.
Compare to the flying height the accuracy in the Z coordinates is better at higher altitudes. (We have experienced that measurement accuracy depends on the structure / texture of the surface and thus in digital images it sometimes needs more experience to identify points on the ground.)

More thoroughly investigation using GPS and IMU information could help to figure out more details.

INSTITUT CARTOGRÀFIC DE CATALUNYA

REPORT

EuroSDR "Digital Camera Calibration".
Data set: DMC data on Fredrikstad test site

R.Alamús, W. Kornus, J.Talaya
Institut Cartogràfic de Catalunya
Parc de Montjuïc 08038 Barcelona SPAIN
ralamus@icc.es, wkornus@icc.es, talaya@icc.es

INTRODUCTION

GOAL

Description of analysis carried out at the ICC with the EuroSDR data. Method and models used are described.

REFERENCE DOCUMENTS

Reference	DOCUMENT	DATE
D_1	EuroSDR-Phase2-Schedule.pdf	Stuttgart, February 17, 2006
D_2	EuroSDR-Phase2-Data.pdf	Stuttgart, February 20, 2006
D_3	EuroSDR-Members-Feb202006.pdf	Stuttgart, February 20, 2006
D_4	README-DMC-DataDisc.pdf	Stuttgart, March 24, 2006
D_5	Informe_EUROSDR.doc	Barcelona, April 27, 2006
D_6	Readme.pdf (Experimental Phase 2b – DMC and UltracamD)	Stuttgart, January 23, 2007

GENERAL OVERVIEW

In this section a general overview description of the data set and process is done.

DATA SET

Data set evaluated is “DMC data, test site Fredrikstad” described in documents D_2 and, in a closer detail, D_4.

A full aerotriangulation has already been performed and reported in document D_5. Current analysis is performed using the data described in document D_6.

WORKFLOW

Ground control points (GCP), check points and tie points image observations are provided by Michael Cramer, Institut für Photogrammetry (ifp),Universität Stuttgart (see document D_6),

Bundle block adjustment is carried out with the in-house ACX-GeoTex software .

Since neither GPS data nor information about the reference coordinate system of the control points are provided, the bundle block adjustment is performed in Cartesian coordinates. 4 sets of additional parameters have been included in the adjustment: one set of 12 self-calibration parameters per image quarter.

This is exactly the same configuration as used in D_5.

DATA SET ANALYSIS

The data sets have been processed independently.

DMC HG 900m

In this block 4 362 photogrammetric observations of 1 647 points (tie points, GCP and check points) are applied.

In the bundle block adjustment there is estimated an additional set of 12 self-calibration parameters for each image quadrant.

Table 1 summarizes the different block weighting using the same configuration of additional parameters.

run	A priori standard deviation				Annex data
	Object space		Image space		
	Plan _GCP [m]	H_GCP [m]	Manual [μm]	Autom. [μm]	
1	0.030	0.050	2.0	6.0	Annex_1
2	0.020	0.025	2.0	2.5	Annex_2
3	0.020	0.025	4.0	5.0	Annex_3

Table 1: A priori weighting for 3 different runs of ACX

It has to be noticed that run no.1 has been performed with photogrammetric observations of GCP 11 in image 101 and GCP 47 in image 516, which have been removed in runs no. 2 and 3 due to large residuals in image space.

Notice that there are some areas with weak strip connection. In figure 1 such areas are signalized with a red circle. In this case ICC usually would add manual observations in order to improve strip connections.

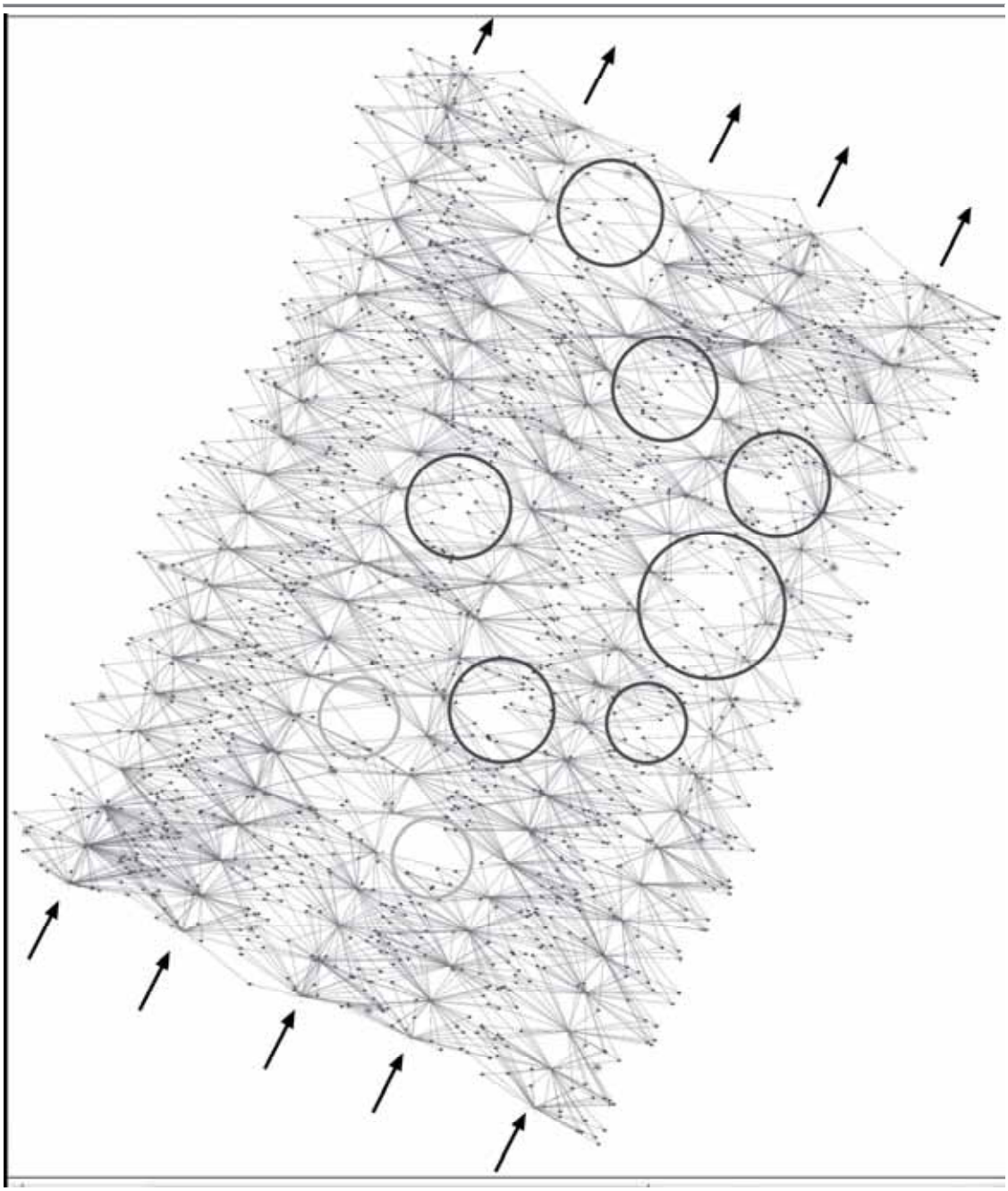

Figure 1: Point to exterior orientation connections in DMC_low Block. Black arrows shows flight lines, black dots represents observed points on ground, blue lines connect the ground points with these images where they have been observed. Red circles show zones with a weak connection between strips. Orange circles show other possible weakly connected zones.

DMC HG 1800m

In this block 2 322 photogrammetric observations of 805 points (tie points, GCP and check points) are applied.

In the bundle block adjustment there is estimated an additional set of 12 self-calibration parameters for each image quadrant.

Table 2 summarizes the different block weighting using same configuration of additional parameters.

run	A priori standard deviation				Annex data
	Object space		Image space		
	Plan _GCP [m]	H_GCP [m]	Manual [μm]	Autom. [μm]	
1	0.030	0.050	2.0	6.0	Annex_4
2	0.020	0.025	2.0	2.5	Annex_5
3	0.020	0.025	5.0	5.0	Annex_6

Table 2: A priori weighting for 3 different runs of ACX

SOME COMMENTS ON THE DMC PROCESSING

We have observed that there is a larger error propagation with a better block connection (which is usually, but not necessarily, related to a larger number of image observation) under the same block adjustment conditions. Similar effects are also described in the paper of Ralph Schroth [1], which shows significantly larger height residuals at check points in a block with an 80% sidelap than in the same block with 60% sidelap or less. We have also observed this behavior with the RUBI block (which has a 50% sidelap aprox.) using different tie point distribution and tie point density instead of varying sidelap. As already mentioned at the beginning, the resulting height accuracy is getting worse as better the geometric block stability is established in terms of image to image connections by image observations.

We have also experienced that by decreasing the weight of image observations and using GPS aerial observations we can get good results in check points heights even without using any set of self-calibration parameters (see table 8 in [2]). Of course, such approximation (low weight of image observations) is dangerous in a productive environment, especially if good GPS observations are not available (as it happens in the EuroSDR test). Referenced results in [2] suggest that image observations could be influenced by systematic errors. If the *a priori* standard deviations of the image observations are relaxed, these systematic errors, together with effects of other error sources, are projected into image space and can be seen as image residuals in the bundle adjustment (see figure 8 in [2]).

The risk of handling an aerotriangulation with unbalanced weights is to get a biased or a not sufficiently accurate (wrong) solution for the exterior orientation.

REFERENCES

[1] R.W.Schroth, 2007. LARGE FORMAT DIGITAL CAMERAS FOR AERIAL SURVEY OF GEOSPATIAL INFORMATION, Strategic Integration of Surveying Services (TS 5.3 – Airborne Surveying – Laser Scanners and Cameras), FIG Working Week 2007, Hong Kong SAR, China 13-17 May 2007).

[2] R.Alamús, W.Kornus, J.Talaya, 2006. STUDIES ON DMC GEOMETRY, ISPRS Journal of Photogrammetry & Remote Sensing 60 (2006) pp. 375-386.

ANNEX 1: DMCHG 900 m

A priori standard deviation fot GCP: 3 cm in plan and 5 cm in height, and 2 μm for automatic and 6 μm for manual image observations.

... deleted M. Cramer ...

ANNEX 2: DMCHG 900 m

A priori standard deviation fot GCP: 2 cm in plan and 2.5 cm in height, and 2 μm for automatic and 2.5 μm for manual image observations.

... deleted M. Cramer ...

ANNEX 3: DMCHG 900 m

A priori standard deviation fot GCP: 2 cm in plan and 2.5 cm in height, and 4 μm for automatic and 5 μm for manual image observations.

... deleted M. Cramer ...

ANNEX 4: DMCHG 1800 m

A priori standard deviation fot GCP: 3 cm in plan and 5 cm in height, and 2 μm for automatic and 6 μm for manual image observations.

... deleted M. Cramer ...

ANNEX 5: DMCHG 1800 m

A priori standard deviation fot GCP: 2 cm in plan and 2.5 cm in height, and 2 μm for automatic and 2.5 μm for manual image observations.

... deleted M. Cramer ...

ANNEX 6: DMCHG 1800 m

A priori standard deviation fot GCP: 2 cm in plan and 2.5 cm in height, and 5 μm for automatic and manual image observations.

... deleted M. Cramer ...

Institut für Photogrammetrie und GeoInformation
Leibniz Universität Hannover

Nienburger Str. 1
D-30167 Hannover

Tel.: +49-511/762-2485
Fax: +49-511/762-2483
e-mail: jacobsen@ipi.uni-hannover.de
http://www.ipi.uni-hannover.de

Dr.-Ing. Karsten Jacobsen

Hannover, 15.3.2007

Analysis of EuroSDR Camera Calibration test block Frederikstaad
DMC
Phase II

1. Lower Flying elevation

```
MAX PHOTOS/POINT            :      6
OBJECT POINTS               :   1648
PHOTOS                      :    115
PHOTO POINTS                :   4363

MINIMUM AND MAXIMUM OF PHOTO COORDINATES
 X MINIMUM =  -45.996  X MAXIMUM =   45.781
 Y MINIMUM =  -77.399  Y MAXIMUM =   77.842

 NUMBER OF PHOTOS/OBJECT POINT
PHOTOS/POINT    1     2     3     4     5     6
POINTS:         0   794   711    87    42    14

   CAMERA PROJECTION CENTER  TERRAIN   PHOTO SCALE
       1          988.        63.        7709.
```

9.3cm GSD

	RMSX	RMSY	RMSZ	sigma0
no selfcalibration	2.1 cm	1.5 cm	3.0 cm	2.81 µm
param. 1-12	1.9 cm	1.3 cm	2.7 cm	2.73 µm
param. 1-12, 79-80	2.0 cm	1.4 cm	2.7 cm	2.67 µm
param. 1-12, 30-41, 74-77	2.0 cm	1.3 cm	2.5 cm	2.64 µm

table 1: discrepancies at control points
parameters 1-12 = standard BLUH-parameters
parameters 79 – 80 = special common DMC-parameters
parameters 30 – 41, 74 – 77 = special individual DMC parameters

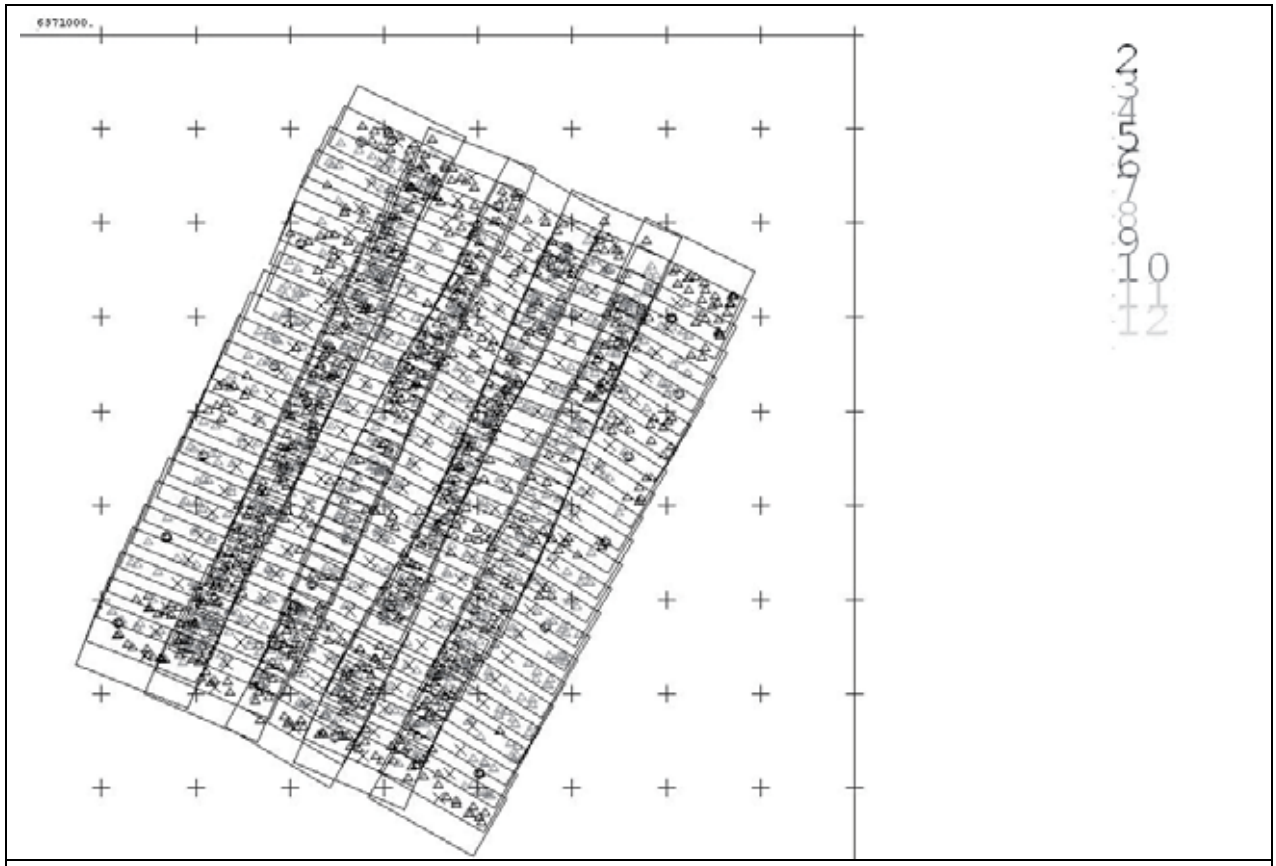

figure 1: DMC lower flying elevation – block configuration
color of points corresponds to number of images / point (see upper right)

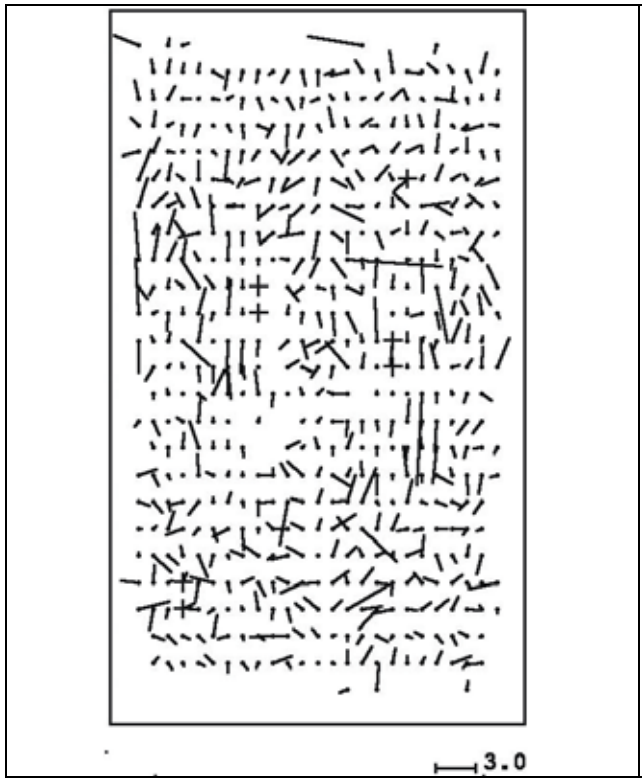

figure 2: averaged and overlaid image residuals of block adjustment without self calibration

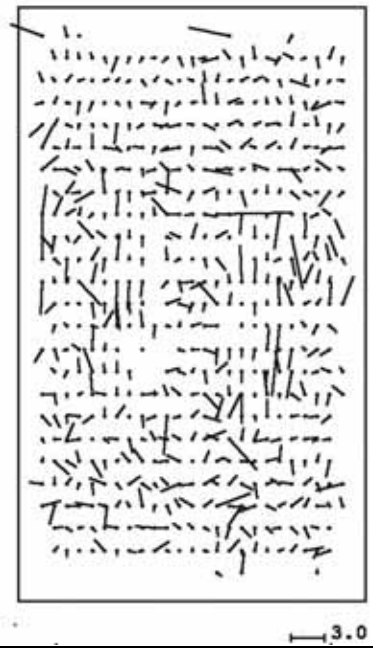

figure 3a: averaged and overlaid residuals

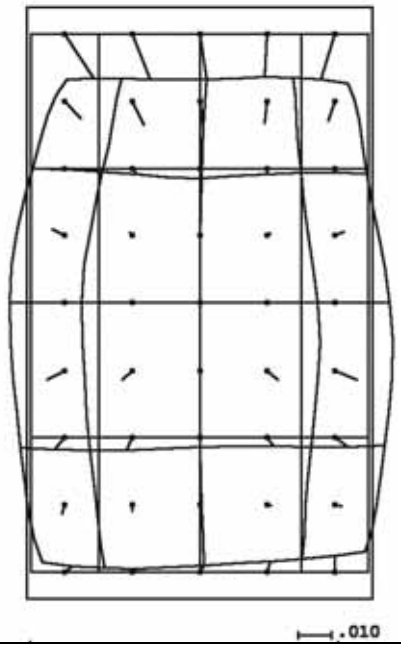

figure 3b: systematic image errors

block adjustment with self calibration – additional parameters 1 – 12 (standard parameters for aerial images)

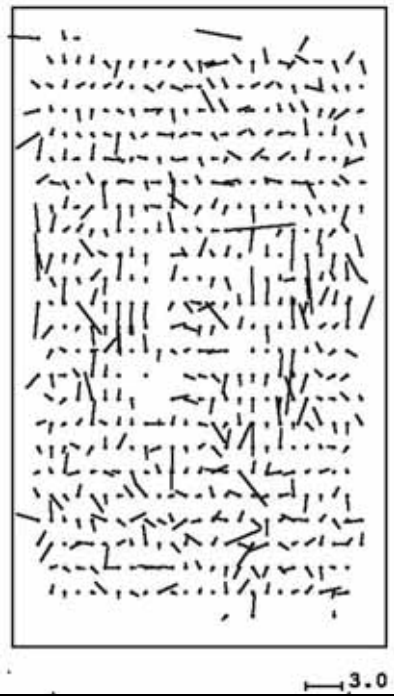

figure 4a: averaged and overlaid residuals

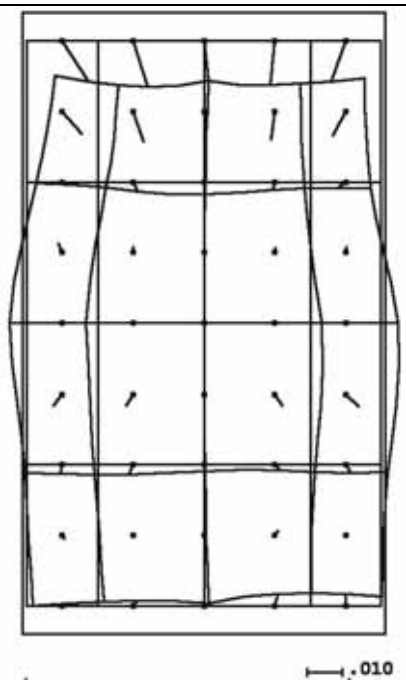

figure 4b: systematic image errors

block adjustment with self calibration – additional parameters 1 – 12 + 79-80 (standard parameters for aerial images + special common DMC-parameters – same value for all 4 quarters)

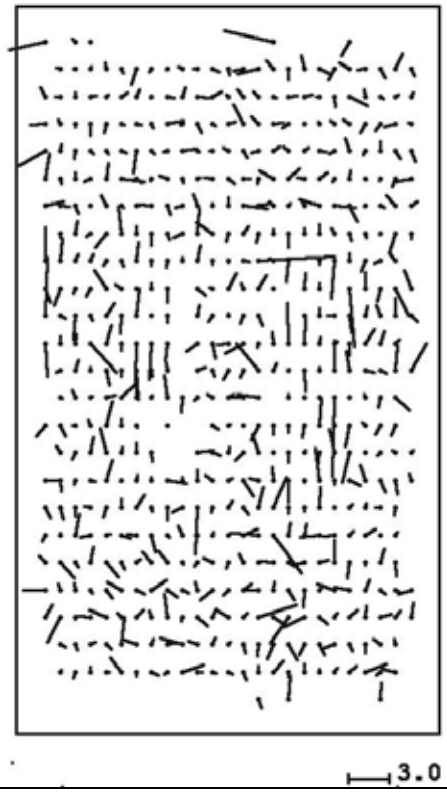

figure 5a: averaged and overlaid residuals

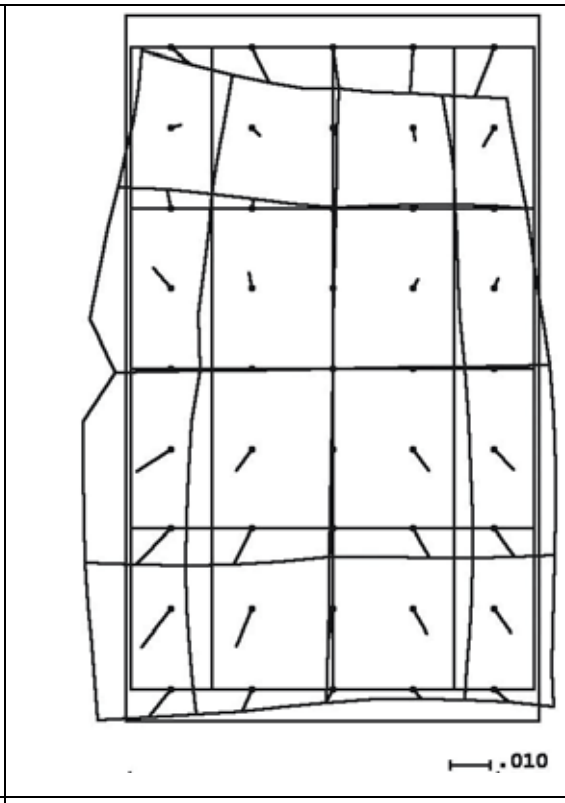

figure 5b: systematic image errors

block adjustment with self calibration – additional parameters 1 – 12 + 30-41, 74-77 (standard parameters for aerial images + special individual DMC-parameters – different for all 4 quarters)

2. Upper Flying elevation

```
MAX PHOTOS/POINT            :       6
OBJECT POINTS               :     805
PHOTOS                      :      34
PHOTO POINTS                :    2322

MINIMUM AND MAXIMUM OF PHOTO COORDINATES
 X MINIMUM =   -45.796  X MAXIMUM =    45.906
 Y MINIMUM =   -82.844  Y MAXIMUM =    82.518

NUMBER OF PHOTOS/OBJECT POINT
PHOTOS/POINT    1     2     3     4     5     6
POINTS:         0   349   312    71    34    39

    CAMERA PROJECTION CENTER  TERRAIN   PHOTO SCALE
        1          1866.        66.       1 :14998.
```

18cm GSD

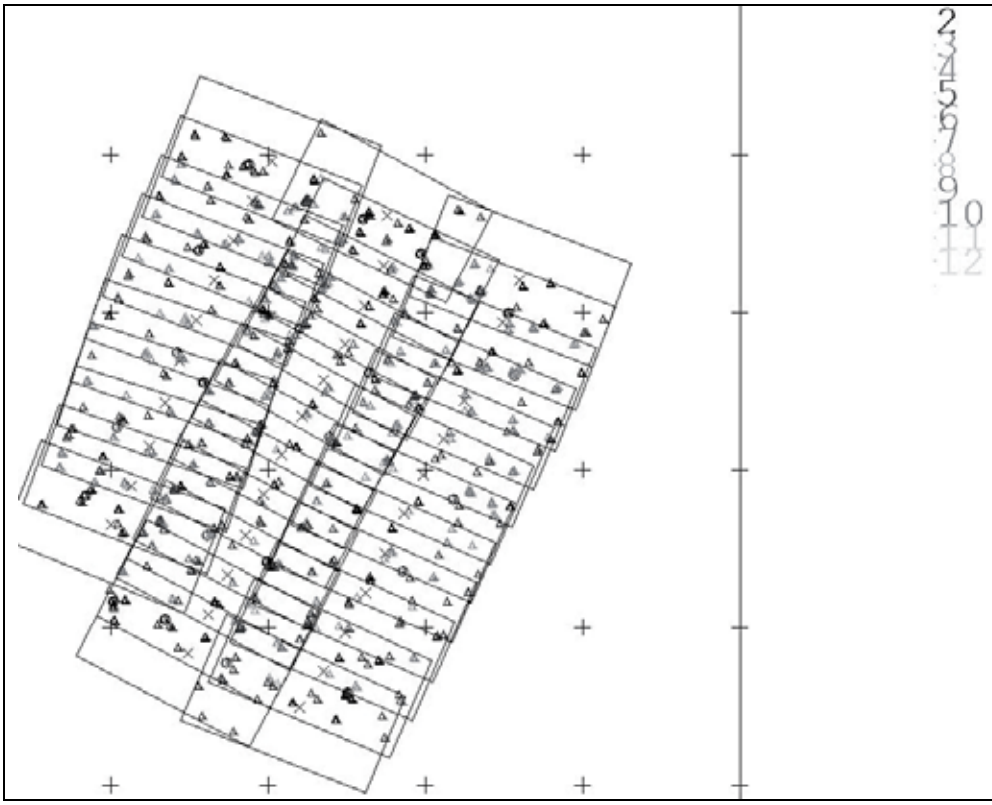

figure 5: DMC upper flying elevation – block configuration color of points corresponds to number of images / point (see upper right)

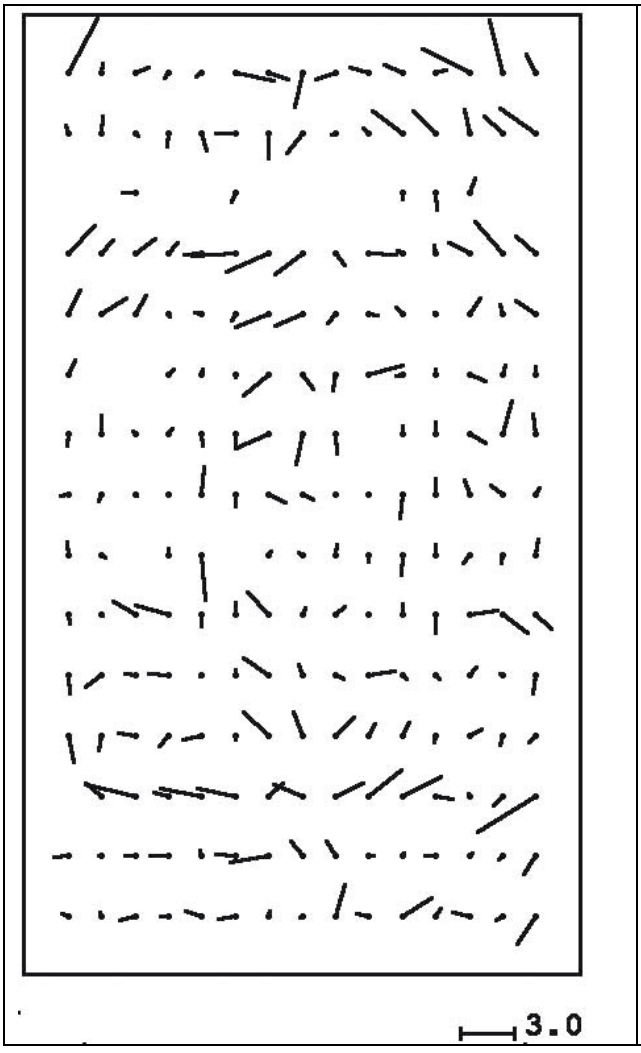

figure 6: averaged and overlaid image residuals of block adjustment without self calibration

	RMSX	RMSY	RMSZ	sigma0
no selfcalibration	8.4 cm	4.0 cm	11.5 cm	2.69 µm
param. 1-12	6.0 cm	3.5 cm	9.1cm	2.51 µm
param. 1-12, 79-80	5.8 cm	3.1 cm	9.5cm	2.42 µm
param. 1-12, 30–41, 74–77	4.3 cm	2.7 cm	9.5 cm	2.32 µm

table 2: discrepancies at control points
parameters 1-12 = standard BLUH-parameters
parameters 79 – 80 = special common DMC-parameters
parameters 30 – 41, 74 – 77 = special individual DMC parameters

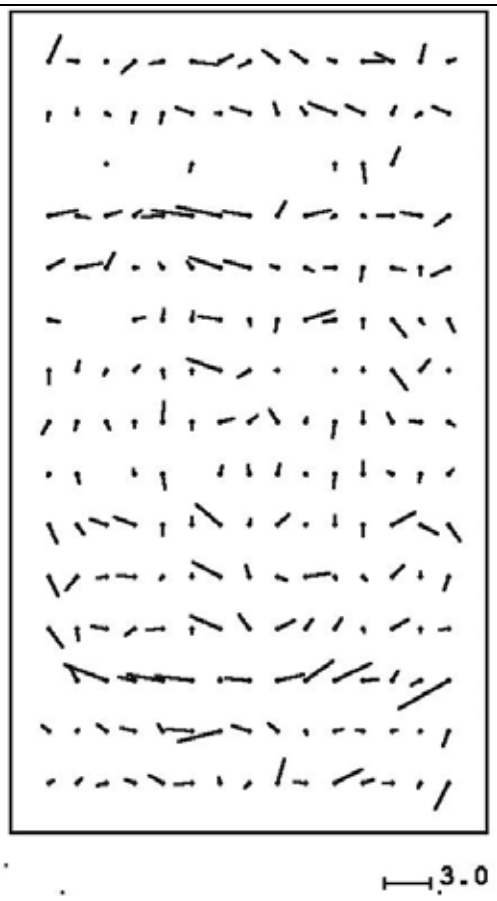

figure 7a: averaged and overlaid residuals

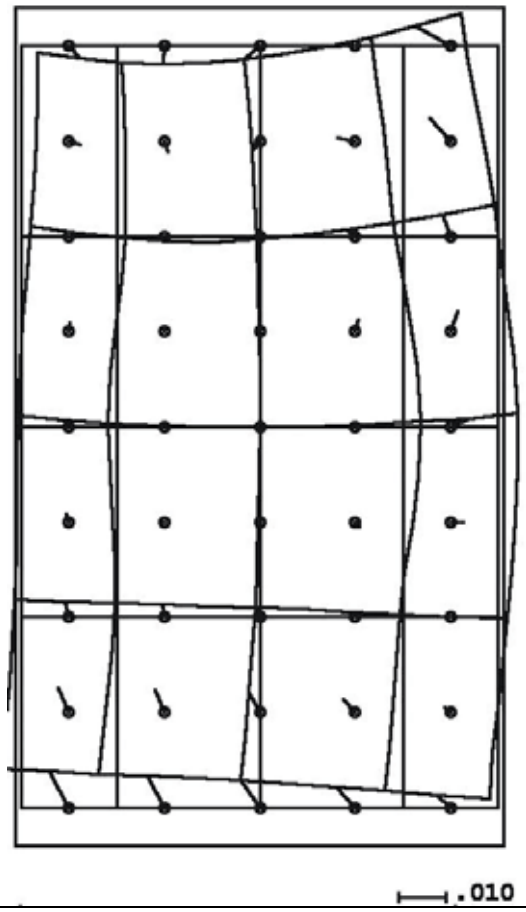

figure 7b: systematic image errors

block adjustment with self calibration – additional parameters 1 – 12 (standard parameters for aerial images)

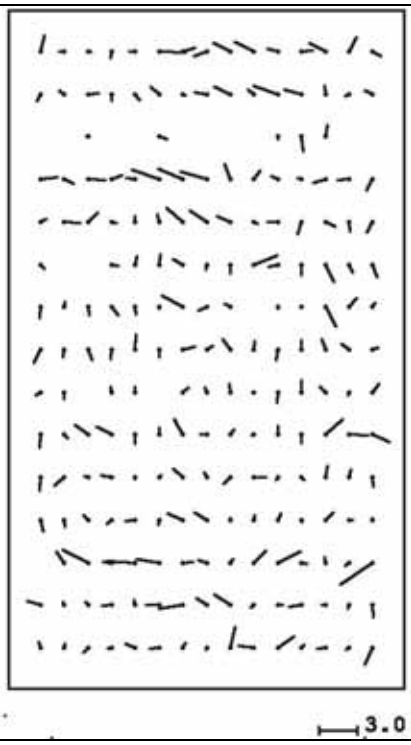

figure 8a: averaged and overlaid residuals

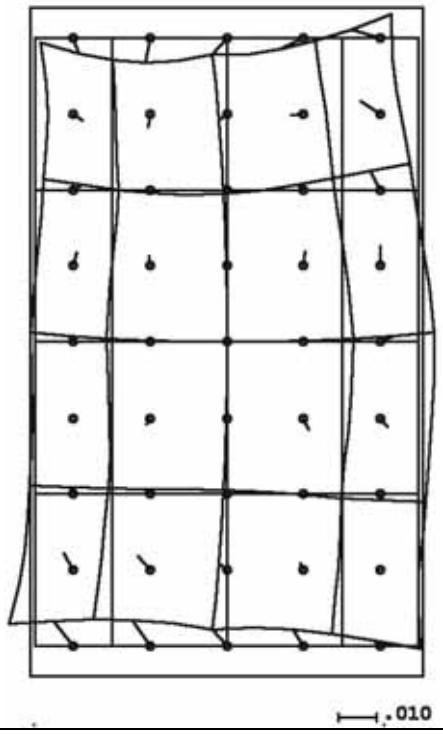

figure 8b: systematic image errors

block adjustment with self calibration – additional parameters 1 – 12 + 79-80 (standard parameters for aerial images + special common DMC-parameters – same values for all 4 quarters)

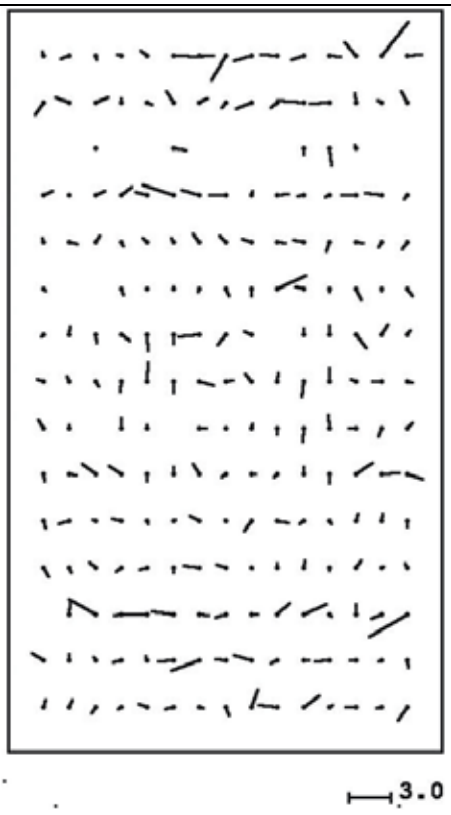

figure 9a: averaged and overlaid residuals

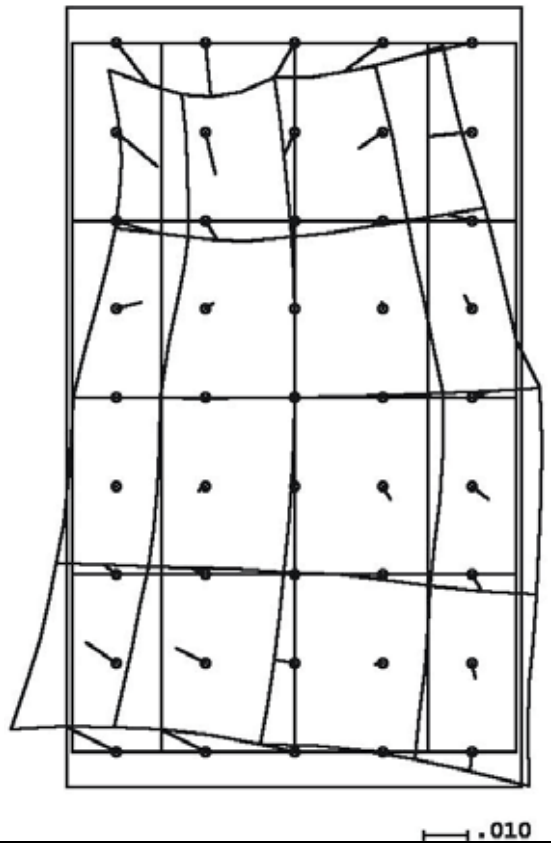

figure 9b: systematic image errors

block adjustment with self calibration – additional parameters 1 – 12 + 30-41, 74-77 (standard parameters for aerial images + special individual DMC-parameters – individual values for all 4 quarters)

3. Upper + lower flying elevation

```
 MAX PHOTOS/POINT            :      10
 OBJECT POINTS               :    2423
 PHOTOS                      :     149
 PHOTO POINTS                :    6685
  NUMBER OF PHOTOS/OBJECT POINT
NUMBER OF PHOTOS/OBJECT POINT
 PHOTOS/POINT    1     2     3     4     5     6     7     8     9    10
 POINTS:         0  1124  1006   150    72    53     7     8     2     1
    IMAGE SCALE   1 :    7385.12 -  1 :   15296.70
```

9.3cm + 18cm GSD

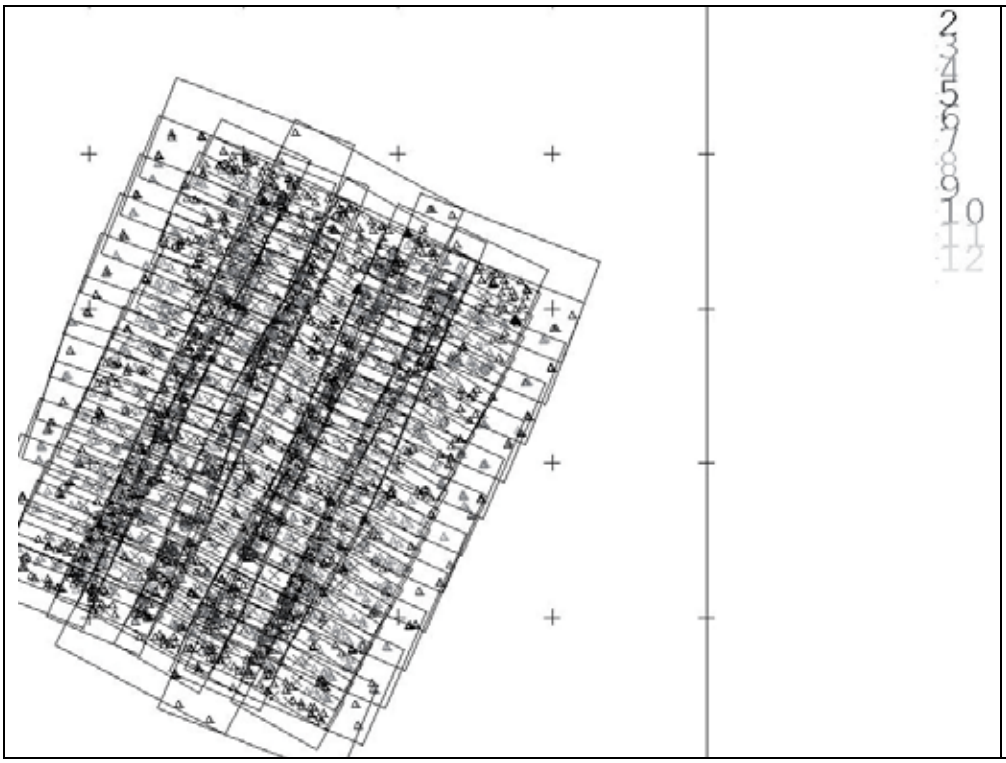

figure 10: UltraCamD upper + lower flying elevation – block configuration color of points corresponds to number of images / point (see upper right)

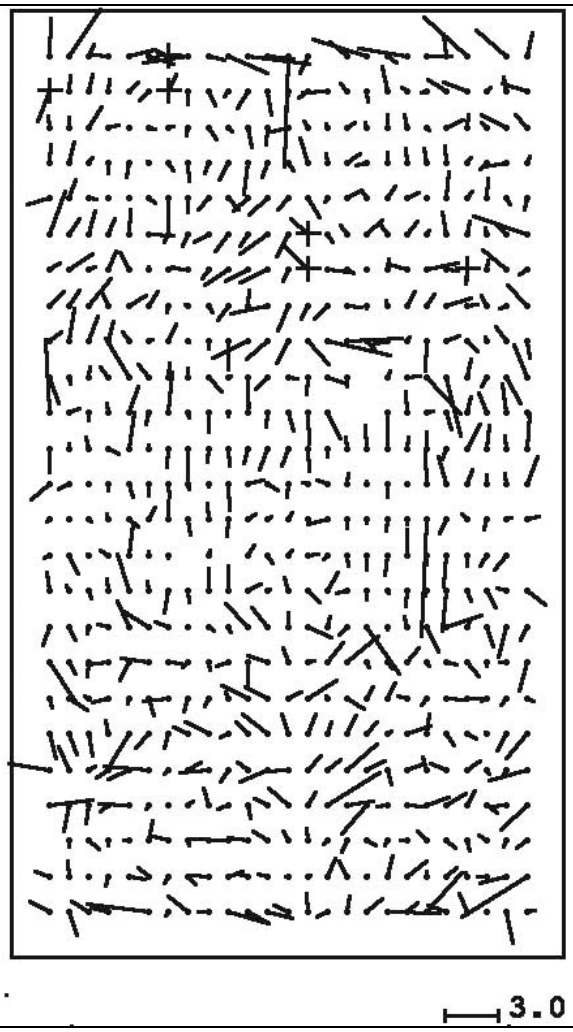

figure 11: averaged and overlaid image residuals of block adjustment without self calibration

	RMSX	RMSY	RMSZ	sigma0
no selfcalibration	3.2 cm	1.7 cm	3.6 cm	2.76 µm
param. 1-12	2.3 cm	1.3 cm	2.3 cm	2.65 µm
param. 1-12, 79-80	2.3 cm	1.3 cm	2.7cm	2.57 µm
param. 1-12, 30–41, 74–77	1.8 cm	1.3 cm	2.2 cm	2.51 µm

table 3: discrepancies at control points
parameters 1-12 = standard BLUH-parameters
parameters 79 – 80 = special common DMC-parameters
parameters 30 – 41, 74 – 77 = special individual DMC parameters

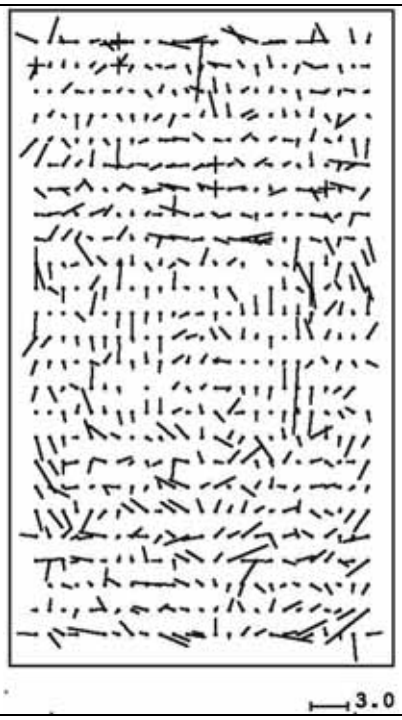

figure 12a: averaged and overlaid residuals

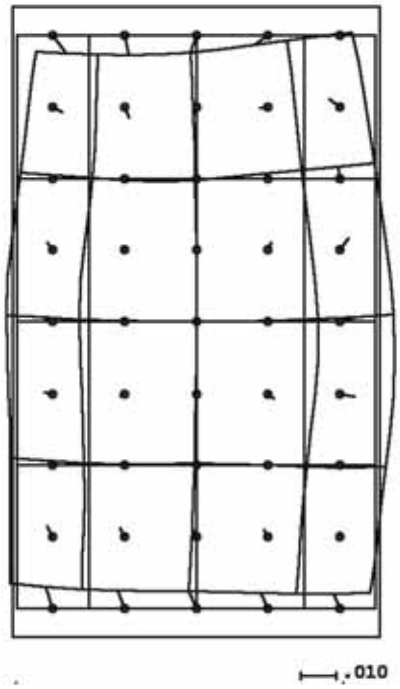

figure 12b: systematic image errors

block adjustment with self calibration – additional parameters 1 – 12 (standard parameters for aerial images)

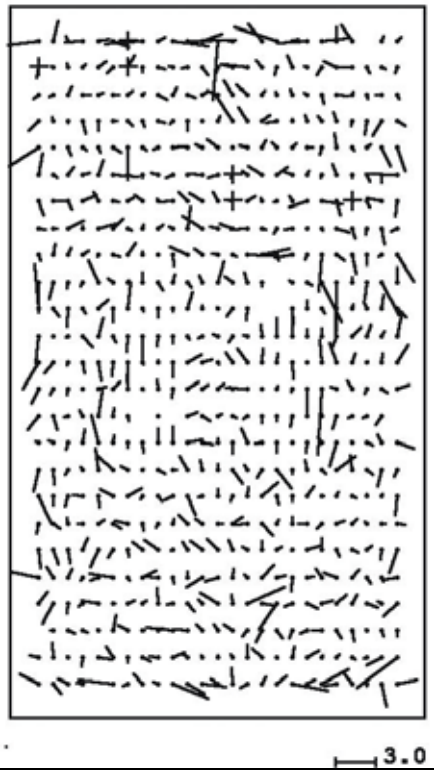

figure 13a: averaged and overlaid residuals

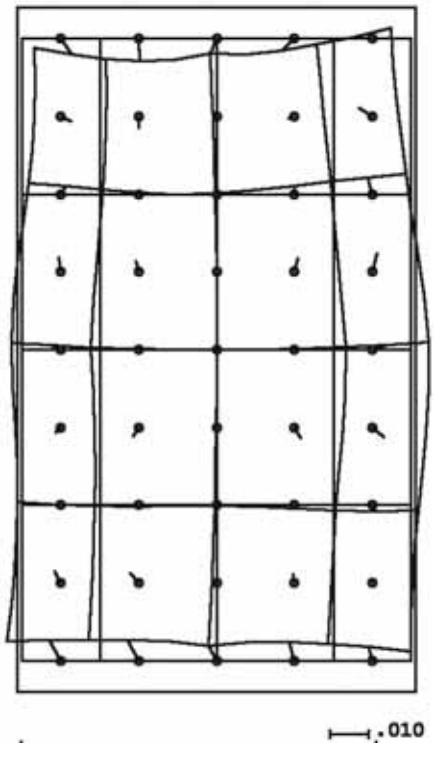

figure 13b: systematic image errors

block adjustment with self calibration – additional parameters 1 – 12 + 79-80 (standard parameters for aerial images + special common DMC-parameters)

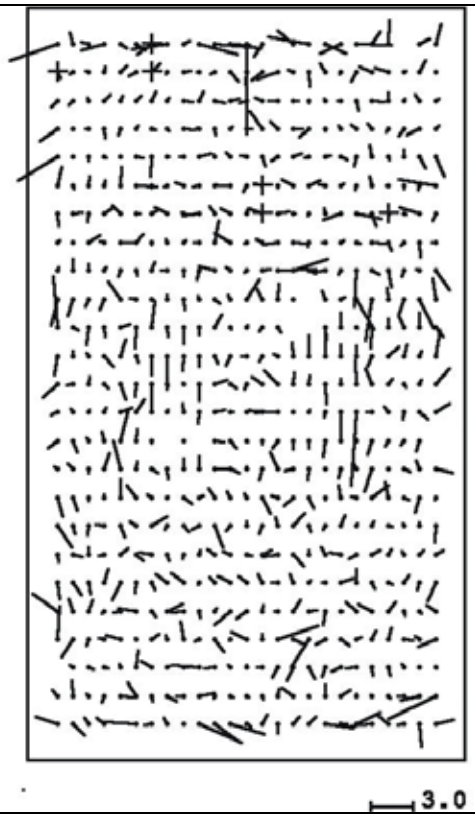

figure 14a: averaged and overlaid residuals

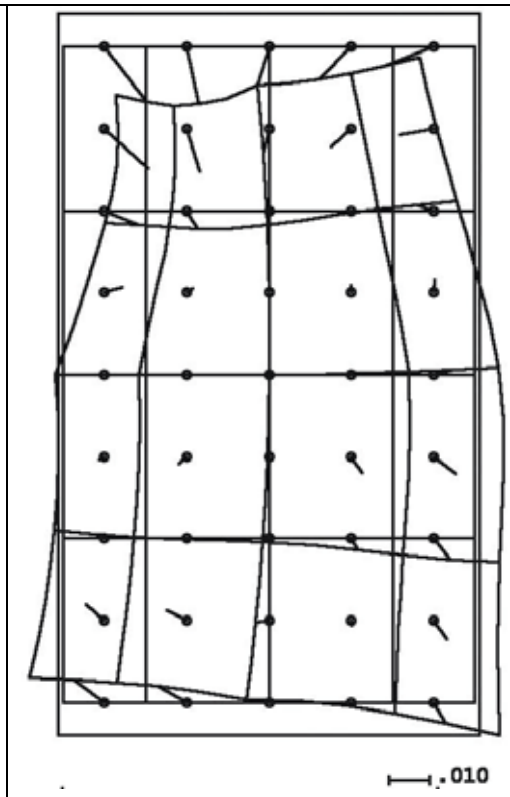

figure 14b: systematic image errors

block adjustment with self calibration – additional parameters 1 – 12 + 30-41, 74-77 (standard parameters for aerial images + special individual DMC-parameters – individual values for all 4 quarters)

EuroSDR DMC Data Sets – Bundle Adjustment Results

(using the image coordinates provided by the pilot centre)

Xiaoliang Wu

CSIRO Mathematical and Information Sciences
Private Bag 5, Wembley, WA 6913, Australia
Phone: +61 8 9333 6162, Fax: +61 8 9333 6121
Email: Xiaoliang.Wu@csiro.au

February 2007

In this report the DMC bundle adjustment results obtained using the image coordinates (Phase 2b) provided by EuroSDR Pilot Centre [1] were presented.

1. Results of bundle adjustments

Three block adjustment configurations were conducted, they are: the low-flying height, the high-flying height and the combined low- and high- flying heights. No GPS or PATB orientation data was used during block adjustment processing, therefore the results were obtained purely based on the image/space coordinates provided by the Pilot Centre. In the following description, "adjusted coordinates" mean the bundle adjusted coordinates for those points that were used as control points during bundle adjustment processing, "obtained coordinates" mean the new computed coordinates for those check points (space coordinates are unknown during bundle adjustment). In order to make control and check points easily discernible, the control and check point numbers are prefixed by 90..0 and 80..0 respectively.

1.1 Adjusted coordinates of control points

The block adjustment results for DMC data sets are shown in the following tables. Tables 1-3 list the adjusted coordinates of control points and their differences to the supplied coordinates. The root mean squares (RMS) values of X, Y and Z differences are also given in the last rows.

Table 1: The adjusted coordinates of 23 control points and the differences between supplied coordinates and adjusted coordinates for DMC low-flying height (unit is in metre)

… deleted M. Cramer …

Table 2: The adjusted coordinates of 21 control points and the differences between supplied coordinates and adjusted coordinates for DMC high-flying height (unit is in metre)

… deleted M. Cramer …

Table 3: The adjusted coordinates of 23 control points and the differences between supplied coordinates and adjusted coordinates for DMC low- and high- flying heights (unit is in metre)

… deleted M. Cramer …

1.2 Obtained coordinates of check points

Tables 4-6 list the obtained coordinates of check points.

Table 4: The obtained coordinates of 21 check points for DMC low-flying height (unit is in metre)

… deleted M. Cramer …

Table 5: The obtained coordinates of 20 check points for DMC high-flying height (unit is in metre)
… deleted M. Cramer …

Table 6: The obtained coordinates of 21 check points for DMC low- and high- flying heights (unit is in metre)
… deleted M. Cramer …

4. Discussion about the processing and results

A special program was written to import image coordinates provided by the Pilot Centre [1] into our in-house bundle adjustment software. All image coordinates were successfully imported and no additional points were introduced. High-flying point identification names (except the control points) were renamed because there are identical point names between high-flying and low-flying points (same point names but not the same points).

A relative orientation and model connection scheme was applied to all images using imported image coordinates. For the high-flying data set, the relative orientation started from the first stereo pair in the first run (image 6003 was set as the origin in high-flying height), while for the low-flying data set, the relative orientation started from the first stereo pair in first run (image 101 was set as the origin in low-flying height). The relative orientation parameters from the first stereo pairs were then used for model connection for the rest stereo pairs in order to join all models spatially.

Once all relative models were connected, the initial image orientation values and initial model coordinates for all points were determined using the relative model parameters, and bundle adjustment was then performed. The in-house developed software was used to perform bundle adjustment.

No GPS and PATB orientation data was used for any purposes during block adjustment processing. The known (fixed) parameters for each image are the pixel size: 0.012mm in both pixel directions and the focal length: 120.00mm. Six unknowns for each image are the camera position (X, Y and Z) and image rotation angles (omega, phi and kappa). No additional parameters were introduced within bundle adjustment processing. Cartesian coordinate system was assumed for control points and therefore no map projection processing was performed during bundle adjustment processing.

From the results presented in the previous section, we observe that the adjusted space coordinates for the control points have very good agreement (low residual error between the supplied space coordinates and the adjusted space coordinates) for all DMC flying heights: X, Y, Z RMS are less than 0.05m, 0.03m and 0.01m, respectively. The X, Y, Z RMS of the control points for the low-flying height are quite stunning: 0.007m, 0.008m and 0.002m, respectively. However, the final assessment for bundle adjustment results will be analysed by the Pilot Centre using the provided coordinates of check points.

References

1. Cramer M., 2007, Experimental Phase 2b – DMC and UltracamD Remarks. Institute for Photogrammetry, University of Stuttgart.

Bundle Block Adjustment Results of
EuroSDR Phase 2 –DMC Blocks

Intergraph, Huntsville

1) DMC-High Block Specifications

- Number of Images: 34 (in three strips)
- Number of Control Points: 21
- Number of Check Points: 20
- Coordinate system: UTM (easting, northing, zone 32) on WGS84 ellipsoid and ellipsoidal heights [m]
- Standard deviation of image measurement: 3 microns
- Standard deviation of Control Points: 0.06m, 0.06m, 0.08m for X, Y, and Z
- Number of rays per point: Please see following plot.

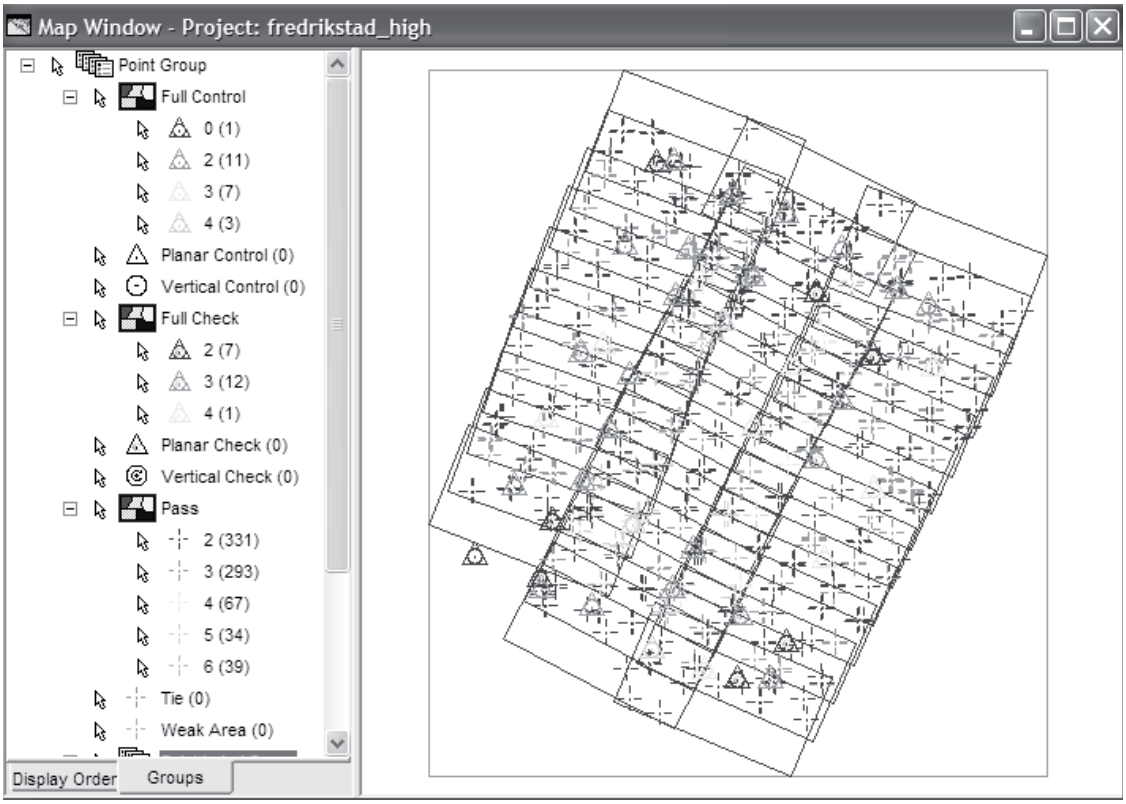

Figure 1. DMC-High Block Geometry with Point Distribution

Bundle Block Adjustment Results:

a) Without Self-Calibration

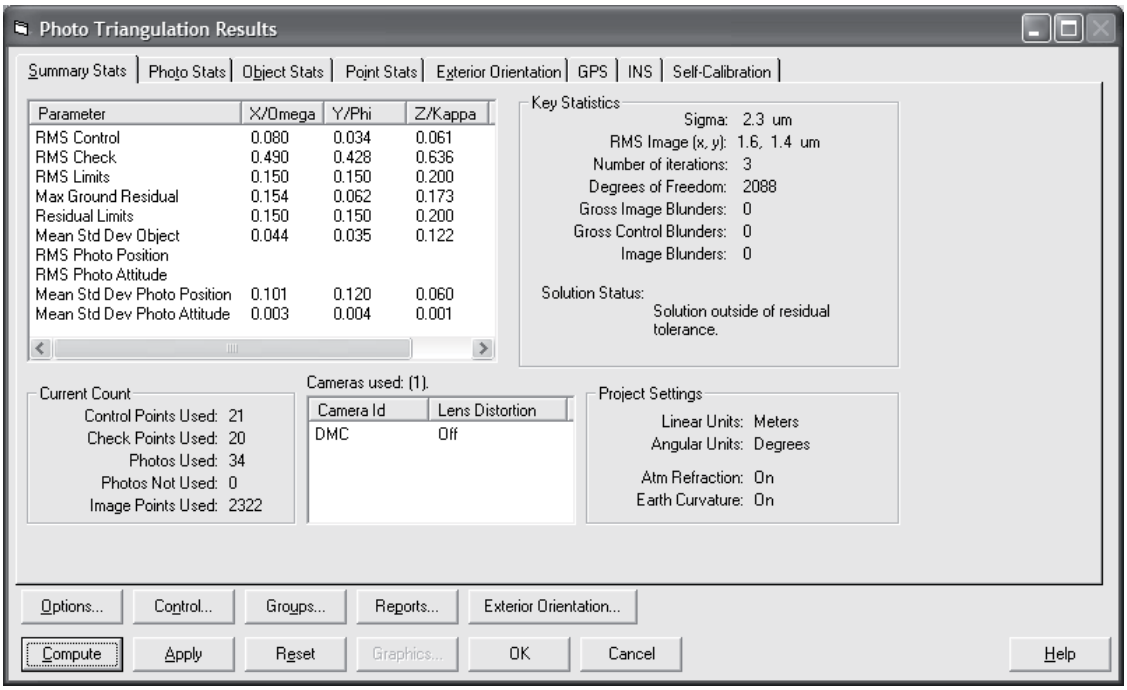

Figure 2. Summary Statistics of Bundle Adjustment without Self-Calibration

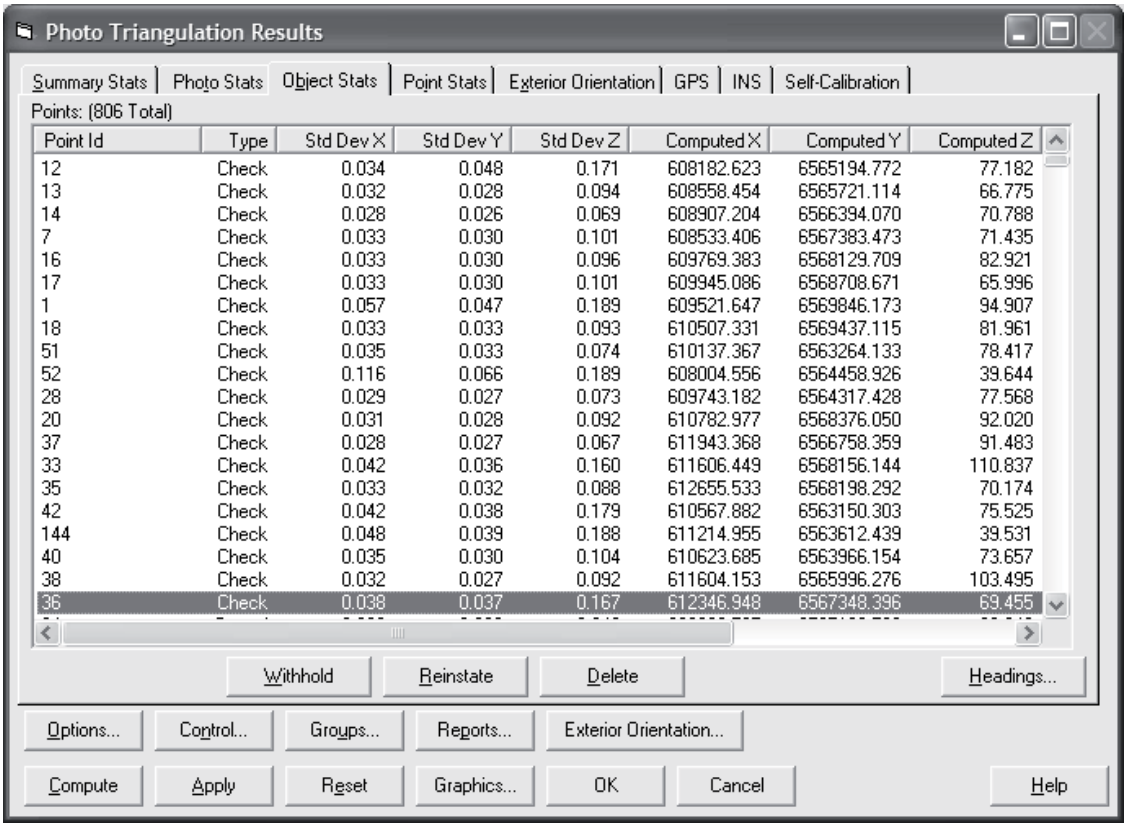

Figure 3. Check Point Coordinates with Their a Posteriori Standard Deviations

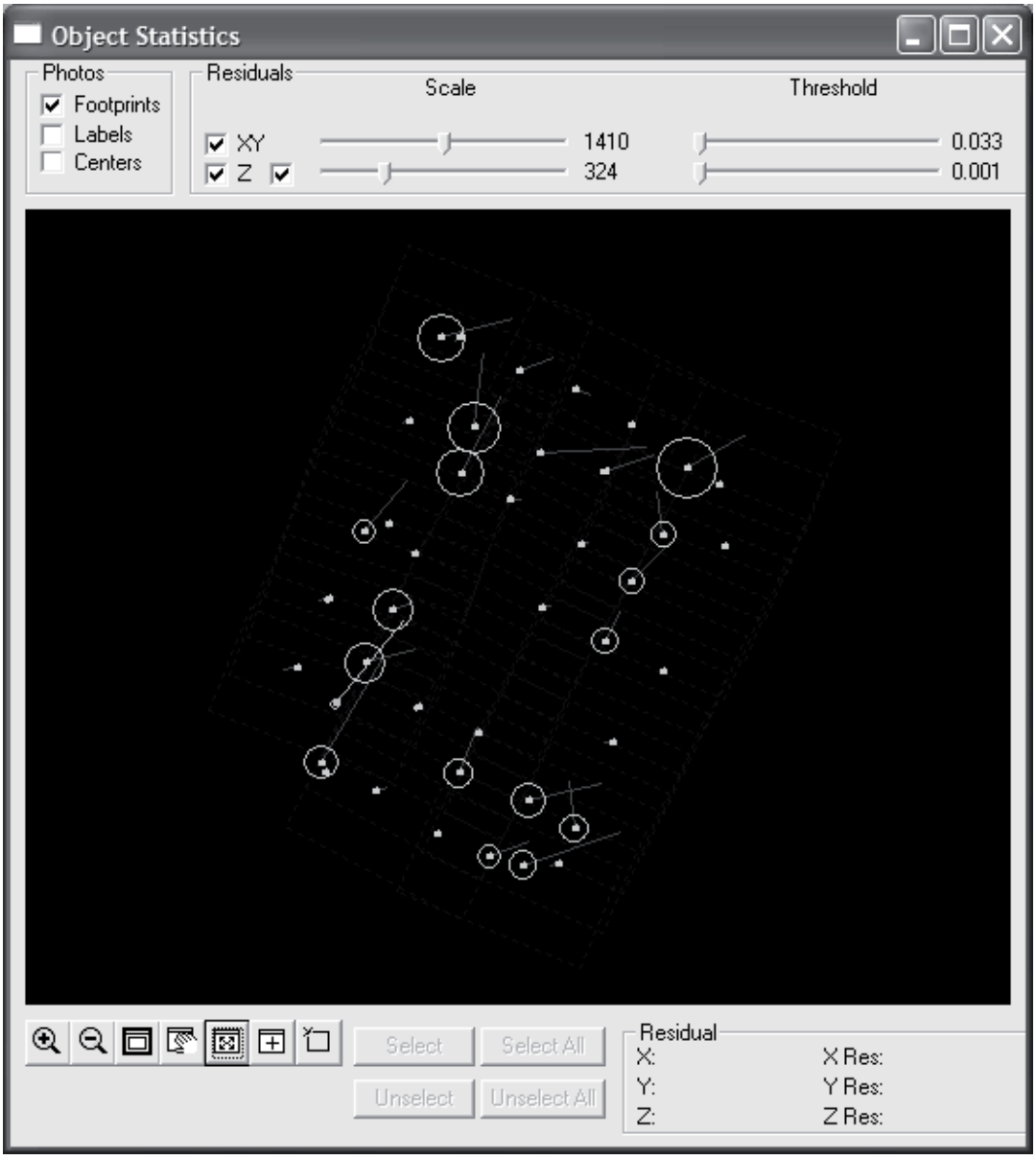

Figure 4. Control Point Residuals Plot

Please see "DMC-High-Without-SC-Detail-Results.doc" file for details.

b) With Self Calibration (One set of Ebner Model)

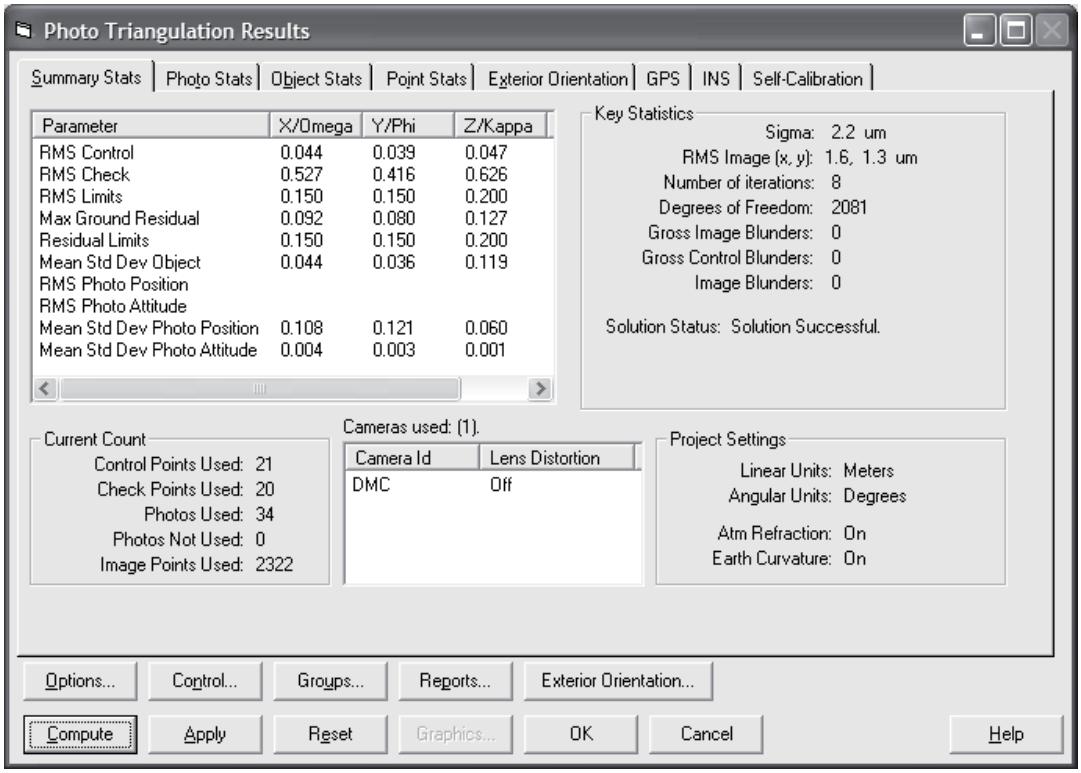

Figure 5. Summary Statistics of Bundle Adjustment with Self-Calibration

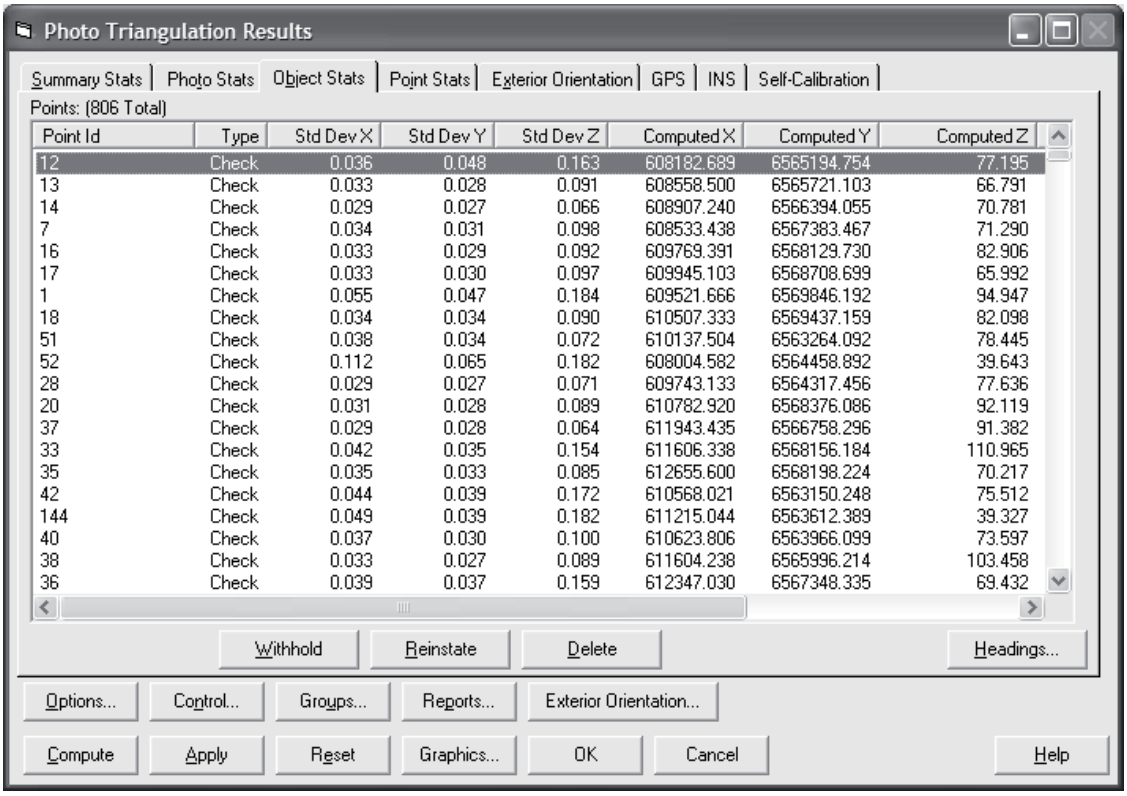

Figure 6. Check Point Coordinates with Their a Posteriori Standard Deviations

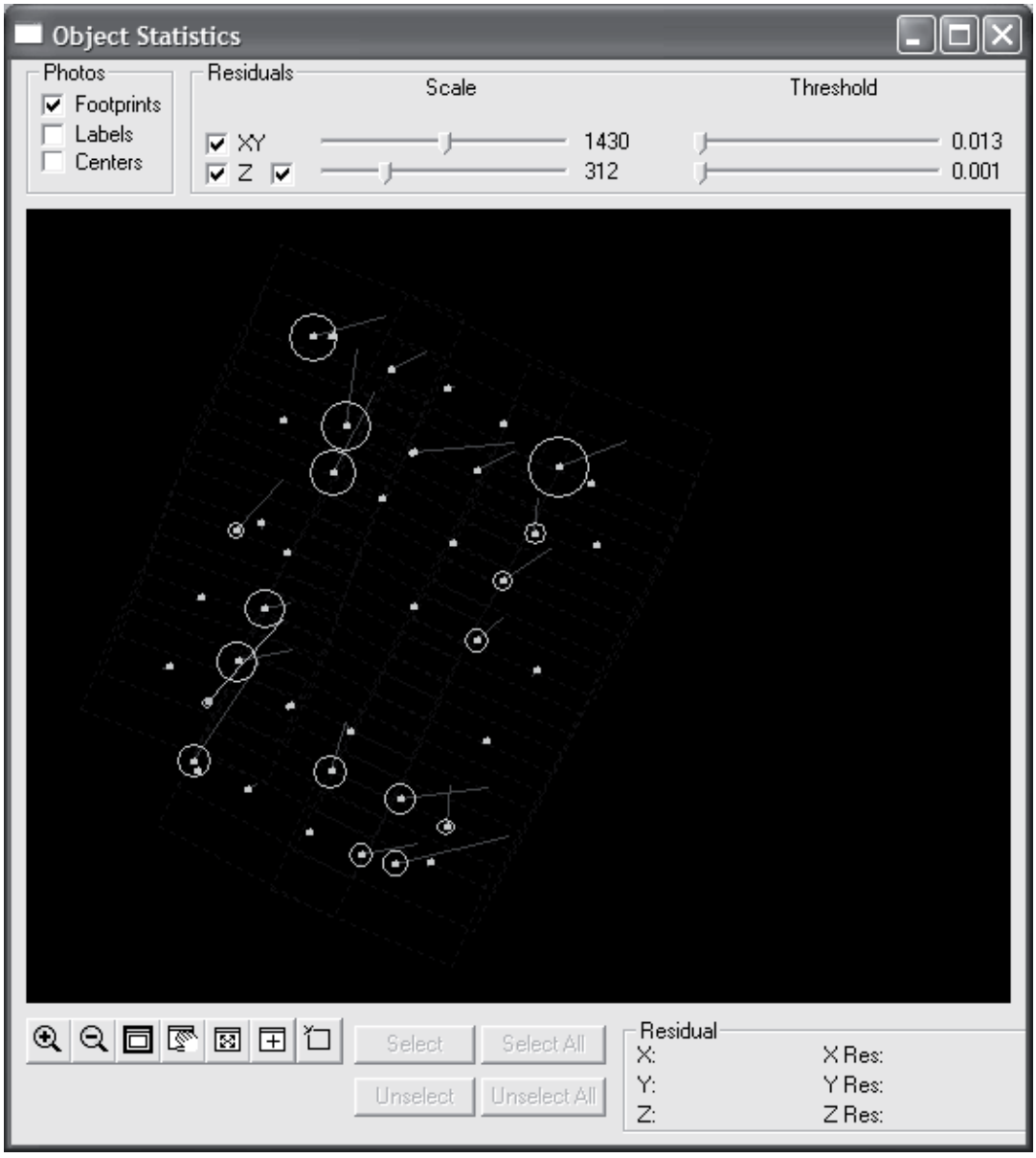

Figure 7. Control Point Residuals Plot

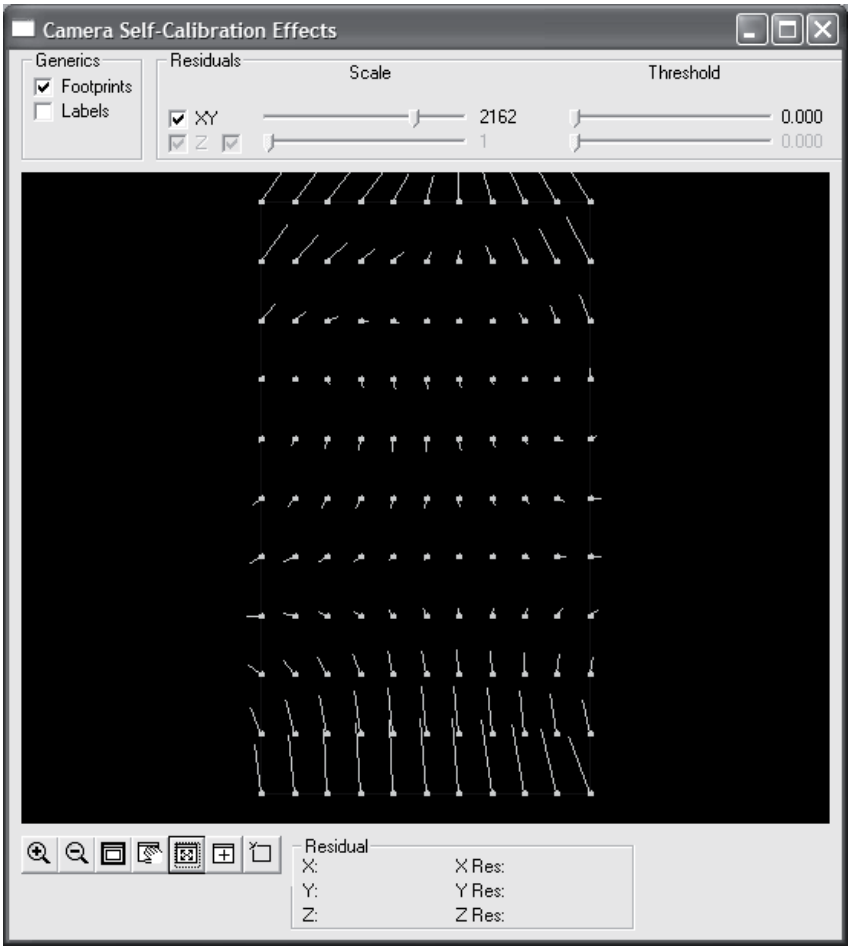

Figure 8. Self-Calibration Distortion Plot

Please see "DMC-High-With-SC-Detail-Results.doc" for a complete adjustment report.

2) DMC-Low Block Specifications

- Number of Images: 155 (in five strips)
- Number of Control Points: 22
- Number of Check Points: 22
- Coordinate system: UTM (easting, northing, zone 32) on WGS84 ellipsoid and ellipsoidal heights [m]
- Standard deviation of image measurement: 3 microns
- Standard deviation of Control Points: 0.06m, 0.06m, 0.08m for X, Y, and Z
- Number of rays per point: Please see following plot.

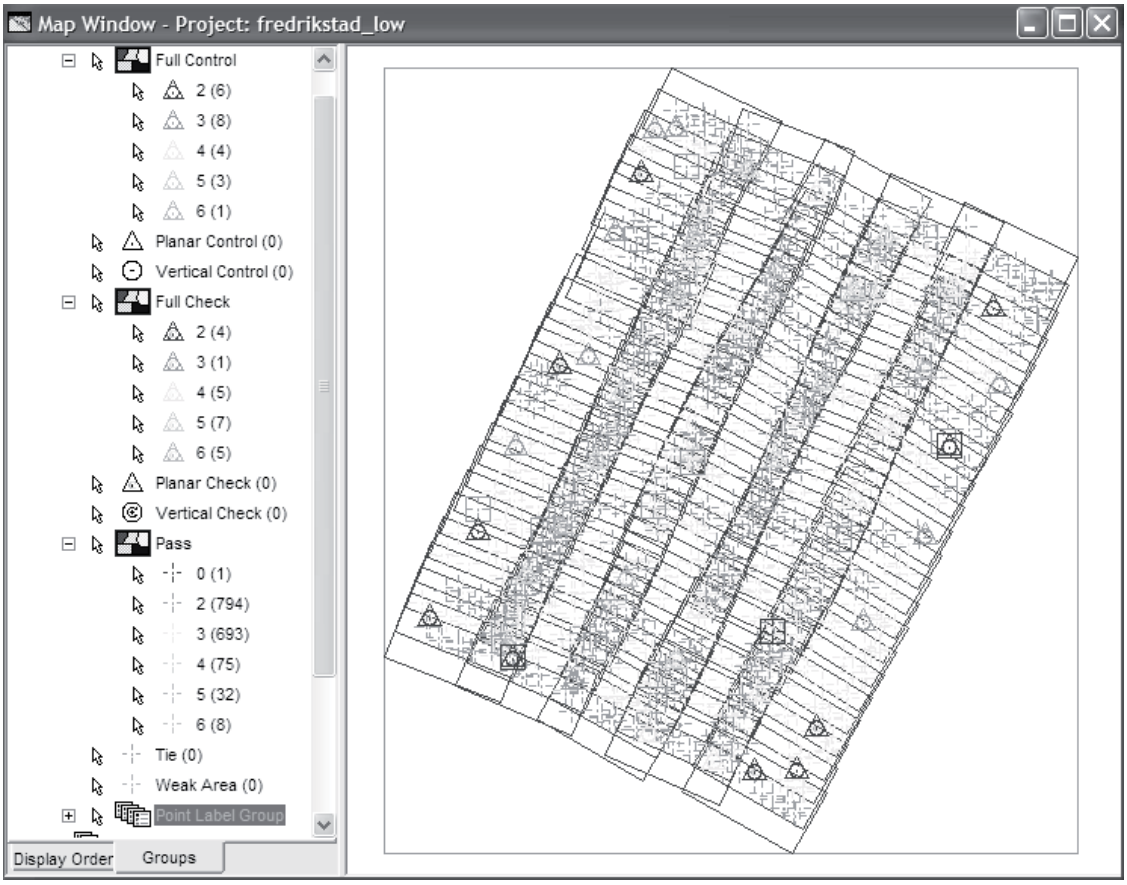

Figure 9. DMC-Low Block Geometry with Point Distribution

Bundle Adjustment Results

a) Without Self-Calibration

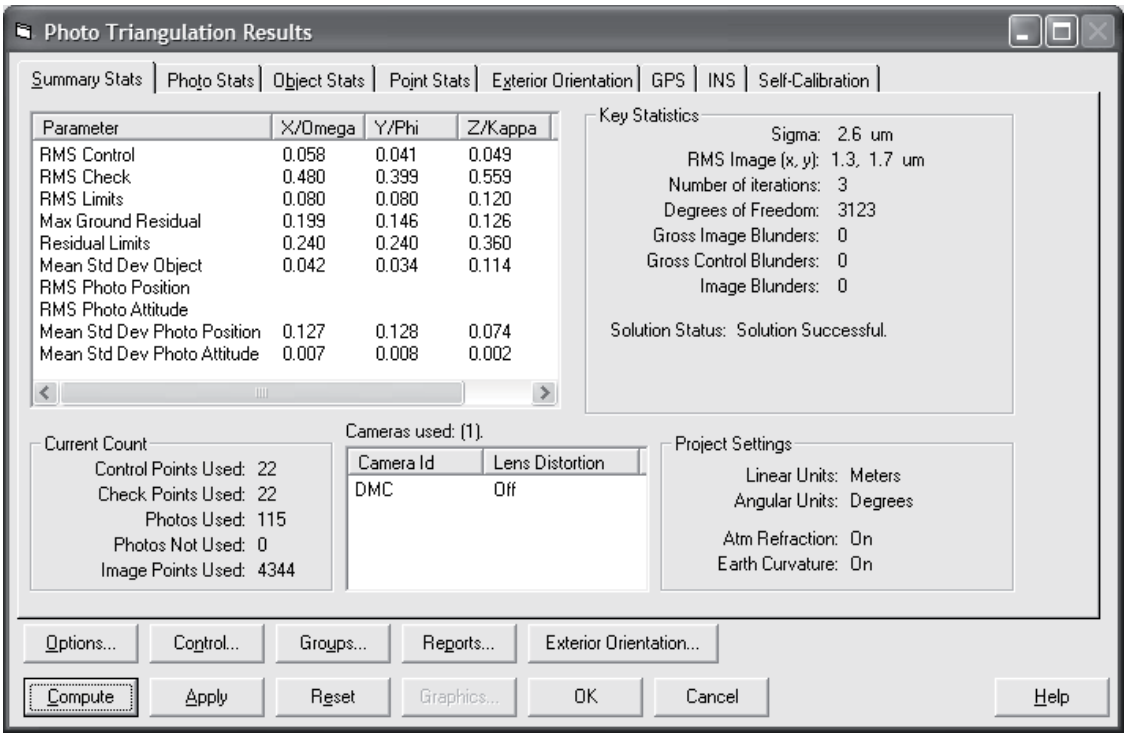

Figure 10. Summary Statistics of Bundle Adjustment without Self-calibration

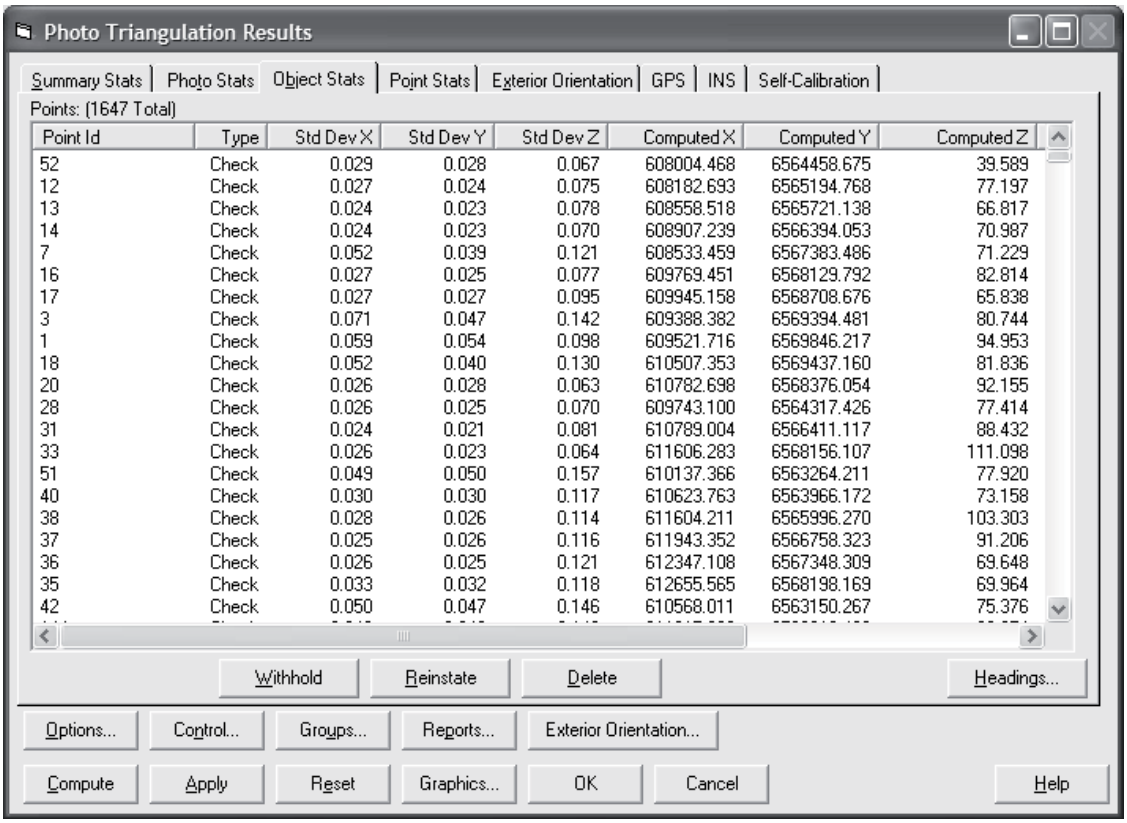

Figure 11. Check Point Coordinates with Their a Posteriori Standard Deviations

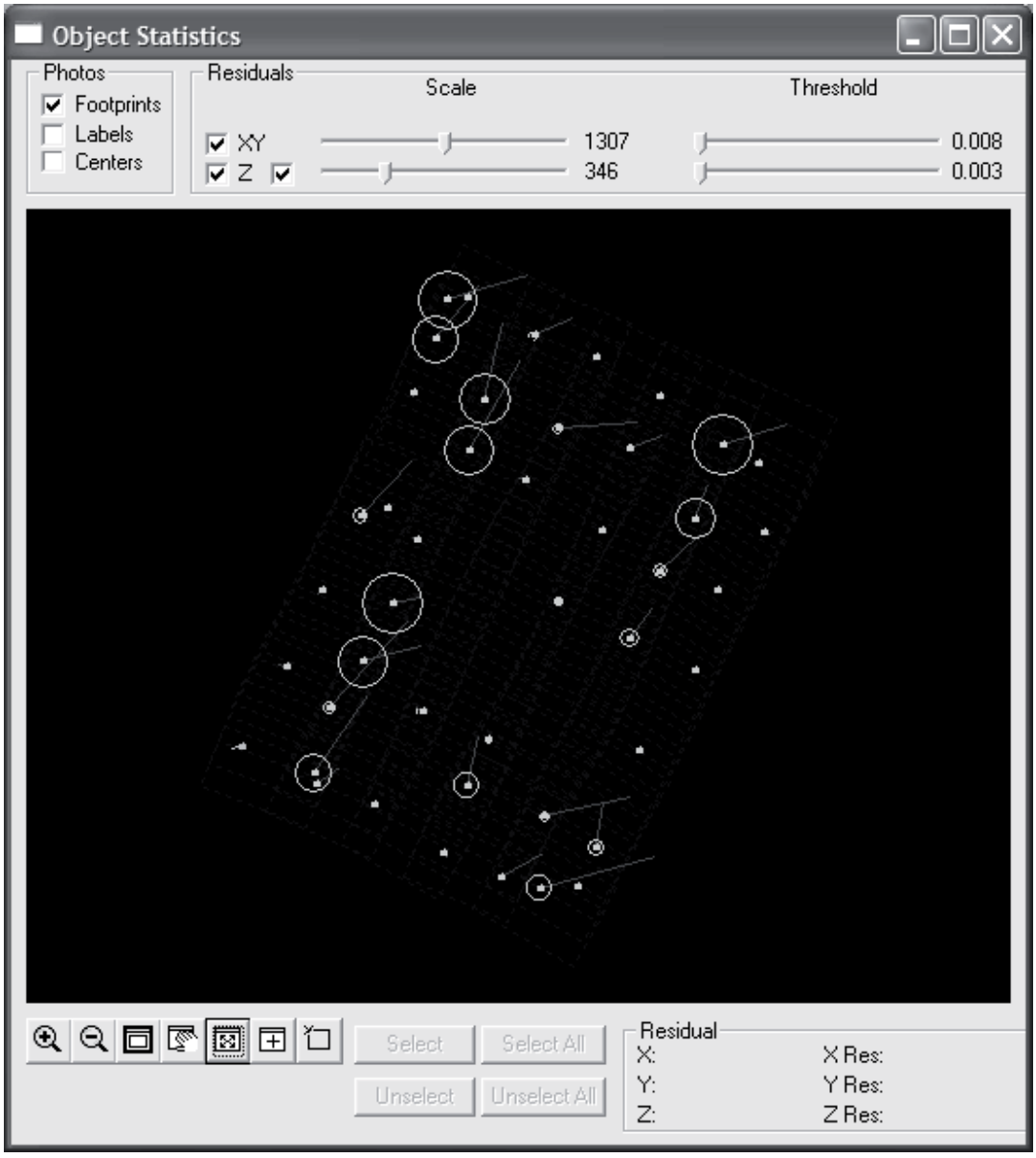

Figure 12. Control Point Residual Plot

Please see "DMC-Low-Without-SC-Detail-Results.doc" file for details

b) With Self-Calibration (one set of Ebner Model)

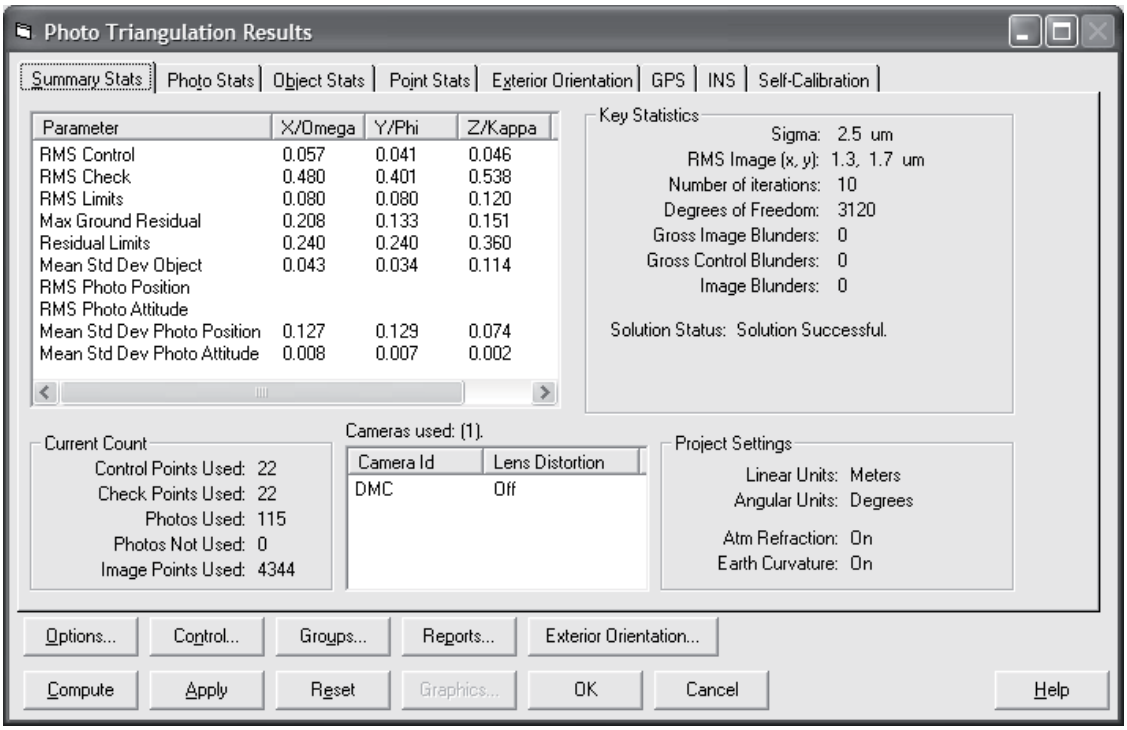

Figure 13. Summary Statistics of Bundle Adjustment with Self-Calibration

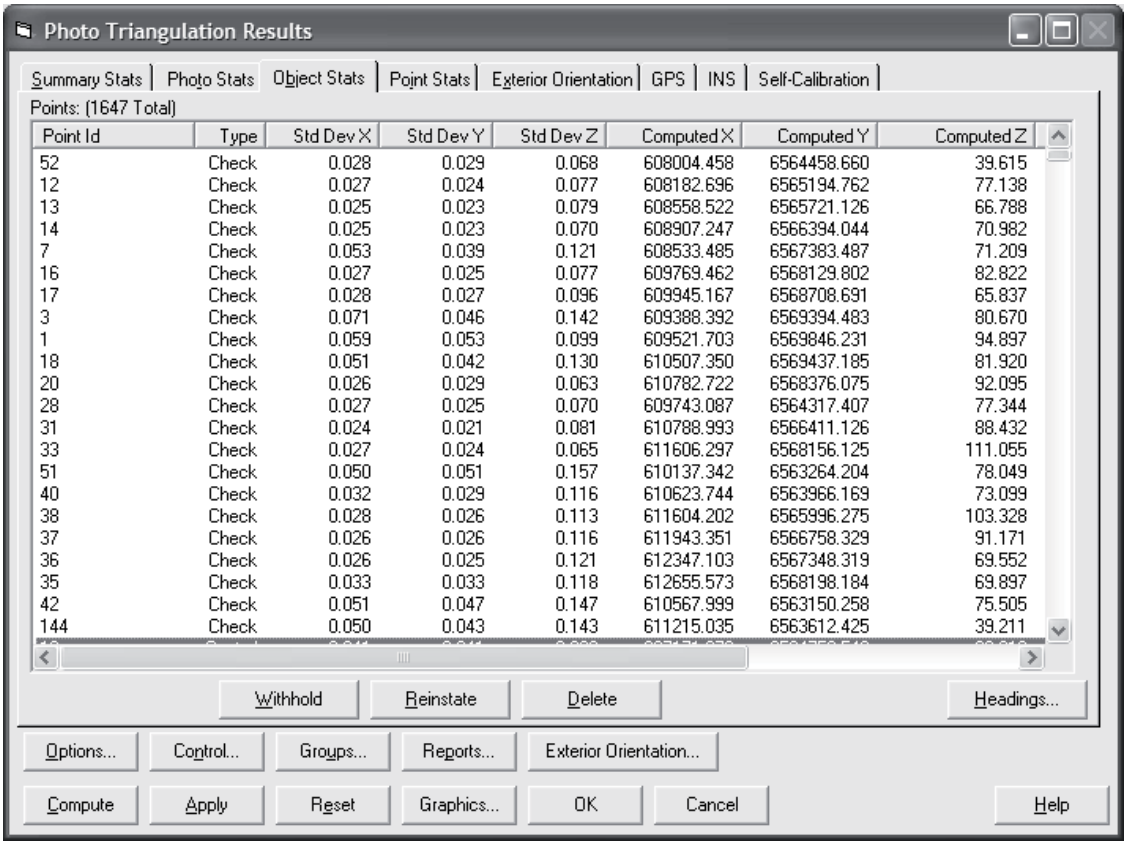

Point Id	Type	Std Dev X	Std Dev Y	Std Dev Z	Computed X	Computed Y	Computed Z
52	Check	0.028	0.029	0.068	608004.458	6564458.660	39.615
12	Check	0.027	0.024	0.077	608182.696	6565194.762	77.138
13	Check	0.025	0.023	0.079	608558.522	6565721.126	66.788
14	Check	0.025	0.023	0.070	608907.247	6566394.044	70.982
7	Check	0.053	0.039	0.121	608533.485	6567383.487	71.209
16	Check	0.027	0.025	0.077	609769.462	6568129.802	82.822
17	Check	0.028	0.027	0.096	609945.167	6568708.691	65.837
3	Check	0.071	0.046	0.142	609388.392	6569394.483	80.670
1	Check	0.059	0.053	0.099	609521.703	6569846.231	94.897
18	Check	0.051	0.042	0.130	610507.350	6569437.185	81.920
20	Check	0.026	0.029	0.063	610782.722	6568376.075	92.095
28	Check	0.027	0.025	0.070	609743.087	6564317.407	77.344
31	Check	0.024	0.021	0.081	610788.993	6566411.126	88.432
33	Check	0.027	0.024	0.065	611606.297	6568156.125	111.055
51	Check	0.050	0.051	0.157	610137.342	6563264.204	78.049
40	Check	0.032	0.029	0.116	610623.744	6563966.169	73.099
38	Check	0.028	0.026	0.113	611604.202	6565996.275	103.328
37	Check	0.026	0.026	0.116	611943.351	6566758.329	91.171
36	Check	0.026	0.025	0.121	612347.103	6567348.319	69.552
35	Check	0.033	0.033	0.118	612655.573	6568198.184	69.897
42	Check	0.051	0.047	0.147	610567.999	6563150.258	75.505
144	Check	0.050	0.043	0.143	611215.035	6563612.425	39.211

Figure 14. Check Point Coordinates with Their a Posteriori Standard Deviations

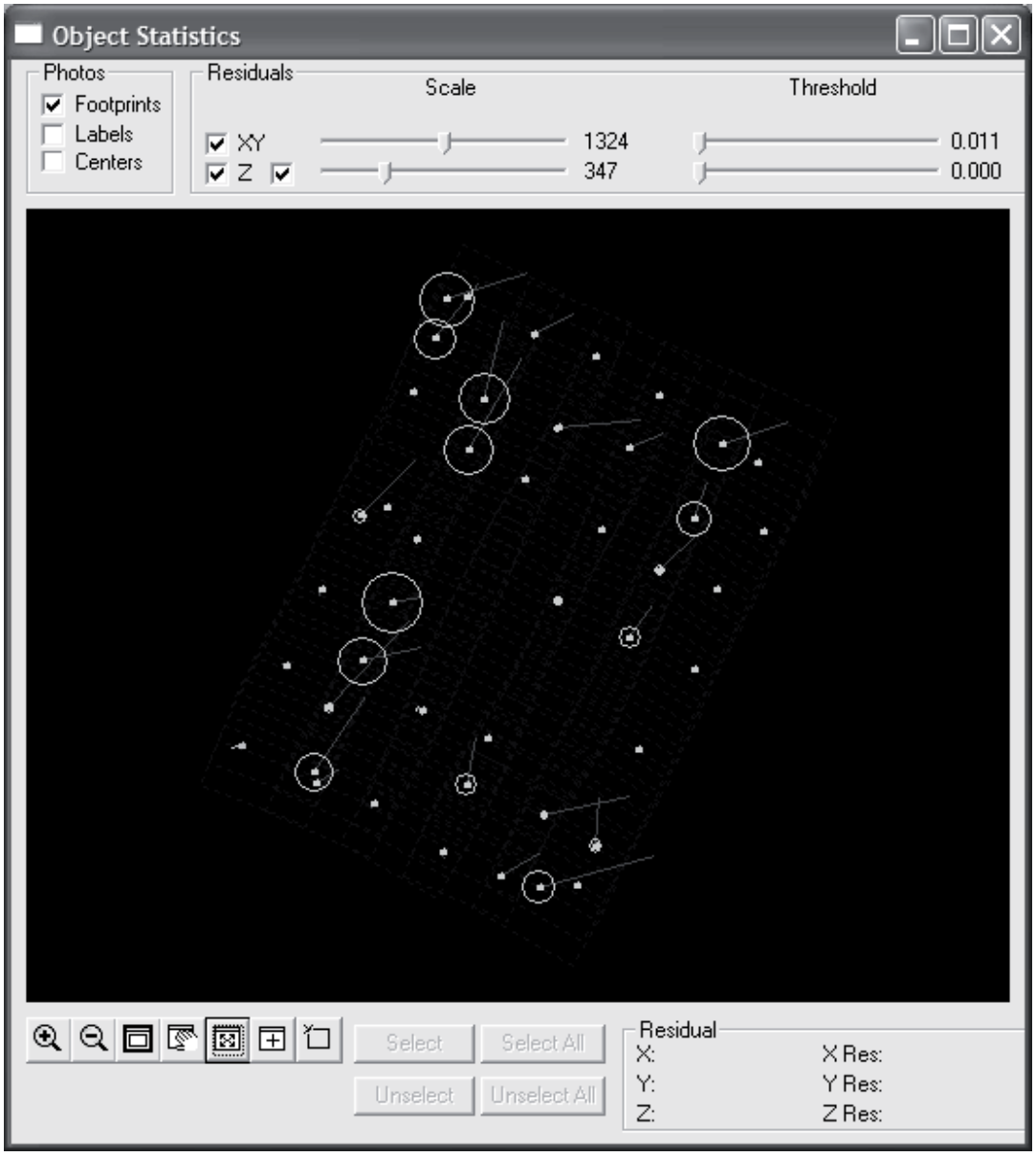

Figure 15. Control Point Residual Plot

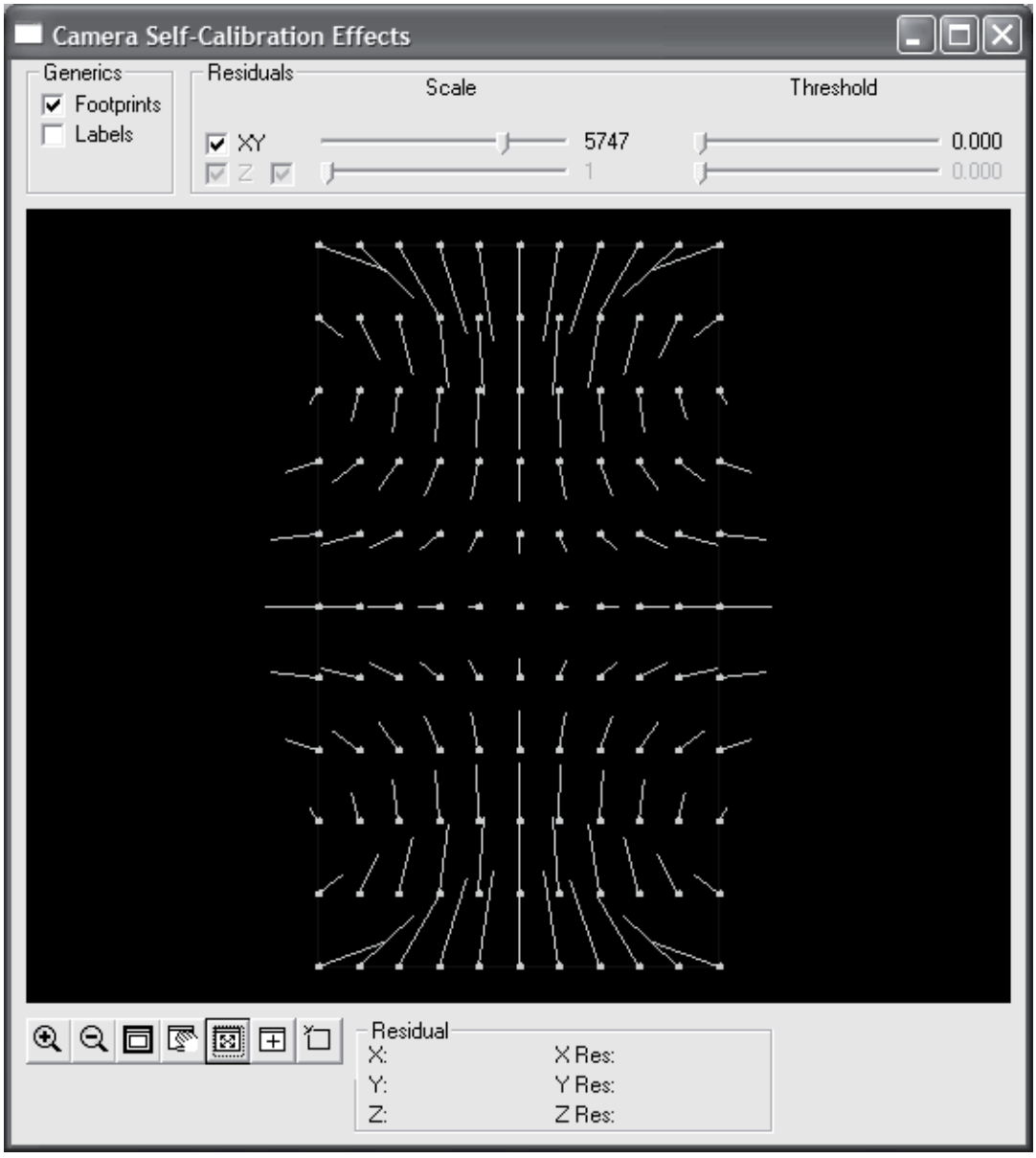

Figure 16. Self Calibration Distortion Plot

Please see “DMC-Low-With-SC-Detail-Results.doc” file for details

Preliminary report for the EuroSDR Ultracam Test in ITACYL (Spain)

Oscar O. Rodríguez-Rico (ita-rodricos@itacyl.es)
David A. Nafría (nafgarda@itacyl.es)

Introduction

According to the EuroSDR digital camera test schedule, the individual reports must be finished around 19th may 2006. Due several reasons we haven't been able to write the report on time, so we write this document with some preliminary results in order to inform de ongoing process.

Until now we have only processed the low flight of UltracamD data and those are the results we are showing in this document.

Details for the data processing

Processing Software: Point Measurement and bundle adjustment with Match-AT.

Parameters in use: A priori we prefer to avoid using autocalibration parameters because the ones included in Match-AT are specifics for film cameras.

We have used the following weights values for the bundle adjustment:

Observation	Sigma
Image measurements	±4 µm
Ground control (X,Y)	±0.033 m
Ground control (Z)	±0.010 m
GPS Photocentre (X,Y)	±0.10 m
GPS Photocentre (Z)	±0.15 m

Using two different flight height:

We did an automatic tie point extraction with Match-AT, therefore it was impossible to transfer points between images with more than a 30% of difference in flight height. In order to join both flights we will introduce manual tie points.

Personal feeling about the UltracamD data:

We have plenty of experience with UltracamD data. During 2005 we took more than 25000 photos with two different UltracamD cameras from Spanish contractors. The images supplied by our contractors (also 16 bits deep) have better radiometric performance compared with the data supplied by the EuroSDR. To run the point measurement process we did a contrast stretch (equal for all images).

The automatic tie point measurement didn't work as expected according to our experience with UltracamD images. In our production blocks with a 60% overlap we usually get around 145 tie points per image while in this block we only have got 90 tie points per image with a more complex surface and higher overlap.

From our point of view the processing methodology for the GPS trajectory is not clear enough. In our contracts with UltracamD data we usually employ GPS/INS from IGI Aerocontrol IId. For this project we actually don't know if the flight was done with gyrostabilized mount and if so, if the moving lever arm was taken into account. According with the provided data (only a fixed lever arm) we suppose that there isn't gyrostabilized mount.

According with the distance between the GPS base and the plane GPS rover we decided to introduce drift parameters in the bundle adjustment and leave the lever arm of the GPS antenna at values of (0,0,0) to check if the shift parameters are similar to the lever arm. The results show that the linear drifts for the GPS data have an important effect in contrast with a theoretical absolute GPS solution.

Also we want to empathize that some terrain control and check points are very difficult to identify on the images so we prefer to avoid use them.

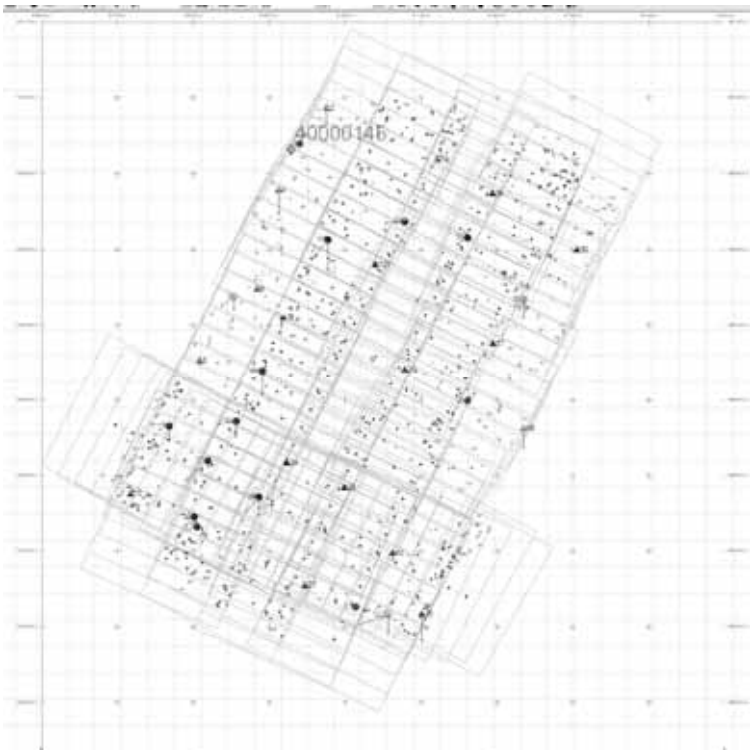

Preliminary results

According with the test procedure the participants should provide the adjusted coordinates for the check points. In the next table we show these coordinates for the low flight.

ID	X	Y	Z	SX	SY	SZ	CHECK POINT
2	609754.062	6569860.921	75.413	0.0150	0.0140	0.0410	
4	609122.878	6568780.359	82.679	0.0140	0.0130	0.0380	
6	608840.218	6567477.201	45.682	0.0130	0.0130	0.0400	
7	608533.474	6567383.416	71.278	0.0360	0.0270	0.0960	YES
8	608083.083	6566532.333	68.488	0.0140	0.0130	0.0380	
9	607680.640	6565659.976	84.479	0.0200	0.0180	0.0560	YES
10	607171.771	6564752.610	98.832	0.0140	0.0140	0.0400	
11	608038.351	6564322.152	68.989	0.0160	0.0150	0.0460	YES
12	608182.780	6565194.772	77.007	0.0150	0.0140	0.0460	YES
13	608558.649	6565721.144	66.630	0.0140	0.0140	0.0400	YES
14	608907.460	6566394.009	70.871	0.0170	0.0140	0.0480	YES
15	609181.141	6567102.708	39.231	0.0120	0.0110	0.0340	
16	609769.578	6568129.739	82.921	0.0160	0.0150	0.0480	YES
19	611214.477	6569184.148	106.613	0.0120	0.0120	0.0340	
20	610782.733	6568376.057	91.850	0.0140	0.0130	0.0380	YES
24	609229.469	6565160.751	39.291	0.0100	0.0090	0.0290	
25	608859.477	6564716.564	39.588	0.0120	0.0120	0.0380	YES

27	609470.076	6563542.371	80.113	0.0110	0.0110	0.0330	
29	609991.985	6564832.889	74.037	0.0090	0.0090	0.0280	
31	610789.054	6566411.108	88.146	0.0100	0.0100	0.0280	
33	611606.354	6568156.210	110.764	0.0140	0.0140	0.0400	YES
34	611942.832	6568736.161	110.062	0.0120	0.0120	0.0360	
36	612346.870	6567348.381	69.535	0.0250	0.0270	0.1340	YES
40	610623.797	6563966.197	73.644	0.0110	0.0110	0.0360	
42	610568.081	6563150.342	75.152	0.0450	0.0250	0.1320	YES
43	611009.192	6563159.079	57.264	0.0130	0.0130	0.0390	
46	612350.142	6565615.222	55.680	0.0150	0.0140	0.0400	
52	608004.620	6564458.815	39.460	0.0160	0.0150	0.0470	YES
121	610399.116	6567796.098	67.565	0.0100	0.0100	0.0290	

In Valladolid, 23rd june 2006

The Bundle Adjustment Results of EuroSDR UltraCamD Data Sets

Xiaoliang Wu

CSIRO Mathematical and Information Sciences
Private Bag 5, Wembley, WA 6913, Australia
Phone: +61 8 9333 6162, Fax: +61 8 9333 6121
Email: Xiaoliang.Wu@csiro.au

July 2006

This report briefly presents the bundle adjustment results of the EuroSDR UltraCamD data set provided by EuroSDR Pilot Centre (www.eurosdr.net) and the Calibration Network (www.ifp.uni-stuttgart.de/eurosdr/index.html). Both the high-flying and the low-flying data sets were processed, and bundle adjustment results under various configurations are presented and some discussions are made based on the UltraCamD data set experiences. The recommended coordinates of check points are also given for further accuracy analysis which will be taken by Pilot Centre.

1. Control and check points

The UltraCamD test site is located at Fredrikstad, Norway. The flight direction is from north-east to south-west and the site cover area is about 5km by 6.5km (see Figure 1). Digital images were taken using UltraCamD camera [1-4]. The digital image frame size is 11500 by 7500 and each pixel of the captured panchromatic band data is stored in 12bits. 51 signalised object points are available and well distributed around the site (not all of them visible on all images). Tables 1 and 2 list the 19 control points and 18 check points and their object space coordinates for EuroSDR UltraCamD high-flying data set. For each control point or check point, there is a chip images provided by Pilot Centre (except check point 80052). In order to make control and check points easily discernible, a control point number has been added by 90000 and a check point number has been added by 80000. All 19 control points and 18 check points were well identified and matched on all appeared images (both the high-flying and the low-flying data sets) based on the provided chip images. Since check point 80052's chip image is unavailable from ancillary data provided, 80052 was identified by back projecting its space coordinates onto images using the estimated image orientation parameters. In the following context, the data set of 19 control points is referred as the control point set and the data set of 18 check points is referred as the check point set.

Table 1: Control Points and their supplied object space coordinates (19 points)

… deleted M. Cramer …

Table 2: Check Points and their supplied object space coordinates (18 points)

… deleted M. Cramer …

2. Bundle Adjustment Configurations

As illustrated in Figure 1, there are 2 flying strips in the high-flying data set and 5 flying strips in the high-flying data set. Based on the available strips, 5 bundle adjustment configurations are designed as described as follows:

A. Using 2 long strips from the high-flying data set;
B. Using 4 long strips from the low-flying data set;
C. Using 4 long strips and 1 cross strip from the low-flying data set;
D. Using 2 long strips from the high-flying data set and 4 long strips from the low-flying data set; and
E. Using 2 long strips from the high-flying data set and 4 long strips and 1 cross strip from the low-flying data set.

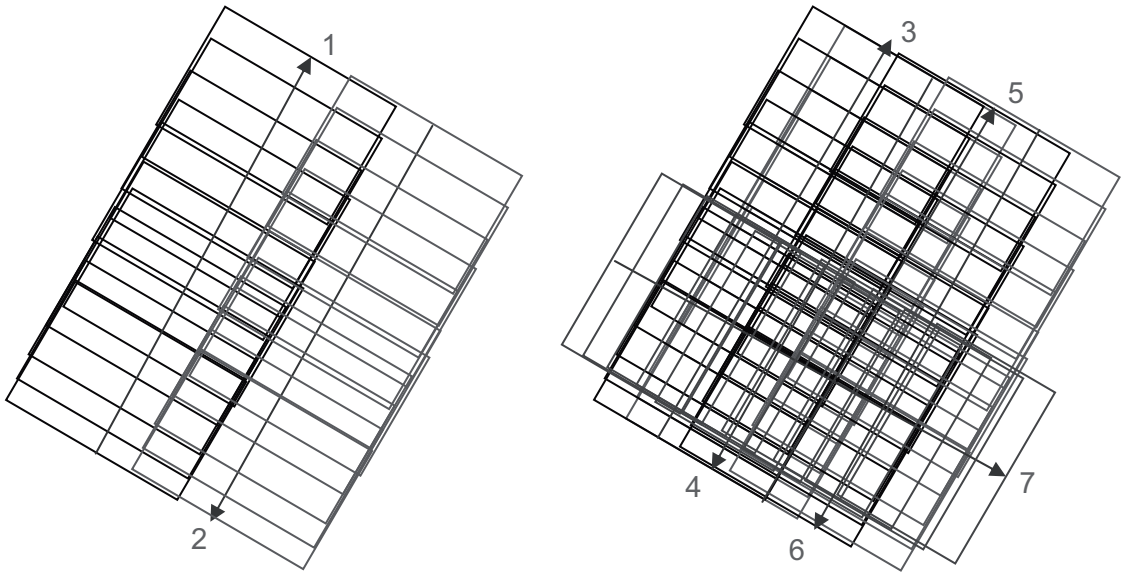

Figure 1: UltraCamD test site Fredrikstad flight configuration. Left: the low-flying data set contains 2 long strips, the flying height is 3800m, the ground distance sample (GDS) is 0.34m and there are total 29 images. Right: the low-flying data set contains 4 long strips and 1 cross strip, the flying height is 1900m, GSD is 0.17m and the there are total 132 images.

3. Experiments and Results of Image Orientation and Bundle Adjustment

All points of the control point set and check point set were well measured on their appeared images in both the high-flying and the low-flying data sets. An image matching technique was used to pass points to other images. Most stereo pairs have enough (more than 6) combined control and check points appeared within the overlapping areas, in the situation while less than 6 combined control and check points appeared on a particular stereo pair, a few pass points were added to guarantee the minimum point number required to perform relative orientation. A relative orientation and model connection scheme was applied to all images. For the high-flying data set, the relative orientation started from the first stereo pair in Strip 1, while for the low-flying data set, the relative orientation started from the first stereo pair in Strip 3 (Figure 1). The relative orientation parameters from the first stereo pairs were then used for model connection for next stereo pairs in order to join all models spatially [5].

Once all relative models were connected, the initial image orientation values and initial model coordinates for all points were determined using the relative model parameters, and bundle adjustment was then performed. The in-house developed software was used to perform

bundle adjustment. The bundle adjustment equations used are based on the well-known co-linearity equations (Wang, pp.93). The known parameters for each image are the pixel size: 0.009mm in both pixel directions and the focal length: 101.4mm [1], no GPS and PATB data is used for any purposes. Six unknowns per image are the camera position (X, Y and Z) and image rotation angles (omega, phi and kappa). No additional parameters were introduced within bundle adjustment processing. Cartesian coordinate system is assumed for control points and therefore no map projection processing involved during bundle adjustment.

All available control points used as control points during bundle adjustment and all available check points and other pass points were used as pass points (supplied check points' space coordinates are not used during any bundle adjustment).

In the following description, "adjusted coordinates" mean the bundle adjusted coordinates for those points that were used as control points during bundle adjustment, "obtained coordinates" mean the new computed coordinates for those check points (space coordinates are unknown during bundle adjustment), and "supplied coordinates" mean the coordinates which were provided by Pilot Centre.

Tables 3A-3E list the adjusted coordinates of control points and their differences between supplied coordinates and adjusted coordinates from 5 bundle adjustment configurations. The root mean squares (RMS) values of X, Y and Z differences are also given. Tables 4A-4E list the obtained coordinates of check points from 5 bundle adjustment configurations.

Table 3A: The adjusted coordinates of 19 control points and the differences between supplied coordinates and adjusted coordinates for Configuration A (unit is in metre)

… deleted M. Cramer …

Table 3B: The adjusted coordinates of 18 control points and the differences between supplied coordinates and adjusted coordinates for Configuration B (unit is in metre)

… deleted M. Cramer …

Table 3C: The adjusted coordinates of 18 control points and the differences between supplied coordinates and adjusted coordinates for Configuration C (unit is in metre)

… deleted M. Cramer …

Table 3D: The adjusted coordinates of 19 control points and the differences between supplied coordinates and adjusted coordinates for Configuration D (unit is in metre)

… deleted M. Cramer …

Table 3E: The adjusted coordinates of 19 control points and the differences between supplied coordinates and adjusted coordinates for Configuration E (unit is in metre)

… deleted M. Cramer …

Table 4A: The obtained coordinates of 17 check points for Configuration A (unit is in metre)

… deleted M. Cramer …

Table 4B: The obtained coordinates of 16 check points for Configuration B (unit is in metre)

… deleted M. Cramer …

Table 4C: The obtained coordinates of 16 check points for Configuration C (unit is in metre)

… deleted M. Cramer …

Table 4D: The obtained coordinates of 18 check points for Configuration D (unit is in metre)

… deleted M. Cramer …

Table 4E: The obtained coordinates of 18 check points for Configuration E (unit is in metre)

… deleted M. Cramer …

4. Discussion about the results

From results shown in the previous section, the adjusted space coordinates for control points have very good agreements between the supplied space coordinates and the adjusted space coordinates for all configurations: X, Y, Z RMS are less than 0.06m, 0.1m and 0.02m, respectively. Based on the overall assessment for all bundle adjustment configurations, the recommended space coordinates for check points, which are to be used for accuracy analysis are from Configuration C. Since check points 80001 and 80048 are not covered under Configuration C, results taken from Configuration A. Therefore, the suggested space coordinates for check points are given in Table 5.

Table 5: The recommended coordinates of 18 check points for accuracy analysis (unit is in metre). Note: 80001 and 80048's coordinates were taken from Configuration A since they are not covered by low-flying data set.

… deleted M. Cramer …

5. Experiences with the high-flying UltraCamD data and some remarks

- What processing software was used for data evaluation?
  In-house developed software was used for bundle adjustment.

- What kind of parameter set was used for AT?
  They parameters are 6 parameters per image and 3 parameters per point. No additional parameters were investigated or tested.

- Were the two flying heights used separately or in a combined approach?
  Two flying heights were used either in separate mode or combined mode (see Section 2).

- What are the general findings obtained from this specific data set? What is your personal feeling on the data quality and performance of this specific data set?
  Although this specific data set was captured under very low light condition, the data quality for both UltraCamD high-flying and low-flying data sets is still sufficient for doing any photogrammetric processing. 14-bit data is very valuable in terms of identifying control and check points on screen visually. The measurement task was performed directly on the 14-bit image data. It was well noticeable that 14-bit data is superior matching performance to 8-bit data through the measurement task. Detailed matching comparison needs to be conducted to investigate the matching differences further.
  The XY accuracy derived from the low-flying data set is almost twice higher than the XY accuracy derived from the high-flying data set based on the control point residual analysis (see Tables 3A and 3C), while the elevation accuracy seems not improved by such amount.
  Some signalised points were difficult to be identified due to the poor light condition, which may reduce the estimated accuracy for these points, especially for points 90037 and 90047.

- What are your personal experiences with other digital sensor flights of the same type of sensor? Does this result match the experiences from former flights?
  The author does not have other same type of sensor experiences.

- What is your personal recommendation on optimal processing flow for this specific type of digital sensor data? How will you handle such kind of data in future?
  An ideal processing flow should use the image data without applying any transformation, conversion and reformatting. It seems extra data handling is common to digital sensor data. For both the high-flying and low-flying data set processing (point measurement and point transferring), in order to allow in-house software to

process efficiently and visual stereo view easily, the author rotated all images 90 degrees counter clockwise for south-west to north-east strips and 90 degrees clockwise for north-east to south-west strips, images were reformatted into new TIIF images (new TIFF images are strip based instead of tile based like the original TIFF images).

Regarding the optimal processing, the author would like to recommend that some standardisations, such as data formats, ancillary data formats associated with images should be agreed by various parties (sensor manufacturers, software providers and major), and EuroSDR Digital Camera Calibration project might set up some tasks for these purposes. In addition to the panchromatic data, it would be desirable to have multi-spectral data as well to improve visual identification process. The author also would like to raise the overlapping issue: what is the optimal overlapping configuration for digital camera systems? Obviously, more overlaps can improve matching results and therefore improve the quality of derived DEM and orthoimages, but too many overlaps may also increase processing costs (labour and time).

Acknowledgements

The author would like thank to Dr Michael Cramer (Institute of Photogrammetry, University of Stuttgart) for his kind support to allow us to participate in EuroSDR project on Digital Camera Calibration and prompt data set provision. Thanks are given to EuroSDR Pilot Centre (www.eurosdr.net), the Calibration Network (www.ifp.uni-stuttgart.de/eurosdr/index.html), the UltraCamD manufacturer (www.vexcel.com) and also the data provider IFMS Pasewalk (www.arcforest.com).

References

1. Vexcel Imaging, Calibration Report, Geometric Calibration for UltraCam D, S/N UCD-SU-1-0002, Graz, April-28-2004, Vexcel GmbH, A-8010 Graz, Austria
2. Kröpfl M., Kruck E. and Gruber M., 2004, Geometric Calibration of the Digital Large Format Aerial Camera UltraCamD, ISPRS 2004, Istanbul
3. Leberl F. and Gruber M., 2005, Understanding some Noteworthy Capabilities, Photogameetric Week 2005, Stuttgart, Germany
4. Cramer M., 2006, Phase II - Empirical Data Set Description UltraCamD Data, Test Site Fredrikstad, Institute for Photogrammetry, University of Stuttgart, D-70174
5. Wang Z. Z., 1990, Principles of Photogrammetry (with Remote Sensing), Publishing House of Surveying and Mapping, Beijing

Institut für Photogrammetrie und GeoInformation
Universität Hannover

Nienburger Str. 1
D-30167 Hannover

Tel.: ++49-511/762-2485
Fax: ++49-511/762-2483
e-mail: jacobsen@ipi.uni-hannover.de
http://www.ipi.uni-hannover.de

Dr.-Ing. Karsten Jacobsen

Hannover, Nov., 29th ,2006

EuroSDR Digital camera test

investigation of UltraCamD block Frederickstad, Norway lower flight level

1. STATISTICS

block configuration:

132 images flying height: 1964m, mean ground height 65m image scale 1 : 18 909
→ ground sampling distance (GSD) = 17cm
An automatic aero triangulation has been made with LPS, the block adjustment and analysis has been made with the Hannover program system BLUH.

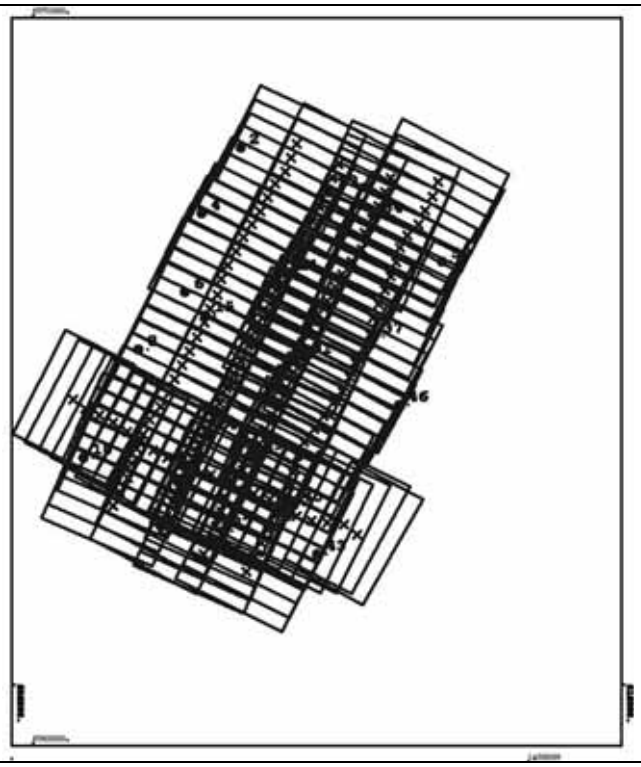

Fig. 1: configuration of lower flight level

the image numbers have been changed like shown to ascending numbers in the flight lines

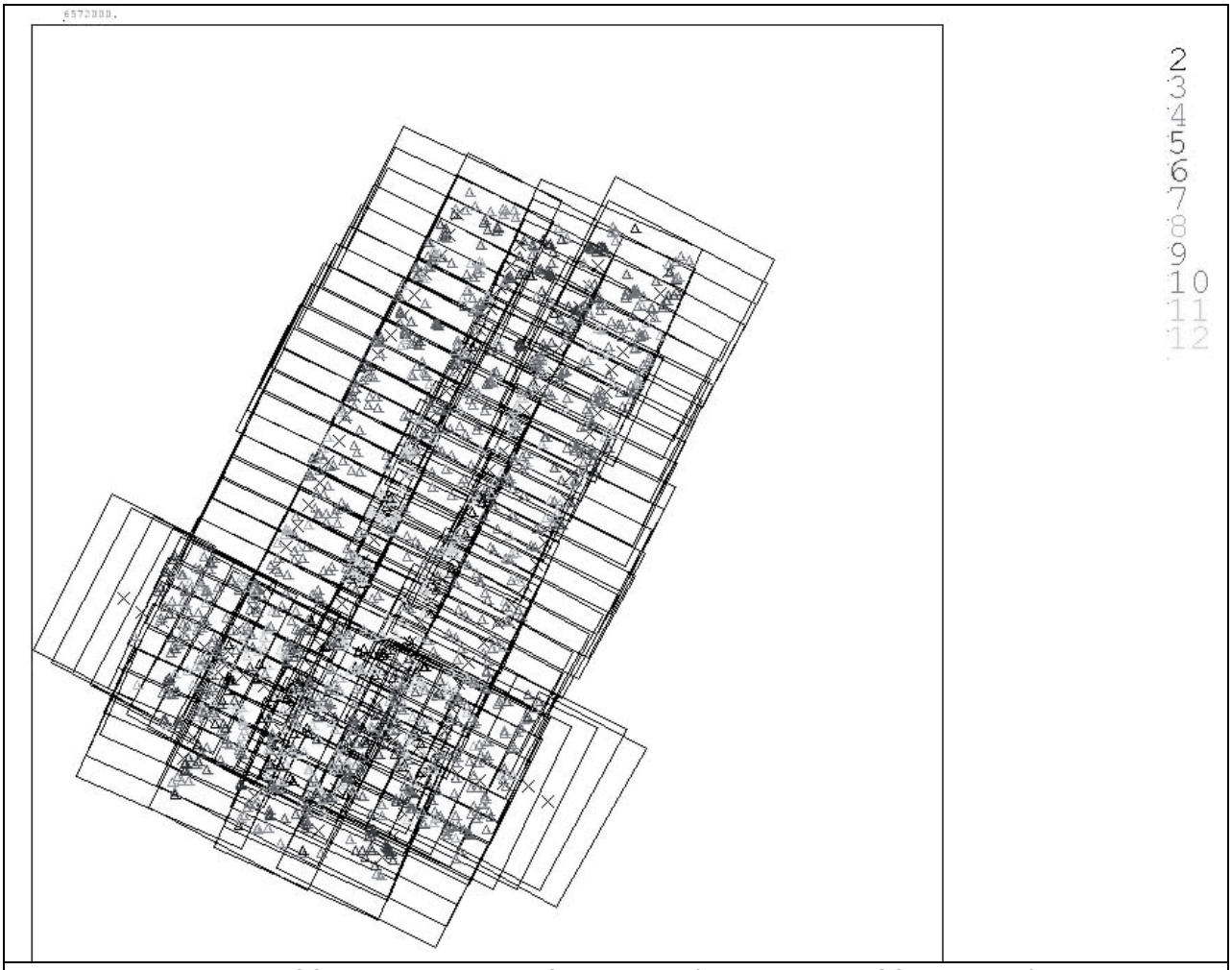

Fig. 2: pass points of flight lines lower flight level (connection of flight lines)
the colour corresponds to the number of images / point (see upper right)

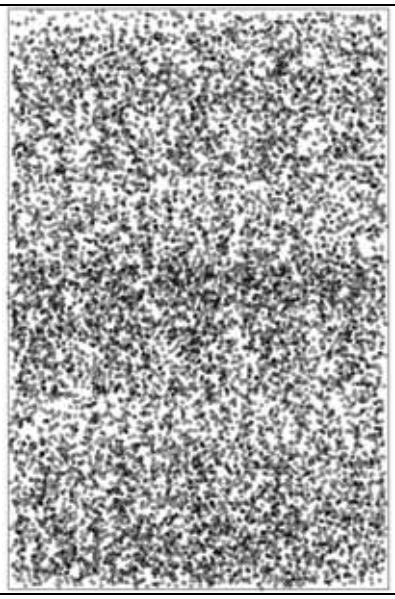

Fig. 3: distribution of points in the images – overlay of all images

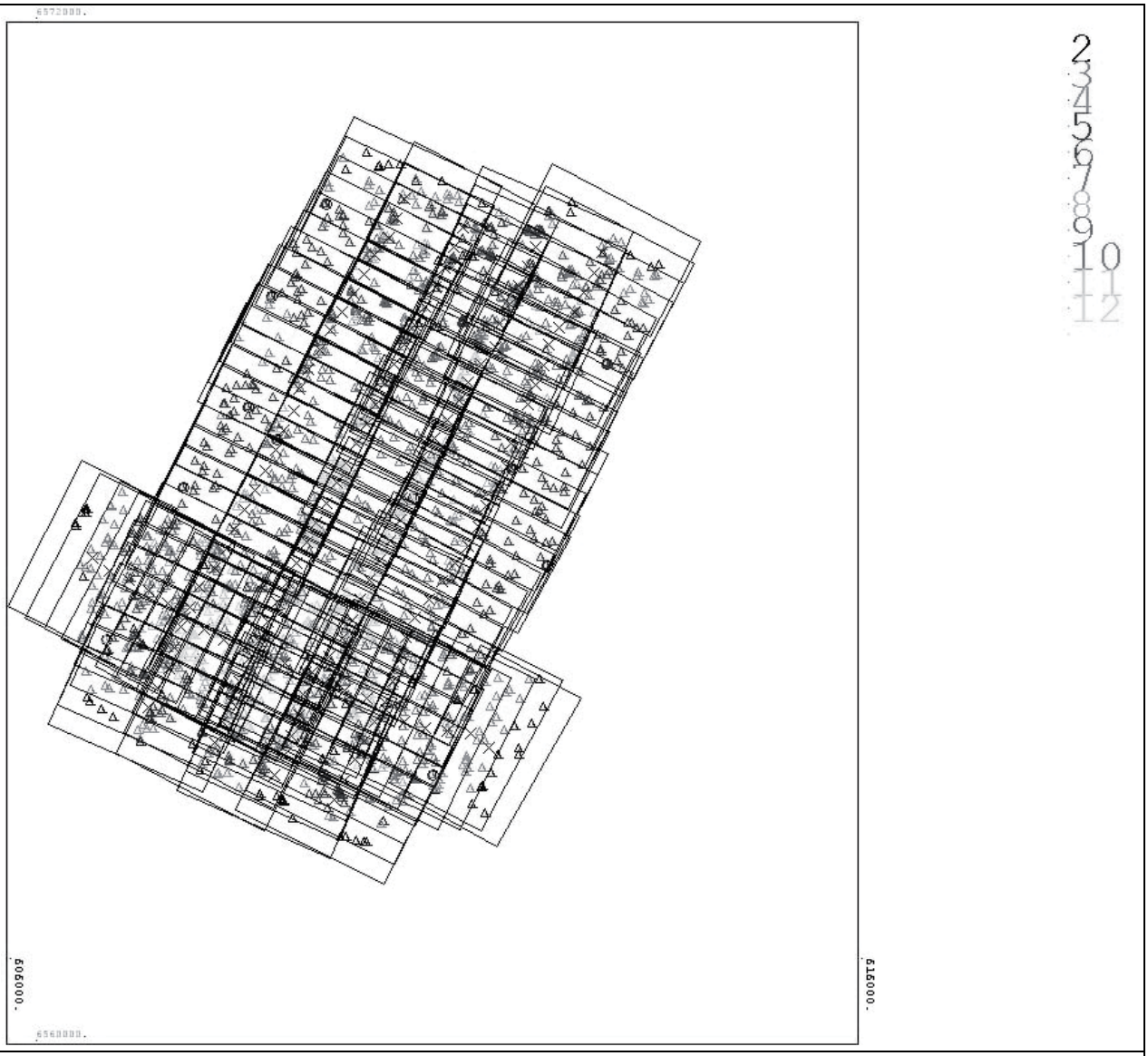

Fig. 4: all points of lower flight level
colour coded corresponding to the number of images / points (see upper right)

```
IN PHOTO        615    56 POINTS = LOWEST NUMBER
IN PHOTO        508   156 POINTS = HIGHEST NUMBER


NUMBER OF PHOTOS/OBJECT POINT
PHOTOS/POINT    1     2     3     4     5     6     7     8     9    10
POINTS:        13    84    79   134   240   144   136   175   253   234

PHOTOS/POINT   11    12    13    14    15    16    17    18    19    20
POINTS:       111    78    55    26    18     3     1     2     0     1

MAX PHOTOS/POINT           :     20
OBJECT POINTS              :   1774
PHOTOS                     :    132
PHOTO POINTS               :  13601
```

General information about data acquisition and block characteristics

Not all control and check points are reliable; they could not be measured in all theoretic possible images because of the forest. In addition the point identification was very difficult. By this reason the block is not optimal for test of the best data handling, but nevertheless an analysis of the image geometry for systematic image errors is possible. Because of the just parallel flight lines the systematic image errors cannot be separated totally from the influence of the control points – for such an analysis crossing flight lines should be used.

The points are distributed well in the images (figure 4), so systematic image errors can be analysed well.

2. ADDITIONAL PARAMETERS

The detailed analysis has been made with program system BLUH. BLUH includes general additional parameters and a set of parameters especially fitted to the geometry of the DMC as well as the UltraCam. The self calibration with additional parameters is able to determine geometric discrepancies between the mathematical model of perspective images and the real image geometry – this difference is called “systematic image errors” even if it is an error of the mathematic model.

The additional parameters may be correlated. High correlations may cause geometric problems in block areas not well supported by control points. By this reason in program BLUH the additional parameters are checked for correlation, total correlation and by Student-test. Too high correlated parameters and parameters with too small Student – test values are removed automatic from the adjustment.

Additional parameters in BLUH

```
1 = ANGULAR AFFINITY
2 = AFFINITY
3 - 6 = GENERAL DEFORMATION
7 - 8 = TANGENTIAL DISTORTION
9 = RADIAL SYMMETRIC R*R*R  10 - 11 RADIAL SYMMETRIC HIGHER DEGREE
12 = GENERAL DISTORTION

13 = FOCAL LENGTH  14, 15 = PRINCIPAL POINT
   FOR COMBINED ADJUSTMENT WITH GPS 13 - 15 REQUIRED FOR GPS-SHIFT
16 - 18 POSSIBLE GPS-DRIFT   19-20 GPS-DATUM  21= T*T
22 - 26 FOR PANORAMIC CAMERA
27 - 28 RADIAL SYMMETRIC FOR FISHEYE
29      DMC EXCENTRICITY   30 - 33 DMC SYNCHRONIZATION
34 - 41 DMC PERSPECTIVE DEFORMATION OF SINGLE CAMERAS
42 - 49 ULTRACAM SCALE  50 - 65 ULTRACAM SHIFT  66 - 73 ULTRACAM ROTATION
74 - 77 DMC RADIAL SYMMETRIC ORIGINAL IMAGES  78 - 81 DMC FOCAL LENGTH
ORIGINAL IMAGES
```

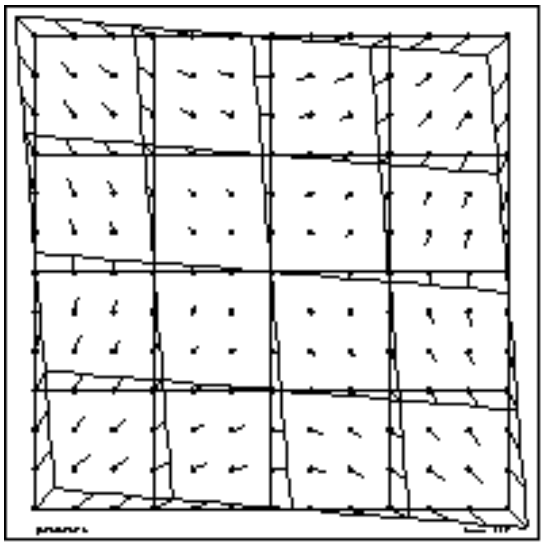

parameter 1

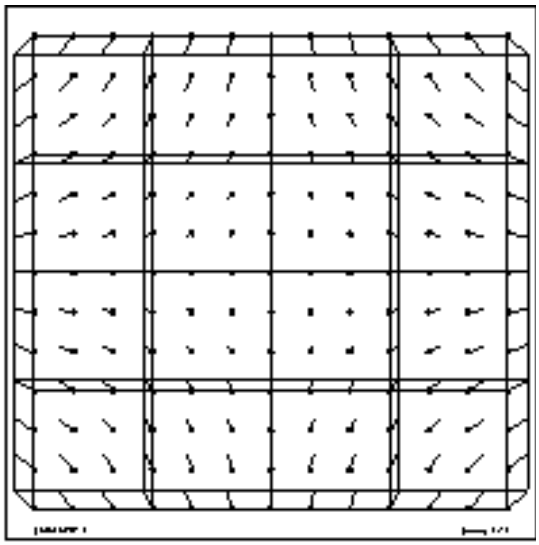

parameter 2

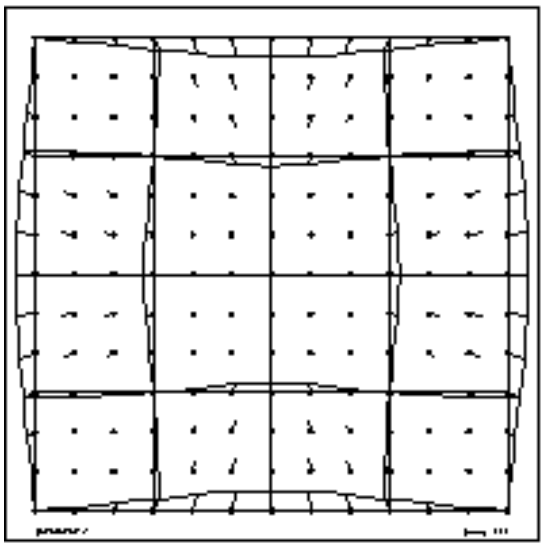

parameter 3 ↑

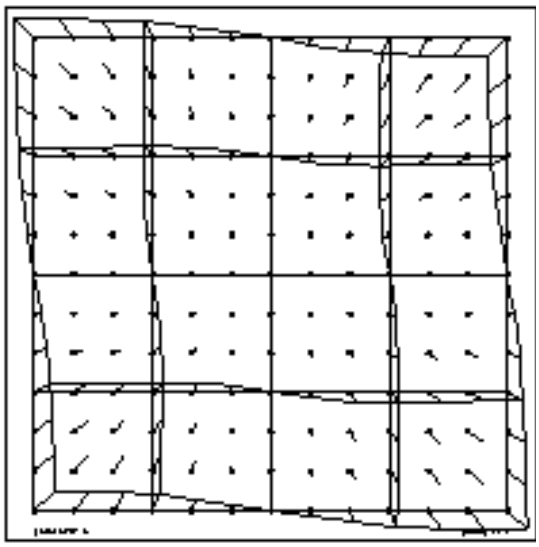

parameter 4 ↑

parameter 5 ↓

parameter 6 ↓

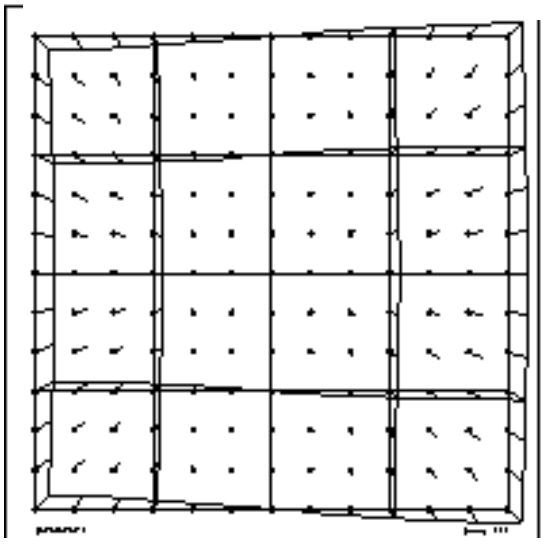

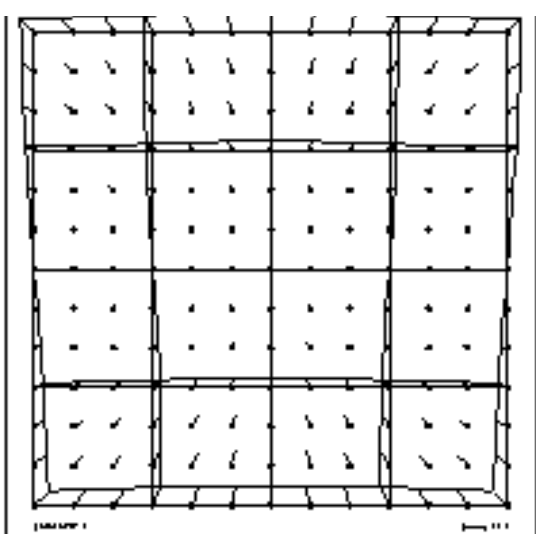

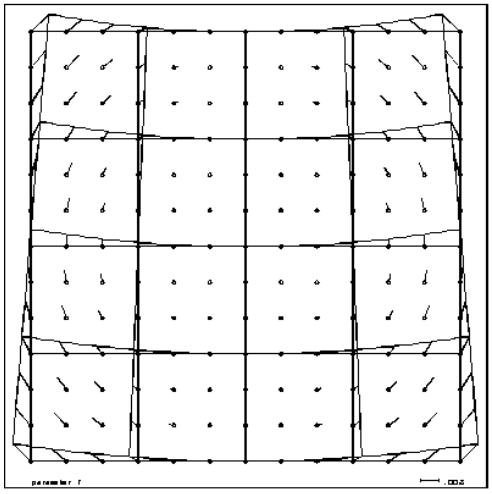

parameter 7

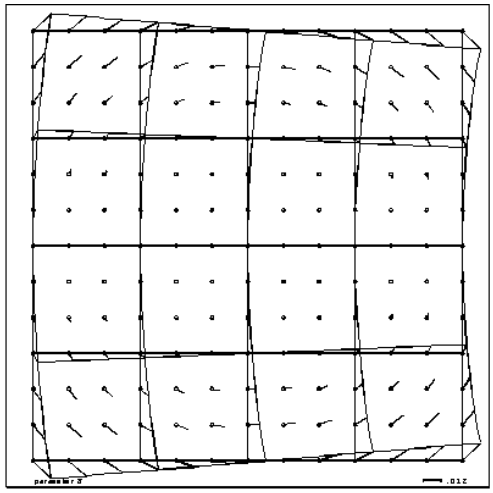

parameter 8

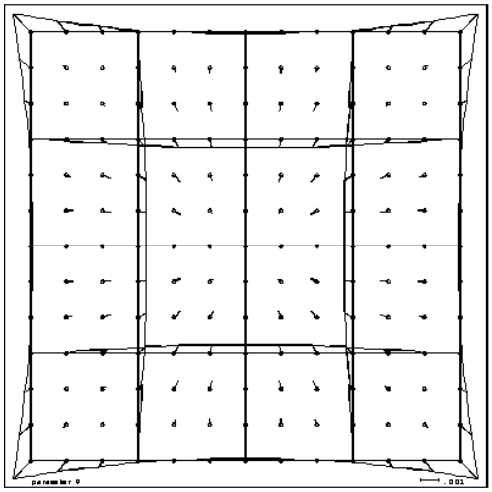

parameter 9 ↑

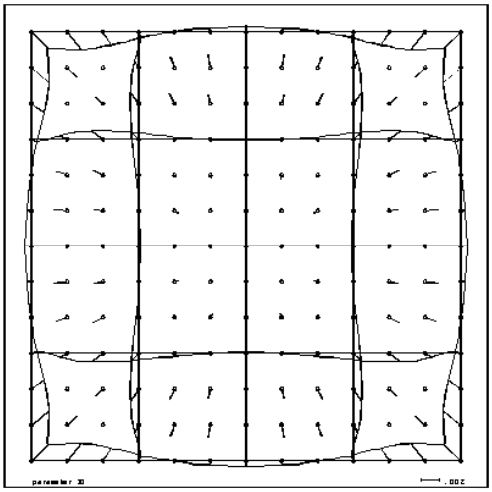

parameter 10 ↑

parameter 11 ↓

parameter 12 ↓

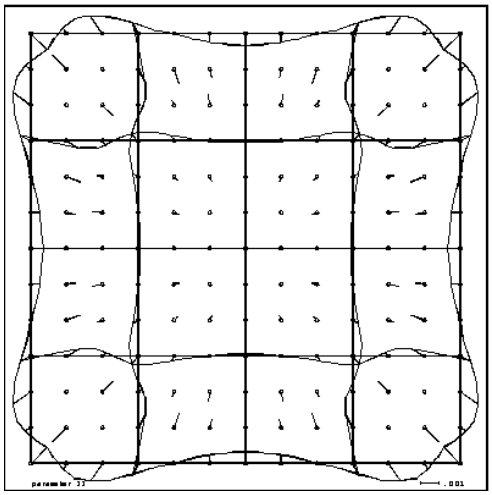

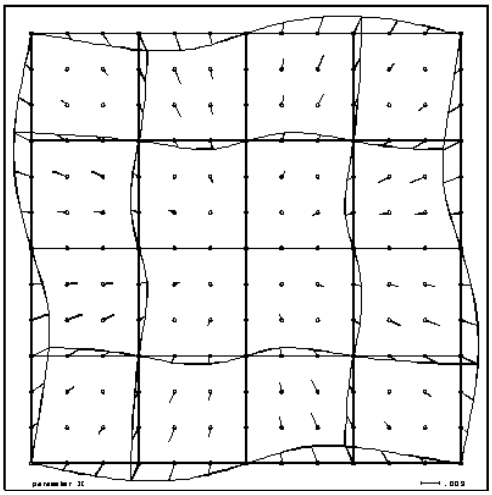

Special additional parameters for Vexcel UltraCamD

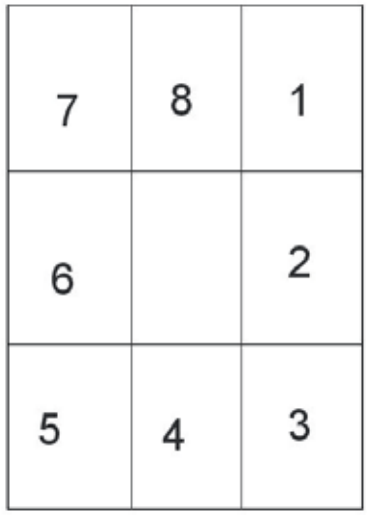

The UltraCamD has a synthetic image based on 9 individual CCD-arrays. With the additional parameters 42 up to 73 problems of the CCD-array merge can be determined. For 8 different sub-areas special parameters are available.

parameter 42 – 49 = scale parameters	42 for sub-unit 1 49 for sub-unit 8
parameters 50 – 57 = shift X	50 for sub-unit 1 57 for sub-unit 8
parameters 58 – 65 = shift Y	58 for sub-unit 1 65 for sub-unit 8
parameters 66 – 73 = rotation	66 for sub-unit 1 73 for sub-unit 8

3. ANALYSIS OF BLOCK FREDERICKSTAD

		control points			check points		
	sigma0 [µm]	SX [cm]	SY [cm]	SZ [cm]	SX [cm]	SY [cm]	SZ [cm]
no AP	2.46	6.1	5.5	24.6	7.8	5.3	15.7
AP 1-12	2.34	5.4	4.8	14.4	5.3	5.7	12.6
AP 1-12, 42-65	2.22	5.6	4.8	13.3	4.8	5.7	12.4

Table 1: discrepancies at check and control points AP = additional parameters

As check points, ground coordinates of the old OEEPE direct sensor orientation block have been used (search for identical points with 1m search radius).

all used check points, with numbers of images / object point

12 … deleted M. Cramer …
13 … deleted M. Cramer …
14 … deleted M. Cramer …
16 … deleted M. Cramer …
20 … deleted M. Cramer …
33 … deleted M. Cramer …
36 … deleted M. Cramer …
38 … deleted M. Cramer …

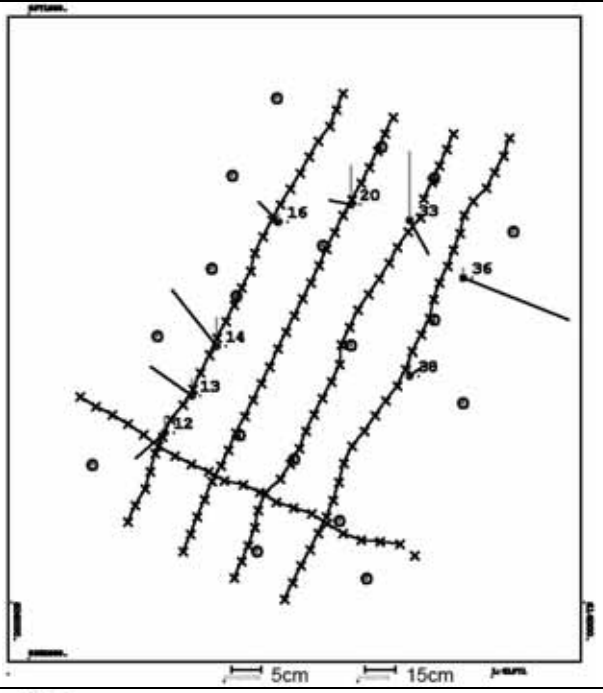

Fig. 5: discrepancies at check points
vector scale for X, Y = 5cm (blue vector)
vector scale for Z = 15cm (green vector)
circles = control points

upper left: without additional parameters

lower left: with parameters 1 – 12

lower right: with all parameters

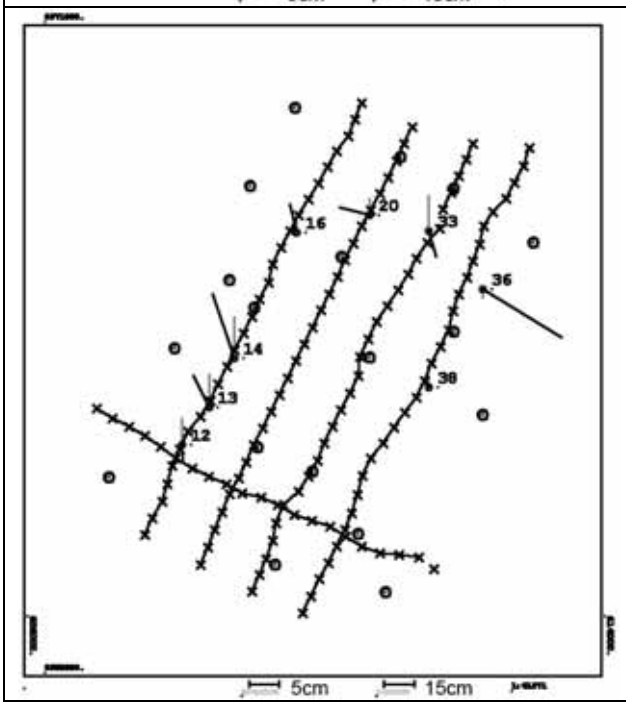

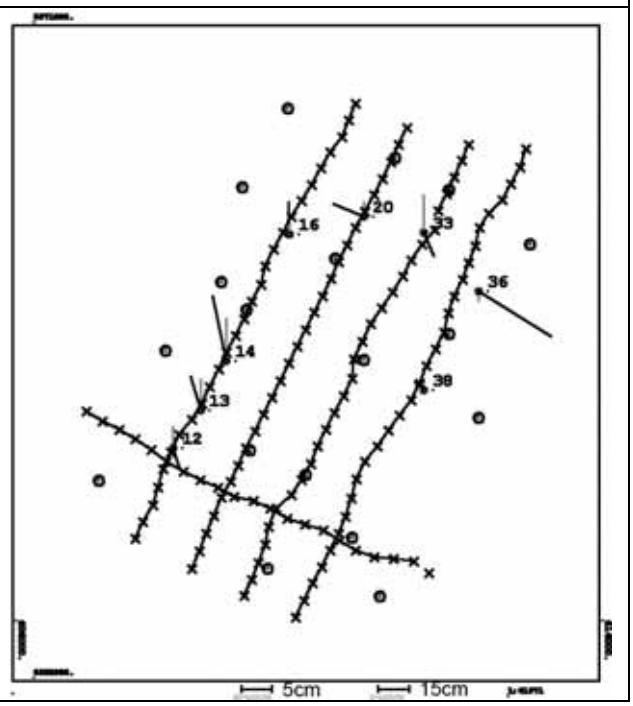

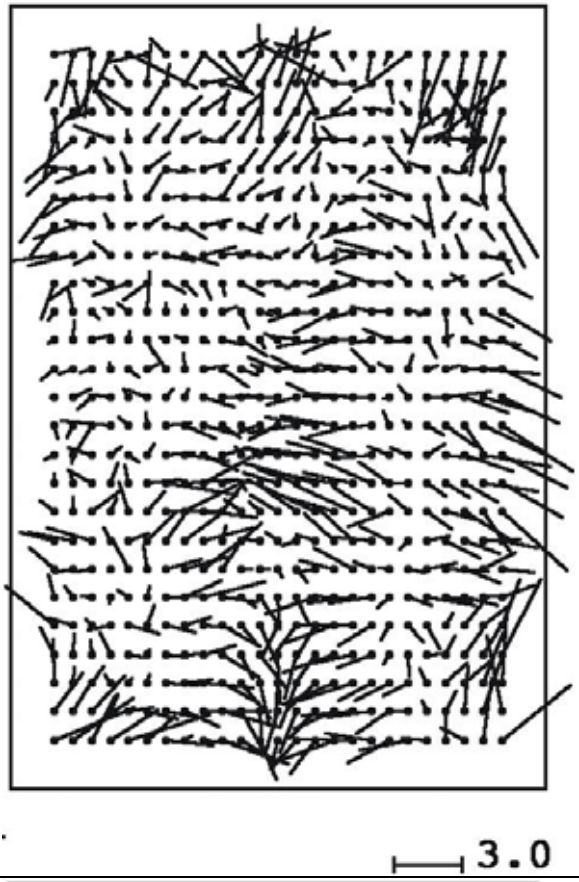

Fig. 6: averaged image coordinate residuals of block adjustment

upper left: without additional parameters
root mean square = 1.07µm

lower left: with parameters 1 – 12
root mean square = 0.82µm

lower right: with all parameters
root mean square = 0.69µm

vector scale = 3µm

in average 27 original discrepancies / vector

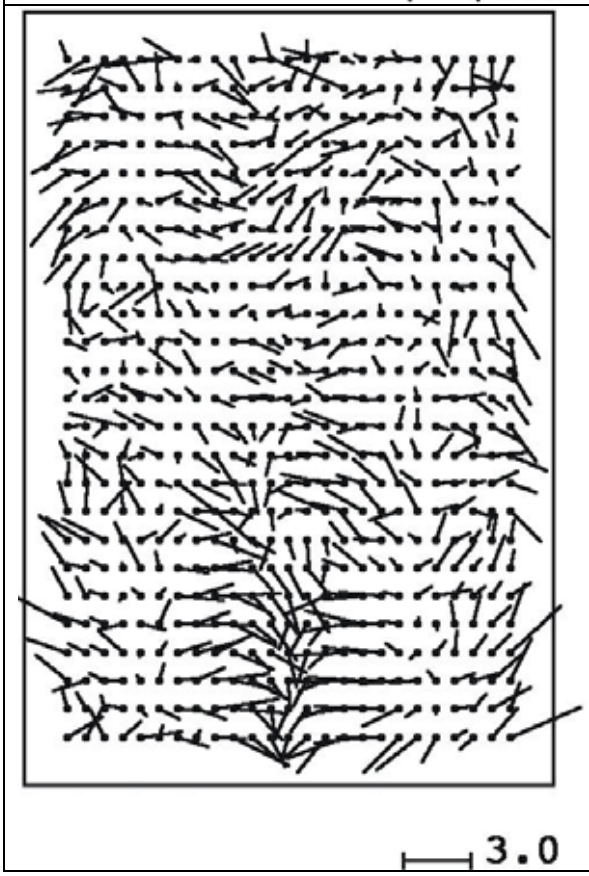

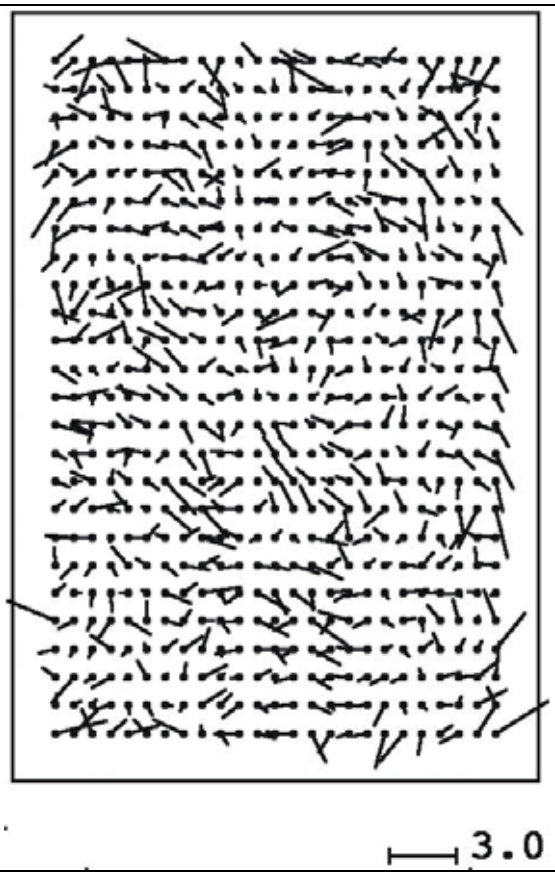

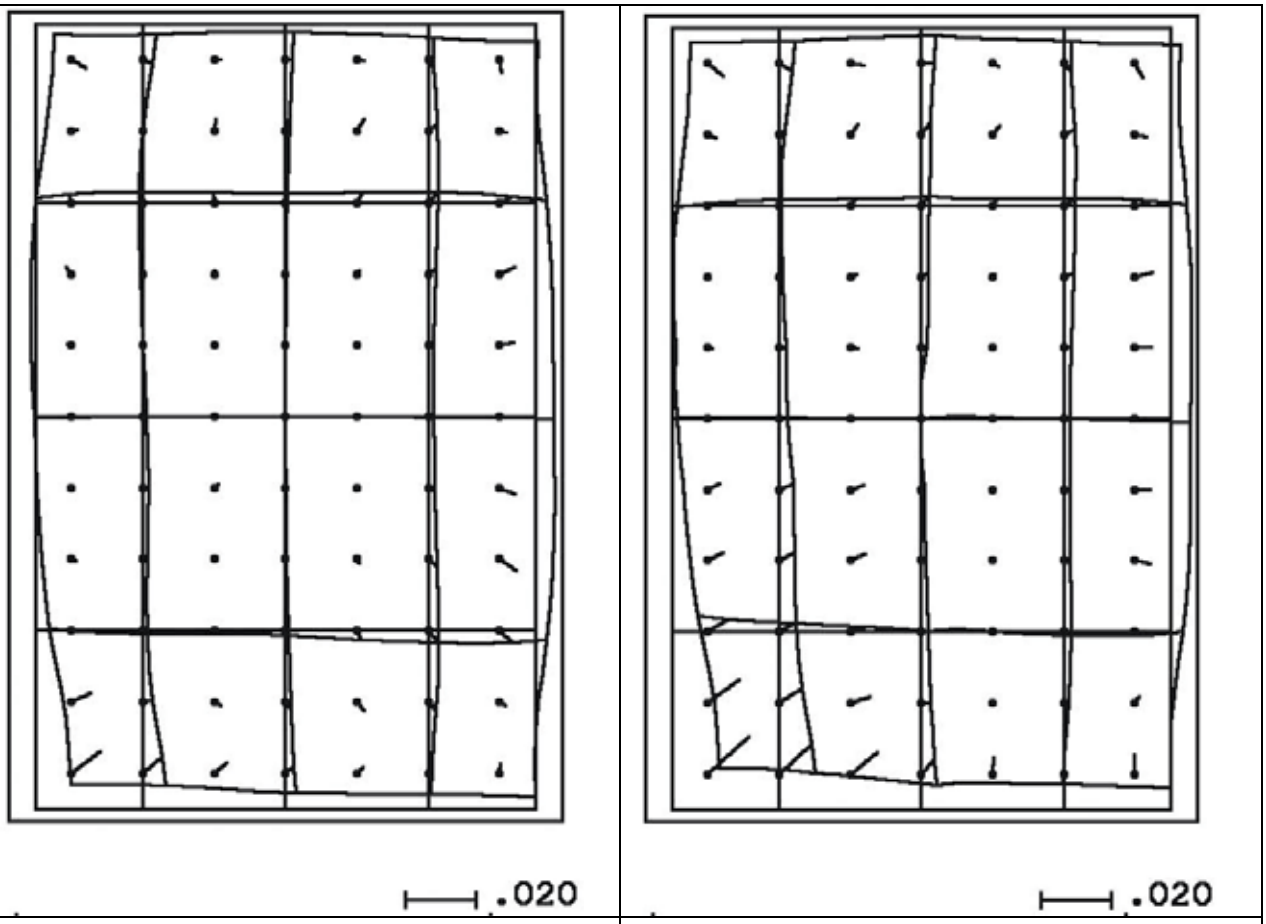

parameters 1 - 12	parameters 1 -12 + 42 - 73

Figure 7: effect of additional parameters to image coordinates (“systematic image errors”)

The averaged residuals (figure 6) show only the tendency of the systematic image errors. Caused by the correlation to the exterior orientation they are usually quite smaller like the systematic image errors (figure 7).
The averaged residuals of the adjustment with the parameters 1 – 12 indicate very clear remaining systematic image errors which can be fitted with the 12 standard parameters plus the special UltraCamD-parameters. The adjustment with the full set of additional parameters has only negligible averaged residuals (figure 6, lower right), indicated also with the covariance function of the averaged residuals (figure 8). The adjustment with the standard additional parameters 1 – 12 is reducing the covariance of the averaged residuals only slightly – the maximal value is just reduced from 0.33 to 0.31, but the dominating figure remains. The adjustment with all additional parameters (1-12 + 42-73) is strongly reducing the covariance – the maximal value is reduced to 0.13 and after 20mm distance in the image, there is only some noise remaining. From this side the adjustment should be made with all additional parameters.

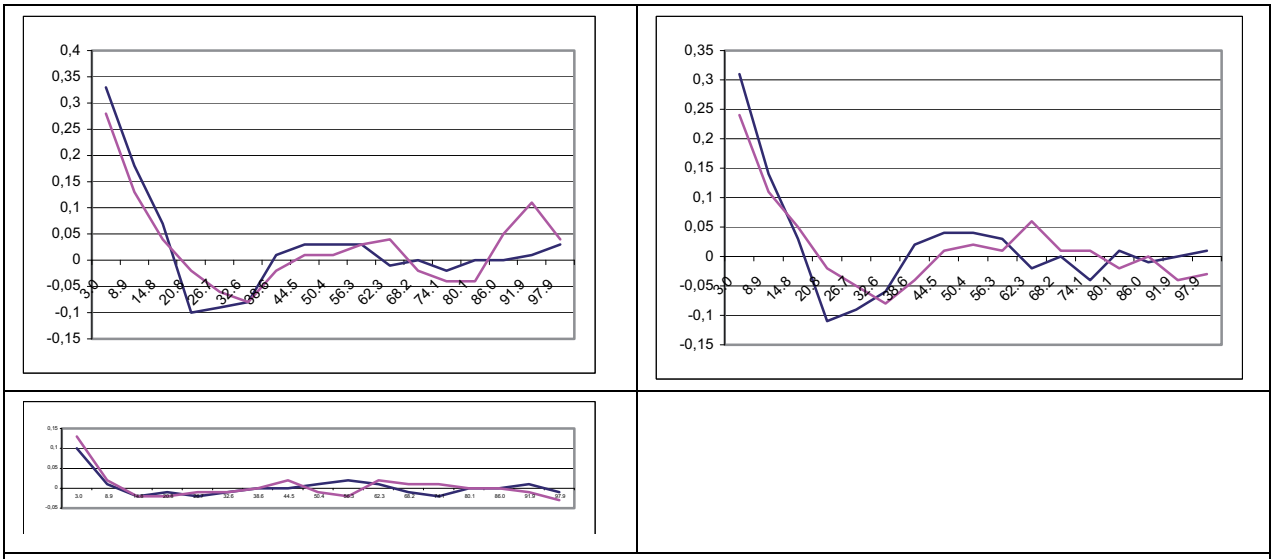

Figure 7: covariance function of the averaged residuals (figure 5)
vertical: covariance value horizontal: distance of points in image [mm]
red: covariance for dx' green: covariance for dy'
upper left: adjustment without additional parameters (maximal = 0.33)
upper right: adjustment with additional parameters 1 – 12 (maximal = 0.31)
lower left: adjustment with all additional parameters (maximal = 0.13)

The block adjustment should be done with self calibration by additional parameters. At least the standard parameters 1 – 12 are required; with the special UltraCam-parameters the results are improved just a little. The discrepancies at the independent check points correspond to 0.3 GSD for X and Y and to 0.2 GSD for the x-parallax under the condition of a height to base relation of 3.7. Because of the high number of image points for each check point this is not a too good result, but it is caused by the limited identification of the control and check points.

The shape and size of the systematic image errors seams to be typical for the UltraCamD. A similar size and also shape has been achieved also with data from other UltraCamD cameras.

Institut für Photogrammetrie und GeoInformation
Universität Hannover

Nienburger Str. 1
D-30167 Hannover

Tel.: ++49-511/762-2485
Fax: ++49-511/762-2483
e-mail: jacobsen@ipi.uni-hannover.de
http://www.ipi.uni-hannover.de

Dr.-Ing. Karsten Jacobsen

Hannover, Oct., 22nd ,2006

EuroSDR Digital camera test

investigation of UltraCamD block Frederickstad, Norway upper flight level

1. STATISTICS

block configuration:

28 images flying height: 3906m, mean ground height 69m image scale 1 : 37 839

An automatic aero triangulation has been made with LPS, the block adjustment and analysis has been made with the Hannover program system BLUH.

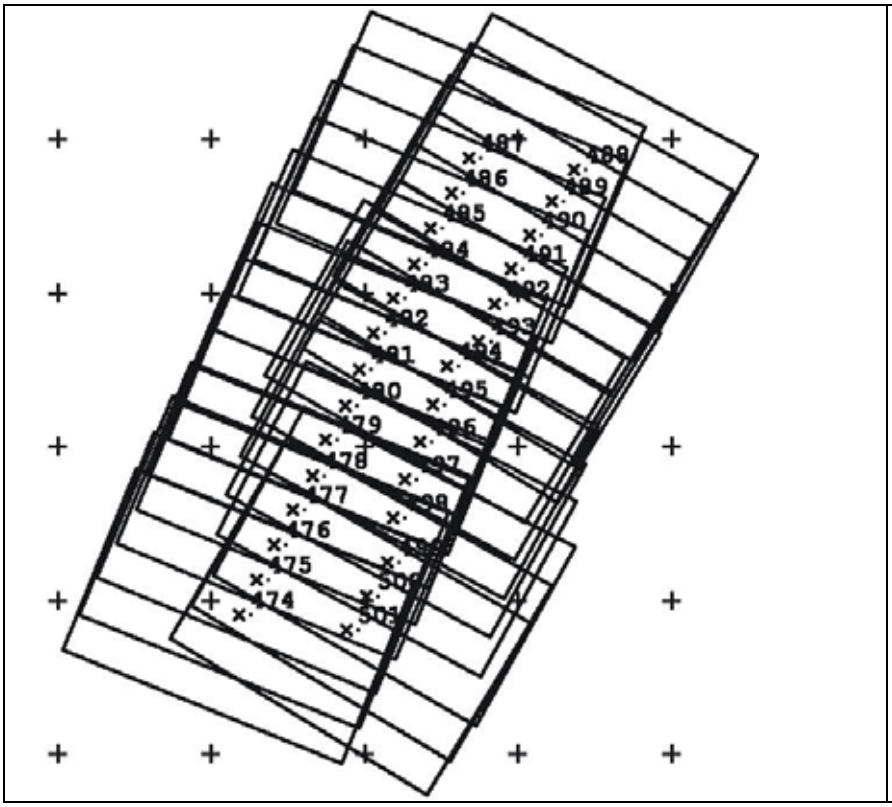

Fig. 1: configuration of upper flight level

the image numbers have been changed like shown to ascending numbers in the flight lines

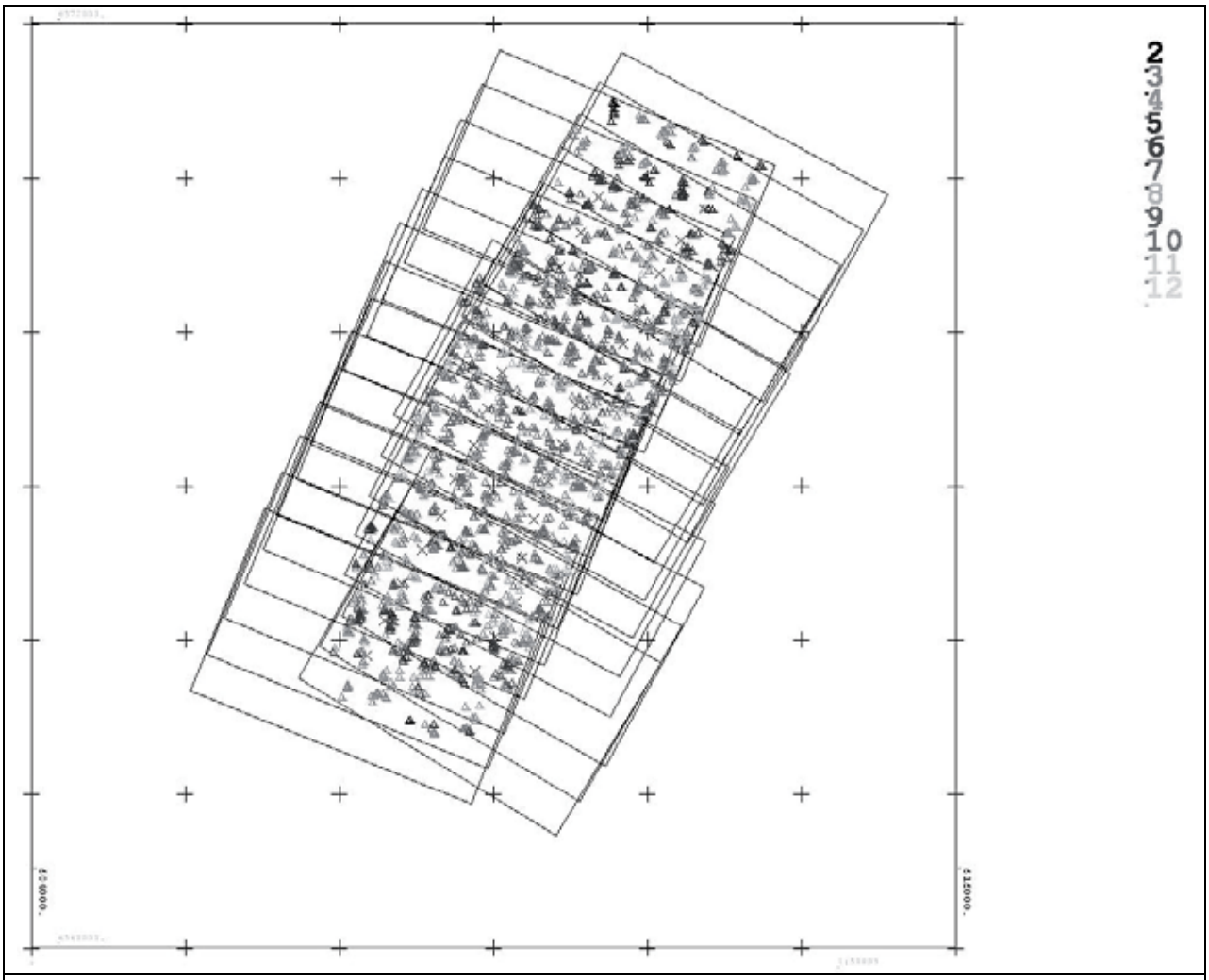

Fig. 2: tie points of flight lines upper flight level
the colour corresponds to the number of images / point (see upper right)

Fig. 3: distribution of points in the images – overlay of all images

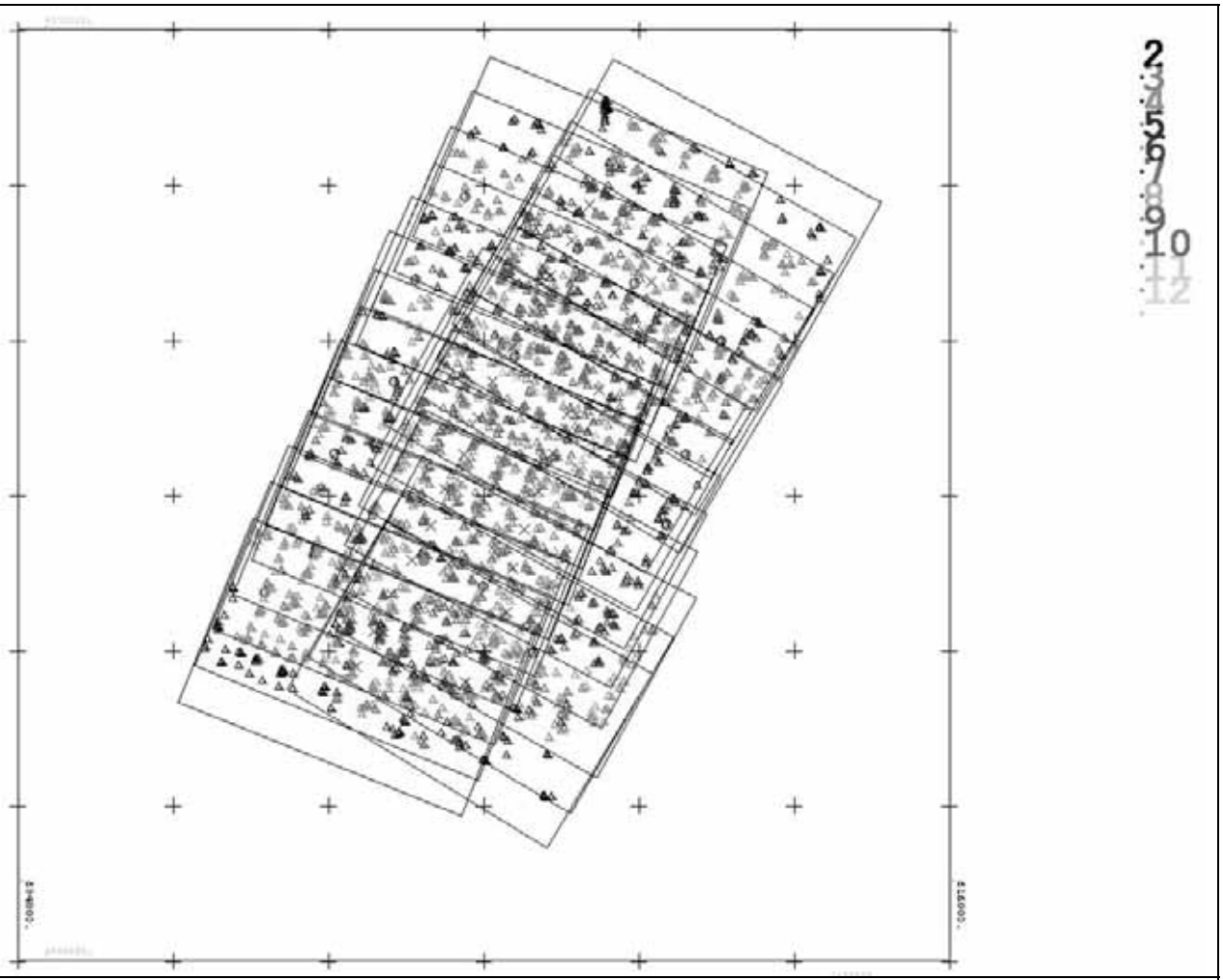

Fig. 4: all points of upper flight level
colour coded corresponding to the number of images / points (see upper right)

```
 NUMBER OF PHOTOS/OBJECT POINT
 PHOTOS/POINT    1     2     3     4     5     6     7     8     9    10
 POINTS:        22   199   430   509   572   262   317   373   390   216

 MAX PHOTOS/POINT           :     11
 OBJECT POINTS              :   3269
 PHOTOS                     :     28
 PHOTO POINTS               :  19040

 MINIMUM AND MAXIMUM OF PHOTO COORDINATES
  X MINIMUM =  -33.600  X MAXIMUM =   33.593
  Y MINIMUM =  -51.740  Y MAXIMUM =   51.579


NUMBER OF POINTS PER PHOTO
 ========================

       474  384       475  731       476  798       477  713       478  679
       479  684       480  752       481  796       482  739       483  754
       484  799       485  739       486  671       487  599       488  447
       489  514       490  658       491  772       492  838       493  768
       494  714       495  675       496  678       497  643       498  635
       499  631       500  677       501  552

 IN PHOTO       474   384 POINTS = LOWEST NUMBER
 IN PHOTO       492   838 POINTS = HIGHEST NUMBER
```

General information about data acquisition and block characteristics

Not all control and check points are reliable; they could not be measured in all theoretic possible images because of the forest. In addition the point identification was very difficult. By this reason the block is not optimal for test of the best data handling, but nevertheless an analysis of the image geometry for systematic image errors is possible. Because of the just parallel flight lines the systematic image errors cannot be separated totally from the influence of the control points – for such an analysis crossing flight lines should be used.

The points are distributed well in the images (figure 5), so systematic image errors can be analysed well.

2. ADDITIONAL PARAMETERS

The detailed analysis has been made with program system BLUH. BLUH includes general additional parameters and a set of parameters especially fitted to the geometry of the DMC as well as the UltraCam. The self calibration with additional parameters is able to determine geometric discrepancies between the mathematical model of perspective images and the real image geometry – this difference is called “systematic image errors” even if it is an error of the mathematic model.

The additional parameters may be correlated. High correlations may cause geometric problems in block areas not well supported by control points. By this reason in program BLUH the additional parameters are checked for correlation, total correlation and by Student-test. Too high correlated parameters and parameters with too small Student – test values are removed automatic from the adjustment.

Additional parameters in BLUH

```
1 = ANGULAR AFFINITY
2 = AFFINITY
3 - 6 = GENERAL DEFORMATION
7 - 8 = TANGENTIAL DISTORTION
9 = RADIAL SYMMETRIC R*R*R  10 - 11 RADIAL SYMMETRIC HIGHER DEGREE
12 = GENERAL DISTORTION

13 = FOCAL LENGTH  14, 15 = PRINCIPAL POINT
   FOR COMBINED ADJUSTMENT WITH GPS 13 - 15 REQUIRED FOR GPS-SHIFT
16 - 18 POSSIBLE GPS-DRIFT   19-20 GPS-DATUM  21= T*T
22 - 26 FOR PANORAMIC CAMERA
27 - 28 RADIAL SYMMETRIC FOR FISHEYE
29      DMC EXCENTRICITY   30 - 33 DMC SYNCHRONIZATION
34 - 41 DMC PERSPECTIVE DEFORMATION OF SINGLE CAMERAS
42 - 49 ULTRACAM SCALE  50 - 65 ULTRACAM SHIFT  66 - 73 ULTRACAM ROTATION
74 - 77 DMC RADIAL SYMMETRIC ORIGINAL IMAGES  78 - 81 DMC FOCAL LENGTH
ORIGINAL IMAGES
```

Special additional parameters for Vexcel UltraCamD

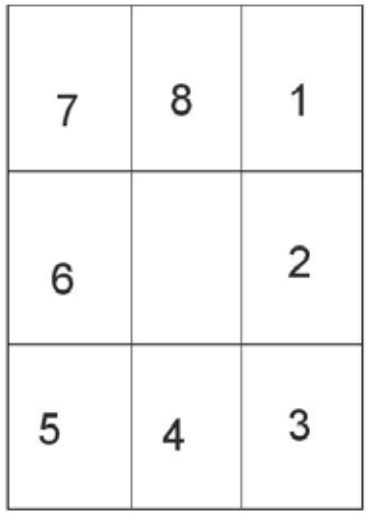

The UltraCamD has a synthetic image based on 9 individual CCD-arrays. With the additional parameters 42 up to 73 problems of the CCD-array merge can be determined. For 8 different sub-areas special parameters are available.

parameter 42 – 49 = scale parameters	42 for sub-unit 1 49 for sub-unit 8
parameters 50 – 57 = shift X	50 for sub-unit 1 57 for sub-unit 8
parameters 58 – 65 = shift Y	58 for sub-unit 1 65 for sub-unit 8
parameters 66 – 73 = rotation	66 for sub-unit 1 73 for sub-unit 8

3. ANALYSIS OF BLOCK FREDERICKSTAD

Only control points have been available, an analysis with check points was not possible.

	add. parameters	used	sigma0 [µm]	RMSX [cm]	RMSY [cm]	RMSZ [cm]
1	without		2.75	11.0	13.8	29.6
2	1 - 12	1, 3-8, 10-12	2.63	10.2	11.7	31.2
3	1-12, 42-73	26 parameters	2.55	10.1	11.9	30.0

Table 1: comparison of different block adjustments, sigma0 and discrepancies at control points add. parameters = initiated additional parameters
used = finally used parameters

	all check points			check points inside control points		
	SX	SY	SZ	SX	SY	SZ
1	11.9	7.4	40.4	8.1	7.1	21.2
2	13.3	8.4	33.2	9.1	8.8	20.6
3	12.1	8.5	30.5	8.9	9.1	19.8

Table 2: results at independent check points [cm]

As check points, ground coordinates of the old OEEPE direct sensor orientation block have been used (search for identical points with 1m search radius).

“all check points”

1 … deleted M. Cramer …
3 … deleted M. Cramer …
7 … deleted M. Cramer …
12 … deleted M. Cramer …
13 … deleted M. Cramer …
14 … deleted M. Cramer …
16 … deleted M. Cramer …
20 … deleted M. Cramer …
33 … deleted M. Cramer …
36 … deleted M. Cramer …
38 … deleted M. Cramer …

Partially these points are located outside the area of the control points, by this reason a reduced check point file with points just located inside the area of the control points has been used.
“check points inside control points” without points 1, 3, 7

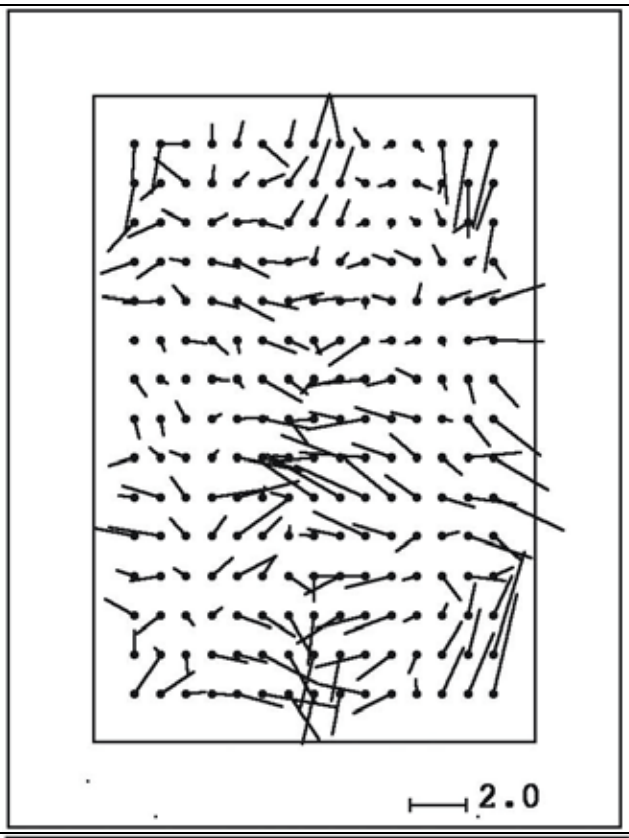

Fig. 5: averaged image coordinate residuals of block adjustment

upper left: without additional parameters

lower left: with parameters 1 – 12

lower right: with all parameters

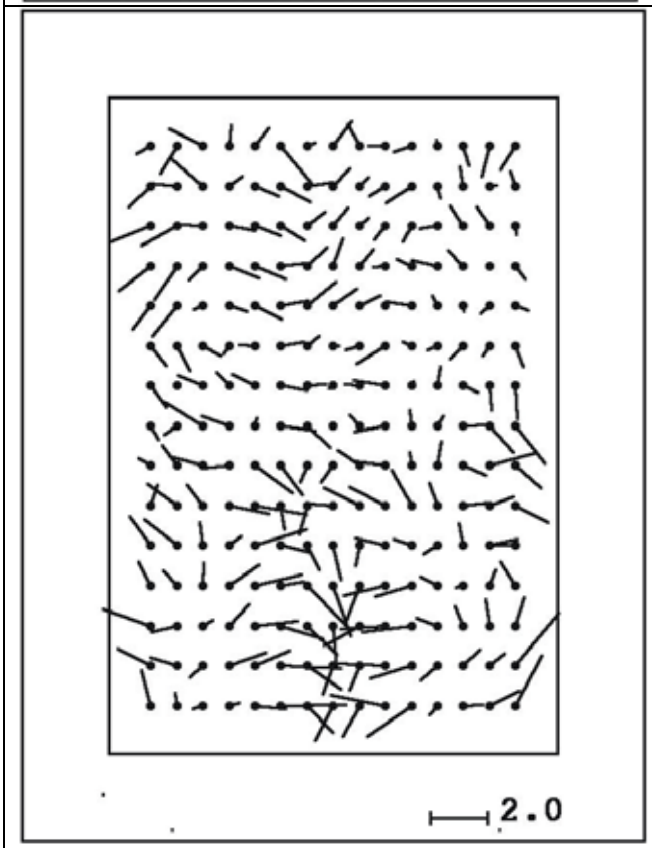

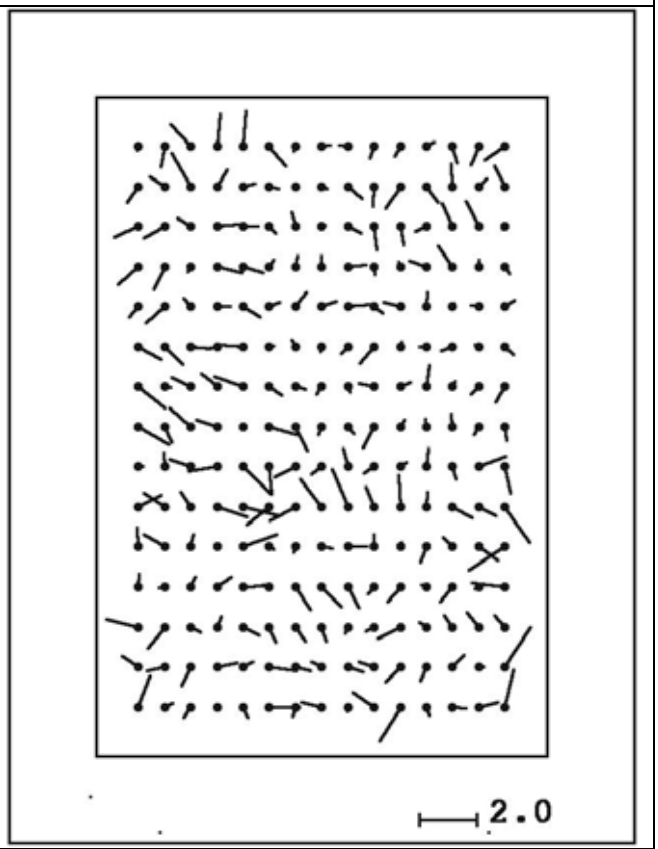

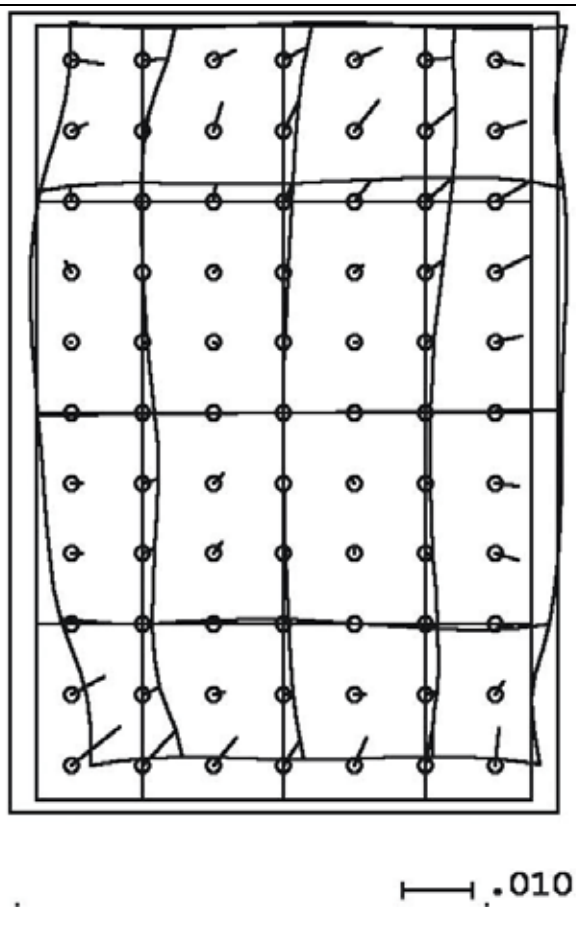

parameters 1 - 12

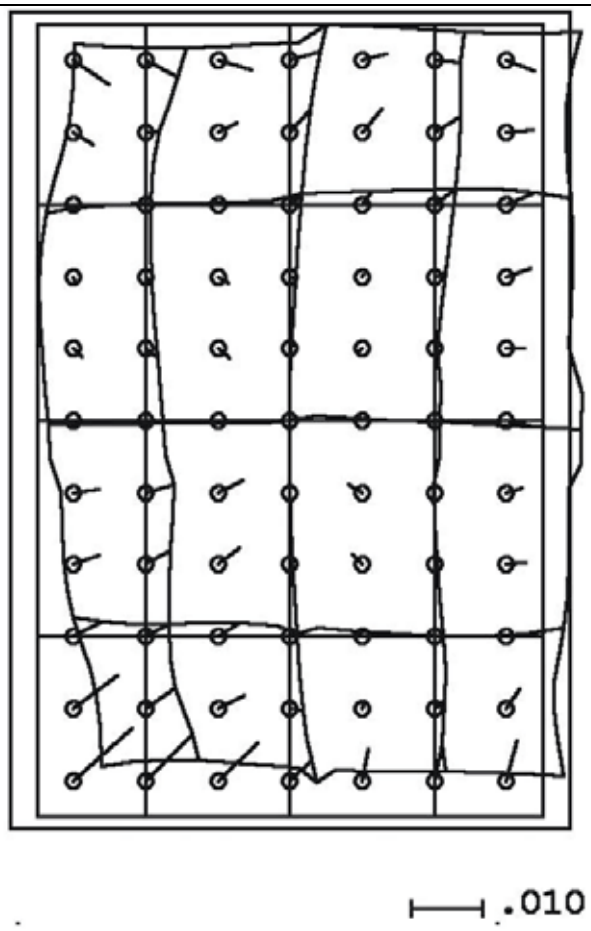

parameters 1 -12 + 42 - 73

Figure 6: effect of additional parameters to image coordinates (“systematic image errors”)

The averaged residuals (figure 5) show only the tendency of the systematic image errors. Caused by the correlation to the exterior orientation they are usually quite smaller like the systematic image errors (figure 6).
The averaged residuals of the adjustment with the parameters 1 – 12 indicate very clear remaining systematic image errors which can be fitted with the 12 standard parameters plus the special UltraCamD-parameters. The adjustment with the full set of additional parameters has only negligible averaged residuals (figure 5, lower right), indicated also with the covariance function of the averaged residuals (figure 7). The adjustment with the standard additional parameters 1 – 12 is reducing the covariance of the averaged residuals only slightly – the maximal value is just reduced from 0.34 to 0.31, but the dominating figure remains. The adjustment with all additional parameters (1-12 + 42-73) is strongly reducing the covariance – the maximal value is reduced to 0.16 and after 20mm distance in the image, there is only some noise remaining. From this side the adjustment should be made with all additional parameters.

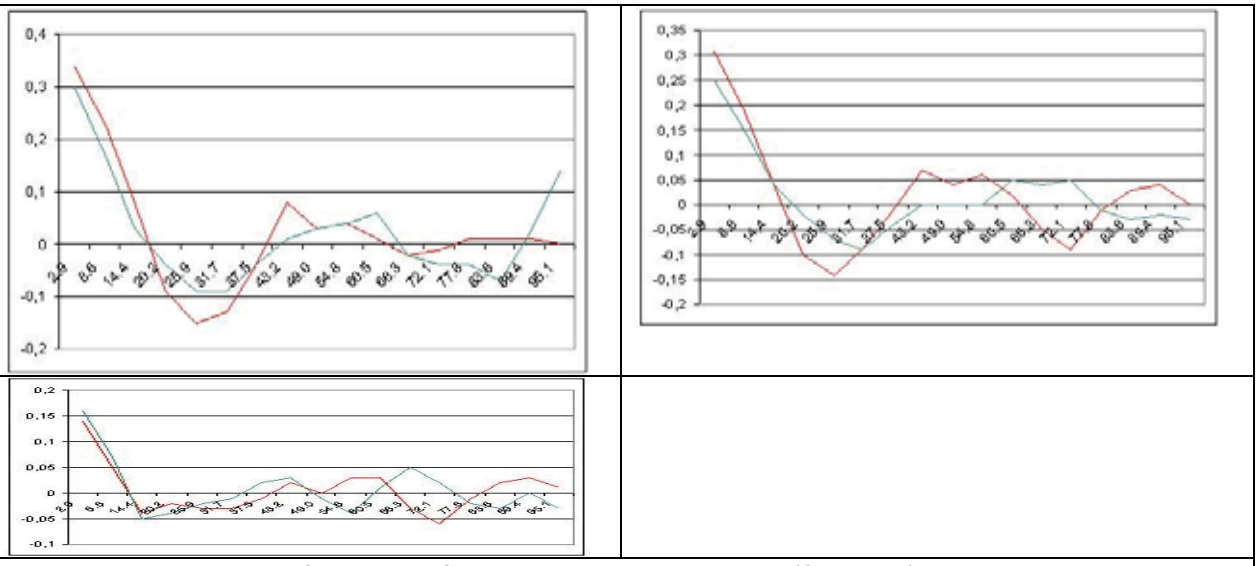

Figure 7: covariance function of the averaged residuals (figure 5)
vertical: covariance value horizontal: distance of points in image [mm]
red: covariance for dx' green: covariance for dy'
upper left: adjustment without additional parameters
upper right: adjustment with additional parameters 1 – 12
lower left: adjustment with all additional parameters

The discrepancies at the independent check points do not reflect the results of the independent check points very clear. The best results in X and Y are still achieved without self calibration. Only the more sensible height values show the best results at the adjustment with self calibration and here with all additional parameters. This becomes more clear at the points located outside the frame of the control points, but this is typical because such points are quite more effected by systematic image errors.

The achieved accuracy is not far away from sigma0 multiplied with the image scale for X and Y and this multiplied with the height to base relation (for p=60%) for Z. Because of the high number of images/point it should be more accurate. Also the height to base relation is better because of the endlap of 80%. Finally this indicates again the problem of the identification of the control and check points, dominating the result.

The shape and size of the systematic image errors seams to be typical for the UltraCamD. A similar size and also shape has been achieved also with data from other UltraCamD cameras. In general the size is 2 to 3 times larger than for the DMC.

Institut für Photogrammetrie und GeoInformation
Universität Hannover

Nienburger Str. 1
D-30167 Hannover

Tel.: ++49-511/762-2485
Fax: ++49-511/762-2483
e-mail: jacobsen@ipi.uni-hannover.de
http://www.ipi.uni-hannover.de

Dr.-Ing. Karsten Jacobsen

Hannover, Nov., 29th ,2006

EuroSDR Digital camera test

investigation of UltraCamD block Frederickstad, Norway adjustment of both flight levels together

1. STATISTICS

block configuration:

160 images flying height: 1964m, mean ground height 65m image scale 1 : 18 909 and 3906m, image scale 1 : 37 839
→ ground sampling distance (GSD) = 17cm and 34cm
An automatic aero triangulation has been made with LPS, the block adjustment and analysis has been made with the Hannover program system BLUH.

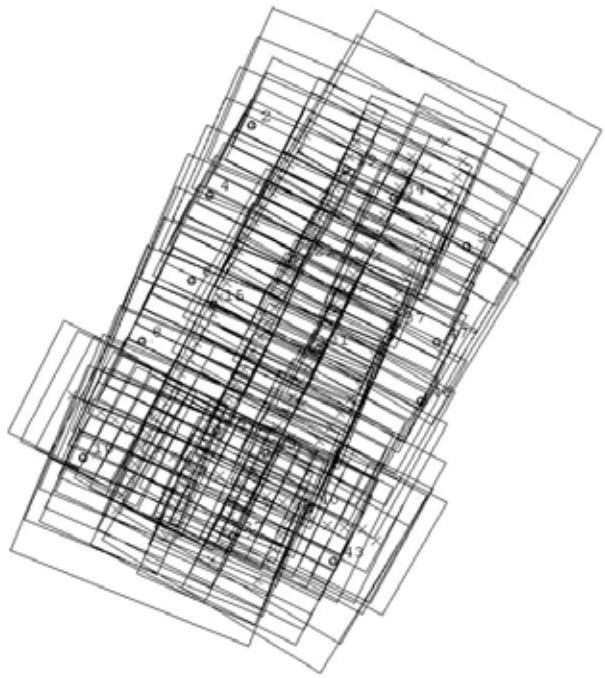

Fig. 1: configuration of both flight levels

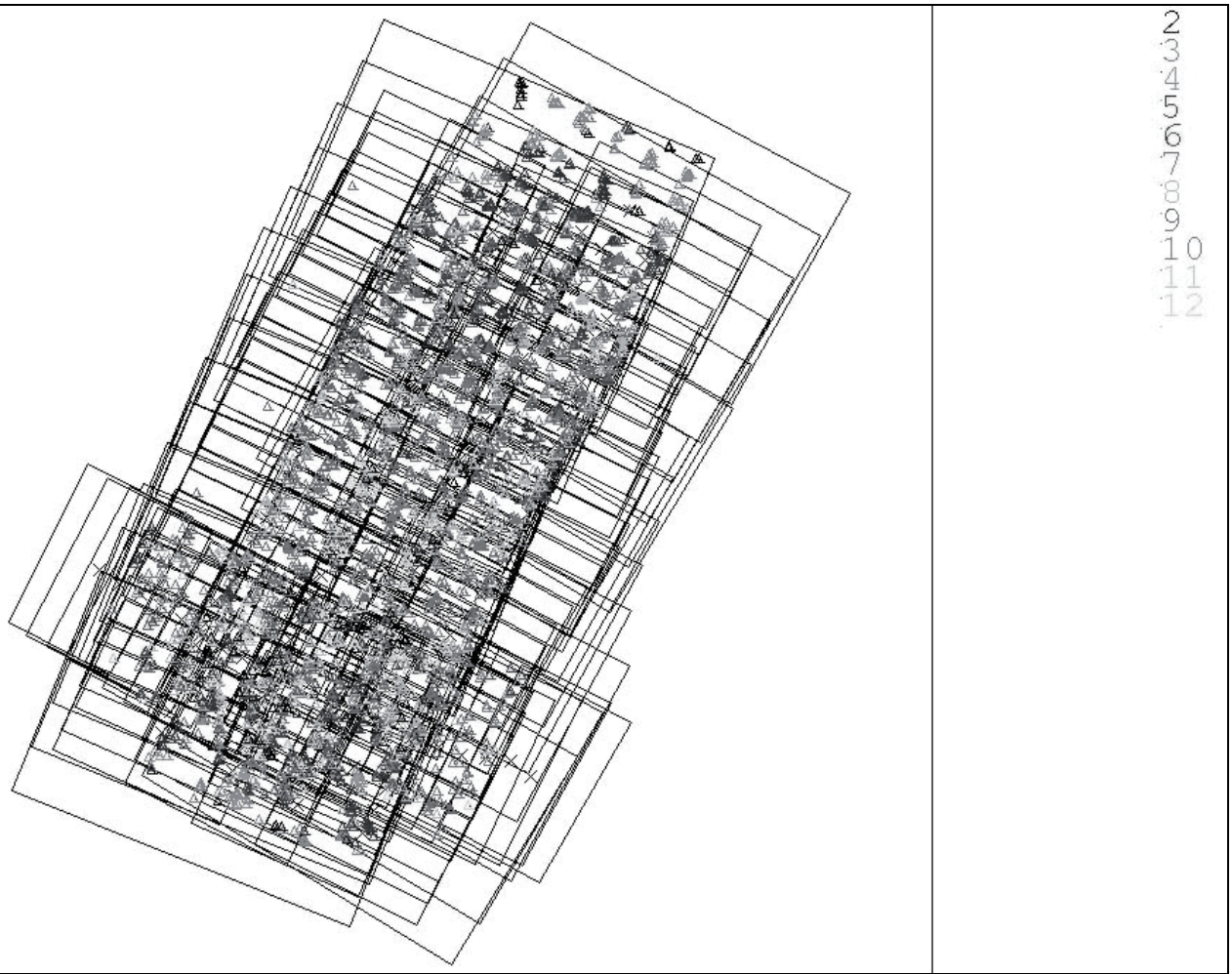

Fig. 2: pass points of flight lines - both flight levels (connection of flight lines)
the colour corresponds to the number of images / point (see upper right)

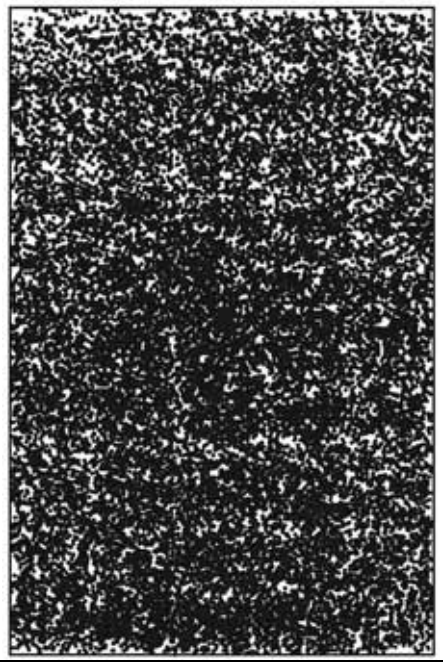

Fig. 3: distribution of points in the images – overlay of all images

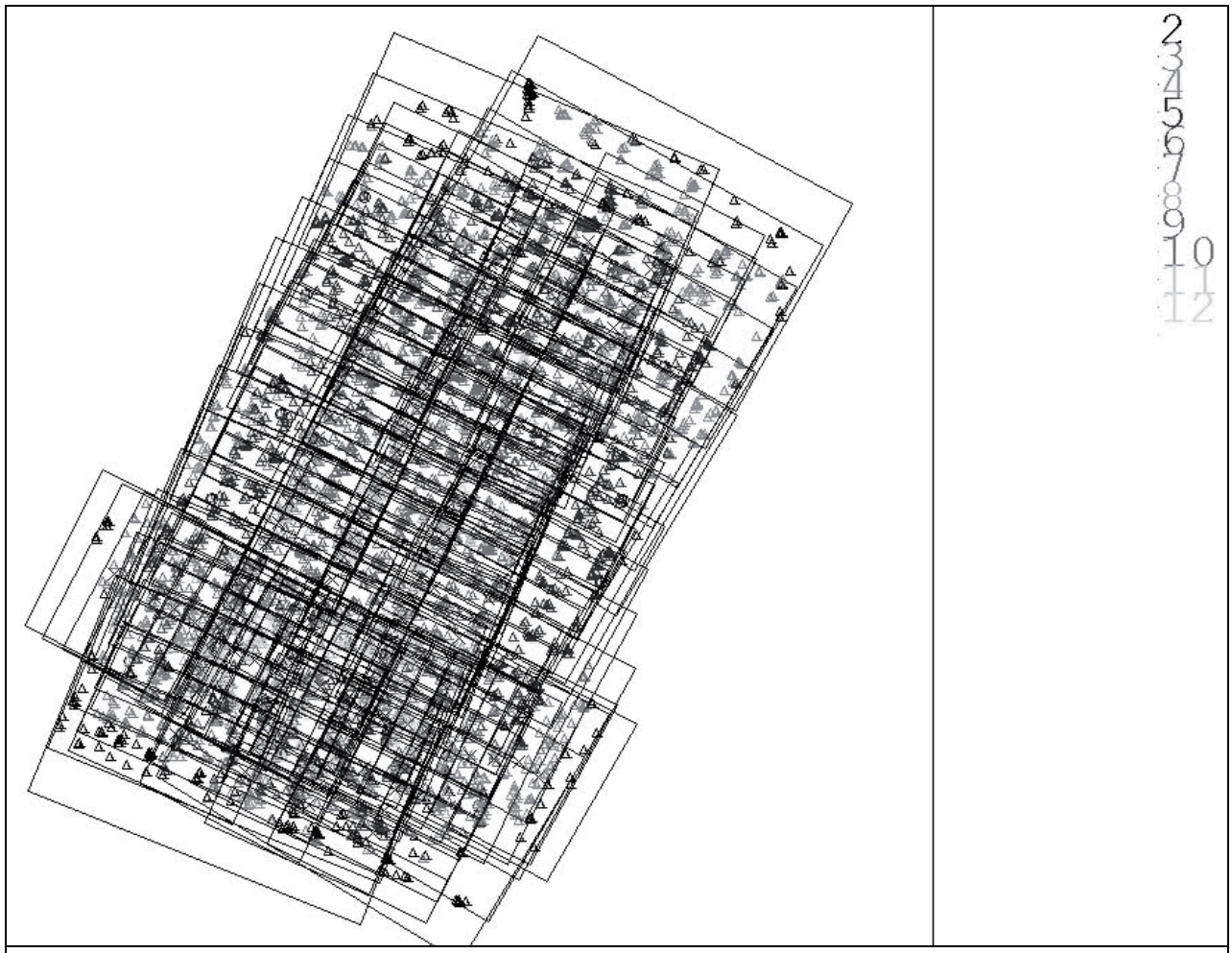

Fig. 4: all points of both flight levels
colour coded corresponding to the number of images / points (see upper right)

```
IN PHOTO       615    56 POINTS = LOWEST NUMBER
IN PHOTO       492   838 POINTS = HIGHEST NUMBER


NUMBER OF PHOTOS/OBJECT POINT
PHOTOS/POINT    1     2     3     4     5     6     7     8     9    10
POINTS:        40   293   507   637   803   397   451   543   640   443

PHOTOS/POINT   11    12    13    14    15    16    17    18    19    20
POINTS:       111    79    58    26    16     5     2     0     3     2

PHOTOS/POINT   21    22    23    24    25
POINTS:         0     2     1     1     1

 MAX PHOTOS/POINT           :     25
 OBJECT POINTS              :   5021
 PHOTOS                     :    160
 PHOTO POINTS               :  32597

 MINIMUM AND MAXIMUM OF PHOTO COORDINATES
  X MINIMUM =  -33.679  X MAXIMUM =   33.593
  Y MINIMUM =  -51.740  Y MAXIMUM =   51.579
```

The upper and the lower flight level are only connected by a limited number of points:

```
STRIP         PHOTOS
    1       474 -        487  upper flight level
    2       488 -        501  upper flight level
    3       503 -        529  lower flight level
    4       530 -        556          "
    5       557 -        584          "
    6       585 -        613          "
    7       615 -        635          "
```

CONNECTION OF STRIPS

		N		N		N		N		N	
		STRIP		STRIP		STRIP		STRIP		STRIP	
STRIP 1 CONNECTED TO		2	2125	3	10	4	8	5	2	7	3
STRIP 2 CONNECTED TO		1	2125	4	1	5	1	6	4	7	2
STRIP 3 CONNECTED TO		1	10	4	446	5	72	7	243		
STRIP 4 CONNECTED TO		1	8	2	1	3	446	5	395	6	116
		7	250								
STRIP 5 CONNECTED TO		1	2	2	1	3	72	4	395	6	449
		7	247								
STRIP 6 CONNECTED TO		2	4	4	116	5	449	7	216		
STRIP 7 CONNECTED TO		1	3	2	2	3	243	4	250	5	247
		6	216								

General information about data acquisition and block characteristics

Not all control and check points are reliable; they could not be measured in all theoretic possible images because of the forest. In addition the point identification was very difficult. By this reason the block is not optimal for test of the best data handling, but nevertheless an analysis of the image geometry for systematic image errors is possible. Because of the just parallel flight lines the systematic image errors cannot be separated totally from the influence of the control points – for such an analysis crossing flight lines should be used.

The points are distributed well in the images (figure 4), so systematic image errors can be analysed well.

2. ADDITIONAL PARAMETERS

The detailed analysis has been made with program system BLUH. BLUH includes general additional parameters and a set of parameters especially fitted to the geometry of the DMC as well as the UltraCam. The self calibration with additional parameters is able to determine geometric discrepancies between the mathematical model of perspective images and the real image geometry – this difference is called “systematic image errors” even if it is an error of the mathematic model.

The additional parameters may be correlated. High correlations may cause geometric problems in block areas not well supported by control points. By this reason in program BLUH the additional parameters are checked for correlation, total correlation and by Student-test. Too high correlated parameters and parameters with too small Student – test values are removed automatic from the adjustment.

Additional parameters in BLUH

```
1 = ANGULAR AFFINITY
2 = AFFINITY
3 - 6 = GENERAL DEFORMATION
7 - 8 = TANGENTIAL DISTORTION
9 = RADIAL SYMMETRIC R*R*R  10 - 11 RADIAL SYMMETRIC HIGHER DEGREE
12 = GENERAL DISTORTION

13 = FOCAL LENGTH  14, 15 = PRINCIPAL POINT
   FOR COMBINED ADJUSTMENT WITH GPS 13 - 15 REQUIRED FOR GPS-SHIFT
16 - 18 POSSIBLE GPS-DRIFT   19-20 GPS-DATUM  21= T*T
22 - 26 FOR PANORAMIC CAMERA
27 - 28 RADIAL SYMMETRIC FOR FISHEYE
29      DMC EXCENTRICITY   30 - 33 DMC SYNCHRONIZATION
34 - 41 DMC PERSPECTIVE DEFORMATION OF SINGLE CAMERAS
42 - 49 ULTRACAM SCALE  50 - 65 ULTRACAM SHIFT  66 - 73 ULTRACAM ROTATION
74 - 77 DMC RADIAL SYMMETRIC ORIGINAL IMAGES  78 - 81 DMC FOCAL LENGTH
ORIGINAL IMAGES
```

Special additional parameters for Vexcel UltraCamD

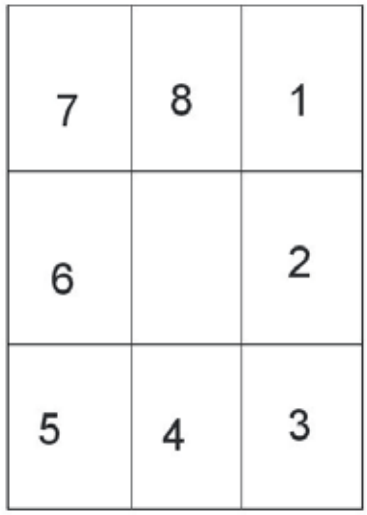

The UltraCamD has a synthetic image based on 9 individual CCD-arrays. With the additional parameters 42 up to 73 problems of the CCD-array merge can be determined. For 8 different sub-areas special parameters are available.

parameter 42 – 49 = scale parameters	42 for sub-unit 1 49 for sub-unit 8
parameters 50 – 57 = shift X	50 for sub-unit 1 57 for sub-unit 8
parameters 58 – 65 = shift Y	58 for sub-unit 1 65 for sub-unit 8
parameters 66 – 73 = rotation	66 for sub-unit 1 73 for sub-unit 8

3. ANALYSIS OF BLOCK FREDERICKSTAD both flight levels

		control points			check points		
	sigma0 [µm]	SX [cm]	SY [cm]	SZ [cm]	SX [cm]	SY [cm]	SZ [cm]
no AP	2.63	6.4	9.9	20.1	6.8	5.4	18.0
AP 1-12	2.50	5.2	6.8	21.8	4.4	6.3	15.7
AP 1-12, 42-65	2.40	5.4	8.2	17.6	3.9	6.3	15.2

Table 1: discrepancies at check and control points AP = additional parameters

As check points, ground coordinates of the old OEEPE direct sensor orientation block have been used (search for identical points with 1m search radius).

all used check points, with numbers of images / object point

12 … deleted M. Cramer …
13 … deleted M. Cramer …
14 … deleted M. Cramer …
16 … deleted M. Cramer …
20 … deleted M. Cramer …
33 … deleted M. Cramer …
36 … deleted M. Cramer …
38 … deleted M. Cramer …

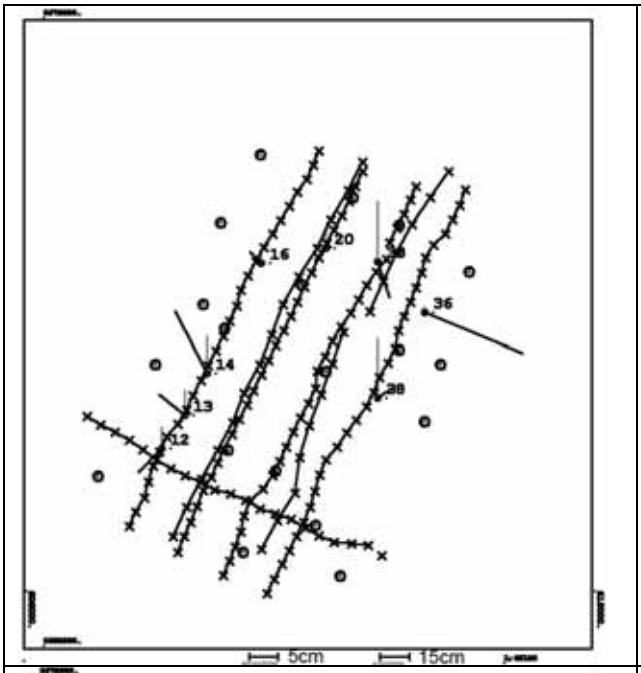

Fig. 5: discrepancies at check points
vector scale for X, Y = 5cm (blue vector)
vector scale for Z = 15cm (green vector)
circles = control points

upper left: without additional parameters

lower left: with parameters 1 – 12

lower right: with all parameters

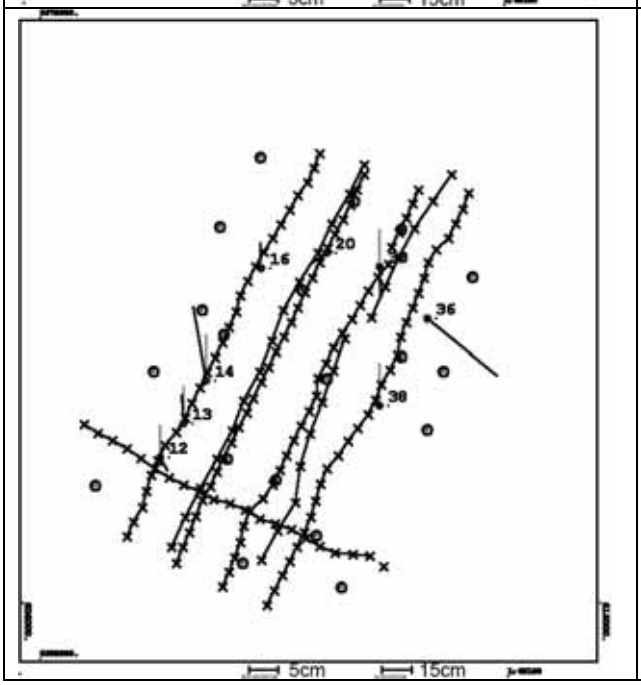

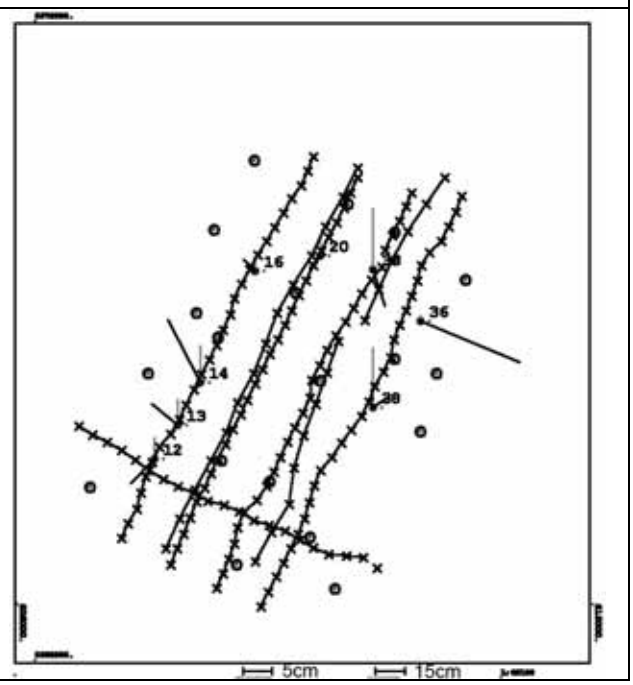

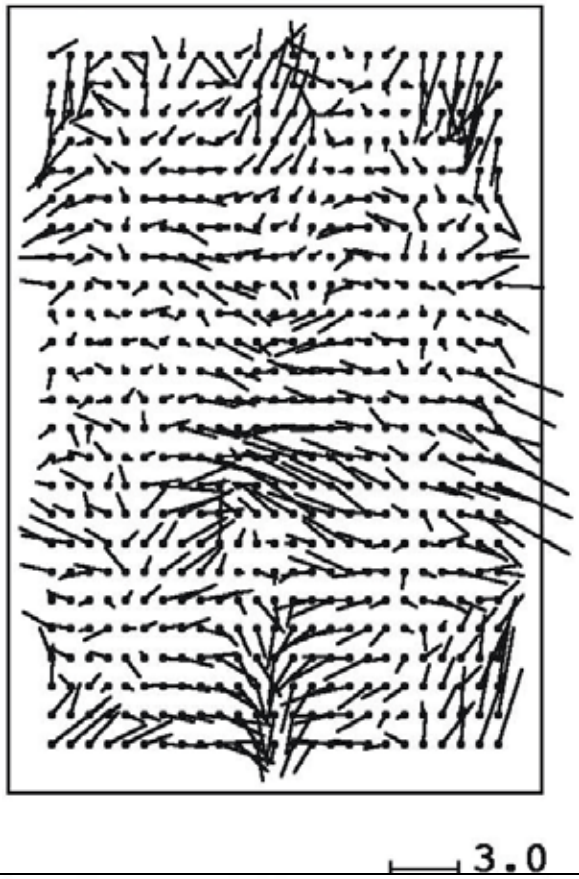

Fig. 6: averaged image coordinate residuals of block adjustment

upper left: without additional parameters
root mean square = 0.99µm

lower left: with parameters 1 – 12
root mean square = 0.78µm

lower right: with all parameters
root mean square = 0.56µm

vector scale = 3µm

in average 52 original discrepancies / vector

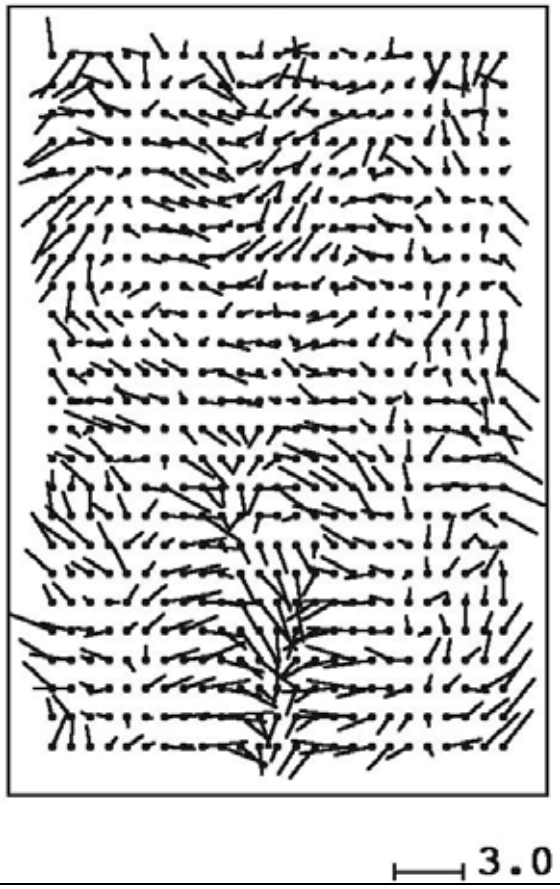

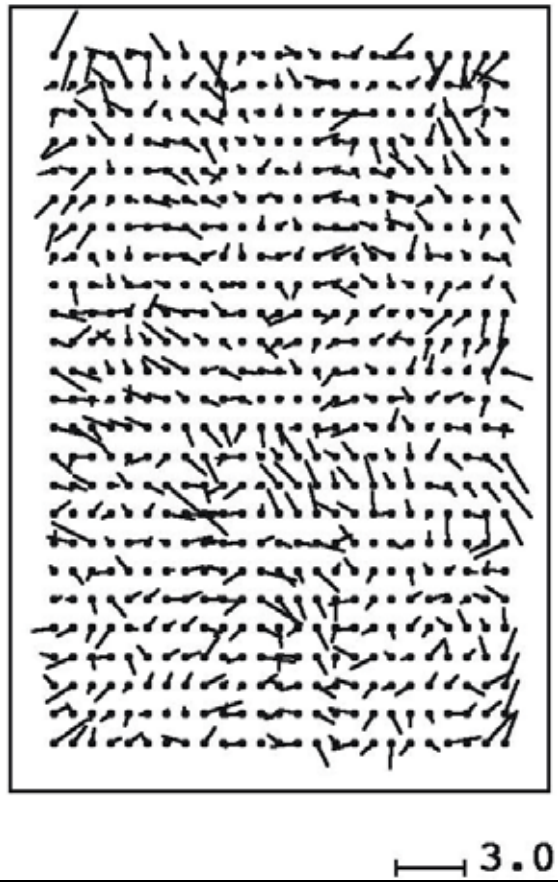

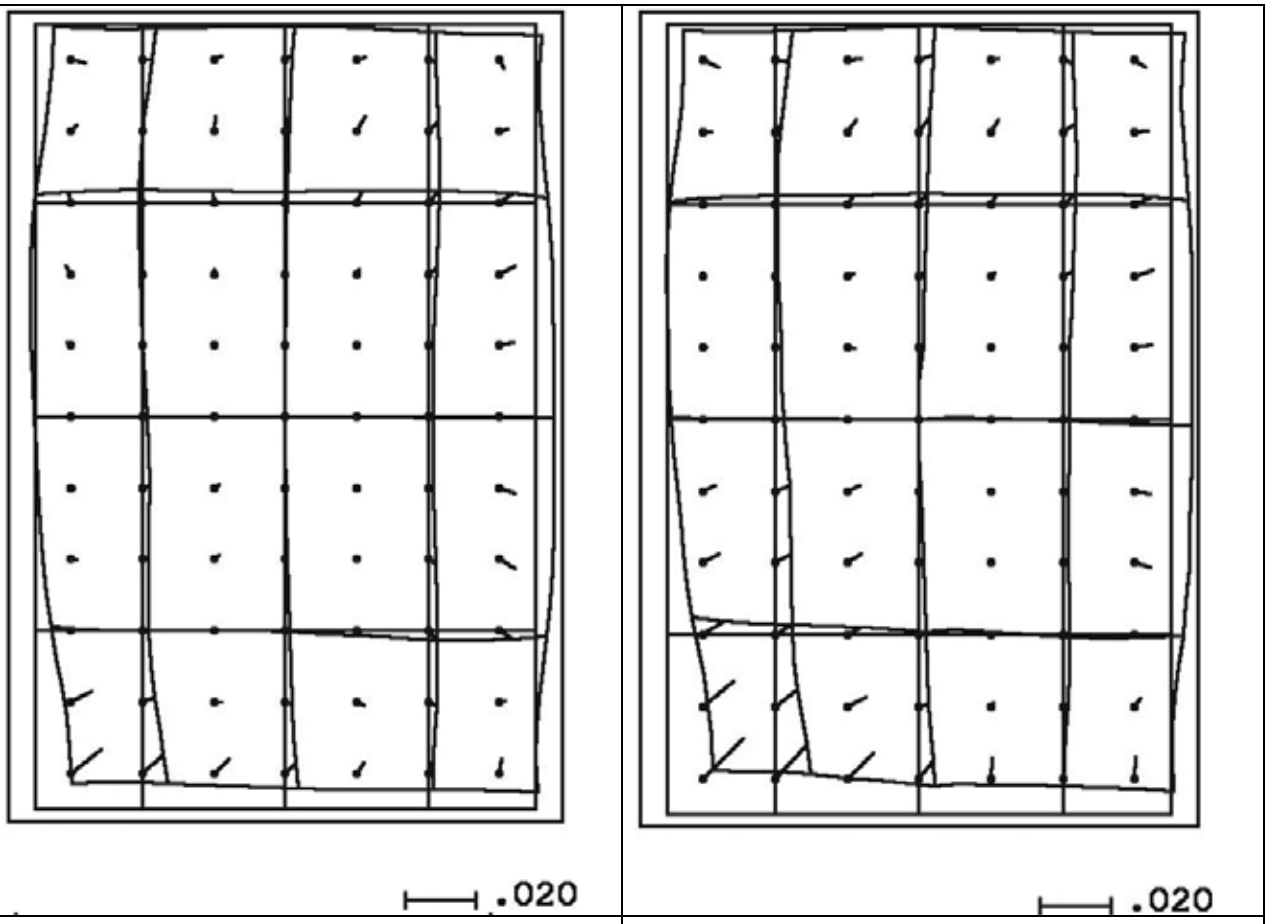

parameters 1 - 12	parameters 1 -12 + 42 - 73

Figure 7: effect of additional parameters to image coordinates (“systematic image errors”)

The averaged residuals (figure 6) show only the tendency of the systematic image errors. Caused by the correlation to the exterior orientation they are usually quite smaller like the systematic image errors (figure 7).
The averaged residuals of the adjustment with the parameters 1 – 12 indicate very clear remaining systematic image errors which can be fitted with the 12 standard parameters plus the special UltraCamD-parameters. The adjustment with the full set of additional parameters has only negligible averaged residuals (figure 6, lower right), indicated also with the covariance function of the averaged residuals (figure 8). The adjustment with the standard additional parameters 1 – 12 is reducing the covariance of the averaged residuals only slightly – the maximal value is just reduced from 0.34 to 0.31, but the dominating figure remains. The adjustment with all additional parameters (1-12 + 42-73) is strongly reducing the covariance – the maximal value is reduced to 0.16 and after 20mm distance in the image, there is only some noise remaining. From this side the adjustment should be made with all additional parameters.

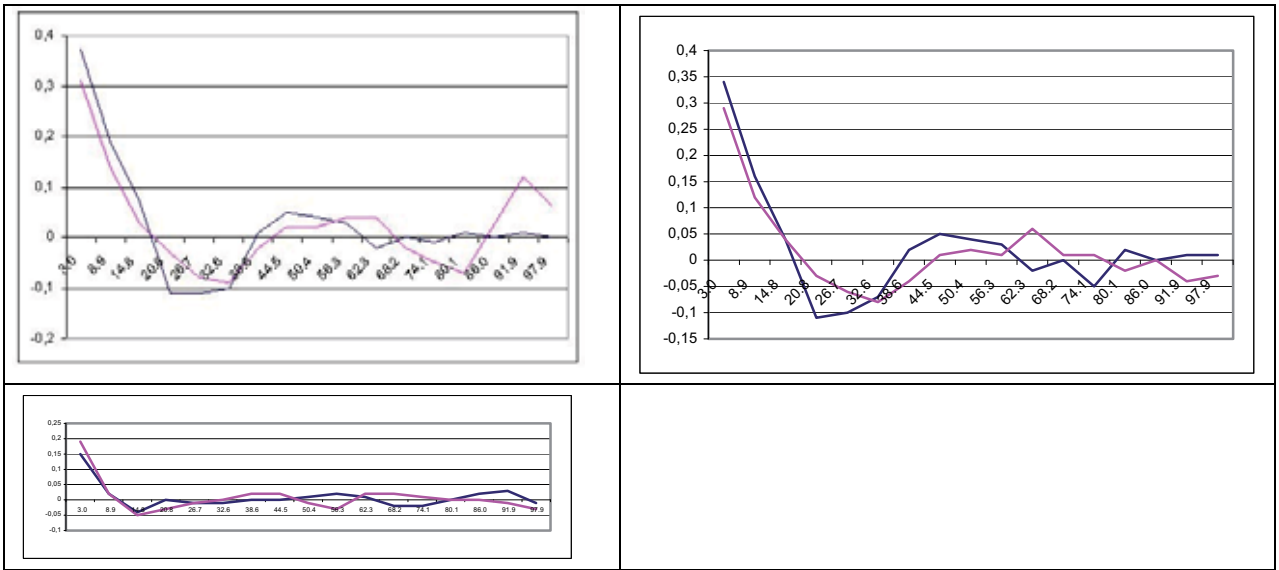

Figure 7: covariance function of the averaged residuals (figure 5)
vertical: covariance value horizontal: distance of points in image [mm]
red: covariance for dx' green: covariance for dy'
upper left: adjustment without additional parameters (maximal = 0.37)
upper right: adjustment with additional parameters 1 – 12 (maximal = 0.34)
lower left: adjustment with all additional parameters (maximal = 0.19)

The block adjustment should be done with self calibration by additional parameters. At least the standard parameters 1 – 12 are required; with the special UltraCam-parameters the results are improved just a little. The discrepancies at the independent check points correspond to 0.3 GSD for X and Y and to 0.2 GSD for the x-parallax in relation to the dominating lower flying level under the condition of a height to base relation of 3.7. Because of the high number of image points for each check point this is not a too good result, but it is caused by the limited identification of the control and check points.

The shape and size of the systematic image errors seams to be typical for the UltraCamD. A similar size and also shape has been achieved also with data from other UltraCamD cameras.

The result of the adjustment of all images together is very similar to the individual flying heights. The re is no significant difference of the systematic image errors for both flying heights and of course, for the handling of all images together.

Institut für Photogrammetrie und GeoInformation
Universität Hannover

Nienburger Str. 1
D-30167 Hannover

Tel.: ++49-511/762-2485
Fax: ++49-511/762-2483
e-mail: jacobsen@ipi.uni-hannover.de
http://www.ipi.uni-hannover.de

Dr.-Ing. Karsten Jacobsen

Hannover, Oct., 22nd ,2006

EuroSDR Digital camera test remarks

The original plan of the accuracy evaluation of digital cameras could not be reached totally because of the dominating influence of the control and check point measurements. By this reason also the results of the different participants cannot be compared directly. This of course, effects also the comparison of the adjustment results. The negative influence of the very difficult control and check point determination can be seen also by the comparison of the lower and the upper DMC flying height results. By theory there should be a relation of 2 between the achieved accuracies, but in reality the relation is approximately 2.4, indicating the larger problems of the control point identification in the smaller scale. Of course this is influenced also by 3.3 images/control points for the lower flying height and 2.5 images/control point for the upper flying height, but this should not have such a strong influence. Also the combined results should be better than just the lower flying elevation, but this is not the case.

For a better comparison of the results achieved by the different participants, a set of image coordinates of the control and check points should be distributed. But nevertheless this allows not the comparison of the method of block adjustment with the different sets of additional parameters – this will just show the quality of the used automatic aero triangulation. For the direct comparison of the numerical handling of the block adjustment also the same image coordinates of tie points are required.

Nevertheless, there is no discussion, that a block adjustment with self calibration is required for achieving optimal results.

EuroSDR Digital Camera Calibration

Report on: UltraCam D Digital Aerial Camera Calibration

Authors: Dr M J Smith, Mr N Kokkas, Mr K S Qtaishat

Affiliation: IESSG, The University of Nottingham, University Park, Nottingham, NG7 2RD, UK; email: martin.smith@nottingham.ac.uk

1. Introduction

There are now many different digital sensor systems available for photogrammetry, remote sensing and digital image analysis. Cramer (2005) provides a summary of the systems available in 2005 and these include; single and multi-cone/lens systems as well as high resolution push broom scanners. Before any imagery can be used for high precision measurement purposes in photogrammetry there is a need to determine the geometric model of the sensing system. In the case of frame cameras there is a need to establish the sensor model and determine the relationship of this model in comparison to the standard normally (and traditionally) used in photogrammetry which is perspective geometry. The process of measuring the relationship of a 'real' frame camera geometry in comparison to perspective geometry is known as camera calibration. Camera calibration is normally undertaken by the manufacturer before supplying a camera for photogrammetry then periodically, and when necessary, during the life of the camera.

The 'new' multi cone digital camera systems are geometrically complex systems. The image used for photogrammetric analysis is made up of a number of images produced by a cluster of camera cones and possibly various groups of CCD arrays. This produces a resultant image which is not just based on traditional single lens/focal plane camera geometries but is dependant on the joining of images from multiple lens (different perspectives), handling groups of focal planes and the matching of overlapping image areas. For optimal use of this imagery there is a need to:

1. understand this complex geometric model;
2. undertake a calibration of the 'real' camera;
3. analyse the relationship between the calibrated camera geometry and perspective geometry;
4. establish whether existing calibration procedures are adequate;
5. possibly establish new procedures;
6. establish how long a camera calibration lasts before periodic recalibration is required.

Some of these requirements can only be determined through long-term experience/research and some can be determined through investigation and short-term research. This report provides an investigation into the camera calibration of a Vexcel UltraCam D aerial camera based on results achieved from two flights flown over a test site over Fredrikstad-Norway as part of the EuroSDR Digital Camera Calibration project.

2. Aim

The aim of this research was to investigate the calibration of a Vexcel UltraCam D digital aerial camera. This will involve investigating the following objectives:

1. understanding the geometry of the UltraCam D;

2. establishing whether existing camera calibration techniques are suitable;
3. possibly proposing an alternative camera calibration approach.

3. Methodology

Provided for this project is a data set consisting of two UltraCam D sorties taken at different altitudes over a targeted (pre-marked) test site in Norway, see ' 3.1 *Test site and data provided*'. The facilities available for undertaking the investigation at the IESSG are given in the section '3.2 *Facilities for digital image processing and camera calibration*'. The available data and facilities influences the methodology that can be adopted. A brief description of the camera geometry is given in the section '4. *Camera geometry*' and this provides the guide for the detailed issues to be investigated.

The methods used for the investigation are as follows and based on the objectives:

1. The geometry of the camera is obtained from a literature review (objective 1.) and this is reported in section 4. '*Camera geometry'*.
2. The proposed method of camera calibration will be based on the self-calibration technique using the Collinearity equations (objective 2. and 3.) and this is reported in section 5. '*Trials and analysis'*. The following trials will be undertaken for the;
    a. high flight;
    b. low flight.

    Variables in the self-calibration technique to be investigated are as follows:
    1. number of tie points used in joining the images;
       This will be investigated on the benchmark result only (see point 3.1. below), making a reasonable assumption that this would be typical of all other triangulations.
    2. number of control points and number of check points;
       This will be investigated on the benchmark result only (see 3.1. below), making a reasonable assumption that this would be typical of all other triangulations.
    3. calibration model used;
        3.1. As a camera calibration has already been performed by Vexcel and applied by IFMS a triangulation will be performed without a calibration model which can be used as a 'benchmark result' against which other results can be compared.
        3.2. The 'best ' result from existing traditional models will be identified based on the smallest image residuals and RMSE of ground and check points. In theory, the existing traditional self-calibration models have been based on knowledge and experience of single cone frame camera geometries and environmental effects. As such it might be reasonable to expect only limited benefit from using these models with a multi lens system.
        3.3. As the geometry of the UltraCam D is different from the traditional single cone/CCD camera an analysis will be undertaken to try to identify any systematic patterns in the image residuals (objective 3.). This will enable alternative calibration procedures (objective 3.) to be considered. The potential camera features which may cause variations from the traditional self-calibration models (see section 4.) will be investigated through analysis of triangulation image residuals within the:
            a. whole image;
            b. individual sub-images;
            c. common overlap areas between the sub-images; and
            d. sub-images taken from the same cone, with the same letter (see figure 2).

        Two methods can be identified to apply a new calibration model to the image coordinates:
        a. self-calibration during the bundle adjustment;
        b. by identification and quantification of systematic residuals followed by application to image coordinates and re-computation of the bundle adjustment.

        The purists would argue that approach 'a' is the 'best' approach with some justification but approach 'b' does have some advantages:
        a. it can be applied to any multi-lens camera system with little or no change to the method;

b. it only requires some post processing software to analyse the residuals not a change to existing aerial triangulation software;
c. it can consider systematic effects on image coordinates from any sources and not those just dependent on modelling optical geometry (see section 4.).

Approach 'b' will be adopted in the project for investigation and for convenience it will be identified as the 'IESSG approach'.

The project has requested that the coordinates of a number of prescribed check points are included in the computation enabling a check point analysis to be performed. It has not been possible to include a meaningful analysis of these check points in the report as their coordinates have not been provided to a suitable accuracy. So the same trials (in addition to those discussed in the main report) have been undertaken again (as described in this section) but with all observed ground control points and prescribed check points included. These results are presented in Appendix A.

3.1 Test site and data provided

Data Provider:	IFMS-Pasewalk / Germany	
Test Site:	Fredrikstad-Norway	
Mission Flight:	16 September 2004	
Image used:	Panchromatic image	
In-flight GPS/IMU:	None used	
High flight:		
	Flying height:	3800m
	Number of images:	29
	Number of control points available:	14
Low flight:		
	Flying height:	1900m
	Number of images:	132
	Number of control points available:	17
Overlap:	80% forward and 60% lateral overlap	

Standard error of ground control points = ± 0.050m.
Check ground points were provided but at a lower quality than the control points so they are of limited value in the analysis.

3.2 Facilities for digital image processing and camera calibration

Leica LPS – used for image point observations and automatic tie point measurement.
ORIMA – used for aerial triangulation computation with and without self-calibration.
IESSG in-house analysis tools – used to analyse results.

3.3 Presentation of results

The results from the aerial triangulation computations will be presented in two ways:
1. in tables of RMSE on control, check and image points;
2. in graphical form showing the mean image residuals computed from all the image measurements, from all the images, within a small sub-area of the image. Typically this involved dividing the image into 24x24 sub-areas giving 8x8 number of sub-areas/points per CCD. Looking at residual plots of various number of subdivisions from one residual per CCD up to a high density of points per CCD the 24x24 division seems to give a reasonably detailed distribution of residuals. The 24x24 also appeared to give a reasonable indication of any systematic patterns and therefore image coordinate correction, without swamping with detail and random error. It is important to note the scale of the residuals varies between plots, see the scale arrow in the bottom right hand corner of each figure.

A summary table is given for both the high flown and low flown results.

4. Camera geometry (summary related to camera and image geometry)

The Vexcel UltraCam D digital aerial camera consists of 8 lens cones as shown in figure 1 (Smith et al., 2005, Kruck, 2006, Gruber and Ladstädler, 2006). The 4 lens cones in a line through the centre of the cone cluster are used to capture the panchromatic image which is made up of 9 overlapping sub-images to create a composite image as shown schematically in figure 2. The sub-images have been given a letter to show which images were captured by the same lens cone.

Points to note for analysis related to camera geometry:
1. There are more than one CCD in all except one sub-image;
2. Each cone will need to be calibrated and typical frame camera calibration parameters applied:
    a. Focal length;
    b. The relationship of CCD arrays to each other (shift, rotation and scale);
    c. Lens distortion.

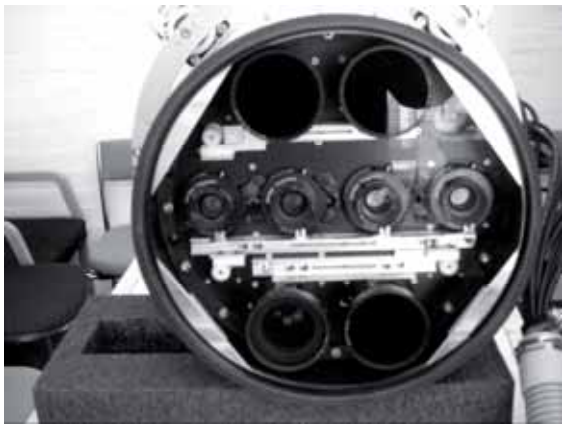

Figure 1. Multiple lens cones; 4 panchromatic across the centre and 4 larger colour cones (Copyright Simmons Aerofilms Ltd) (Smith et al., 2005)

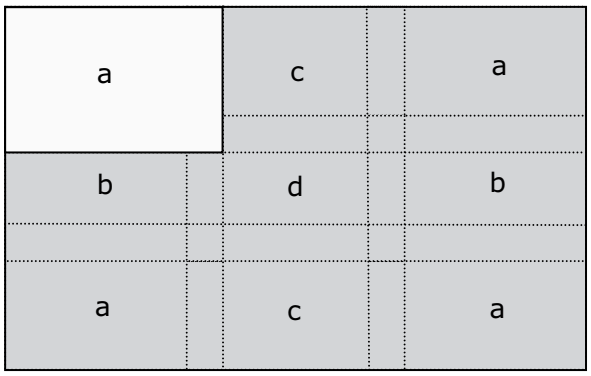

Figure 2. Schematic of the 9 sub-images making up the panchromatic image with one image highlighted

Points to note for analysis of the suitability of self-camera calibration techniques:
1. Self-calibration techniques have not traditionally calibrated for the merging/matching of the sub-images together.
2. Self-calibration techniques could take into consideration in-flight effects:
    a. Overall camera/image parameters for the composite image (2. a-c above);
    b. Image flatness
    c. Environmental effects:
        i. Atmospheric refraction effects;
        ii. Thermal effects on the camera;
        iii. Atmospheric pressure effects on the camera.
    d. Systematic effects of merging/matching of the sub-images together.

5. Trials and analysis

The proposed method of camera calibration will be based on the self-calibration technique using the Collinearity equations (objective 2. and 3.) and the following trials have been undertaken.

5.1. Results and discussion - general

5.1.1. Quality of the images

It should be noted that the precision of the image observation were hindered by the reduced radiometric image quality in both the high and low flight. This made observation of some of the control points difficult and probably had an impact on the quality of automatic tie point generation. In addition, no attempt was made to perform any image enhancement techniques in the entire image but instead the histogram was adjusted accordingly for each separate image observation. The standard error used for the image observations was the σ_o value from a preliminary run of the aerial triangulation for a particular block being analysed, typically 1-2μm.

5.1.2. Number of tie points used in joining the images

900 tie points (132 images) were used in the low flight and 2300 tie points (29 images) were used in the high flight. Due to the low radiometric quality, mismatched and gross errors occurred in several tie points which were identified and excluded by the robust blunder detection algorithm available in LPS.

5.1.3. Number of control points and number of check points

The number of control points and check points used was investigated on the benchmark results only (see section 3.1.), making a reasonable assumption that this would be typical of all other triangulations. After making a number of test runs it was found that using the low accuracy check points did not help much in the analysis to identify the best results for the AT. For the low flight it was decided to use 14 ground control points plus 3 ground control points as check points. For the high flight it was decided to use 11 ground control points plus 3 ground control points as check points.

5.2. Results and discussion - high flight (3800m)

5.2.1. Calibration model used

5.2.1.1. No calibration model - benchmark result

As a camera calibration has already been performed by Vexcel and results applied by IFMS a triangulation was performed without a calibration model which can be used as a 'benchmark result' against which other results can be compared.

Self Calibration method	Ground control points RMSE (m) of residuals			Ground check points RMSE (m) of residuals			Image coordinates RMSE (μm) of residuals	
	X	Y	Z	X	Y	Z	x	y
No Calibration	0.048	0.026	0.031	0.108	0.102	0.278	1.69	1.82

Table 1. *Results of high flight AT without any calibration model*

The following figure indicates the image residuals of the observations in the image space for the results presented in table 1.

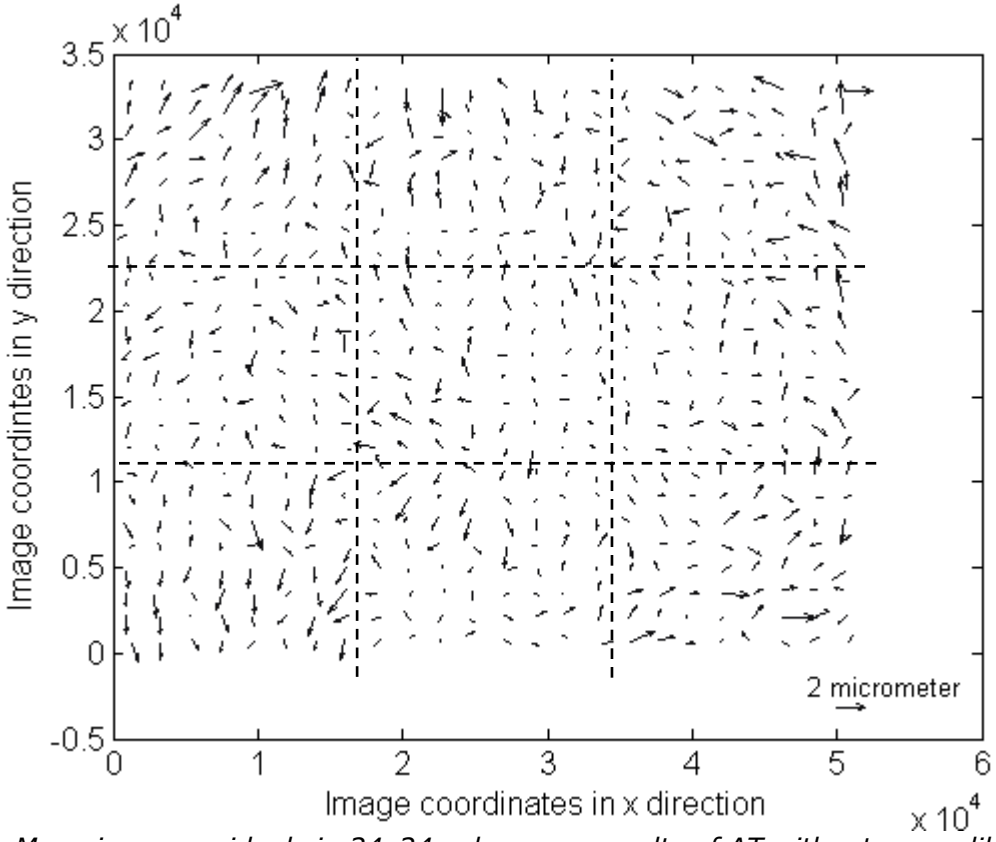

Figure 3. *Mean image residuals in 24x24 sub-areas, results of AT without any calibration model (coordinates in µm, partitioning shows approximate boundaries of the CCD arrays)*

On visual inspection of figure 3., there is no overall identifiable systematic patterns in the whole image. There are small areas where systematic patterns can be identified, some showing a relationship to the CCDs (for example see bottom left corner) but it should be noted that in general the image residuals over the whole image are very small. As these residuals could come from a variety of sources and this is only results from one block, these patterns may not be due to just uncorrected systematic characteristics of camera/image geometry. This raises the question 'is this pattern of residuals repeatable between blocks of images?'.

5.2.1.2. The 'best' result from existing self-calibration models

A number of self calibration models where tested from Leica LPS and ORIMA software to assess the most suitable for this type of imagery. The results presented here come from ORIMA and are considered the 'best' result from existing self-calibration models based on the smallest image residuals and RMSE of ground and check points. The parameters of the self-calibration model are as follows:
c = principal distance
x_o, y_o = principal point position
a_1, a_2, a_3 = polynomial coefficients for radial lens distortions

The results in table 2 show a very small improvement (except check point RMSE in X and Y) compared to the benchmark values in table 1. The above self-calibration parameters were free (had large standard errors) during the AT solution in ORIMA.

The following figure 4. shows a similar pattern of the image residuals to those in figure 3 (as defined in section 3), for the results presented in table 2.

Self Calibration method	Ground control points RMSE (m) of residuals			Ground check points RMSE (m) of residuals			Image coordinates RMSE (μm)of residuals	
	X	Y	Z	X	Y	Z	x	y
Self Calibration	0.042	0.024	0.020	0.120	0.104	0.248	1.59	1.73

Table 2. *Results of high flight AT with self-calibration model*

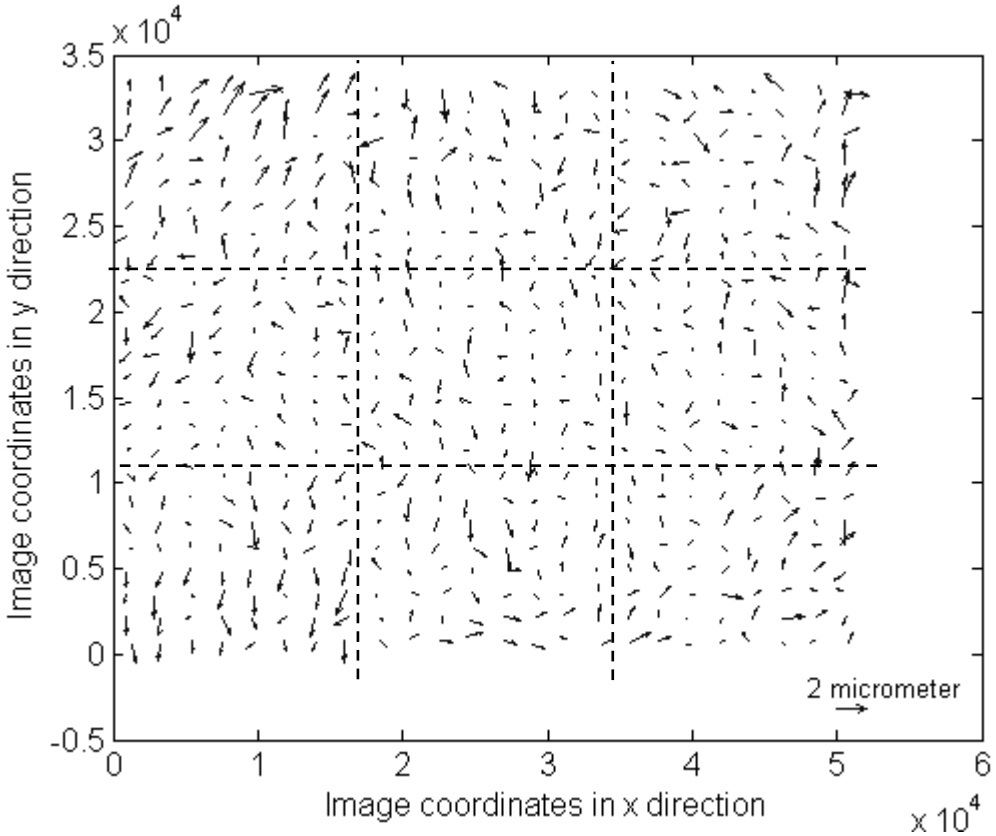

Figure 4. *Mean image residuals in 24x24 sub-areas, results of AT with self-calibration model (coordinates in μm, partitioning shows approximate boundaries of the CCD arrays)*

5.2.1.3. Analysis of aerial triangulation image residuals – IESSG approach

As the geometry of the UltraCam D is different from the traditional single cone/CCD camera an analysis will be undertaken to try to identify any systematic patterns in the image residuals (objective 3.). This will enable alternative calibration procedures (objective 3.) to be considered. The potential camera features which may cause variations from the traditional self-calibration models (see section 4.) will be investigating through analysis of triangulation image residuals.

Self Calibration method	Ground control points RMSE (m) of residuals			Ground check points RMSE (m) of residuals			Image coordinates RMSE (μm)of residuals	
	X	Y	Z	X	Y	Z	x	y
IESSG Approach	0.038	0.022	0.018	0.129	0.098	0.280	1.53	1.62

Table 3. *Results of high flight AT with IESSG approach*

The following figure 5 shows the mean image residuals of the observations for the sub- areas in the image.

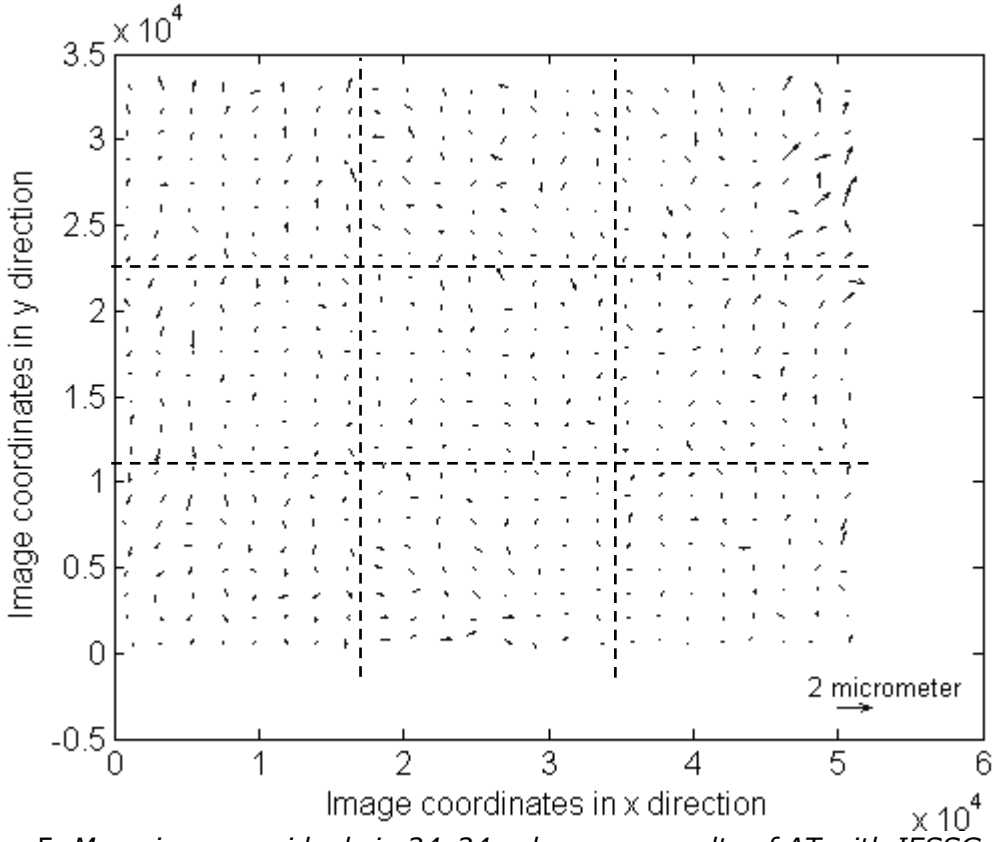

Figure 5. *Mean image residuals in 24x24 sub-areas, results of AT with IESSG approach (coordinates in µm, partitioning shows approximate boundaries of the CCD arrays)*

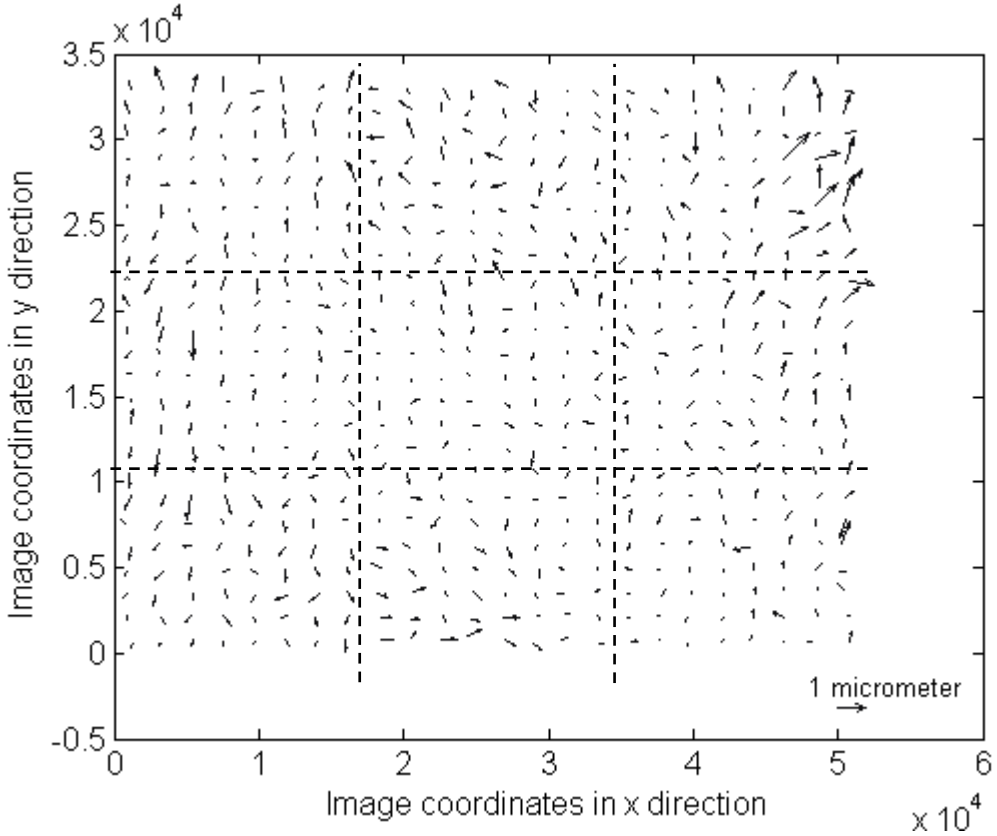

Figure 6. *Mean image residuals in 24x24 sub-areas, results of AT with IESSG approach (note the residual scale has been changed 1 µm, coordinates in µm, partitioning shows approximate boundaries of the CCD arrays)*

Applying the results shown in figure 3. to the measured image coordinates as described in section 3. give the results in table 3., figure 5 and figure 6. using ORIMA without any self-calibrating model. As the residuals are so small in figure 5, figure 6 has been presented which is the same results but with a larger residual scale. The solution appears to have reduced some of the residual pattern although, the top right hand corner seems to still have some relatively large residuals.

5.2.2. Summary Table 4. of high flight results

Self Calibration method	Ground control points RMSE (m) of residuals			Ground check points RMSE (m) of residuals			Image coordinates RMSE (μm) of residuals	
	X	Y	Z	X	Y	Z	x	y
No Calibration	0.048	0.026	0.031	0.108	0.102	0.278	1.69	1.82
Self Calibration	0.042	0.024	0.020	0.120	0.104	0.248	1.59	1.73
IESSG Approach	0.038	0.022	0.018	0.129	0.098	0.280	1.53	1.62

Table 4. *Summary of high flight results*

Table 4. shows the results of the ground control RMSE are significantly better than the ground control check point RMSE values. The ground control RMSE values are influenced by the standard errors of the image coordinates and the ground control. The standard error of ±0.05m for the ground control was provided and the standard error used for the image observations was the σ_o value from a preliminary run of the aerial triangulation for a particular block being analysed, typically 1-2μm. So we are not aware of using any incorrect weighting or unduly 'forcing' a fit to the control. Table 4. also shows in general, a very slight improvement has been obtained from the self-calibration model. The self-calibration model is probably correcting for some environmental effects. The IESSG approach has slightly improved the RMSE of the image residuals, minimal improvement on the ground control RMSE but has made the check point RMSE slightly worse (considering RMSE in X and Z).

The Z RMSE for the check points in all three cases is dominated by one large Z residual which is greater than -0.3m in each case. If this value is removed the RMSE of the remaining points is around the 0.1m level.

5.3. Results and discussion - low flight (1900m)

A similar process used for analysing the high flown images has been used to assess the low flown images except for the IESSG approach the high flown residual corrections have been used in the low flown computation. This correction was used because the ideal scenario would be to compute the residual corrections from a block of triangulation and then assuming this was a systematic pattern for all images, this would be applied until a new correction was computed. It is important to note that the results from the aerial triangulation in ORIMA were obtained *without* using the cross strip in the low flight.

5.3.1. Calibration model used

5.3.1.1. No calibration model - benchmark result

Self Calibration method	Ground control points RMSE (m) of residuals			Ground check points RMSE (m) of residuals			Image coordinates RMSE (μm)of residuals	
	X	Y	Z	X	Y	Z	x	y
No Calibration	0.054	0.034	0.042	0.042	0.038	0.186	1.32	1.31

Table 5. *Results of low flight AT without self-calibration model*

It is interesting to note that the image coordinate RMSE values are smaller than for the high flight indicating a better quality of measurement and/or image quality. In addition, the difference in the image residuals could have been also influenced by the difference in the number of tie points between the low and high flight. The RMSE values of the ground check points are good in X and Y but the Z value for the check points is a little large compared with the ground control Z value and the comparable value from the high flight. Figure 7. shows the image residuals of the observations in the image space for the results presented in table 5. If there is any systematic pattern in the images then there should be a similarity with the pattern of residuals in figure 3. By visual inspection there is some similarities between the figures see top and bottom left corners.

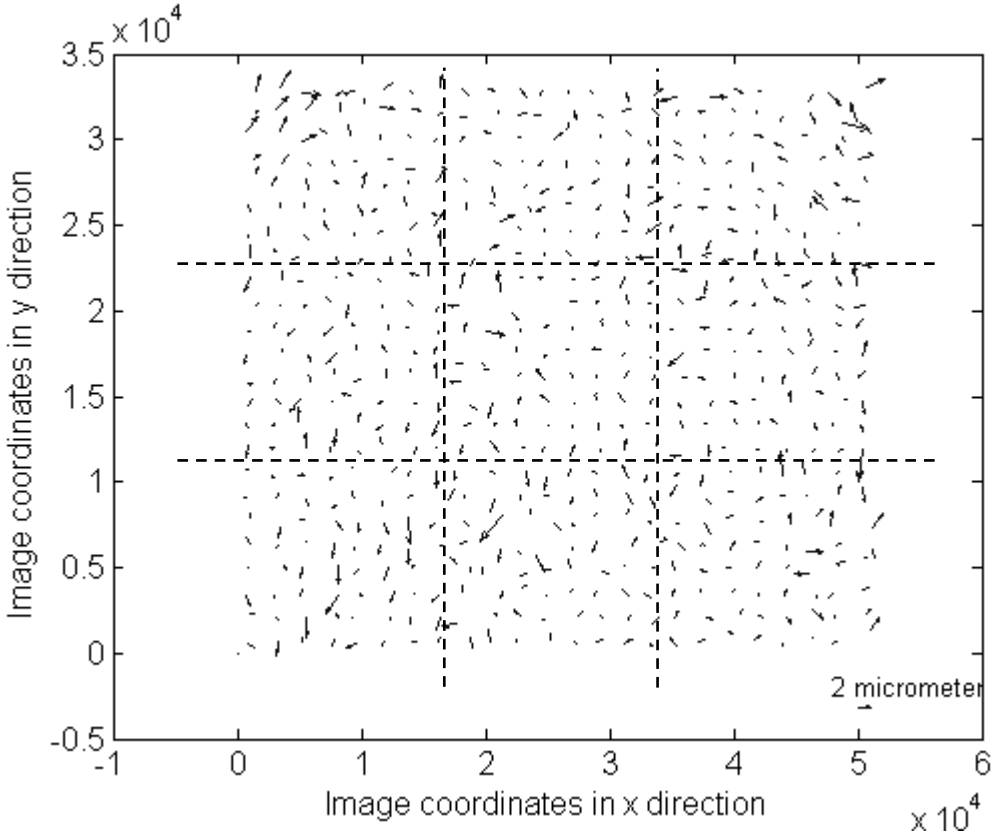

Figure 7. *Mean image residuals in 24x24 sub-areas, results of AT without calibration model (coordinates in μm, partitioning shows approximate boundaries of the CCD arrays)*

5.3.1.2. The 'best ' result from existing self-calibration

A number of self-calibration models where tested from Leica LPS and ORIMA software to assess the most suitable for this type of imagery. The results presented here come from ORIMA and are considered the 'best' result from existing self-calibration models based on the smallest image residuals and RMSE of ground and check points. The parameters of the self-calibration model are as follows:
c = principal distance
x_o, y_o = principal point position
a_1, a_2, a_3 = polynomial coefficients for radial lens distortions
The above self-calibration parameters were free (had large standard errors) during the AT solution in ORIMA.

Self Calibration method	Ground control points RMSE (m) of residuals			Ground check points RMSE (m) of residuals			Image coordinates RMSE (μm)of residuals	
	X	Y	Z	X	Y	Z	x	y
Self Calibration	0.052	0.037	0.033	0.031	0.032	0.093	1.24	1.20

Table 6. *Results of low flight AT with self-calibration model*

The following figure 8 indicates the image residuals of the observations in the image space for the results presented in table 6. There is a similar pattern of residuals to those shown in figure 7.

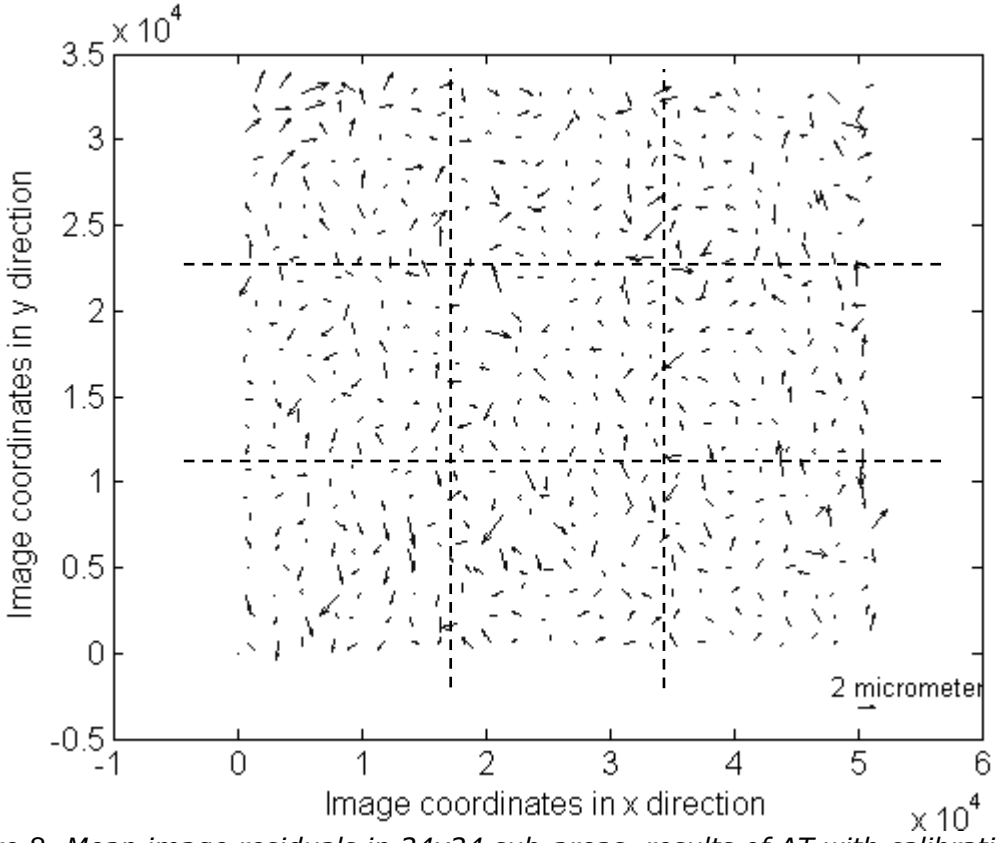

Figure 8. *Mean image residuals in 24x24 sub-areas, results of AT with calibration model (coordinates in μm, partitioning shows approximate boundaries of the CCD arrays)*

5.3.1.3. Analysis of aerial triangulation image residuals – IESSG approach

Self Calibration method	Ground control points RMSE (m) of residuals			Ground check points RMSE (m) of residuals			Image coordinates RMSE (μm)of residuals	
	X	Y	Z	X	Y	Z	x	y
IESSG Approach	0.055	0.038	0.028	0.037	0.037	0.038	1.06	1.00

Table 7. *Results of AT with IESSG calibration model*

In this trial, the image coordinate corrections that have been applied are the values computed from the high-flown block. The following figure 9 indicates the image residuals of the observations in the image space for the results presented in table 7. It appears, from visual inspection, that some of the patterns have been reduced.

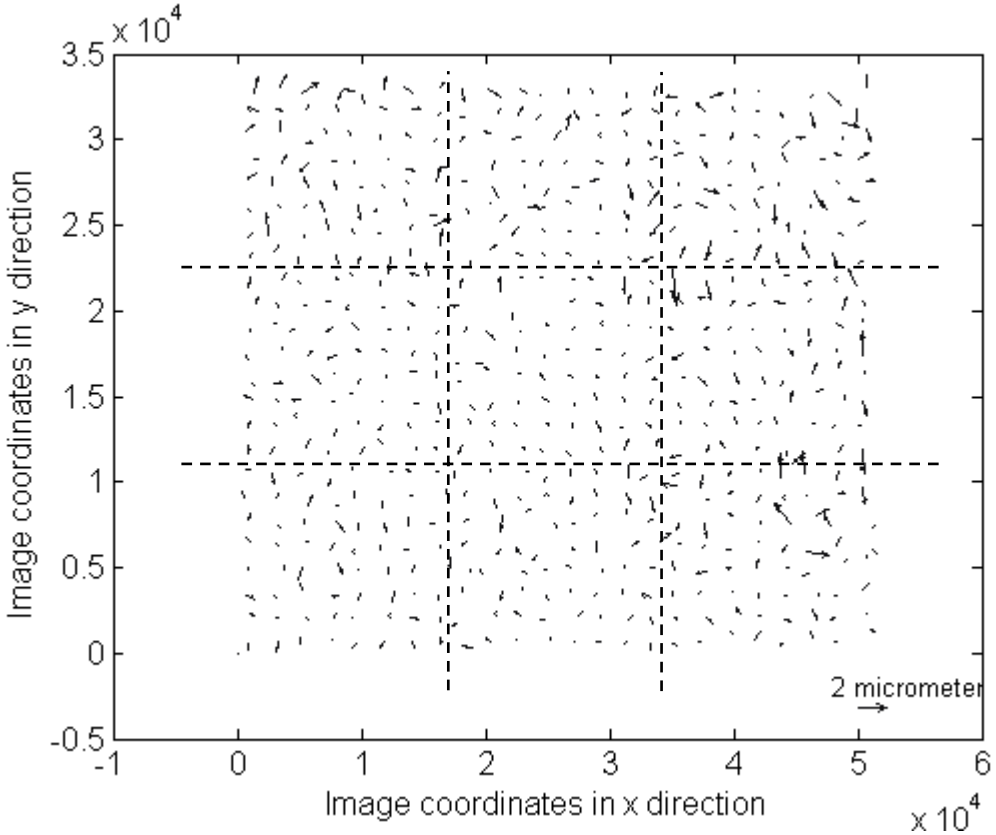

Figure 9. *Mean image residuals in 24x24 sub-areas, results of AT with IESSG calibration model (coordinates in μm, partitioning shows approximate boundaries of the CCD arrays)*

5.3.2. Summary Table 8 of low flight results

Table 8. shows again small RMSE values for the ground control points as identified in the high flown trials. It also shows a small improvement in applying a traditional single lens self-calibration model technique. The really interesting improvement comes from applying the IESSG approach which has reduced relatively significantly the x and y image residuals and the Z RMSE values for the check points compared to the their bench mark values. This is using the residual corrections from the high flown block. The relatively large Z RMSE for the check points in the 'no calibration' computation is dominated, like the high flight, by one residual greater than 0.3.

Self Calibration method	Ground control points RMSE (m) of residuals			Ground check points RMSE (m) of residuals			Image coordinates RMSE (μm)of residuals	
	X	Y	Z	X	Y	Z	x	y
No Calibration	0.054	0.034	0.042	0.042	0.038	0.186	1.32	1.31
Self Calibration	0.052	0.037	0.033	0.031	0.032	0.093	1.24	1.20
IESSG Approach	0.055	0.038	0.028	0.037	0.037	0.038	1.06	1.00

Table 8. *Summary of low flight results*

6. Application of camera calibration parameters

As far as the application of the additional parameters is concerned in further photogrammetric processing chains, it would be proposed to apply any corrections to each image before their future use.

7. Conclusions

Both flights show results where the ground control RMSE are better than the ground control check point RMSE values. This is a little surprising as we are not aware of using any incorrect weighting or duly 'forcing' a fit to the control. From the significantly small residuals of the ground control points, it is evident that the use of in-flight GPS/IMU data could have being very helpful for controlling the exterior orientation parameters.

Only very small systematic patterns could be visually identified in small areas of the image. The existing self-calibration methods and the IESSG approach have made a small improvement on the results. The IESSG calibration approach for the low flight has been particularly beneficial in improving the RMSE in Z and reducing image residuals. However, the method was less successful at improving the high flown results.

More tests and trials are required with a number of blocks to fully understand the residual patterns that are being produced not only within the images of a block but also between blocks.

The IESSG approach has shown that is has potential but needs further investigation to fully assess its capabilities. It is a little surprising that this approach did not make as much improvement with the high flown block, which was used to compute the correction, as it did with the low flown block. Issues such as optimum subdivision of the image would also need to form part of this investigation.

A similar trial and analysis is being undertaken using both the high and the low flown flights together.

8. References

Cramer, M., 2005. Digital Airborne Cameras- Status and Future. ISPRS Hannover Workshop on High resolution Earth imaging for geospatial information Proceedings, Volume XXXVI Part I/W3 ISSN No. 1682-1777.

Kruck, E., 2006. Simultaneous Calibration of Digital Aerial Survey Cameras. International Calibration and Orientation Workshop, EuroCOW 2006. January 2006, Castelldefels, Spain. EuroSDR Commission I and ISPRS Working Group 1/3.

Gruber M., Ladstädler R., 2006. Geometric Issues of the digital large format aerial camera UltraCamD. International Calibration and Orientation Workshop, EuroCOW 2006. January 2006, Castelldefels, Spain. EuroSDR Commission I and ISPRS Working Group 1/3.

Smith, M. J., Qtaishat, K., Park, D., and Jamieson, A., 2005. Initial Results from the Vexcel UltraCam D Digital Aerial Camera. ISPRS Hannover Workshop on High resolution Earth imaging for geospatial information Proceedings, Volume XXXVI Part I/W3 ISSN No. 1682-1777.

9. Acknowledgements

The authors would like to thank Dr Michael Cramer, The University of Stuttgart and EuroSDR for providing the data and the opportunity to take part in this research project. The authors would also like to thank The University of Nottingham and the Jordanian Government for their support.

APPENDIX A

These results have been produced by using all the ground control points observed (14 points high flight and 17 low flight) and including the prescribed check points (approximately 14 points).

These tables show the result of the same tests used in the original report. They are results from ORIMA with the blunder detection on but has not excluded any of the ground control points. Note Sigma Zero has been included instead of the RMSE of the image coordinates. Comparing the ground RMSE values obtained from these trials to the values obtained in the main report trials (with slightly less control) the values in Table A1 (see Table 4) are in general, very similar (slightly larger in some coordinates) and Table A5 (see Table 8) are in general, slightly smaller.

	Ground control points RMSE (m) of residuals			Image coordinates Sigma Zero (μm)
	X	Y	Z	
No Calibration	0.047	0.037	0.027	2.0
Self Calibration	0.044	0.038	0.019	1.9
IESSG Calibration models	0.046	0.038	0.022	1.8

Table A1 Summary of High flight results

… deleted M. Cramer …
Table A2 Check point coordinates for No calibration solution (High flight)

… deleted M. Cramer …
Table A3 Check point coordinates for Self calibration solution (High flight)

… deleted M. Cramer …
Table A4 Check point coordinates for IESSG calibration solution (High flight)

Self Calibration	Ground control points RMSE (m) of residuals			Image coordinates Sigma Zero (μm)
	X	Y	Z	
No Calibration	0.052	0.031	0.038	1.7
Self Calibration	0.049	0.036	0.032	1.6
IESSG Calibration models	0.051	0.037	0.024	1.3

Table A5 Summary of Low flight results

… deleted M. Cramer …
Table A6 Check point coordinates for No calibration solution (Low flight)

… deleted M. Cramer …
Table A7 Check point coordinates for Self calibration solution (Low flight)

… deleted M. Cramer …
Table A8 Check point coordinates for IESSG calibration solution (Low flight)

EuroSDR UltraCamD Data Sets – Bundle Adjustment Results

(using the image coordinates provided by the pilot centre)

Xiaoliang Wu

CSIRO Mathematical and Information Sciences
Private Bag 5, Wembley, WA 6913, Australia
Phone: +61 8 9333 6162, Fax: +61 8 9333 6121
Email: Xiaoliang.Wu@csiro.au

February 2007

This report presents follow-up results to the previous report "EuroSDR UltraCamD Data Sets – Bundle Adjustment Results" [1] by the author. In this report the bundle adjustment results obtained using the image coordinates (Phase 2b) provided by EuroSDR Pilot Centre [2] were presented.

The bundle adjustments were performed under the same configurations as described in [1]. The bundle adjustment process used the image coordinates (both control points, check points and pass points) provided by the Pilot Centre [2] instead of our own measured coordinates. The recommended coordinates of the check points under various configurations are provided, of which further accuracy analysis will be performed by the Pilot Centre.

1. EuroSDR UltraCamD data sets and control/check points

Figure 1 shows the low-flying and high-flying diagrams of the UltraCamD image data sets. In the following, the data set of 19 control points is referred as the ground control point (GCP) set and the data set of 18 check points is referred as the check point (CHP) set. In order to make control and check points easily discernible, the control and check point numbers are prefixed by 90..0 and 80..0 respectively.

Table 1: Control Points and their supplied object space coordinates (19 points)

… deleted M. Cramer …

Table 2: Check Points and their supplied object space coordinates (17 points)

… deleted M. Cramer …

2. Bundle adjustment configurations

As illustrated in Figure 1, there are 2 flying strips in the high-flying data set and 5 flying strips in the high-flying data set. Based on the available strips, 5 bundle adjustment configurations are designed as described as follows:

A. Using 2 long strips from the high-flying data set;
B. Using 4 long strips from the low-flying data set;
C. Using 4 long strips and 1 cross strip from the low-flying data set;
D. Using 2 long strips from the high-flying data set and 4 long strips from the low-flying data set; and
E. Using 2 long strips from the high-flying data set, 4 long strips and 1 cross strip from the low-flying data set.

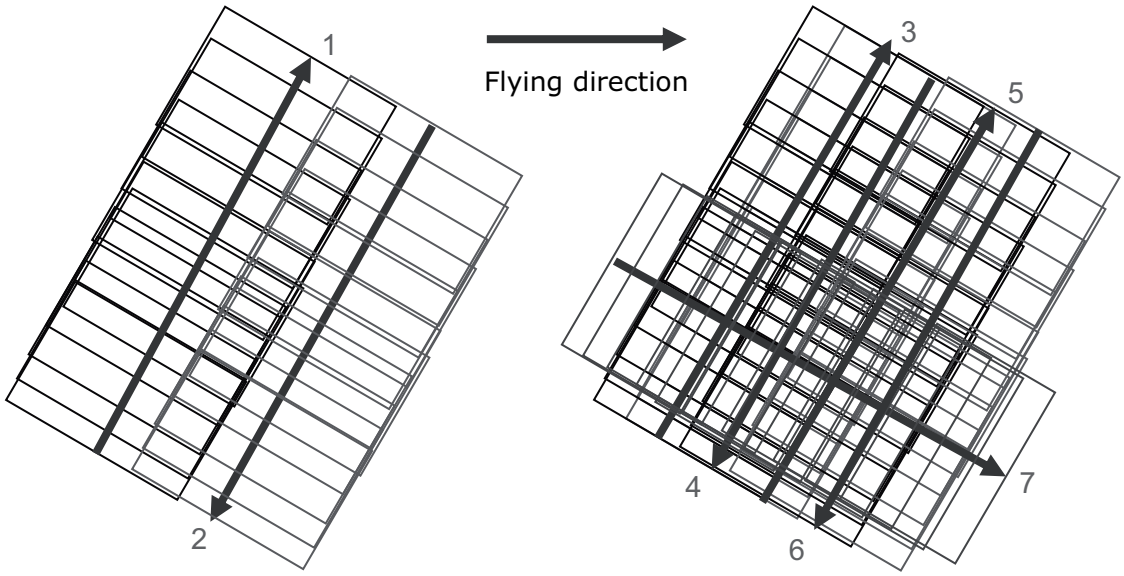

Figure 1: UltraCamD test site Fredrikstad flight configuration. Left: the low-flying data set: acquired in 2 long strips at a flying height of 3800m; the ground distance sample (GDS) is 0.34m; total of 29 images. Right: the low-flying data set; acquired in 4 long strips and 1 cross strip at a flying height of 1900m; GSD is 0.17m; total of 132 images.

3. Results of bundle adjustments

In the following description, “adjusted coordinates” mean the bundle adjusted coordinates for those points that were used as control points during bundle adjustment processing, “obtained coordinates” mean the new computed coordinates for those check points (space coordinates are unknown during bundle adjustment).

3.1 Adjusted coordinates of control points

Tables 3A-3E list the adjusted coordinates of control points and their differences to the supplied coordinates under 5 bundle adjustment configurations. The root mean squares (RMS) values of X, Y and Z differences are also given in the last rows.

Table 3A: The adjusted coordinates of 18 control points and the differences between supplied coordinates and adjusted coordinates for Configuration A (unit is in metre)

… deleted M. Cramer …

Table 3B: The adjusted coordinates of 18 control points and the differences between supplied coordinates and adjusted coordinates for Configuration B (unit is in metre)

… deleted M. Cramer …

Table 3C: The adjusted coordinates of 18 control points and the differences between supplied coordinates and adjusted coordinates for Configuration C (unit is in metre)

… deleted M. Cramer …

Table 3D: The adjusted coordinates of 17 control points and the differences between supplied coordinates and adjusted coordinates for Configuration D (unit is in metre)

… deleted M. Cramer …

Table 3E: The adjusted coordinates of 17 control points and the differences between supplied coordinates and adjusted coordinates for Configuration E (unit is in metre)

… deleted M. Cramer …

3.2 Obtained coordinates of check points

Tables 4A-4E list the obtained coordinates of check points under 5 bundle adjustment configurations.

Table 4A: The obtained coordinates of 15 check points for Configuration A (unit is in metre)

… deleted M. Cramer …

Table 4B: The obtained coordinates of 15 check points for Configuration B (unit is in metre)

… deleted M. Cramer …

Table 4C: The obtained coordinates of 15 check points for Configuration C (unit is in metre)

… deleted M. Cramer …

Table 4D: The obtained coordinates of 13 check points for Configuration D (unit is in metre)

… deleted M. Cramer …

Table 4E: The obtained coordinates of 13 check points for Configuration E (unit is in metre)

… deleted M. Cramer …

4. Discussion about the processing and results

A special program was written to import image coordinates provided by the Pilot Centre [2] into our in-house bundle adjustment software. All image coordinates were successfully imported and no other points were added. High-flying point identification names (except the control points) were renamed because there are identical point names between high-flying and low-flying points (same point names but not the same points).

A relative orientation and model connection scheme was applied to all images using imported image coordinates. For the high-flying data set, the relative orientation started from the first stereo pair in Strip 1, while for the low-flying data set, the relative orientation started from the first stereo pair in Strip 3 (Figure 1). The relative orientation parameters from the first stereo pairs were then used for model connection for the next stereo pairs in order to join all models spatially.

Once all relative models were connected, the initial image orientation values and initial model coordinates for all points were determined using the relative model parameters, and bundle adjustment was then performed. The in-house developed software was used to perform bundle adjustment.

No GPS and PATB orientation data was used for any purposes during block adjustment processing. The known (fixed) parameters for each image are the pixel size: 0.009mm in both pixel directions and the focal length: 101.4mm. Six unknowns for each image are the camera position (X, Y and Z) and image rotation angles (omega, phi and kappa). No additional parameters were introduced within bundle adjustment processing. Cartesian coordinate system was assumed for control points and therefore no map projection processing was performed during bundle adjustment processing.

It is worth to mention that the numbers of control points and check points provided by the Pilot Centre in for high-flying and low-flying configurations are different. For example, 90037 was only used in Configurations B and C (low-flying) while 90047 was only used in Configuration A (high-flying). However, during the block adjustment processing for Configurations D and E, both 90037 and 90047 were not used, and check points which did not appear on both low-flying and high-flying images were not provided to the Pilot Centre.

From the results presented in the previous section, we observe that the adjusted space coordinates for the control points have very good agreement (low residual error between the supplied space coordinates and the adjusted space coordinates) for all configurations: X, Y, Z RMS are less than 0.06m, 0.08m and 0.05m, respectively. However, the final assessment for bundle adjustment results will be analysed by the Pilot Centre using the provided coordinates of check points.

References

1. Wu X., 2006, EuroSDR UltraCamD Data Sets — Bundle Adjustment Results. CMIS Technical Report 06/158.
2. Cramer M., 2007, Experimental Phase 2b – DMC and UltracamD Remarks. Institute for Photogrammetry, University of Stuttgart.

Institut für Photogrammetrie und GeoInformation
Leibniz Universität Hannover

Nienburger Str. 1
D-30167 Hannover

Tel.: +49-511/762-2485
Fax: +49-511/762-2483
e-mail: jacobsen@ipi.uni-hannover.de
http://www.ipi.uni-hannover.de

Dr.-Ing. Karsten Jacobsen

Hannover, 15.3.2007

Analysis of EuroSDR Camera Calibration test block Frederikstaad
UltraCamD
Phase II

1. Lower Flying elevation

```
MAX PHOTOS/POINT            :     20
OBJECT POINTS               :   2373
PHOTOS                      :    132
PHOTO POINTS                :  16875

MINIMUM AND MAXIMUM OF PHOTO COORDINATES
 X MINIMUM =  -51.697  X MAXIMUM =   51.671
 Y MINIMUM =  -33.723  Y MAXIMUM =   33.684

NUMBER OF PHOTOS/OBJECT POINT
PHOTOS/POINT    1     2     3     4     5     6     7     8     9    10
POINTS:         0   136   184   211   610   140   120   124   188   363

PHOTOS/POINT   11    12    13    14    15    16    17    18    19    20
POINTS:        57    30    39    42    82    10     7    11     6    13

CAMERA PROJECTION CENTER  TERRAIN   PHOTO SCALE
   1          1982.m        69.m       1:18873
```

17cm GSD

	RMSX	RMSY	RMSZ	sigma0
no selfcalibration	4.6 cm	3.5 cm	13.5 cm	1.96 µm
param. 1-12	4.5 cm	3.0 cm	3.7 cm	1.73 µm
param. 1-12, 42-73	4.5 cm	3.0 cm	4.3 cm	1.57 µm

table 1: discrepancies at control points
parameters 1-12 = standard BLUH-parameters
parameters 42-73 = special UltraCam-parameters

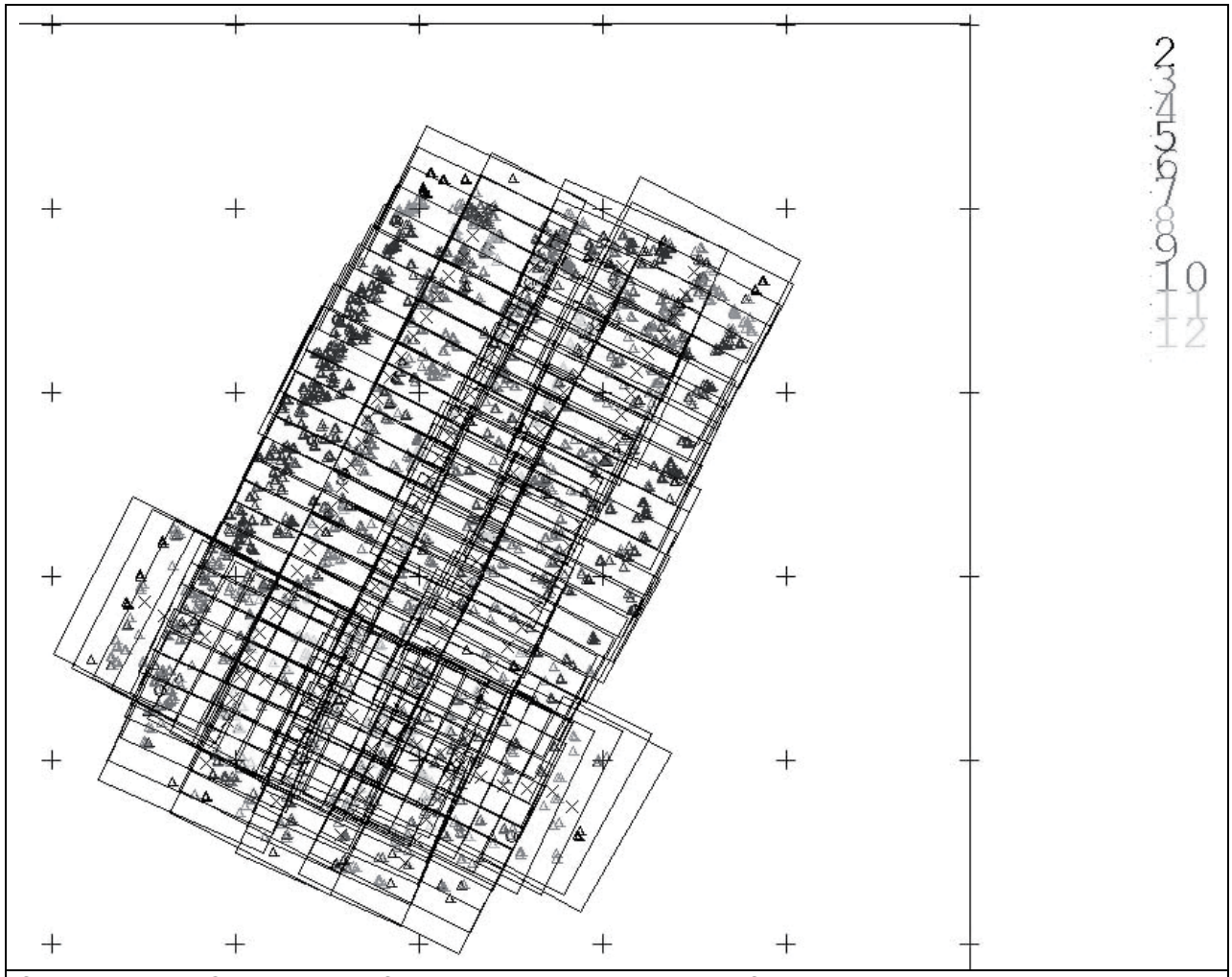

figure 1: UltraCamD lower flying elevation – block configuration
color of points corresponds to number of images / point (see upper right)

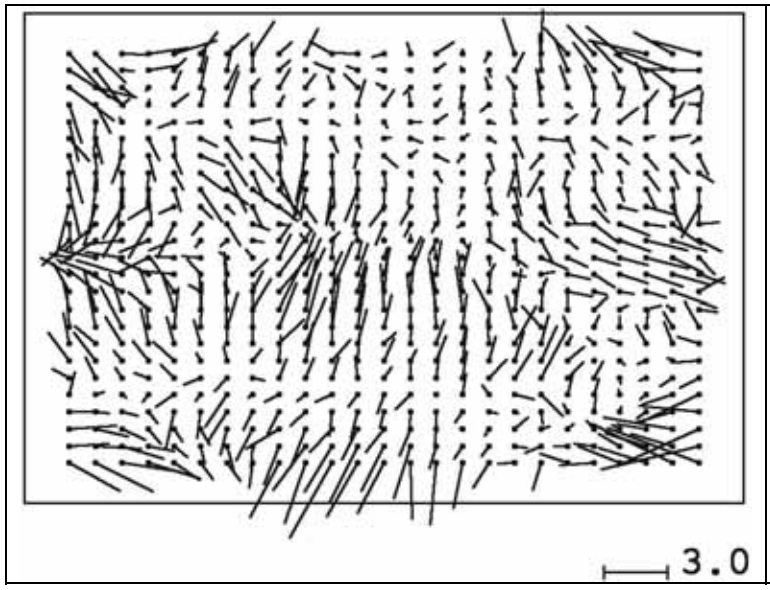

figure 2: averaged and overlaid image residuals of block adjustment without self calibration

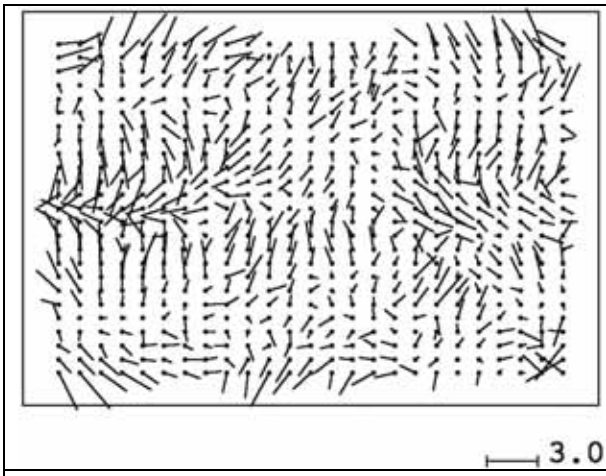

figure 3a: averaged and overlaid residuals

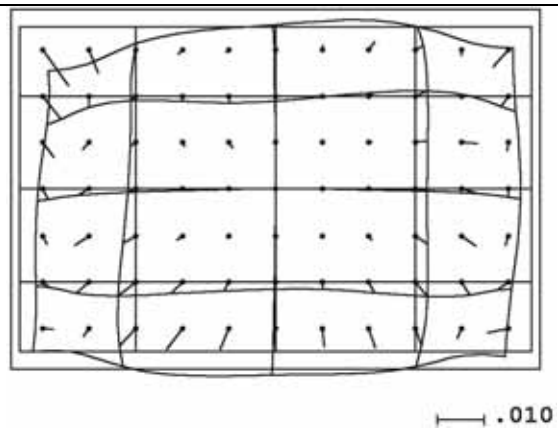

figure 3b: systematic image errors

block adjustment with self calibration – additional parameters 1 – 12 (standard parameters for aerial images)

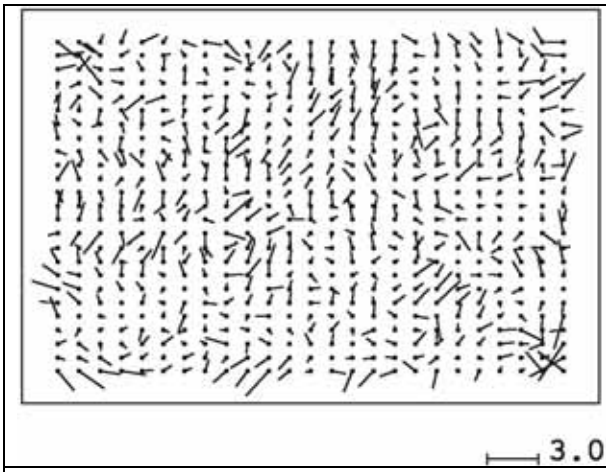

figure 4a: averaged and overlaid residuals

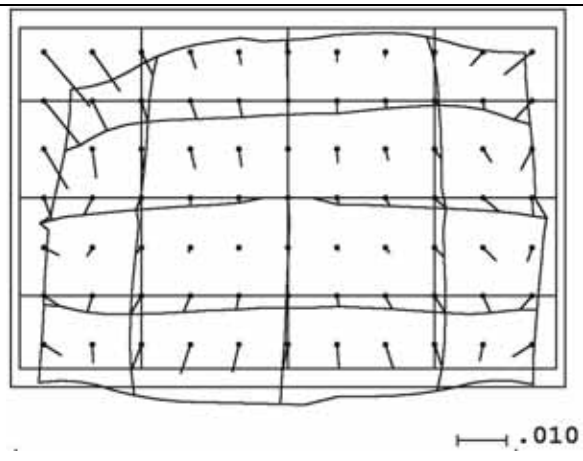

figure 4b: systematic image errors

block adjustment with self calibration – additional parameters 1 – 12 + 42-73 (standard parameters for aerial images + special UltraCamD-parameters)

2. Upper Flying elevation

```
 MAX PHOTOS/POINT              :     11
 OBJECT POINTS                 :   2358
 PHOTOS                        :     29
 PHOTO POINTS                  :  12649

 NUMBER OF PHOTOS/OBJECT POINT
 PHOTOS/POINT    1     2     3     4     5     6     7     8     9    10
 POINTS:         0   240   311   446   591   113   121   101   187   247

CAMERA PROJECTION CENTER  TERRAIN   PHOTO SCALE
    1          3906.m        67.m     1:37861.
```

34cm GSD

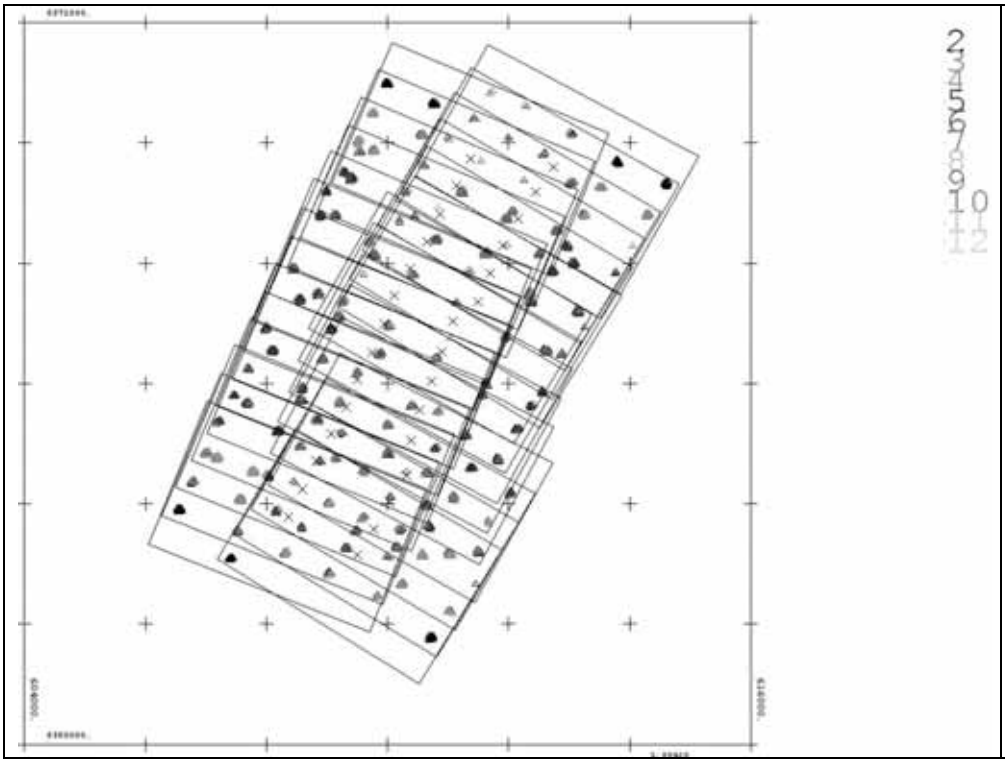

figure 5: UltraCamD upper flying elevation – block configuration color of points corresponds to number of images / point (see upper right)

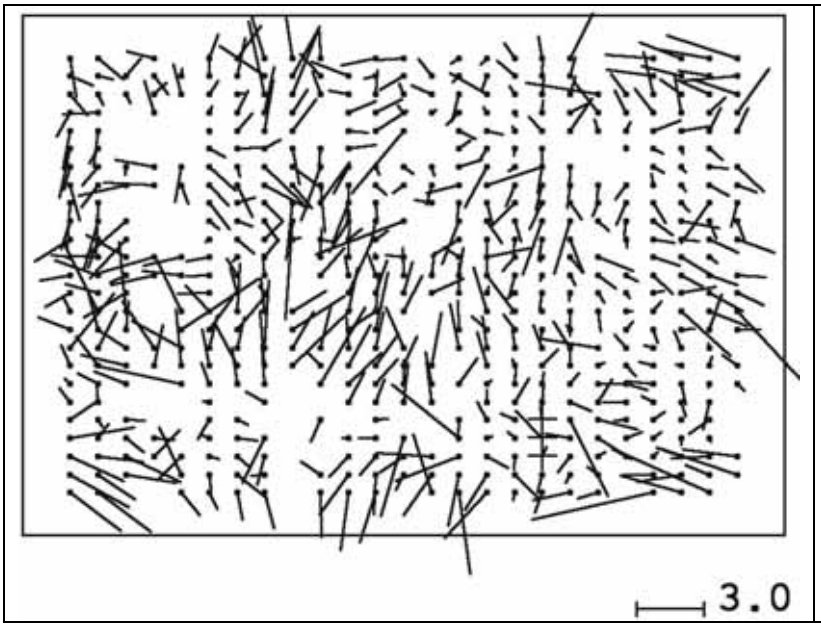

figure 6: averaged and overlaid image residuals of block adjustment without self calibration

	RMSX	RMSY	RMSZ	sigma0
no selfcalibration	8.1 cm	8.7 cm	23.5 cm	1.91 µm
param. 1-12	8.9 cm	8.3 cm	11.0 cm	1.76 µm
param. 1-12, 42-73	7.4 cm	7.1 cm	10.6cm	1.63 µm

table 2: discrepancies at control points
parameters 1-12 = standard BLUH-parameters
parameters 42-73 = special UltraCam-parameters

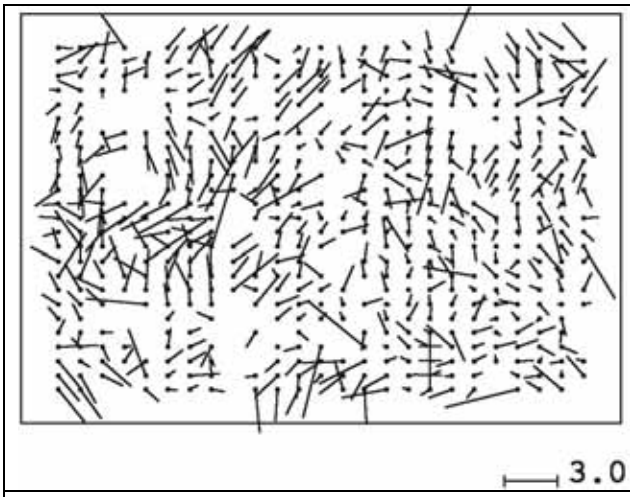

figure 7a: averaged and overlaid residuals

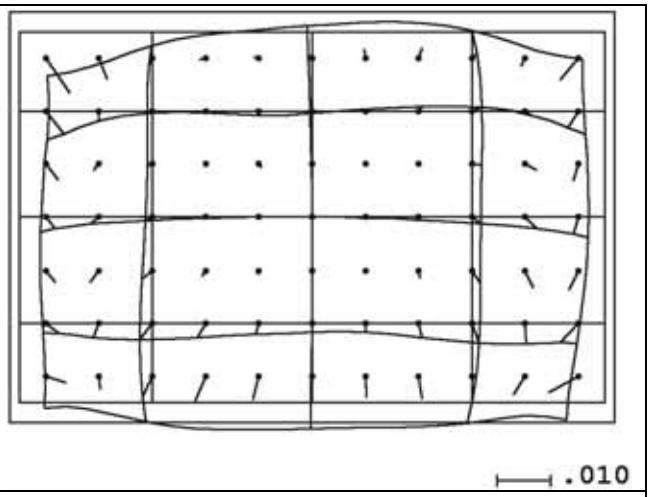

figure 7b: systematic image errors

block adjustment with self calibration – additional parameters 1 – 12 (standard parameters for aerial images)

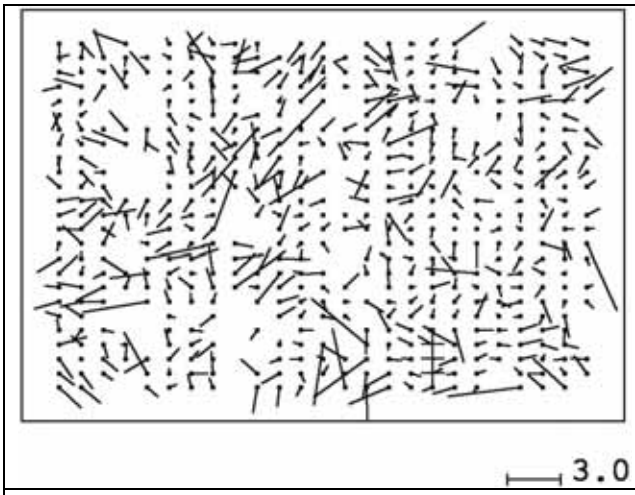

figure 8a: averaged and overlaid residuals

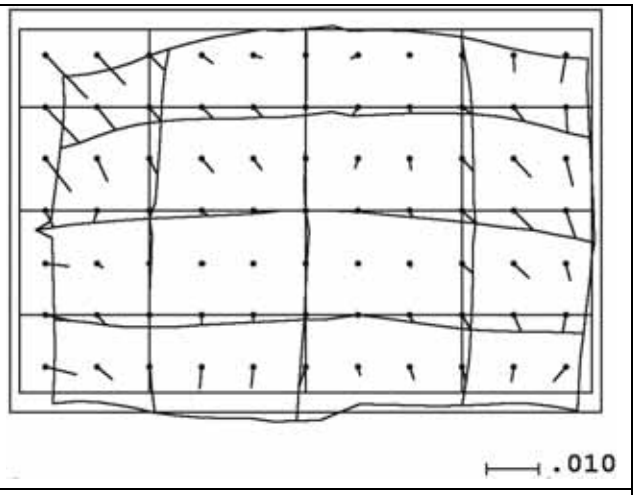

figure 8b: systematic image errors

block adjustment with self calibration – additional parameters 1 – 12 + 42-73 (standard parameters for aerial images + special UltraCamD-parameters)

3. Upper + lower flying elevation

```
MAX PHOTOS/POINT              :      30
OBJECT POINTS                 :    4699
PHOTOS                        :     161
PHOTO POINTS                  :   29524
 NUMBER OF PHOTOS/OBJECT POINT
PHOTOS/POINT    1     2     3     4     5     6     7     8     9    10
POINTS:         0   376   495   654  1184   252   231   225   371   602

PHOTOS/POINT   11    12    13    14    15    16    17    18    19    20
POINTS:        59    30    39    45    75    10     8    10     6    15

PHOTOS/POINT   21    22    23    24    25    26    27    28    29    30
POINTS:         0     2     0     4     3     0     0     1     1     1
```

IMAGE SCALE 1 : 18138.26 - 1 : 38035.35

17cm + 34cm GSD

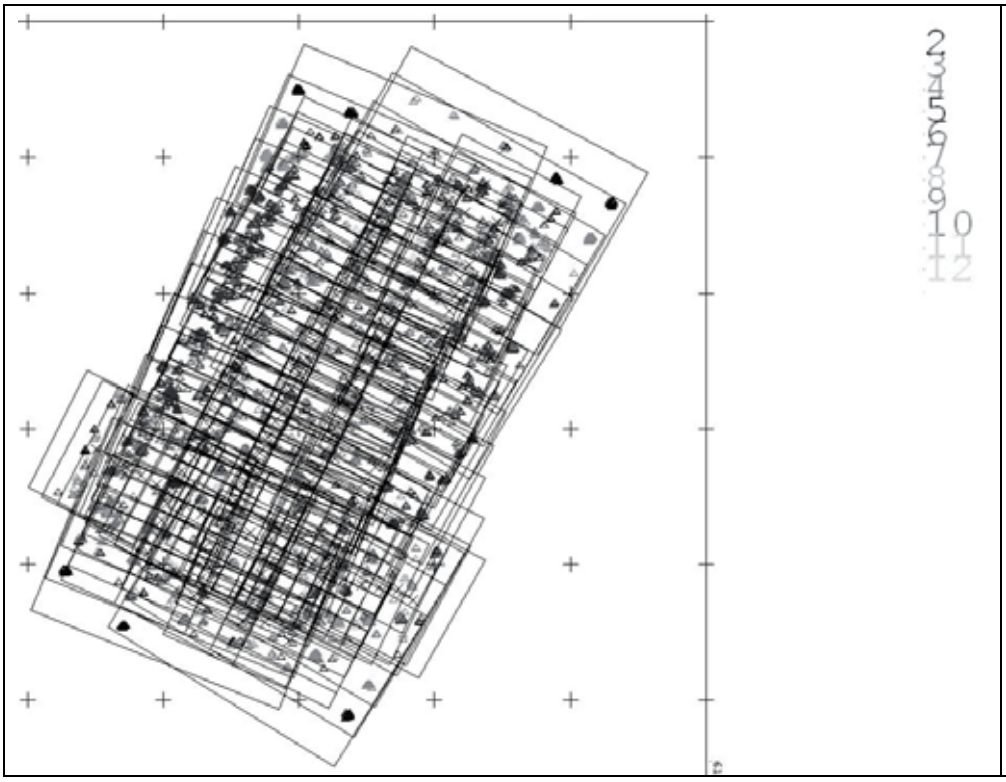

figure 9: UltraCamD upper + lower flying elevation – block configuration color of points corresponds to number of images / point (see upper right)

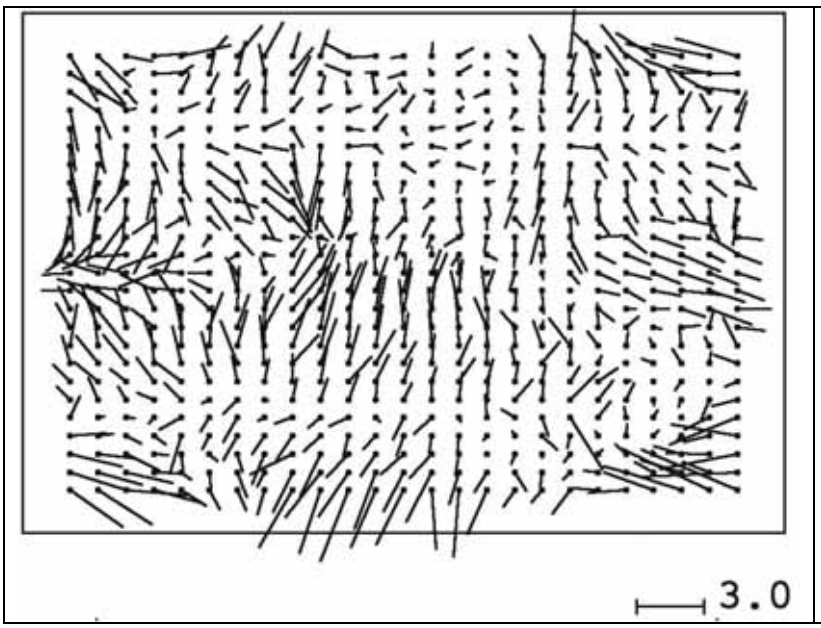

figure 10: averaged and overlaid image residuals of block adjustment without self calibration

	RMSX	RMSY	RMSZ	sigma0
no selfcalibration	5.0 cm	3.7 cm	16.7cm	1.89 µm
param. 1-12	4.1 cm	3.3 cm	6.2 cm	1.70 µm
param. 1-12, 42-73	3.8 cm	3.1 cm	6.9cm	1.55 µm

table 3: discrepancies at control points
parameters 1-12 = standard BLUH-parameters
parameters 42-73 = special UltraCam-parameters

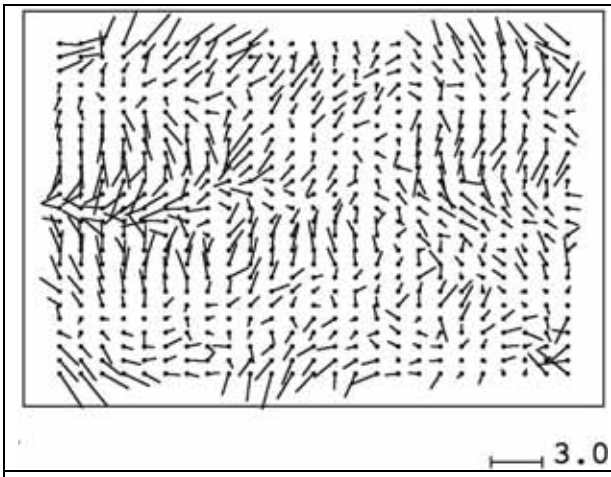	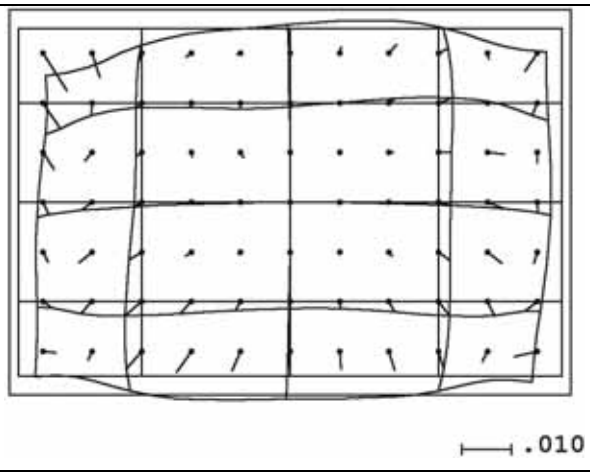
figure 11a: averaged and overlaid residuals	figure 11b: systematic image errors
block adjustment with self calibration – additional parameters 1 – 12 (standard parameters for aerial images)	

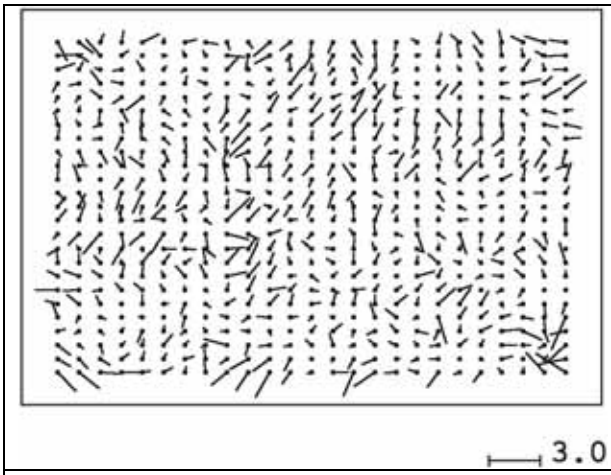	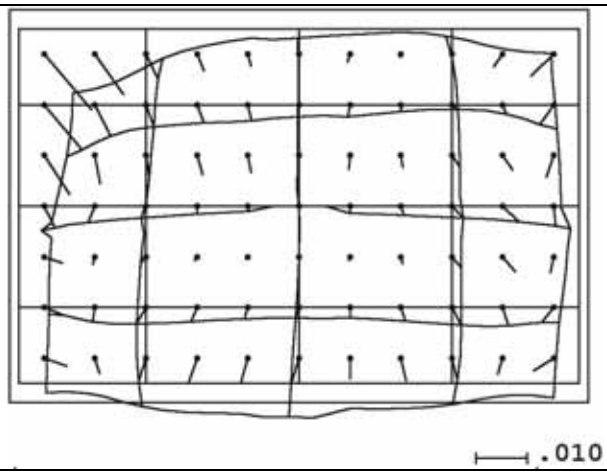
figure 12a: averaged and overlaid residuals	figure 12b: systematic image errors
block adjustment with self calibration – additional parameters 1 – 12 + 42-73 (standard parameters for aerial images + special UltraCamD-parameters)	

LIST OF OEEPE/EuroSDR OFFICIAL PUBLICATIONS

State – May 2008

1 *Trombetti, C.:* „Activité de la Commission A de l'OEEPE de 1960 à 1964" – *Cunietti, M.:* „Activité de la Commission B de l'OEEPE pendant la période septembre 1960 – janvier 1964" – *Förstner, R.:* „Rapport sur les travaux et les résultats de la Commission C de l'OEEPE (1960–1964)" – *Neumaier, K.:* „Rapport de la Commission E pour Lisbonne" – *Weele, A. J. v. d.:* „Report of Commission F." – Frankfurt a. M. 1964, 50 pages with 7 tables and 9 annexes.

2 *Neumaier, K.:* „Essais d'interprétation de »Bedford« et de »Waterbury«. Rapport commun établi par les Centres de la Commission E de l'OEEPE ayant participé aux tests" – „The Interpretation Tests of »Bedford« and »Waterbury«. Common Report Established by all Participating Centres of Commission E of OEEPE" – „Essais de restitution »Bloc Suisse«. Rapport commun établi par les Centres de la Commission E de l'OEEPE ayant participé aux tests" – „Test »Schweizer Block«. Joint Report of all Centres of Commission E of OEEPE." – Frankfurt a. M. 1966, 60 pages with 44 annexes.

3 *Cunietti, M.:* „Emploi des blocs de bandes pour la cartographie à grande échelle – Résultats des recherches expérimentales organisées par la Commission B de l'O.E.E.P.E. au cours de la période 1959–1966" – „Use of Strips Connected to Blocks for Large Scale Mapping – Results of Experimental Research Organized by Commission B of the O.E.E.P.E. from 1959 through 1966." – Frankfurt a. M. 1968, 157 pages with 50 figures and 24 tables.

4 *Förstner, R.:* „Sur la précision de mesures photogrammétriques de coordonnées en terrain montagneux. Rapport sur les résultats de l'essai de Reichenbach de la Commission C de l'OEEPE" – „The Accuracy of Photogrammetric Co-ordinate Measurements in Mountainous Terrain. Report on the Results of the Reichenbach Test Commission C of the OEEPE." – Frankfurt a. M. 1968, Part I: 145 pages with 9 figures; Part II: 23 pages with 65 tables.

5 *Trombetti, C.:* „Les recherches expérimentales exécutées sur de longues bandes par la Commission A de l'OEEPE." – Frankfurt a. M. 1972, 41 pages with 1 figure, 2 tables, 96 annexes and 19 plates.

6 *Neumaier, K.:* „Essai d'interprétation. Rapports des Centres de la Commission E de l'OEEPE." – Frankfurt a. M. 1972, 38 pages with 12 tables and 5 annexes.

7 *Wiser, P.:* „Etude expérimentale de l'aérotriangulation semi-analytique. Rapport sur l'essai »Gramastetten«." – Frankfurt a. M. 1972, 36 pages with 6 figures and 8 tables.

8 „Proceedings of the OEEPE Symposium on Experimental Research on Accuracy of Aerial Triangulation (Results of Oberschwaben Tests)" *Ackermann, F.:* „On Statistical Investigation into the Accuracy of Aerial Triangulation. The Test Project Oberschwaben" – „Recherches statistiques sur la précision de l'aérotriangulation. Le champ d'essai Oberschwaben"– *Belzner, H.:* „The Planning. Establishing and Flying of the Test Field Oberschwaben" – *Stark, E.:* Testblock Oberschwaben, Programme I. Results of Strip Adjustments" – *Ackermann, F.:* „Testblock Oberschwaben, Program I. Results of Block-Adjustment by Independent Models" – *Ebner, H.:* Comparison of Different Methods of Block Adjustment" – *Wiser, P.:* „Propositions pour le traitement des erreurs non-accidentelles"– *Camps, F.:* „Résultats obtenus dans le cadre du project Oberschwaben 2A" – *Cunietti, M.; Vanossi, A.:* „Etude statistique expérimentale des erreurs d'enchaînement des photogrammes"– *Kupfer, G.:* „Image Geometry as Obtained from Rheidt Test Area Photography" – *Förstner, R.:* „The Signal-Field of Baustetten. A Short Report" – *Visser, J.; Leberl, F.; Kure, J.:* „OEEPE Oberschwaben Reseau Investigations" – *Bauer, H.:* „Compensation of Systematic Errors by Analytical Block Adjustment with Common Image Deformation Parameters." – Frankfurt a. M. 1973, 350 pages with 119 figures, 68 tables and 1 annex.

9 *Beck, W.:* „The Production of Topographic Maps at 1 : 10,000 by Photogrammetric Methods. – With statistical evaluations, reproductions, style sheet and sample fragments by

Landesvermessungsamt Baden-Württemberg Stuttgart." – Frankfurt a. M. 1976, 89 pages with 10 figures, 20 tables and 20 annexes.

10 „Résultats complémentaires de l'essai d'«Oberriet» of the Commission C de l'OEEPE – Further Results of the Photogrammetric Tests of «Oberriet» of the Commission C of the OEEPE"
Hárry, H.: „Mesure de points de terrain non signalisés dans le champ d'essai d'«Oberriet» – Measurements of Non-Signalized Points in the Test Field «Oberriet» (Abstract)" – *Stickler, A.; Waldhäusl, P.:* „Restitution graphique des points et des lignes non signalisés et leur comparaison avec des résultats de mesures sur le terrain dans le champ d'essai d'«Oberriet» – Graphical Plotting of Non-Signalized Points and Lines, and Comparison with Terrestrial Surveys in the Test Field «Oberriet»" – *Förstner, R.:* „Résultats complémentaires des transformations de coordonnées de l'essai d'«Oberriet» de la Commission C de l'OEEPE – Further Results from Co-ordinate Transformations of the Test «Oberriet» of Commission C of the OEEPE" – *Schürer, K.:* „Comparaison des distances d'«Oberriet» – Comparison of Distances of «Oberriet» (Abstract)." – Frankfurt a. M. 1975, 158 pages with 22 figures and 26 tables.

11 „25 années de l'OEEPE"
Verlaine, R.: „25 années d'activité de l'OEEPE" – „25 Years of OEEPE (Summary)" – *Baarda, W.:* „Mathematical Models." – Frankfurt a. M. 1979, 104 pages with 22 figures.

12 *Spiess, E.:* „Revision of 1 : 25,000 Topographic Maps by Photogrammetric Methods." – Frankfurt a. M. 1985, 228 pages with 102 figures and 30 tables.

13 *Timmerman, J.; Roos, P. A.; Schürer, K.; Förstner, R.:* On the Accuracy of Photogrammetric Measurements of Buildings – Report on the Results of the Test "Dordrecht", Carried out by Commission C of the OEEPE. – Frankfurt a. M. 1982, 144 pages with 14 figures and 36 tables.

14 *Thompson C. N.:* Test of Digitising Methods. – Frankfurt a. M. 1984, 120 pages with 38 figures and 18 tables.

15 *Jaakkola, M.; Brindöpke, W.; Kölbl, O.; Noukka, P.:* Optimal Emulsions for Large-Scale Mapping – Test of "Steinwedel" – Commission C of the OEEPE 1981–84. – Frankfurt a. M. 1985, 102 pages with 53 figures.

16 *Waldhäusl, P.:* Results of the Vienna Test of OEEPE Commission C. – *Kölbl, O.:* Photogrammetric Versus Terrestrial Town Survey. – Frankfurt a. M. 1986, 57 pages with 16 figures, 10 tables and 7 annexes.

17 *Commission E of the OEEPE:* Influences of Reproduction Techniques on the Identification of Topographic Details on Orthophotomaps. – Frankfurt a. M. 1986, 138 pages with 51 figures, 25 tables and 6 appendices.

18 *Förstner, W.:* Final Report on the Joint Test on Gross Error Detection of OEEPE and ISP WG III/1. – Frankfurt a. M. 1986, 97 pages with 27 tables and 20 figures.

19 *Dowman, I. J.; Ducher, G.:* Spacelab Metric Camera Experiment – Test of Image Accuracy. – Frankfurt a. M. 1987, 112 pages with 13 figures, 25 tables and 7 appendices.

20 *Eichhorn, G.:* Summary of Replies to Questionnaire on Land Information Systems – Commission V – Land Information Systems. – Frankfurt a. M. 1988, 129 pages with 49 tables and 1 annex.

21 *Kölbl, O.:* Proceedings of the Workshop on Cadastral Renovation – Ecole polytechnique fédérale, Lausanne, 9–11 September, 1987. – Frankfurt a. M. 1988, 337 pages with figures, tables and appendices.

22 *Rollin, J.; Dowman, I. J.:* Map Compilation and Revision in Developing Areas – Test of Large Format Camera Imagery. – Frankfurt a. M. 1988, 35 pages with 3 figures, 9 tables and 3 appendices.

23 *Drummond, J.* (ed.): Automatic Digitizing – A Report Submitted by a Working Group of Commission D (Photogrammetry and Cartography). – Frankfurt a. M. 1990, 224 pages with 85 figures, 6 tables and 6 appendices.

24 *Ahokas, E.; Jaakkola, J.; Sotkas, P.:* Interpretability of SPOT data for General Mapping. – Frankfurt a. M. 1990, 120 pages with 11 figures, 7 tables and 10 appendices.

25 *Ducher, G.:* Test on Orthophoto and Stereo-Orthophoto Accuracy. – Frankfurt a. M. 1991, 227 pages with 16 figures and 44 tables.

26 *Dowman, I. J.* (ed.): Test of Triangulation of SPOT Data – Frankfurt a. M. 1991, 206 pages with 67 figures, 52 tables and 3 appendices.

27 *Newby, P. R. T.; Thompson, C. N.* (ed.): Proceedings of the ISPRS and OEEPE Joint Workshop on Updating Digital Data by Photogrammetric Methods. – Frankfurt a. M. 1992, 278 pages with 79 figures, 10 tables and 2 appendices.

28 *Koen, L. A.; Kölbl, O.* (ed.): Proceedings of the OEEPE-Workshop on Data Quality in Land Information Systems, Apeldoorn, Netherlands, 4–6 September 1991. – Frankfurt a. M. 1992, 243 pages with 62 figures, 14 tables and 2 appendices.

29 *Burman, H.; Torlegård, K.:* Empirical Results of GPS – Supported Block Triangulation. – Frankfurt a. M. 1994, 86 pages with 5 figures, 3 tables and 8 appendices.

30 *Gray, S.* (ed.): Updating of Complex Topographic Databases. – Frankfurt a. M. 1995, 133 pages with 2 figures and 12 appendices.

31 *Jaakkola, J.; Sarjakoski, T.*: Experimental Test on Digital Aerial Triangulation. – Frankfurt a. M. 1996, 155 pages with 24 figures, 7 tables and 2 appendices.

32 *Dowman, I. J.*: The OEEPE GEOSAR Test of Geocoding ERS-1 SAR Data. – Frankfurt a. M. 1996, 126 pages with 5 figures, 2 tables and 2 appendices.

33 *Kölbl, O.*: Proceedings of the OEEPE-Workshop on Application of Digital Photogrammetric Workstations. – Frankfurt a. M. 1996, 453 pages with numerous figures and tables.

34 *Blau, E.; Boochs, F.; Schulz, B.-S.*: Digital Landscape Model for Europe (DLME). – Frankfurt a. M. 1997, 72 pages with 21 figures, 9 tables, 4 diagrams and 15 appendices.

35 *Fuchs, C.; Gülch, E.; Förstner, W.*: OEEPE Survey on 3D-City Models.
Heipke, C.; Eder, K.: Performance of Tie-Point Extraction in Automatic Aerial Triangulation. – Frankfurt a. M. 1998, 185 pages with 42 figures, 27 tables and 15 appendices.

36 *Kirby, R. P.*: Revision Measurement of Large Scale Topographic Data.
Höhle, J.: Automatic Orientation of Aerial Images on Database Information.
Dequal, S.; Koen, L. A.; Rinaudo, F.: Comparison of National Guidelines for Technical and Cadastral Mapping in Europe ("Ferrara Test") – Frankfurt a. M. 1999, 273 pages with 26 figures, 42 tables, 7 special contributions and 9 appendices.

37 *Koelbl, O.* (ed.): Proceedings of the OEEPE – Workshop on Automation in Digital Photogrammetric Production. – Frankfurt a. M. 1999, 475 pages with numerous figures and tables.

38 *Gower, R.*: Workshop on National Mapping Agencies and the Internet. *Flotron, A.; Koelbl, O.*: Precision Terrain Model for Civil Engineering. – Frankfurt a. M. 2000, 140 pages with numerous figures, tables and a CD.

39 *Ruas, A.*: Automatic Generalisation Project: Learning Process from Interactive Generalisation. – Frankfurt a. M. 2001, 98 pages with 43 figures, 46 tables and 1 appendix.

40 *Torlegård, K.; Jonas, N.*: OEEPE workshop on Airborne Laserscanning and Interferometric SAR for Detailed Digital Elevation Models. – Frankfurt a. M. 2001, CD: 299 pages with 132 figures, 26 tables, 5 presentations and 2 videos.

41 *Radwan, M.; Onchaga, R.; Morales, J.*: A Structural Approach to the Management and Optimization of Geoinformation Processes. – Frankfurt a. M. 2001, 174 pages with 74 figures, 63 tables and 1 CD.

42 *Heipke, C.; Sester, M.; Willrich, F.* (eds.): Joint OEEPE/ISPRS Workshop – From 2D to 3D – Establishment and maintenance of national core geospatial databases. *Woodsford, P.* (ed.): OEEPE Commission 5 Workshop: Use of XML/GML. – Frankfurt a. M. 2002, CD.

43 *Heipke, C.; Jacobsen, K.; Wegmann, H.*: Integrated Sensor Orientation – Test Report and Workshop Proceedings. – Frankfurt a. M. 2002, 302 pages with 215 figures, 139 tables and 2 appendices.

44 *Holland, D.; Guilford, B.; Murray, K.*: Topographic Mapping from High Resolution Space Sensors. – Frankfurt a. M. 2002, 155 pages with numerous figures, tables and 7 appendices.

45 *Murray, K.* (ed.): OEEPE Workshop on Next Generation Spatial Database – 2005. *Altan, M. O.; Tastan, H.* (eds.): OEEPE/ISPRS Joint Workshop on Spatial Data Quality Management. 2003, CD.

46 *Heipke, C.; Kuittinen, R.; Nagel, G.* (eds.): From OEEPE to EuroSDR: 50 years of European Spatial Data Research and beyond – Seminar of Honour. 2003, 103 pages and CD.

47 *Woodsford, P.; Kraak, M.; Murray, K.; Chapman, D.* (eds.): Visualisation and Rendering – Proceedings EuroSDR Commission 5 Workshop. 2003, CD.

48 *Woodsford, P.* (ed.): Ontologies & Schema Translation – 2004. *Bray, C.* (ed.): Positional Accuracy Improvement – 2004. *Woodsford, P.* (ed.): E-delivery – 2005. Workshops. 2005, CD.

49 *Bray, C.; Rönsdorf, C.* (eds.): Achieving Geometric Interoperability of Spatial Data, Workshop – 2005. *Kolbe, T. H.; Gröger, G.* (eds.): International Workshop on Next Generation 3D City Models – 2005. *Woodsford, P.* (ed.): Workshop on Feature/Object Data Models. 2006, CD.

50 *Kaartinen, H.; Hyyppä J.*: Evaluation of Building Extraction. *Steinnocher, K.; Kressler, F.*: Change Detection. *Bellmann, A.; Hellwich, O.*: Sensor and Data Fusion Contest: Information for Mapping from Airborne SAR and Optical Imagery (Phase I). *Mayer, H.; Baltsavias, E.; Bacher, U.*: Automated Extraction, Refinement, and Update of Road Databases from Imagery and Other Data. 2006, 280 pages.

51 *Höhle, J.; Potuckova J.*: The EuroSDR Test "Checking and Improving of Digital Terrain Models". *Skaloud, J.*: Reliability of Direct Georeferencing, Phase 1: An Overview of the Current Approaches and Possibilities. *Legat, K.; Skaloud, J.; Schmidt, R.*: Reliability of Direct Georeferencing, Phase 2: A Case Study on Practical Problems and Solutions. 2006, 184 pages.

52 *Murray, K.* (ed.): Proceedings of the International Workshop on Land and Marine Information Integration. 2007, CD.

53 *Kaartinen, H., Hyyppä, J.*: Tree Extraction. 2008, 56 pages.

54 *Patrucco, R., Murray, K.*. (eds.): Production Partnership Management Workshop – 2007. Ismael *Colomina, I,. Hernández, E.* (eds.): International Calibration and Orientation Workshop, EuroCOW 2008. *Heipke, C., Sester, M.* (eds.): Geosensor Networks Workshop. *Kolbe, T. H.;* (ed.): Final Report on the EuroSDR CityGML Project. 2008, CD.

The publications can be ordered using the electronic order form of the EuroSDR website
www.eurosdr.net